Multivariate Methods for Life Safety Analysis in Case of Fire

Benjamin Schröder

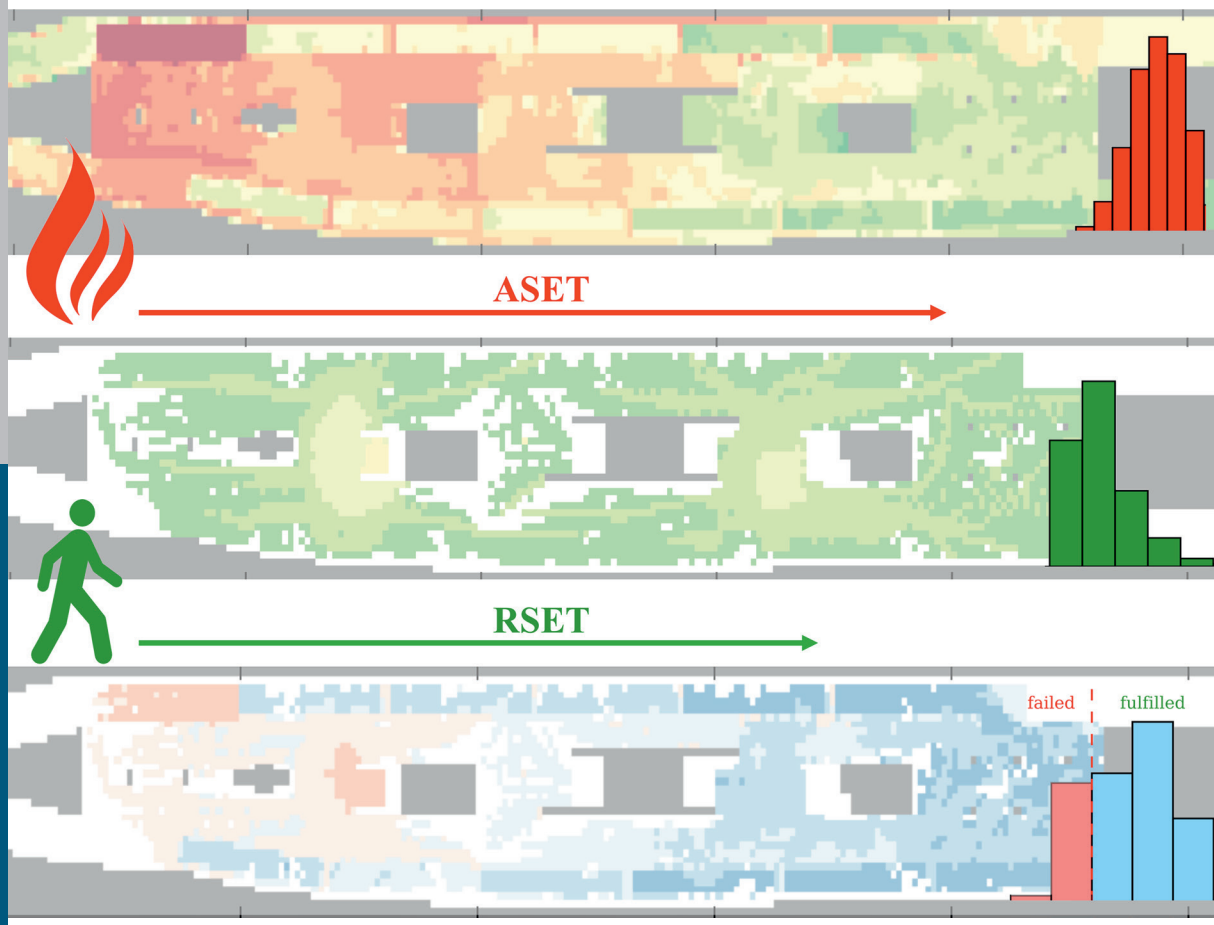

IAS
Band / Volume 34
ISBN 978-3-95806-254-2

JÜLICH
FORSCHUNGSZENTRUM

BERGISCHE
UNIVERSITÄT
WUPPERTAL

Multivariate Methods for Life Safety Analysis in Case of Fire

Fakultät für Architektur und Bauingenieurwesen

Dissertation zur Erlangung eines Doktorgrades
(Dr.-Ing.)

vorgelegt von

Benjamin Schröder
aus Jena

Wuppertal 2016

Die Dissertation kann wie folgt zitiert werden:

urn:nbn:de:hbz:468-20170911-140837-8
[http://nbn-resolving.de/urn/resolver.pl?urn=urn%3Anbn%3Ade%3Ahbz%3A468-20170911-140837-8]

Forschungszentrum Jülich GmbH
Institute for Advanced Simulation (IAS)
Jülich Supercomputing Centre (JSC)

Multivariate Methods for Life Safety Analysis in Case of Fire

Benjamin Schröder

Schriften des Forschungszentrums Jülich
IAS Series Band 34

ISSN 1868-8489 ISBN 978-3-95806-254-2

Bibliographic information published by the Deutsche Nationalbibliothek.
Die Deutsche Nationalbibliothek lists this publication in the Deutsche
ationalbibliografie; detailed bibliographic data are available in the Internet
at http://dnb.d-nb.de.

Herausgeber und Vertrieb: Forschungszentrum Jülich GmbH
Zentralbibliothek, Verlag
52425 Jülich
Tel.: +49 2461 61-5368
Fax: +49 2461 61-6103
E-Mail: zb-publikation@fz-juelich.de
www.fz-juelich.de/zb

Umschlaggestaltung: Jülich Supercomputing Centre, Forschungszentrum Jülich GmbH

Druck: Grafische Medien, Forschungszentrum Jülich GmbH

Schriften des Forschungszentrums Jülich
IAS Series Volume 34

D 468 (Diss., Wuppertal, Univ., 2016)

ISSN 1868-8489
ISBN 978-3-95806-254-2

Persistent Identifier: urn:nbn:de:0001-2017081810

The complete volume is freely available on the Internet on the Jülicher Open Access Server (JuSER) at
www.fz-juelich.de/zb/openaccess

Nomenclature

Abbreviations	Description
ASCII	American Standard Code for Information Interchange
BMBF	Bundesministerium für Bildung und Forschung
BOStrab	Verordnung über den Bau und Betrieb der Straßenbahnen
BR F	Baureihe F
BR H	Baureihe H
BVG	Berliner Verkehrsbetriebe
DNS	Direct numerical simulation
DoE	Design of experiment
EMD	Earth mover's distance
ENT	Emergent norm theory
FDS	Fire Dynamics Simulator
FDSgeogen	Framework for automated processing of FDS simulations
FEC	Fractional effective concentration
FED	Fractional effective dose
FIC	Fractional irritant concentration
FSE	Fire safety engineering
JPSfire	Pre-processing interface between FDS and JuPedSim
JuPedSim	Jülich Pedestrian Simulator
LES	Large eddy simulation
LHS	Latin hypercube sampling
MBO	Musterbauordnung
MPI	Message Parsing Interface
NIST	National Institute of Standards and Technology
OpenMP	Open Multi-Processing
PADM	Protective active decision model
PA System	Personal announcement system
PBefG	Personenbeförderungsgesetz
RABT	Richtlinien für die Ausstattung und den Betrieb von Straßentunneln
SHE	Smoke and heat extraction system
TRStrab	Technische Regeln für Straßenbahnen – Brandschutz in unterirdischen Betriebsanlagen
XML	Extensible Markup Language

Notations	Description	Units
$ASET$	Available safe egress time	min
c	Consequences	
c_p	Specific heat	$\mathrm{kJ\,kg^{-1}\,K^{-1}}$
d	Diameter, thickness	m
$d(i,j)$	Euclidean distance between observations i and j	
D	Occupant density	$\mathrm{m^{-2}}$
E	Extinction coefficient	$\mathrm{m^{-1}}$
ΔH_c	Heat of combustion	$\mathrm{kJ\,kg^{-1}}$
HRR	Heat release rate	kW
$HRRPUA$	Heat release rate per unit area	$\mathrm{kW\,m^{-2}}$
k	Dimensionality	
λ	Thermal conductivity	$\mathrm{W\,m^{-1}\,K^{-1}}$
l	Length	m
μ	Mean	
n	Number of samples	
N	Number of occupants	
ρ	Density	$\mathrm{kg\,m^{-3}}$
$RSET$	Required safe egress time	min
RTI	Response time index	$\mathrm{m^{1/2}s^{1/2}}$
σ	Standard deviation	
σ_i	Volume concentration of gas i	ppm
T	Temperature	°C
t	Time	s, min
v	Velocity	$\mathrm{ms^{-1}}$
$\dot{V}$	Volume flow	$\mathrm{m^3\,h^{-1}}$
γ	Yield	$\mathrm{g\,g^{-1}}$

Chemical Notations	Description
CO_2	Carbon dioxide
CO	Carbon monoxide
COHb	Carboxyhemoglobin
HCN	Hydrogen cyanide
HCl	Hydrogen chloride
O_2	Oxygen
PVC	Polyvinyl chloride
PUR	Polyurethane

Abstract

The assessment of life safety in case of a building fire is based on the comparison of the available safe egress time ($ASET$) and the required safe egress time ($RSET$). With regards to simulation experiments, this straightforward approach is accompanied by uncertainties including the underlying models, the specification of inputs, and the analysis of outputs.

Concerning the two latter aspects, this thesis introduces methodological extensions in order to conduct $ASET$-$RSET$ analyses in a multivariate fashion. For the specification of inputs, the multitude of possible scenarios is represented with the help of systematic sampling techniques. Uncertainties in terms of analysis are tackled with multi-criterial maps rendering both $ASET$ and $RSET$ in spacious environments. The subtraction of both maps is used to determine a measure of consequences.

These methods are applied to a multi-level underground station which is investigated with numerical simulations based on the formation of two subsystems, namely *Fire* and *Evacuation*. The analysis incorporates an ensemble of $8,640$ combined fire scenarios and evacuation scenarios. Throughout the entire design space, more than 95 % of the scenario combinations account for less than half of the maximal observed consequences. This analysis is refined by agglomerative clustering in order to group all observations hierarchically. It becomes evident that the lowest margins of consequences are represented by two clusters covering approximately 75 % of all observations. The investigation of the parametric relations of all clusters allows for the systematic identification of the determining characteristics of fire and evacuation scenarios. In addition to the consequence measure derived from $ASET$-$RSET$, fractional effective doses (FED) are calculated to supplement the analysis. Within the clusters, the number of occupants exceeding common FED thresholds applicable to incapacitation corresponds to the introduced $ASET$-$RSET$ measure. However, throughout the entire design space, this correspondence is not clear and needs further investigation.

Kurzfassung

Die Bewertung der Personensicherheit bei Bränden in Gebäuden stützt sich auf den Vergleich der verfügbaren Räumungszeit (*ASET*) mit der erforderlichen Räumungszeit (*RSET*). Im Hinblick auf Simulationsexperimente ist dieser nachvollziehbare Ansatz mit Unsicherheiten behaftet. Diese beziehen sich unter anderem auf die verwendeten Modelle, die Festlegung von Eingaben, aber auch die Auswertung der Ausgaben.

Zur Berücksichtigung der beiden letztgenannten Aspekte führt die vorliegende Arbeit eine methodische Erweiterung des *ASET-RSET* Ansatzes ein, die sich an den Prinzipien der multivariaten Analyse orientiert. Zur Repräsentation der Vielzahl denkbarer Szenarien werden die Modelleingaben mit systematischen Stichprobenverfahren spezifiziert. Um Unsicherheiten bei der Auswertung in ausgedehnten Räumen zu begegnen, erfolgt die Darstellung von *ASET* und *RSET* auf multikriteriellen Karten. Die Differenzbildung beider Karten ermöglicht die Bestimmung eines Maßes für die Konsequenzen.

Die Methoden werden auf eine mehrgeschossige, unterirdische Personenverkehrsanlage angewandt. Hierzu werden zwei Subsysteme *Brand* und *Räumung* gebildet und mit numerischen Simulationen untersucht. Die Analyse basiert auf einem Ensemble mit 8 640 kombinierten Brand- und Räumungsszenarien. Ca. 95 % aller Szenarien führen zu Konsequenzen, die geringer als die Hälfte der maximal erwarteten Konsequenzen sind. Diese Auswertung wird durch eine Cluster-Analyse verfeinert, um alle Beobachtungen hierarchisch zu gruppieren. Es stellt sich heraus, dass die niedrigsten Konsequenzen durch zwei Cluster repräsentiert werden, die ca. 75 % aller Beobachtungen beinhalten. Die parametrischen Ursprünge der Cluster erlauben Rückschlüsse auf die bestimmenden Charakteristika der Brand- und Räumungsszenarien. Für die zusätzliche Beschreibung der Cluster wurde neben den mittels *ASET-RSET* ermittelten Konsequenzen das fractional effective dose (*FED*) Konzept angewandt. Innerhalb der Cluster ist ein Zusammenhang zwischen den Personenzahlen,

die gängige *FED* Grenzwerte überschreiten und dem *ASET-RSET* Konsequenzmaß feststellbar. Mit Blick auf den gesamten Ergebnisraum ist jedoch kein eindeutiger Zusammenhang erkennbar, woraus sich weiterer Untersuchungsbedarf ergibt.

Contents

List of Figures

Chapter 1

Introduction

1.1 Motivation

Urbanisation and mobility are two of the so-called mega trends of the 21st century. By 2050, the world's population is expected to increase to 9.3 billion people, whereas 6.3 billion of them will live in cities [United Nations, 2012]. Contrary to popular belief, these trends do not solely impact emerging nations overseas. In Germany, for instance, almost ten million out of eighty million people have left rural areas and have moved to cities since 1960 [World Bank, 2015].

For the most means of urban transportation, these and other circumstances have resulted in increasing traffic volumes throughout the past years [Stadt Berlin, 2014]. Moreover, mobility has been identified as one of the key factors for liveable urban areas in the future. In terms of capacity and environmental protection, individual traffic will not be able to cope with these developments. Thus, the importance of public and, in particular, rail-mounted transportation systems will increase. For reasons of urban planning and system optimisation, these systems are oftentimes engineered underground.

Given these facts, infrastructures will either have to be built entirely new or they will have to be extended. The latter case especially poses big challenges to the stakeholders of an underground transportation system. In Germany, most of the underground systems were designed during the decades after World War II, when requirements as well as available technologies were completely different. Apparently, ageing infrastructures do not only affect operational aspects but also the system's resistance against emergencies. In this respect, a fire in the underground is a notable incident.

Meanwhile, the state of the art in fire safety has moved forward. On the one hand, legal requirements and technical specifications regarding fire safety have continuously

been advanced during the last decades. On the other hand, designers increasingly utilise computer simulations in order to predict the system's resistance against fire incidents. These historic developments imply a diffuse discrepancy between the performance of newly built infrastructures and the ones which have been in service since decades.

In 2014, the German Federal Ministry of Education and Research (*BMBF*) acknowledged these challenges and funded the ORPHEUS project. On the basis of experiments and simulations, the primary project objective is to optimise concepts for smoke control and evacuation – especially for existing infrastructures [ORPHEUS, 2015]. Within work package WP 2.4, the central objective of this thesis is to systematically evaluate the resilience of a complex escape route system in case of fire. In this respect, resilience is understood as a system's capability to resist against a certain disturbance. For this purpose, the existing station *Osloer Straße* located in Berlin will serve as case study.

1.2 Underground Transportation Systems

Underground transportation is the backbone of the mobility of metropolitan areas. The first system was built in London in 1863. At this time, the carriages were powered by steam engines. By the end of the 1890s, electrification advanced the breakthrough of this transportation concept resulting in an increasing number of systems being set up, e.g. in Budapest, Berlin, and Hamburg [Fiedler, 2005].

A multitude of different classifications and terminologies has formed worldwide. According to [URP, 2011], "Urban Guided Transport Systems" are distinguished into metros, trams, and light rails. In this respect, metros are "operated on their own right of way and segregated from general road and pedestrian traffic". In turn, trams "share their right of way with general road and/or pedestrian traffic and are therefore embedded in their relevant national road traffic legislation". Finally, light rails are partly "not segregated from general road and pedestrian traffic". Beside these quasi-isolated systems, conventional rails are operated on an interconnected system and involve commuter and intercity services. The latter also are and will increasingly be operated underground in Germany, e.g. in Leipzig, Munich, or Stuttgart.

Having said that, this study generally aims at the challenges of transportation systems built underground. Hence, in this thesis, the latter will be referred to as underground systems. In this respect, the focus will be exclusively set on the stations.

1.2.1 Challenges

Underground stations pose a variety of challenging system features to the fire safety design. Contrary to the basic idea of prescriptive building design, it is oftentimes not possible to ensure an appropriate compartmentalisation. Hence, the most fundamental issue is that buoyancy-driven smoke spread may potentially affect the ascending means of escape, which are oftentimes the only option for clearing a station. Depending on the scenario, a fire can yield high orders of heat release and remarkable mass flows of fire effluents. These problems may be aggravated by comparatively low ceiling heights and enclosure volumes. Narrow spaces also account to limited capabilities regarding mechanical or natural ventilation. The latter case may additionally be influenced by the specific climatic conditions and resulting airflows in the underground.

By means of operation, underground transportation systems are inherently supposed to handle large crowds of diverse sizes and compositions. Furthermore, the evacuation of occupants towards the surface is a complex sequence of events, which heavily depends on a multitude of physiological and psychological factors. Moreover, underground stations do usually not represent isolated systems. In many cases, they are connected or they even occupy further building uses, such as assembly, retail, or office.

1.2.2 Major Fire Incidents

Over the course of the past decades, numerous fire incidents have occurred in underground stations. A very comprehensive collection of incidents is presented in the Handbook of Tunnel Fire Safety [Carvel and Marlair, 2005]. On the following pages, four major incidents will chronologically be described in more detail. The characteristics of the single events widely differ in terms of cause of fire, outcome, behavioural aspects, intervention and so forth. However, the examination of the particular incidents may be valuable for a more sensible understanding of potential interactions within the entire system.

London 1987 In the evening of November 18th, 1987, a fire incident occurred in *King's Cross St. Pancras* station in London, United Kingdom. The fire resulted in 31 fatalities and 100 injured occupants. The investigation of the incident was carried out by C. Fennell, whose report was submitted to the Department of Transport in 1988 [Fennell, 1988]. The following information are excerpts of this source.

King's Cross St. Pancras station is a multi-modal station unifying both overground and underground services. The fire was most likely ignited by a match and developed – fed by grease and fibrous materials – underneath a wooden escalator. 15 minutes after ignition, the fire flashed over, i.e. rapidly developed to an extensive fire. Due to the slope of the escalator, a kind of jet flame spread into the ticket hall. The subsequent smoke and heat spread killed most of the present occupants. This effect resulted in the loss of the escape routes for occupants still being in lower levels. These were evacuated with the help of a train later on. The fire was extinguished five hours after ignition. Besides the material's lacking fire performance, the report moreover revealed severe drawbacks related to the staff's training, response, communication, and supervision.

The behavioural aspects leading to the outcome have been considered by I. Donald and D. Canter in 1990 [Donald and Canter, 1990]. The following insights are derived from this work. It has been found that social roles had a major influence. In this respect, the authors distinguish between the public, the underground staff, and the police officers. The inquiry revealed that instructions given by the staff mostly were ignored by the public. On the other hand, they immediately followed instructions, that were given by the police officers. To a greater or lesser extent, these role conflicts reappeared when surveying underground passengers in the aftermath. Beside authoritarian instructions, the report shows that only multiple and independent evacuation cues will result in appropriate actions by the occupants. One very impressive example of this mechanism is the statement of a male occupant who requested information from a police officer and already felt heat: "Whilst in this passage I picked up one of the wall phones intending to phone my Wife. I put a lOp piece into the slot but left the phone because the (smoke) became thicker" [Donald and Canter, 1990]. This example clearly shows, that even two evacuation cues, e.g. smoke and heat, did not result in the behaviour expected. After having left the ticket hall, others proceeded to adjacent shopping, coffee, or toilet areas inside the station. The authors concluded that not only the perception of cues is important but also the process of interpreting and cross-checking them.

The impact of spatial knowledge is another very interesting factor that has been examined in more detail. Given the instruction to clear the station via adjacent escalators – right towards the ticket hall – the authors conclude that the police officers were not aware about the station's layout. In this respect, the inquiry figured out that the spatial meaning "of clearing the station" was not consistently interpreted

among the occupants. The authors also worked out that both staff and police officers narrowed their focuses of attention more and more to the escalator over the course of time. Consequently, the consideration of the occurrences in the surrounding decreased.

Baku 1995 Until 2016, the incident in Baku, Azerbaijan has been the most severe underground fire. The following information are excerpts of the work by Hedefalk and Wahlstrom published in 1998 [Hedefalk and Wahlstrom, 1998]. There were 289 fatalities and 270 injured people. In the evening of October 28th, 1995, a train encountered an electrical malfunction just when entering the tunnel between the stations *Ulduz* and *Nariman Narimanov*. The train subsequently came to a stop within the tunnel, which instantly was filled by heat and toxic smoke. Since some of the pneumatic carriage doors did not open properly, passengers attempted to use the windows as emergency exits. However, the majority of fatalities was later found dead inside the carriages. Many of the evacuees, who were able to disembark the train, perished in the tunnel either effected by the fire or by electric shocks. The latter occurred due to the fact that evacuees reached for wall-mounted cables in order to be geared to the tunnel's walls. As the fire broke out in the penultimate carriage, the 200 m path towards *Ulduz* was blocked for most of the evacuees. Another namable fact is that the tunnel was equipped with a ventilation system. The activation of the latter – approximately 15 minutes after ignition – caused a flow reversal worsening the conditions in the areas which were less affected until then. A number of 40 fatalities was later found along the tunnel. It is also notable that the responding fire brigade was not able to start efficient firefighting operations, since they were not equipped with breathing apparatus.

Berlin 2000 Although there were no fatalities, the fire incident at the *Deutsche Oper* station in Berlin, Germany is noteworthy. Until this time the station was only equipped with one exit towards the surface. During the major event *Love Parade* on July 8th, 2000, the station was densely crowded with visitors. At the same time, a carriage caught fire right when arriving at the station. The ignition was caused by electrical problems resulting in an emergency breaking, which again caused an electric arc. The incident has never been investigated systematically. However, an operational report, published by the Berlin fire brigade a few weeks later, allows for some informed conclusions [Kirchner, 2000]; this is the source of the following information. When the fire brigade arrived at the scene, approximately 350 occupants were trapped

underground. The carriage on fire was located at the platform edge towards the only exit; resulting in untenable conditions within the two adjacent staircases and the ticket hall. Fortunately, the remaining areas of the platform were relatively smoke-free. Again, the behavioural aspects of this event are concerning. Based on the report of single fire fighters, there was a certain concern among the occupants. However, others interpreted the incident as a big "happening". In addition, a number of passengers had to be prompted to disembark the carriages. With increasing smoke spread, the fire brigade subsequently decided to evacuate the crowd via the tunnel system. All in all, a number of 26 persons were taken to hospitals. With respect to the time sequence of the incident, the report states that the last occupants were evacuated safely after approximately 45 minutes. The fire was under control after one and a half hours. It is notable that the fire department utilised two large scale ventilation units placed on outlet shafts at the adjacent tunnels. However, the laborious setup of the latter allowed for an activation right after the station was evacuated. Another remarkable factor is the presence of background airflows in the tunnel system. Since crossing underground services in the neighbouring station were stopped very late, the fire brigade reported about batch-wise smoke spread during the tunnel evacuation.

In addition to that, there is video material available capturing approximately 20 minutes from ignition until the time, when the fire brigade guided occupants out of the station through the tunnel system. In terms of various behavioural aspects, such as risk perception, delayed response, or group affiliation, these recordings are valuable for getting an understanding of human behaviour in fire.

Daegu 2003 On February 15th, 2003, a fire incident with 192 fatalities occurred in the *Jungangno* station in Daegu, South Korea. In the aftermath, Jeon and Hong conducted an interview and questionnaire study with 96 recovered survivors. Six years after the incident, they published a journal paper revealing numbers and factors in terms of behavioural aspects [Jeon and Hong, 2009]. In this respect, it is certainly the most comprehensive documentation of an underground fire incident. The following information are sourced from the aforementioned study.

Jungangno station is a three-level underground structure consisting of one platform level, one ticket hall, and one shopping mall. The fire was maliciously set with flammable liquids inside a train. Five minutes after ignition, the opposite train arrived in the station. The fire immediately spread to the latter resulting in extensive smoke and heat release. It has been estimated that approximately 640 persons were inside the station or the trains as the fire started. In terms of familiarity, the study revealed

that almost half of the subjects used the station more than once a day. Worrying facts are the findings related to the individual response of the occupants. After each of the subjects became aware of the fire, 49 % simply "waited". Another 19 % attempted to "contact someone outside". On average, the subjects who escaped instantly made their decision based on the observation of smoke (42 %) or due to hearing the corresponding announcement (33 %). However, the authors identified a relation between the distance from the fire origin and the susceptibility of the different evacuation cues. For instance, 83 % of the passengers inside the carriage furthest away from the fire, escaped after hearing the announcement for three times. Beside the response behaviour, the authors also investigated the route choice of the subjects. The platform level of the *Jungangno* station is equipped with four exits towards the surface. It was found that approximately 65 % of the occupants used the two exits opposite to the burning carriages. Only 10 % chose the exits nearby the latter. Another 23 % could not provide certain information. Further on, it has been worked out that more than 60 % of the subjects followed an evacuation route they had planned in advance. Only 25 % of this group were able to complete their planned passage. In contrast, the remaining 75 % deviated from their initial route. The authors mainly identified three different reasons for that: movement in a dense crowd, poor visibility conditions, and ineffective escape route lighting systems. In addition to that, half of the subjects repeatedly traversed particular passages due to smoke obscuration. In terms of the structural design, it was found that massive pillars placed on the platform level severely impaired the movement and orientation capabilities of the occupants. The fire was declared out almost four hours after ignition.

Lessons Learned The numbers and facts outlined above give an impressive overview of the complex interactions between all system elements in an underground station. Major elements are, e.g. the occupants, the fire, the built environment, as well as aspects regarding organisation and intervention. It has clearly been shown that the system is not solely driven by physics but also by human factors.

In terms of fire scenarios, it turned out that fully developed fires are possible in principle. Fires in areas other than the platforms may also severely impact the system's performance. Moreover, the presence of smoke yields a variety of interactions with the evacuation of occupants. Notable aspects are, e.g. route choice, walking speed reduction, or incapacitation. Furthermore, the occurring smoke dynamics may be influenced by climatic effects induced either naturally or technically. With regards to occupant behaviour, the incident studies reveal that occupants do not necessarily

respond adequately – especially if no or ambiguous information is provided. These characteristics are distinctively influenced by any action undertaken by staff or authorities.

1.2.3 Case Study: Osloer Straße

History The underground station *Osloer Straße* located in the district Wedding in central Berlin is operated by the Berlin transportation service (*BVG*). It connects the U8 service from *Wittenau* to *Hermannstraße* with the U9 service starting at *Rathaus Steglitz* and terminating at *Osloer Straße*. Construction works started at the beginning of 1973 and were completed in 1977. In line with the extension of the U8 service in 1987, the station became a through station. As further extension plans have meanwhile been abandoned, the station will remain the northbound terminal stop of the U9 service [Schomacker, 2009].

Operation Based on the last major traffic report, *Osloer Straße* is used by 90,000 passengers per day on average. This number is composed of approximately 55,000 customers using the U8 service and another 35,000 using the U9 service [Stadt Berlin, 2014].

The station is served by large structure gauge vehicles providing a variety of different train generations. The two main generations are "Baureihe F" and "Baureihe H", which are referred to as *BR F* and *BR H* from now on. Despite different ratios between seats and stances, both vehicles can carry approximately 750 passengers [BVG, 2007]. Moreover, *BR F* can be operated as two-car, four-car, and six-car trainset, whereas *BR H* represents an inseparable trainset.

Depending on weekday and daytime, the operation intervals are adjusted accordingly. During the peak hour on work days, the trains are operating in five minute intervals. The early and late hours are served with a ten minute interval.

Building Layout In principle, the station can be divided into four floors ordered from lowest to highest elevation above sea level: platform U8 (27 m), platform U9 (31 m), concourse level (35 m) and surface (40 m). Each platform level is approximately 110 m long and 20 m wide and has a slightly curved shape. The ceiling heights above the platform range from 2.85 m to 3.0 m, while notable areas are obstructed by binding beams and display panels. Moreover, the stair lintels are equipped with static smoke curtains, which have a height of approximately 0.45 m. The concourse level comprises traffic and shopping areas and extends to approximately 3,000 m^2.

Finally, the surface area above the station consists of a large crossroad as well as a tramway and several bus stops.

Moreover, ten staircases access the particular areas of the station. Starting from the U8 level, two staircases directly lead towards the concourse level, whereas a double staircase leads to the U9 level. The U9 level itself is connected to the concourse level by two further staircases. Finally, there are five staircases that connect the concourse level with the surface. The layout of the station as well as the main elements of the escape route system are schematically illustrated in Figure 1.1.

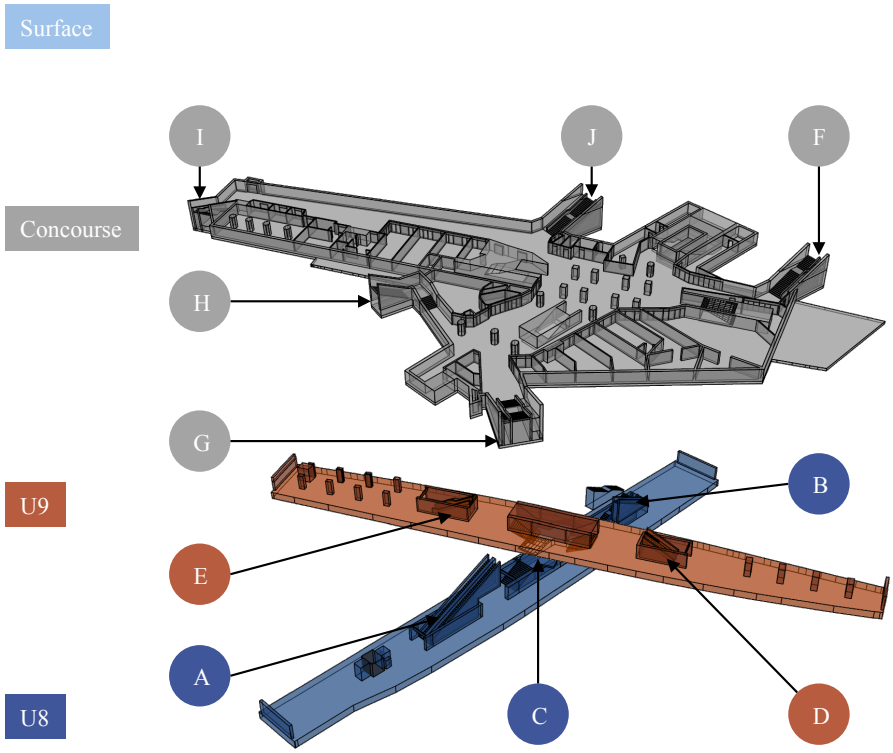

Figure 1.1: Schematic overview of the station.

Both the colour distinction and the nomination presented in Figure 1.1 are used throughout the entire thesis. The staircases are designed in three different ways: conventional stairs, escalators, or a combination of both. Table 1.1 provides an overview of the differently equipped staircases within the station.

Table 1.1: Overview of layout and types of staircases. The ways from origin to destination are assumed from underground to surface. U8 = U8 level, U9 = U9 level, CL = Concourse level, SU = Surface.

Name	Origin	Destination	Stair	Escalator
A	U8	CL	-	x
B	U8	U9	x	-
C	U8	CL	x	x
D	U9	CL	-	x
E	U9	CL	x	x
F	CL	SU	x	x
G	CL	SU	x	x
H	CL	SU	x	-
I	CL	SU	x	x
J	CL	SU	x	x

Technical Building Equipment All rooms that are not accessible by the public are monitored by a fire detection system. In addition to that, each shopping unit on the concourse level is equipped with smoke detectors as well. An occurring alarm is directly transmitted to the technical control centre of the *BVG*.

The shopping units inside the concourse level are equipped with a fire suppression system. The latter is a conventional sprinkler system consisting of 135 glass bulb sprinkler heads with a normal response rating. The system is designed to serve for 40 minutes.

A mechanical smoke and heat extraction system (*SHE*) is installed on the shopping areas in the concourse level. The system serves for both purposes: ventilation in normal service and smoke extraction in the event of fire.

The means of escape are marked with luminescent signs, which are mounted in close proximity to the floor levels. Moreover, emergency and information telephones are provided on the platforms. A personal announcement system (*PA*) paired with surveillance cameras can be utilised to initiate and monitor an evacuation.

1.3 State of the Art

1.3.1 Fire Safety Engineering

Design Methods In principle, fire safety engineering (*FSE*) can be based on the prescriptive or the performance-based design approach. The prescriptive design relies

on the straightforward fulfilment of tangible requirements that are postulated in relevant building codes or comparable specifications. In case of compliance, the proposed design then is "deemed to satisfy" the code's overall protection goals [Hurley and Rosenbaum, 2016, p. 1246]. Despite advantages like simplicity and confirmability, this procedure cannot be applied consistently in some cases, e.g. non-trivial building layouts or varying occupancies. Moreover, in particular situations, the prescriptive design may yield cost-intensive measures.

In these cases, it is possible to conduct the performance-based design approach, which is supposed to provide the answer if a system's resistance is greater than a particular influence. For this purpose, objectives are formulated and quantified by performance criteria. The latter are specified based upon the relevant engineering problem. In fact, this methodology allows for more individual and efficient design solutions. The performance-based design process is utilised within this thesis and is taken up in Chapter 2.

In principle, the performance-based approach is distinguished in deterministic or risk-based analyses. In the first case, "scenarios that are expected to occur with a frequency above a threshold value are analyzed to determine their consequences". In case of a risk-based analysis, "the consequences of each scenario are analyzed; however, these consequences are weighted by the probability of the event occurring" [Hurley and Rosenbaum, 2016]. Regarding the latter, a comprehensive review and application example on risk-based *FSE* has been conducted by Albrecht [Albrecht, 2012].

Finally, depending on the complexity, deterministic and risk-based *FSE* analyses commonly utilise different models for predicting both fire and evacuation processes. In this respect, models are considered as mathematical models.

Fire Modelling Fire modelling involves a diversity of scientific fields. The most relevant are thermodynamics, fluid mechanics, thermochemistry as well as heat and mass transfer. The consolidation of the latter in the form of control volumes and conservation laws allows for the mathematical formulation of different model approaches [Quintiere, 2006]. Based on the classification proposed in the German vfdb guideline, these formulations can be as follows: empirical approaches, zone models, or field models [vfdb, 2013].

Empirical approaches are commonly sourced from experiments, which have been designed regarding a specific scientific question. The gathered experimental data

has been used to derive correlations for partial phenomena, e.g. single enclosure temperatures, plume mass flows, or ceiling jet velocities.

Moreover, zone models and field models are based on the conservation of mass, momentum, and energy, whereas the degrees of abstraction are differing. Given a compartment fire, zone models assume a persistent formation of a cold gas layer and an overlying hot gas layer, while both zones are assigned with homogenous temperatures and densities. Moreover, the mass exchange between the two zones is solely assumed via the plume. Common software frameworks also provide the implementation of openings, vents, or the combination of multiple rectangular compartments.

Field models are characterised by the discretisation of the computational domain into a finite number of elements. For all elements, the governing differential equations of the above-mentioned conservation terms are approximated with certain discretisation schemes, e.g. finite differences. Due to the higher spatial resolution, field models provide more localised information about varying *FSE*-relevant quantities. In addition to that, filigree building components or additional boundary conditions can be incorporated in more detail. In turn, the computational demand is significantly higher compared to zone models.

Evacuation Modelling Evacuation processes incorporate the movement of pedestrians. According to Hoogendoorn, a comprehensive representation of this can be achieved by considering the strategic, tactical, and operational level of motion [Hoogendoorn et al., 2002]. With regards to pedestrians, the strategic level covers the question "which activities they like to perform" as well as "the order of these activities". The tactical level concerns "short-term decisions made by the pedestrians", e.g. route choice. Finally, the operational level "describes the actual walking behavior of pedestrians" [Schadschneider et al., 2009].

Given these fundamentals, the broad variety of available models can be classified based upon multiple characteristics. In terms of the representation of pedestrians, the differentiation in microscopic and macroscopic models has well established. Microscopic models consider pedestrians as agents with individual characteristics whereas macroscopic models assume pedestrians as compact streams with unique attributes such as velocities and densities. The movement of the assumed streams then is calculated according to hydraulic principles. Having said that, macroscopic models can usually be solved by hand calculation methods, while microscopic models require computer resources. In case of microscopic models, the computational domain can be

represented in different ways. In concrete terms, the movement patterns can either be calculated in continuous or discrete space.

Besides these physical aspects, the strategic and tactical levels especially imply a strong necessity of understanding behavioural aspects when modelling evacuation dynamics. The importance of that has been emphasised within the incident studies provided in Section 1.2.2. Similar thoughts are given by Purser, who found that – for a long time – the focus of evacuation modelling was merely set on the underlying physics [Purser, 2016b]. Henceforth, a more exclusive summary of human behaviour in fire is given in the following section.

1.3.2 Human Behaviour in Fire

The need for a consolidation of human factors and fire safety is more or less acknowledged. Since the 1970s, the research field of human behaviour in fire formed as a multi-disciplinary intersection between human scientists, natural scientists, and engineers. A comprehensive review about this branch and the related theories, models, studies, and subsequent engineering implications has been carried out by Kuligowski [Kuligowski, 2016]. If no additional references are given, the following contents and sources are derived from this work.

In general, human behaviour in fire is defined as "the study of human response, including people's awareness, beliefs, attitudes, motivations, decisions, behaviours, and coping strategies in exposure to fire and other similar emergencies in buildings, structures and transportation systems".

In terms of time, behavioural aspects doubtlessly affect both the pre-evacuation phase and the movement phase. As "the pre-evacuation period can be significantly longer than the movement period" in certain cases, an informed understanding of the underlying processes and their particular time demands is inevitable. The same applies to the question whether the movement phase may also be affected by behavioural aspects. These thoughts are taken up in Chapters 2, 3, and 5.

Theories and Models Over the course of the past decades, a number of theories were proposed, advanced, or rejected. This applies to early attempts to explain disasters by *Panic*, *Disaster Shock*, or *Group Mind*. The overwhelming majority of past incidents and subsequent inquiries clearly showed that occupants neither act irrationally or selfishly nor remain in certain states of shock. This statement may not be misinterpreted in the way that anxiety and fear do not play any role. Kuligowski states that "these are natural emotions in emergency situations". Another abandoned

behavioural theory in case of emergency is the assumption that individuals strictly form groups that can be described with one unified response without considering any diversities within the particular group.

The major theory currently accepted is the emergent norm theory (*ENT*). It covers the transition from a routine situation to an emergency, in the sense that certain "norms" no longer apply and new ones have to be agreed. Initially, individuals initiate communication in order to assess the new situation and to "seek coordinated action to find a solution to the shared problem". It should be noted that this communication is not necessarily verbal. Individuals can provide the process with both their "social stock of knowledge" and "conventional norms".

In order to apply and extend the *ENT*, Kuligowski utilises the protective active decision model (*PADM*) which was introduced by Lindell and Perry [Lindell and Perry, 2012]. It represents a versatile, state-of-the-art framework for the description of "information flow and decision-making [...] in response to natural and technological disasters". Initially, the pre-decisional phase of *PADM* consists of individual attributes such as social context, available information, and a number of others. The starting point of the decision process is the perception of cues, which must be noticed and understood by an individual. In terms of different perceptions, the *PADM* distinguishes three different types: threat, protective actions, and stakeholders. Having received an arbitrary set of cues, an evaluation sequence is triggered consisting of the following steps: risk identification, risk assessment, protective action search, protective action assessment, and protective action implementation. However, this sequence is bypassed by a loop that addresses the generation, communication, and assessment of additional information, which an individual deems as necessary before making a decision. The resulting sequence of (protective) actions can be summarised in so-called decomposition diagrams.

Another broad field of theories covers the understanding of group behaviour. Although the group mind theory has been rejected to describe egress dynamics holistically, the consideration of group behaviour is inevitable. In general, Kuligowski employs three different layers to distinguish group behaviour: affiliative behaviour, helping others, and convergence clusters.

The affiliative behaviour theory has been proposed by Sime [Sime, 1983] and states that single persons form groups in case of an emergency evacuation. The coherence of these groups strongly depends on their social relation. In other words: it is rather likely that a group of friends will separate than a family group will do. With regards to physical characteristics, Proulx found that groups will adapt, e.g. movement

speeds to the lowest possible within a particular group [Proulx, 1995]. Moreover, Kuligowski states additional studies that indicate an increasing relation between social familiarity within a group and delays in the response behaviour. With regards to helping others, Kuligowski relies on several incident studies that prove cooperation and mindfulness during emergency evacuations. She explains these observations with the redefinition of the situation within the *PADM*, which results in an implicit "weness" within a group. The third theory about group behaviour is the formation of convergence clusters. The latter occur in areas that are supposed to provide safety. This phenomenon has especially been observed when an evacuation was perceived as impossible.

11 Behavioural Facts Finally, Kuligowski summarises her statements and the contribution of Gwynne in the form of eleven behavioural facts in order to cover the present findings in the research field of human behaviour in fire [Kuligowski, 2016]. The latter are the basis of assumptions made for the model inputs in this study.

- Initially, people rather feel safe than panic in case of a fire emergency,
- Provision of information does not generally result in adequate actions by occupants,
- Occupants must identify a certain threat and personal risk before protective actions are undertaken,
- If evacuation cues are ambiguous or inconsistent, occupants attempt to gather further information,
- Before escaping, occupants take preparative actions, which delay the response,
- Occupants act rationally in case of a building fire,
- An occupant's decision making process is influenced by the surrounding population,
- Stress decreases occupant's capabilities of receiving and understanding cues,
- The response of occupants is influenced by any kind of familiarity (social, spatial and others),
- Roles of occupants prior to an emergency form the basis of their roles when redefining a particular situation,

- Heterogeneity among occupants affects behaviour.

1.3.3 Research Projects

The following paragraphs provide a brief review of the most recent research projects related to fire safety in underground systems.

TRANSFEU The TRANSFEU project was a trans-European project funded for three and a half years. It involved fire laboratories, standardisation organisations, railway producers, and operators across the continent. Although the project mainly focussed on rolling stock – especially for surface transportation – the achieved outcome also has a notable influence on the fire safety of underground transportation systems. Two work packages of the project considered the toxicity of fire effluents on both the laboratory and the numerical scale. In addition, existing *FSE* methodologies and tools were advanced and adapted according to the context of rolling stock. Many of the project's insights were directly introduced to the finalisation of the European standard EN 45545. This standard covers the fire safety design of underground vehicles, which are designed or refurbished nowadays. Further insights into the results and impact of the project are summarised in the final report [Heuze, 2012].

METRO The METRO project was funded by several public bodies in Sweden for a duration of three years. The project team involved a multitude of partners across public transport, fire services, research, academia, and defence. In particular, the project tasks were divided into seven work packages. For the scope of this thesis, the most relevant tasks were: design fires, evacuation, and smoke control. The centrepiece of the work related to design fires was the conduction of medium and full-scale fire tests. These provided valuable insights into tunnel fire dynamics, ignition sources, ventilation influences, and variable interior material performances. In addition to that, field studies on average fire loads resulting from luggage have been conducted. The insights into evacuation were derived from questionnaire studies and small and medium-scale experiments. Experimental data was gathered for scenarios, where an evacuation is initiated inside a smoke-filled tunnel. Further on, the effectivity of varying designs of escape routes and emergency exits was assessed. The smoke control work package mainly consisted of small-scale laboratory and numerical studies. The focus of those works was the performance of different smoke exhaustion systems in a single-exit station. Further reading can be found in the final project report [Ingason et al., 2012].

OrGaMIR and OrGaMIR Plus The OrGaMIR project and the following extension OrGaMIR Plus were German research projects funded by the *BMBF*. All in all, both projects lasted for nearly seven years involving partners across academia, information and micro technology, engineering, and public transport. The project was mainly focussed on terroristic attacks and potential releases of airborne toxins inside the underground system. In order to ensure adequate rescue operations in such cases, a prognosis system was developed. The latter aims at providing the rescue services with information about contaminated areas. In this conjunction, extensive and long-term field studies on climatic effects inside underground systems have been initiated. In order to ensure an appropriate control about the egress processes, the impact of human factors in terms of decision-making as well as aural and visual perception was investigated. More detailed information on both projects can be found in the final reports of the particular work packages [BMBF, 2015].

1.4 Methodology and Objectives

This thesis concerns the assessment of life safety in case of fire applied to a complex escape route system. The latter is represented by the underground station *Osloer Straße*. The basic methodology is to conduct a deterministic system analysis, which is inspired by the principles of multivariate analyses. Using the basic idea of *Systems Engineering*, two subsystems *Fire* and *Evacuation* are formed. Initially, both of them are assessed separately by specifying simulation ensembles, which are combined within the final stage of the analysis.

Based upon the scientific findings, problems, and challenges discussed throughout this chapter, the outlined methodology is applied in order to pursue the following objectives:

1. Automated setup, computation, and post-processing of simulation ensembles for both fire and evacuation simulations covering a multitude of possible scenarios,

2. Conceptual and technical implementation of interfaces between fire simulation data and *JuPedSim*,

3. Data-driven implementation of underground climate for the purpose of fire simulation,

4. Investigation of impact on fire scenarios induced by underground climate,

5. Generation of variable occupant populations accounting for heterogeneity, temporal dynamics and multiple building uses,

6. Extension of the *ASET-RSET* concept by spatiotemporal and multi-criterial distributions,

7. Identification of scenario clusters out of all combined fire and occupant scenarios based on the similarity of consequences,

8. Enrichment analysis regarding the main determinants of the scenario clusters,

9. Provision of a clustered, deterministic data pool for further work in the ORPHEUS project. The data is supposed to serve as basis for a subsequent risk-based analysis, which will be conducted according to the methodology presented in [Berchtold et al., 2016].

1.5 Thesis Outline

This thesis is organised in seven chapters. Chapter 1 already addressed underground systems in general, major fire incidents, as well as the presentation of the station *Osloer Straße*, which will serve as case study. Moreover, the current state of the art regarding fire safety engineering, human behaviour in fire and past research projects was reviewed. On this basis, the methodology and objectives of the thesis were formulated.

Chapter 2 sets up the methodological frame of this study. For this purpose, a system formation is conducted, to which the performance-based design process is applied. In this respect, the main problem resolution of the upcoming analysis is represented by comparing the available safe egress time ($ASET$) and the required safe egress time ($RSET$). In the next instance, scenarios are introduced in order to supply the system with inputs. The resulting complexity requires systematic methods for designing and analysing simulation experiments, which are finally introduced.

Chapter 3 provides information about all conducted modelling works, which were necessary to achieve the objectives of this thesis. In concrete terms, the consideration of climatic conditions in fire simulations as well as the implementation of interfaces between fire and evacuation simulations are presented.

Chapter 4 covers the design, computation, and analysis of the fire simulation ensemble. For this purpose, the specified parameter variations are presented. Within

the analysis, an advanced workflow for determining *ASET* is introduced. The latter is than incorporated into a preliminary correlation analysis.

Chapter 5 addresses the evacuation simulation ensemble. Within the design of experiment, all relevant parameters are discussed. In particular, a new method for generating occupant scenarios is presented. Finally, a preliminary analysis applied to a reference occupant scenario ensemble provides major insights into the expected pedestrian dynamics.

Chapter 6 tackles the life safety analysis and unifies the subsystems assessed in the two preceding chapters. In this respect, a combined simulation ensemble is set up. The subsequent analysis utilises an agglomerative clustering approach, which provides a consequence-based ranking of the particular combinations of fire and occupant scenarios. The identified clusters are then analysed with regards to the expectable consequences.

Chapter 7 finally provides concluding remarks upon the completion of the study. This covers the major conclusions as well as the outlook for future research.

Chapter 2

Methodology

In this chapter, the methodological framework of this study is set up and conjunct with the case study *Osloer Straße*. In order to provide the basis for the system definition, a brief review of *Quality* and *Systems Engineering* is presented initially. After that, the overall system, its underlying subsystems, and their elements are defined.

Once the system is set up, the process steps of the performance-based design approach are presented and – as appropriate for the scope of this thesis – slightly modified or refined respectively. The project scope addresses the system's boundaries as well as the most relevant stakeholders. In the next step, safety goals of the latter are used in order to derive more concrete objectives. In this respect, the engineering time line model unifying both *ASET* and *RSET* is introduced. Moreover, the necessary performance criteria are discussed. Once this fundament is set up, scenarios as well as their classification are introduced in general and then conjunct with the subsystems *Fire* and *Evacuation*. The related methodological and technical challenges are identified for both the engineering time line model and the scenario framework. Finally, the broad topic *Design and Analysis of Simulation Experiments* is propounded in order to cope with the identified challenges.

2.1 System Formation

In the first instance and secluded from any *FSE* context, it may be helpful to go one step back and have a more generalised view on methods of solving complex problems. The following considerations are provided since both methods and vocabulary in *FSE* are occasionally blurred in everyday usage. In addition, guidelines and standards are rather focussed on the process view than on the system view. In order to profit from superordinate and globally acknowledged guidance on engineering tasks, the basic

ideas of *Quality* and *Systems Engineering* will initially be reconsidered. Both terms are closely linked to each other and provide an appropriate and holistic basis for solving complex engineering problems.

Quality and Systems Engineering *Quality* is defined as the "degree to which a set of inherent characteristics of an object fulfils requirements" [ISO 9000, 2015]. Having said that, assuring quality of complex systems is the ultimate objective of *Systems Engineering*. This task basically consists of the subtasks problem definition, problem resolution, and finally the implementation of the solution. A comprehensive review of (generic) *Systems Engineering* and its application for complex tasks is provided by Winzer [Winzer, 2013]. It is moreover characterised by a number of basic principles e.g. that everything generally has system character. Having said that, every system can be described and modelled and thus be combined to more complex systems. Another principle is the decomposition of problems. It is based on the assumption that the solution of a subproblem contributes to the solution of the overall problem. In other works, this approach is also referred to as "divide and conquer strategy" [Mahajan, 2014]. The major challenge of this principle is the identification, arrangement and – where necessary – the minimisation of relations. Moreover, it is possible to utilise different views of the system, e.g. on the basis of components, processes, requirements, or functions.

Setting up the System Since this thesis will not consider concrete design tasks, the *Systems Engineering* term may probably be slightly inappropriate. However, the concept provides a very good methodological and semantic fundament for the systematic evaluation of a fixed, existing design too.

According to the principles stated above, the system definition presented schematically in Figure 2.1 has been set up. In principle, three levels are distinguished: system, subsystems, and elements. Beginning at the top, the superordinate system has been chosen as *Fire Incident during Operation*. This system is supplied by inputs, i.e. scenarios and the system outputs are incorporated into the life safety analysis. Hence, other classical *FSE* tasks, e.g. proofing structural integrity in case of fire are excluded in this study. On the subjacent level, the superordinate system contains the subsystems *Fire* and *Evacuation*. Within its particular boundaries, each subsystem comprises a variety of different elements, which can have different relations to each other. As already stated, systems and subsystems can receive inputs and yield certain outputs. The fact that these are solely exchanged on the system level and subsystem

level is an important convention. Moreover, the system boundaries are defined in terms of space, time, as well as the process view. The detailed specification of these boundaries will be taken up in the following section.

Throughout this chapter, the presented system will successively be updated with all relevant information and assumptions. In the frame of this thesis, the subsequent transformation from the system to the model level is realised within the subsystems. Concretely, numerical models will be applied for the description of both fire and evacuation dynamics. According to [Winzer, 2013, p. 71], both can thus be classified as prognosis models.

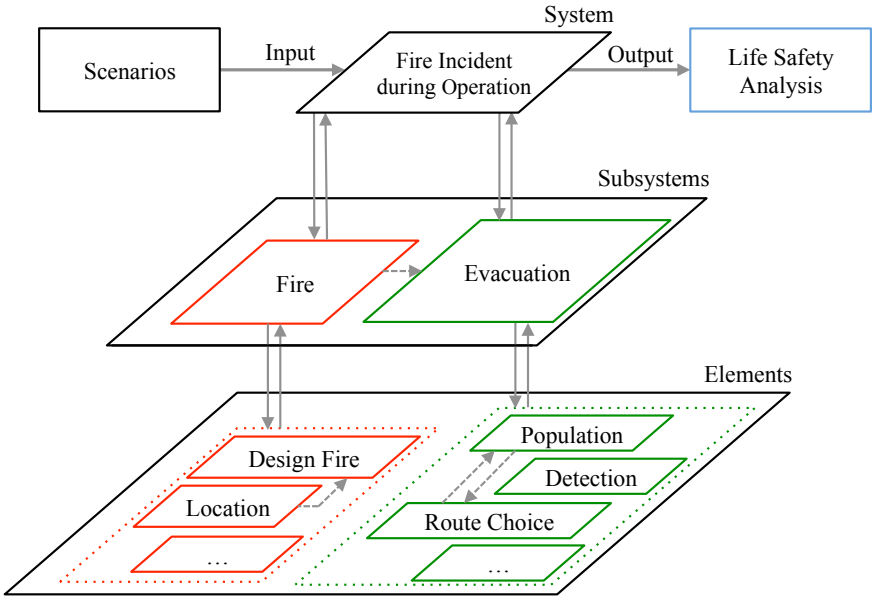

Figure 2.1: Schematic system definition for life safety analysis in case of fire. Based on [Winzer, 2013, p. 69].

2.2 Performance-based Design Process

A general definition of the system to be analysed is now prepared. Henceforth, the system can be unfold to a process in order to focus on the methodological frame. The so-called performance-based design process is supposed to transfer the ideas presented above to the context of *FSE*. It has been incorporated in various standards, guidelines, and handbooks all over the world during the past decades [vfdb, 2013; DIN 18009-1,

2015]. Above all, the basic task has always remained the same: a system is checked against the fundamental question if an arbitrary exposure is lower than the system's resistance. In some cases, the sequences and terminologies slightly differ from each other. Thus, for demonstration purposes, the design process presented in [Hurley and Rosenbaum, 2016] is utilised for the following statements.

In order to implement a performance-based analysis, a whole sequence of definitions and tasks has to be carried out. First of all, the *project scope* needs to be defined. It describes the determination of the system boundaries. In addition to that, all applicable stakeholders and their particular requirements are listed. The subsequent process step is the definition of *goals*, which are intended to be a qualitative description of the desired system performance in case of fire. Depending on the legal framework, this process step represents a direct interface to applicable building codes, which often postulate goals as for instance in Germany [MBO, 2012, § 14]. In the following step, the defined goals are substantiated in terms of *objectives*. This covers the identification of appropriate quantities that allow for a quantification of the system's performance. Having said that, these quantities are evaluated against certain thresholds, henceforth called *performance criteria*. The two following process steps comprise the development of both *scenarios* and so-called *trial designs*. Subsequently, the latter are evaluated on the basis of the agreements stated in the first four steps of this process.

In principle, this process has now reached a decision box consisting of the question if a certain design is compliant with the employed performance criteria. If yes, the trial design can be selected as final design and can be documented respectively. If not, the designer has to adjust either the objectives or the trial designs. In the context of this thesis, the latter case is only of ancillary interest. This also applies to the consideration of multiple trial design as an existing design is exclusively evaluated. A corresponding process modification including the relevant section references is presented in Figure 2.2.

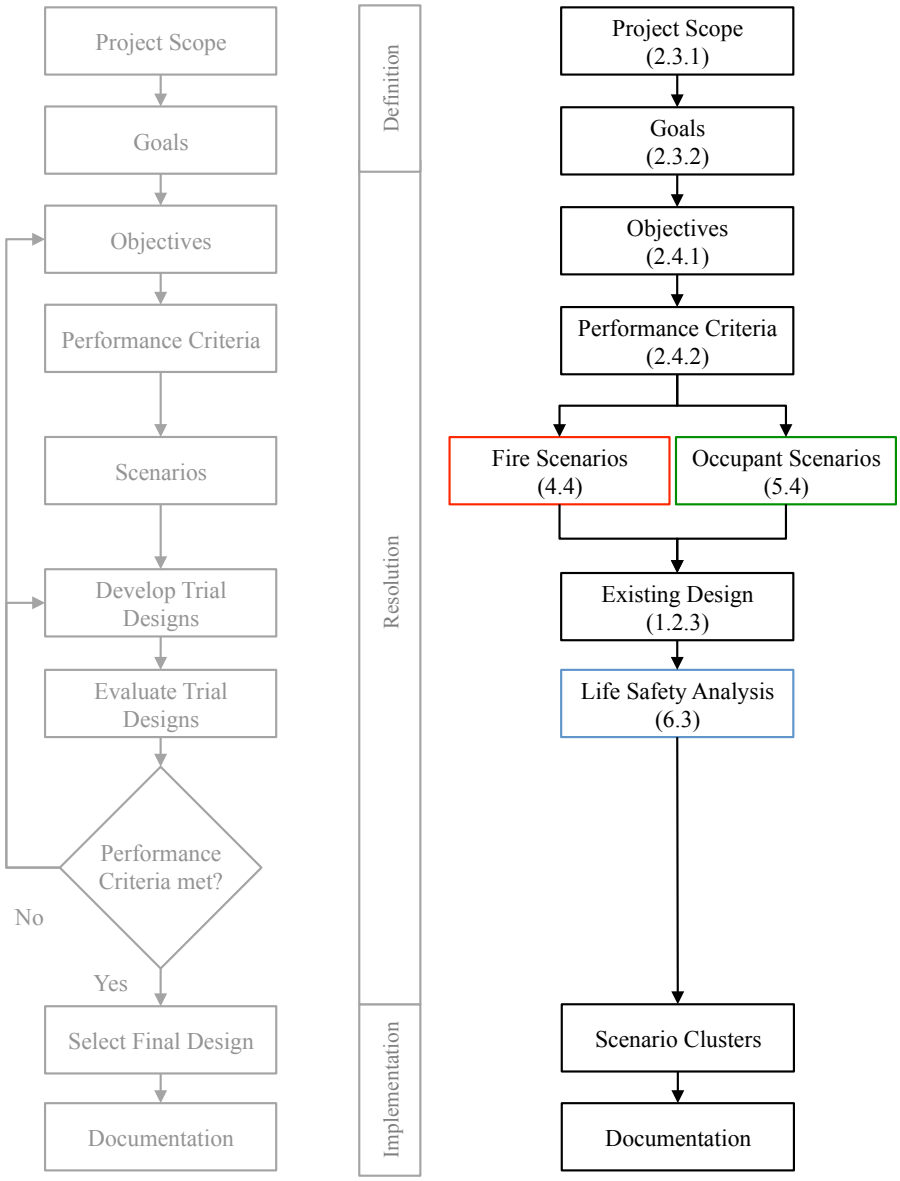

Figure 2.2: Performance-based fire safety design process (left) according to [Hurley and Rosenbaum, 2016] and its adaption (right) for the purpose of this work. The numbers in brackets correspond to the relevant sections of this thesis.

The outlined understanding is more or less the basis of all performance-based

design approaches. However, the real differences arise when considering both the assumption of system inputs and the interpretation of system outputs. This observation is vividly demonstrated during the presentation of national case studies referring to one particular project, e.g. in [SFPE, 2014].

Both the system and the method are now defined and are vitalised throughout the following sections. For this purpose, the three main steps of problem solving are used as central thread: problem definition, problem resolution, and implementation of the solution.

2.3 Problem Definition

2.3.1 Project Scope

System Boundaries The definition of system boundaries for this study has multiple aspects, which, of course, imply some assumptions that can not entirely account for the complexity of the real world. In terms of space, the focus is exclusively set on the underground station. Henceforth, the tunnel system is solely considered rudimentarily. The same applies to the surface, which is partially represented. For sure, the station's life cycle implies ongoing changes of particular design features. However, this study refers to the current design of *Osloer Straße*. Having said that, no so-called trial designs including any additional measures will be considered. The temporal boundaries have two different aspects. In general, the analysis is supposed to cover different times of the year as well as varying daytimes during the hours of operation. In terms of a particular fire incident, a short-termed analysis period of 20 minutes is evaluated. Finally, the definition of process boundaries assumes no firefighting operations by the fire service until the end of this period. On the other hand, staff intervention at an early stage will be considered.

Stakeholders Underground transportation systems involve a multitude of different stakeholders with diverse interests. In the frame of this study, however, the focus will be set on four major groups: customers, transportation department, authorities, and fire service. In this respect, the primary and most extensive group of stakeholders are the customers, whose primary interest is an undisturbed journey. Without doubt, safety is an inherent customer demand as well. However, to some extent, the risk perception when using underground systems may be different compared to other means of transportation, e.g. automobile traffic or aviation. The Berlin transportation department (BVG) is another stakeholder, whose primary objective is to ensure

a profitable and undisturbed operation of the entire transportation system. Likewise, in the sense of responsibility and sustainability, providing a sufficient level of safety for customers is a fundamental interest of the *BVG*. Moreover, authorities have varying interests depending on their responsibilities. On the one hand, public transportation is put out to tender in Germany. This involves demands regarding the fulfilment of requested transportation capacities as well as fines in case of non-performance. On the other hand, the primary interest of approving authorities is the safe design and operation of facilities. Another body is the fire service, who has to ensure efficient and safe rescue operations in case of a fire incident.

Legislative Basis Multiple regulations account for the fire safety-related interests of the above-mentioned stakeholders. The superordinate statute is the German constitutional law. Amongst others, the underlying level accounts for both building legislation and transportation legislation. It consists of the building codes (here: *MBO*) and the passenger transportation act (*PBefG*). By means of fire safety, building codes are concretised by additional regulations applicable to different building uses, e.g. mercantile, assembly, or industry, whereas no specific regulations for transportation facilities are available. On the other hand, the Transportation Act enables the regulation of the operation of tramways (*BOStrab*). For the purpose of fire safety design, the latter is again rendered more precisely by a technical guideline for tramways (*TRStrab BS*).

2.3.2 Safety Goals

The German constitutional law provides every individual with the right to physical integrity. On that basis, *MBO* states that every built environment has to be placed, built, modified, and maintained without posing any hazards to life and health (free and condensed translation) [MBO, 2012, § 3]. Similar intentions are incorporated by the transportation act *PBefG*, whose primary demand for approval is a safe operation [PBefG, 2016, § 13(1)]. In the next instance, *PBefG* empowers *BOStrab*, which ensures safety of both facilities and rolling stock [BOStrab, 2007, § 2].

These general requirements are extended to fire-related hazards by safety goals in both *MBO* [MBO, 2012, § 14] and *BOStrab* [BOStrab, 2007, § 3(1)]. In this respect, the safety goal of particular interest for this study is the following: ensuring rescue of occupants.

In principle, this goal is achieved by two subtasks. Initially, occupants are supposed to engage in self-rescue, whereas rescue operations by the fire services are

assumed in the subsequent phase. The temporal quantification and potential overlap of these phases make for a vivid discussion in engineering practice. Concrete specifications are provided in *TRStrab BS*, which states a calculative quantification of the self-rescue phase. Moreover, rescue operations are assumed to last from the completion of the self-rescue phase until the thirtieth minute of the incident. The focus of this study, however, is exclusively set on the self-rescue phase.

2.4 ASET vs. RSET

2.4.1 Objective

Every occupant has to have left a built environment before any fire effects result in untenable conditions. This objective is simple, reasonable, and comprehensible as well. Relying on the concept of performance-based design, it is incorporated in several standards and regulations for years. Concretely, it is represented by the so-called engineering timeline model [Gwynnee and Boyce, 2016]. It consists of an inequation, opposing the available safe egress time ($ASET$) with the required safe egress time ($RSET$) and a certain margin of safety as shown in Equation 2.1. It is thus also called *ASET-RSET* concept in everyday language.

$$ASET > RSET + \text{safety margin} \tag{2.1}$$

In this respect, $ASET$ describes the performance of a built environment in terms of resistance against the consequences of a particular fire. This is achieved by determining the time when tenability criteria of certain fire effects are exceeded. On the other side, $RSET$ captures the occupant's egress out of the building. The potential difference between these two times is usually referred to as safety margin. The latter may be utilised to cover uncertainties and to characterise the overall performance of a design.

$RSET$ itself is derived from a multitude of relevant time components for the description of egress processes. It is composed of the maximal sum of time periods, such as detection, alarm, pre-movement, and travel as shown in Equation 2.2. It is important to note that this term is accompanied by large uncertainties and may be shaped differently for every particular occupant i (see Section 1.3.2).

$$RSET = max(t_{\text{detection},i} + t_{\text{alarm},i} + t_{\text{pre-movement},i} + t_{\text{travel},i}) \tag{2.2}$$

Finally, the entire *ASET-RSET* concept is summarised in Figure 2.3:

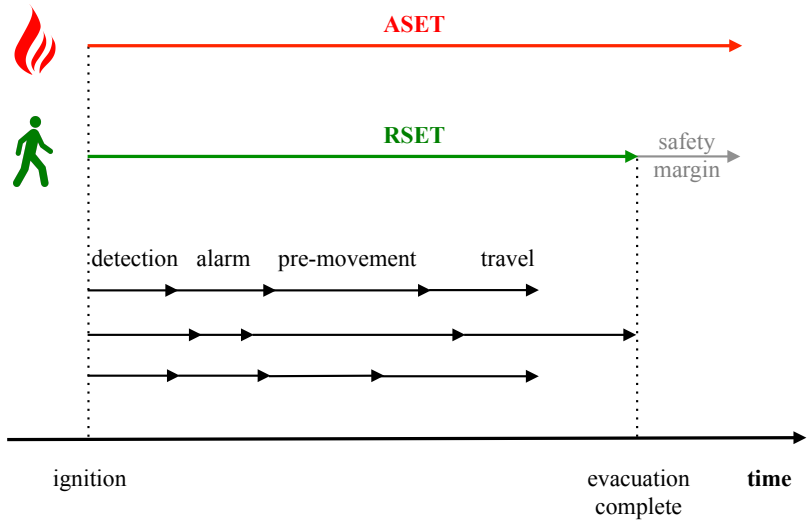

Figure 2.3: Summary of the *ASET-RSET* concept. In orientation to [Gwynnee and Boyce, 2016].

2.4.2 Performance Criteria

In order to determine *ASET*, the performance criteria and corresponding threshold values are used as presented in Table 2.1.

Table 2.1: Performance criteria for determination of *ASET*.

Quantity	**Unit**	**Threshold**
Extinction coefficient	m^{-1}	0.23
Temperature	°C	45
Carbon dioxide	ppm	10,000
Carbon monoxide	ppm	100
Hydrogen cyanide	ppm	8
Hydrogen chloride	ppm	200

The specifications are excerpted from the German vfdb guideline [vfdb, 2013, p. 260]. The recommendations collected there refer to exposure times of up to 30 minutes. The quantities are evaluated at a height of 1.95 m above floor level, which is supposed to represent the upper bound of body heights. Furthermore, this height approximately corresponds to the smoke layer height claimed for existing stations in

TRStrab BS. The further procedure regarding the determination of *ASET* is provided in Chapter 4.

2.4.3 Challenges

So far, the preceding section presented *ASET*-*RSET* as a conceptual framework for the life safety analysis in case of fire. The vitalisation of the latter is achieved by the introduction of scenarios, which will be described in more detail in Section 2.5. Henceforward, the concept's initial simplicity evolves into a highly complex and non-linear problem. The introduction of scenarios for both fire and evacuation incorporates a certain variability into the inputs of both subsystems. Having said that, one generally has to consider any modes of (probability) distributions regarding the output as well. As an example of an acceptable design, Figure 2.4 illustrates the probability distributions of *ASET* and *RSET* qualitatively.

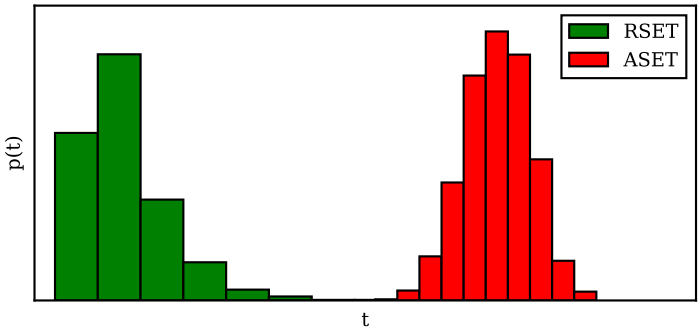

Figure 2.4: Qualitative illustration of *ASET* and *RSET* (probability) distributions of an acceptable design.

In this respect, distributions of both *ASET* and *RSET* induced by parameter variations have already been utilised in a number of works, e.g. in probabilistic studies such as [Albrecht, 2012] or [Kong et al., 2016].

However, additional questions arise with regards to the determination of *RSET* and *ASET* itself. With respect to *RSET*, the total egress time may be noted as the time when the last occupant has left the building. This convention is rather simple but may lead to an extensive underestimation of the design's performance. It gets even more complicated when considering *ASET*. Which quantity shall be considered? What tenability criteria is relevant and last but not least what should the resolution

look like in terms of space and time? At least here, it should become obvious that it is hardly possible to determine one single *ASET* for a particular enclosure or building. The spatiotemporal resolution of the concept needs to be considered during the exploration and selection of scenarios as well. In addition to that, it has to be noted that any uncertainties originating in the model application are excluded in this discussion.

To sum up: the concept is appropriate but its application is by far non-trivial, as it also has been discussed in [Seyfried et al., 2015]. In concrete terms, the proper application of the *ASET-RSET* concept is not only a problem in terms of design and computation of (simulation) experiments, it is also an analysis problem that has to be solved.

2.5 Scenarios

Scenarios are the centrepiece of performance-based fire safety design. In terms of literary usage, the scenario term has become rather popular since the 1980's [Michel et al., 2011] and is even identified as a buzzword in [Kosow and Gaßner, 2008]. As a consequence of that, both definitions and taxonomies may widely differ in daily routines.

The origin of scenario-based techniques can be found in fields like military, politics, and economics. Apart from a specific application, a scenario can be defined as a "hypothetical sequence of events which is constructed in order to assess causal relations" (free translation) [Dudenredaktion, 2006]. According to [Kosow and Gaßner, 2008, pp. 14-17], scenarios cover four major functions: exploration, communication, objective formation, and decision. Referring to this source, the explorative function is supposed to account for the generation, systematisation, and enhancement of knowledge as well as the identification of uncertainties and complexity. In terms of communication, scenarios can either be the result of discussion processes with multiple stakeholders and demands or serve as illustrative input for the latter. Moreover, the objective function of scenarios involves the formulation of nominal states. In terms of the decision function, scenarios serve as orientation points in order to evaluate the consequences of particular measures and strategies.

In general, the scenario term is closely linked to uncertainties since one scenario represents one particular excerpt out of an infinite space of events. Consequently, the utilisation of scenarios represents an indispensable reduction of complexity. However,

the extent of this reduction may obtain a crucial role and will, thus, be pursued in the Sections 2.5.3 and 2.5.4.

Given these general characteristics, this study utilises scenarios in order to simulate the subsystems *Fire* and *Evacuation* as defined in Section 2.1. For this purpose, basic principles of both fire and occupant scenarios are briefly reviewed in the following two sections. Thereafter, the combination of the two as well as the scenario classification applied in this study are discussed.

2.5.1 Fire Scenarios

In conjunction with the performance-based design process, fire scenarios are worldwide addressed in numerous standards and guidelines meanwhile. In this respect, a comprehensive overview is provided in [Hadjisophocleous and Mehaffey, 2016]. Sourced from [ISO/TS 16733, 2006], the definition of fire scenarios needs to consider the following aspects: potential fire hazards, location of fire, type of fire, systems impacting on fire, and occupant response. The following specification of these aspects is excerpted from [Hadjisophocleous and Mehaffey, 2016].

Insofar, fire hazards can either be derived from reviewing statistics or analysing coincidences of combustibles and ignition sources. Challenging fire locations are e.g. rooms with large occupant numbers or places that may affect certain means of escape. Additionally, fires in hidden spaces may advance to a hazardous state before being detected. Other relevant locations may be obstructed spaces that impair the effectivity of active measures or areas which affect plume characteristics, e.g. mass flows or spilled buoyancy. Specifying a fire type involves a qualitative description of the ignition, the intensity, and the development of a fire. Usually, these aspects are closely linked to particular fire locations. If applicable, the impact of passive and active fire protection systems needs to be considered as well. Passive measures may, for instance, be compartmentalisation or structural integrity, while active measures involve the effects of smoke and heat extraction systems or suppression systems. Finally, the potential interactions between a fire incident and the present occupants or staff have to be incorporated in the definition of fire scenarios. These aspects may especially be relevant for extinguishing measures or activities affecting the propagation of fire effects.

2.5.2 Occupant Scenarios

To some extend, the relevance of a fire scenario is always linked to an underlying occupant scenario. Having said that, Nilsson and Fahy conclude that "in *FSE*-analyses, designers often spend a lot of time and effort on the fire problem,, e.g. estimating design *HRR* curves or simulating smoke spread, but occupant aspects may not always be incorporated appropriately in the design" [Nilsson and Fahy, 2016, p. 2048]. Thus, it is inevitable to specify appropriate occupant scenarios carefully. For this purpose, the consideration of different methodologies and aspects is recommended, e.g. in [ISO/TS 29761, 2015] or [RiMEA, 2016]. In this respect, ISO/TS 29761 also includes the definition of fire scenarios, whereas the RiMEA guideline exclusively accounts for occupant scenarios.

Based on the draft work on DIN 18009-2, four major categories have been identified, which will be utilised in this study: *occupancy and occupants*, *built environment*, *safety measures*, and *hazard* [Jäger and Schröder, 2016]. In that regard, *occupancy and occupants* is supposed to account for the emerging variabilities regarding that category. On the one hand, this covers the building use and the related numbers and distribution of occupants. On the other hand, the specification of occupant characteristics is supposed to account for the knowledge in the field of human behaviour in fire as presented in Section 1.3.2. This challenging task has to incorporate diverse factors like age, gender, physical and sensory capabilities, susceptibility, familiarity, experience, knowledge, social and cultural roles, presence of others, or current activities [ISO/TS 29761, 2015]. The category *built environment* covers building characteristics, which are relevant for the evacuation process, e.g. detection and alarm systems, signage, or egress paths. *Safety measures* account for all actions that are applied by means of organisation and intervention in case of an evacuation. Finally, the category *hazard* has two different levels. Initially, arbitrary hazards are assumed as primary cause for an evacuation. Moreover, in terms of considering hazardous effects over the course of an evacuation, this category may represent the interface with the fire scenarios.

2.5.3 Combination and Classification

Once both fire and occupant scenarios are specified, the subsequent step of the analysis is to combine the latter. In this respect, Nilsson and Fahy found that "there is always an occupant scenario paired with each fire scenario. This means that the selection of fire scenarios and occupant scenarios [...] cannot be done independently, but it

is instead a process of finding combined scenarios, which challenge the proposed fire safety design" [Nilsson and Fahy, 2016, p. 2048].

In Section 2.4.3, it has been concluded that each fire scenario corresponds to unique distributions of *ASET* within a built environment. The same applies to occupant scenarios, which may additionally be influenced by the fire scenario's characteristics. Thus and except of fire scenarios that exclude certain occupant scenarios and vice versa, the parameter space of a life safety analysis is spanned by a non-hierarchical, full-factorial combination of the identified fire and occupant scenarios as illustrated in Figure 2.5. In this regard, full-factorial involves $m \times n$ combinations out of m fire scenarios and n occupant scenarios, while non-hierarchical means that there is no sequential relation between the fire and occupant scenarios.

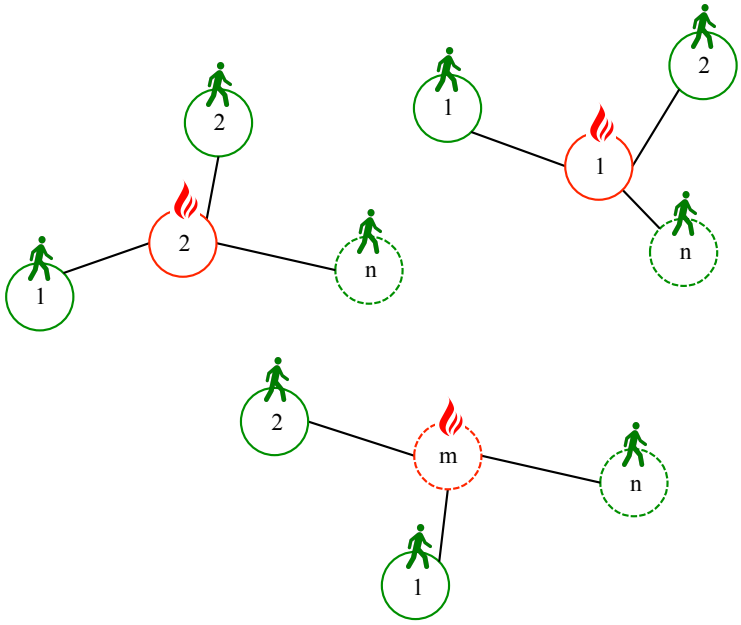

Figure 2.5: Combination of fire and occupant scenarios. In orientation to [DIN NABau 005-52-21 AK2, Personal notes, March 9, 2016].

The challenging character of a particular scenario combination refers to risk; considering both the consequences and the probability. Having said that, one of the most crucial tasks is the identification of design scenarios as a challenging subset of all possible scenarios. This reduction is necessary because of practical constraints in

terms of design, computation, and analysis of simulation experiments. For this purpose, a general classification of scenarios is incorporated in many handbooks [Hurley et al., 2016] and standards [ISO/TS 29761, 2015], [DIN 18009-1, 2015] meanwhile. The scenario taxonomy of the latter is described below and illustrated in Figure 2.6.

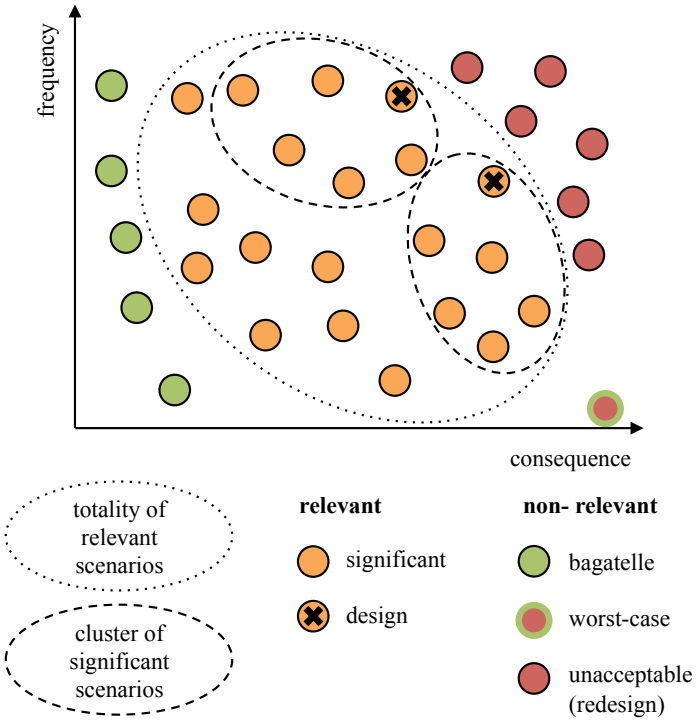

Figure 2.6: Scenario classification [Jäger and Schröder, 2016].

The totality of possible scenarios here is divided into relevant and non-relevant scenarios. On the one hand, the latter consist of bagatelle and worst-case scenarios which oftentimes may be excluded from the analysis by judgement. On the other hand, the analysis may reveal unacceptable scenarios, which do not fulfil an arbitrary requirement. Without further measures, a particular design has to eliminate these scenarios.

The remaining significant scenarios represent the subset, which is relevant for the further design process. For this purpose, these may be grouped into clusters on the basis of comparable risks. Finally, these clusters are represented by design scenarios,

which are supposed to yield the maximum "severe but reasonable" risk [Nilsson and Fahy, 2016, p. 2048].

2.5.4 Challenges

Given the combination of fire and occupant scenarios as well as the classification of the latter, the central engineering task is to reduce the complexity of the introduced scenario space to a smaller extent. In concrete terms, the totality of scenarios is supposed to be represented by design scenarios, which are "amenable to analysis" [ISO/TS 29761, 2015, p. 5]. This process step is also referred to as screening [Hadjisophocleous and Mehaffey, 2016] and is usually conducted a priori using (risk-based) qualitative approaches. These employ statistics or judgement in order to determine design scenarios. Contrary to that, quantitative approaches utilise systematic methods sourced from reliability engineering (e.g. event trees) in order to quantify the risk associated with a scenario.

However, in case of increasing complexity, qualitative approaches may especially suffer from limited predictability caused by non-linear relations and interdependences between the subsystems. In turn, quantitative risk-based approaches are able to cope with these questions but they involve one essential drawback: the lack of data or uncertainties regarding probabilities of particular events.

Moreover, these challenges are not solely affected by input-related uncertainties but also by the consideration of multiple objectives and performance criteria. Thus, it is also an output-related data analysis problem.

According to Braha, the above-mentioned characteristics closely correspond to the classical understanding of engineering processes which aim at system behaviours that "can be predicted and encapsulated by precise description". In that sense, he further states that "there is a strong tendency to control or limit complexity instead of embracing it". Having said that, he concludes limitations regarding the "robustness and resilience" of an engineered system [Braha et al., 2006, p. 7].

Similar thoughts have recently been addressed by Purser when reflecting on current and potential developments in egress modelling. In terms of conceptual challenges for further development, he figured out a number of different aspects e.g. "Examination of the entire escape and hazard development process involving all interactions between the occupants, built systems and fire scenarios". Moreover, he emphasised the necessity for the "Identification of those parameters having the greatest effect on safety outcomes" and to "collect data on the range of variability of each key parameter to facilitate probabilistic analysis of simulation outcomes" [Purser, 2016b].

2.6 Design and Analysis of Simulation Experiments

Inspired by the thoughts stated above, this study is based on a quantitative, deterministic analysis, which is applied to an extensive, pre-computed scenario ensemble. The latter is set up by combining different techniques of experimental design, which allow for a more extensive representation of the infinite scenario space. The analysis of the represented scenario space is supposed to provide an essential basis to the scenario selection process: the grouping of scenario combinations, i.e. the formation of scenario clusters. This analysis is conducted a posteriori based upon the computed consequences of all scenario combinations. In this respect, the probabilities of occurrence are initially not considered further, which is, of course, a limitation.

Having said that, the investigation of system outputs, e.g. consequences, will allow for a more comprehensive understanding of the system behaviour. The subsequent conjunction with system inputs, e.g. scenarios, essentially represents a sensitivity analysis, which is one potential application within the research topic "design and analysis of simulation experiments" [Kleijnen, 2008, p. 7]. According to Winzer, simulation experiments are a powerful tool for the evaluation and implementation of design variants within a modelled system [Winzer, 2013, pp. 198].

Amongst other aspects, the conduction of such studies essentially has to account for two subtasks: designing and analysing the experiment as illustrated in Figure 2.7.

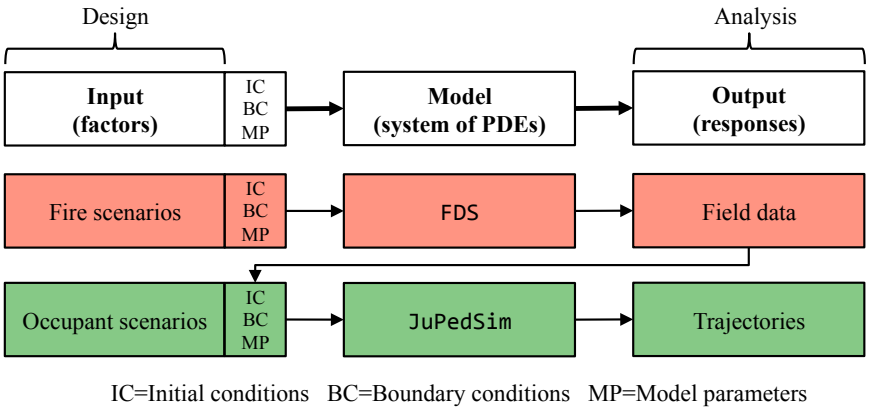

Figure 2.7: General overview of design and analysis of simulation experiments and its application within this study.

In this respect, experimental design essentially covers the definition of inputs. These inputs may be initial and boundary conditions or model parameters that are provided to a certain (black box) model. In the frame of this study, both of the applied models (*FDS* and *JuPedSim*) represent systems of partial differential equations for simulating either fire or pedestrian dynamics. The outputs obtained from the computational realisations are the basis of the subsequent data analysis. The following two sections provide a brief overview of the two above-mentioned subtasks and the corresponding methods applied within this study.

2.6.1 Design of Experiment

Initially, it is important to note that a more extensive scan of the scenario space is not the guarantee for entirely capturing the system behaviour, but it is a good approximation. The quality of the capture may significantly depend on the specifications regarding the design space, e.g. dimensionality, size, or resolution. These aspects are addressed in the design of experiment (*DoE*) research field. *DoE* unifies "mathematical statistics and linear algebra [...] applied to experiments with deterministic and random simulation models" and may serve for diverse goals, e.g. verification and validation, sensitivity analysis, optimisation, or risk analysis [Kleijnen, 2008, pp. 7-10]. *DoE* essentially covers the input configuration of (simulation) experiments. In this respect, a set of inputs is referred to as sample, which is tantamount to the scenario term as introduced in Section 2.5.

According to Kleijnen, the inputs are represented by factors which involve parameters and variables. In that regard, it is important to denote that parameters are "model quantities that have values that cannot be directly observed in the real world", which in turn applies to a variable [Kleijnen, 2008, p. 10]. Experimental designs can be based on several different approaches, e.g. one-factor-at-a-time, full-factorial, fractional-factorial, central composite, or Latin Hypercube. Both applicability and appropriateness of the latter depend on the problem.

Given these general information, the experimental design of the fire simulation ensemble (Section 4.4) has been conducted based upon a full-factorial sampling. For this purpose, every level of the station has been assigned with a separate design space. In case of the platform levels, the design factors consist of three parameters, whereas two of the latter have three levels and one has five levels, i.e. $3 \times 3 \times 5 = 45$ scenarios. The concourse level consists of three factors as well. However, one parameter only involves two levels, i.e. $3 \times 3 \times 2 = 18$ scenarios. The above-mentioned characteristics yield a total number of $45 + 45 + 18 = 108$ scenarios.

Moreover, for the specification of the evacuation scenario ensembles (Section 5.4), Latin Hypercube Sampling (*LHS*) has been applied. General information on this so-called space-filling design method are provided in [Kleijnen, 2008] and [Viana, 2013]. Assuming a space of two factors to be represented by n samples, the basic idea is to divide each parameter domain into n levels. In this respect, the levels can either be distributed uniformly or according to a specified distribution as conducted in [Schröder et al., 2014]. The initial sampling point is randomly chosen and the design space then is expanded according to the following principle: each orthogonal of a sample point may not intersect with another sample point in the particular level. *LHS* henceforth represents an orthogonal sampling method, which can be applied to multi-dimensional spaces. Questions about the random initialisation as well as the spatial representation of the levels by a sample point allow for techniques in order to optimise the coverage of the design space. Regarding these methods, further reading can be found in [Rennen et al., 2010]. In the frame of this study, the levels have been distributed uniformly and the sample points have been allocated centred within the latter. Moreover, the design space coverage is significantly depending on the number of samples. Unfortunately, it is not possible to define versatile thresholds for that since it depends on the problem and the dimensionality to which *LHS* is applied. As an orientation, Kleijnen states 100 samples as a rule of thumb [Kleijnen, 2008, p. 129].

2.6.2 Data Analysis

Data analysis is intended to assess and evaluate a particular design. Depending on the extent of the design space and the complexity of the applied models, a simulation-based life safety analysis can yield massive amounts of data, which can be looked at from two perspectives. Firstly, both fire and evacuation processes are usually described by spatiotemporal data series of diverse quantities. The second perspective accounts for the variabilities introduced by applying design of experiment strategies as described above. These circumstances imply the necessity for advanced analysis workflows for the derivation of superordinate knowledge from the simulation experiments. A comprehensive introduction into methods and tools of this purpose is provided in [Myatt, 2007], which is also the source of the following basics. For the conduction of an exploratory data analysis, Myatt identified four major process steps: problem definition, data preparation, implementation of the analysis, and deployment [Myatt, 2007, p. 6]. Since the first and the last step are part of the performance-based

design process as presented in Section 2.2, data preparation and implementation of the analysis will be the centrepieces of this section.

In this respect, data preparation solves tasks like consolidation, cleaning, and transformation of data. In order to condense information and simultaneously reduce the data extent, these process steps have been applied to the spatiotemporal data derived from the fire and evacuation simulations. With regards to the fire simulations, these data consist of various field quantities, which are highly resolved in space and time. The data obtained from the evacuation simulation are massive sets of trajectories, which comprise the space and time information of every individual pedestrian. In both cases, the data amounts could be reduced by at least three orders of magnitudes, which is achieved by map representations of *ASET* (Section 4.5.1) and *RSET* (Section 5.5.1).

Finally, the implementation of a data analysis itself mainly consists of three tasks: summarising the data, finding hidden relationships, and making predictions, whereby the focus will be set on the first two subtasks in the frame of this study. In this respect, summarising data utilises straightforward formats, e.g. tables or graphs. On the other hand, finding hidden relationships within datasets may involve more sophisticated data formats and methods. In this study for instance, correlation analyses will be conducted in order to provide a principal understanding of the behaviours of the two subsystems *Fire* (Section 4.5.2) and *Evacuation* (Section 5.5.2). Moreover, the outputs of the consolidated simulation ensemble will be investigated using grouping approaches such as hierarchical agglomerative clustering (Section 6.3.2). In order to identify the design scenarios, the clusters will then be further investigated based on relationships regarding the associated inputs (Section 6.3.3).

Chapter 3

Extending the Fire and Evacuation Models

This chapter covers all modelling works which were necessary in order to assess the scientific questions of this study. The model extensions cover both fire simulation and pedestrian simulation. In the first step, the integration of available knowledge and data about underground climate into the field of fire simulation will be discussed. After that, the main extensions of the *JuPedSim* framework for incorporating fire simulation data will be presented.

3.1 Fire Simulations and Underground Climate

In Germany, experiments with thermally-driven, artificial smoke are increasingly applied for the qualitative proof of smoke management concepts [iBMB, 2015, pp. 249-308]. These physical experiments especially account for the fire development phase with comparatively low rates of heat release. In a number of cases, the latter revealed non-trivial airflow regimes, which were – to some extent – caused by climatic effects [Schmundt and Wassermann, 2014]. Similar observations have been made during the first pilot experiments in the frame of the ORPHEUS project. Moreover, some of the incident studies presented in Section 1.2.2 emphasised the importance of airflows in the underground as well. Thus, the necessity to consider potential climatic influences in *FSE* analyses has been more and more acknowledged within the last years.

Underground systems especially can provide very particular climatic conditions, which are likely to be relevant for *FSE* analyses. In this respect, the term "climate" covers a multitude of quantities, such as temperature, airflow velocity, pressure, humidity and many others. However, in the frame of this study, the focus will be set on temperatures and airflow velocities.

In terms of the latter, it is commonly assumed that airflows are predominantly induced by the so-called piston effect caused by moving trains. Having said that, the consideration of climate effects is often neglected arguing that the train traffic is stopped immediately in case of fire.

However, extensive investigations carried out by researchers of the Ruhr-University Bochum clearly proved that airflows in underground stations do not exclusively depend on train movements [Pflitsch et al., 2012]. For instance, long-term field studies conducted in Dortmund, Germany showed that background airflows establish one to three minutes after the train service is ceased [Brüne, 2007]. The characteristics of these background airflows are mainly influenced by the ambient weather conditions. In detail, the temperature differences between the station and the surface as well as temperature differences within the station have been yielded as the main influencing factors.

In general, it has been found that higher temperature gradients result in higher flow velocities. In particular, this is the case during the winter period as the underground temperature profiles are less dynamic than the ambient ones and as partially strong chimney effects arise. In contrast, the summer period is rather characterised by more localised temperature differences and more or less stable stratification phenomena. These conditions lead to airflows with minor velocities that are prone to flow reversals. In this case, the background airflow is predominantly driven by the temperature differences within the station. With regards to safety research, the necessity for further investigations about interactions between background airflows and those which are thermally driven, e.g. by a fire, has already been pointed out in [Pflitsch et al., 2013].

The insights summarised above allow for the assumption that climatic aspects may be relevant for *FSE* analyses in underground stations. Assuming the low-energetic development phase of a carriage fire at the basement of a two-level station, the following two simple cases shall support this thesis.

Winter case: Comparatively low underground temperatures provide good buoyancy conditions for the plume formation, resulting in a stable stratification of the hot gas layer. However, the vertical temperature differences cause remarkable airflows towards the surface. The latter are constricted at the staircases, which are the only connection to the surface. On the one hand, this results in turbulent disruptions of the hot gas layer in these areas but, on the other hand, it provides a notable natural

ventilation of the platform level. In turn, this causes a remarkable smoke spread into the escape routes and the adjacent level.

Summer case: Higher temperatures within the underground system result in a less stable hot gas layer formation. However, the overall temperature equilibrium results in minor airflow velocities and, thus, in less turbulent disruptions. Subsequently, the natural ventilation is predominantly driven by the thermal impact of the fire itself. Hence, the conditions on the platform level become unacceptable rather fast. However, the escape routes and the adjacent level will remain almost smoke-free for a longer time.

The question if climate conditions affect the development of performance criteria cannot readily be answered. It depends on a multitude of aspects, e.g. the project scope, the built environment, the system boundaries, or the occurring fire dynamics. Since there are only few insights available so far, the points stated above shall serve as a starting point for the consideration of these aspects within this study.

In this regard, the following paragraphs cover the implementation of available data and knowledge into a *CFD*-based fire simulation. Since a literature review did not reveal any recommendations for considering the aforementioned aspects in the scope of underground stations, a brief review on other helpful documents is provided.

Across multiple building uses, a number of different design guidelines already account for the consideration of climatic conditions in *FSE* analyses. A first example is the German *RABT* guideline, which applies to road tunnels [FGSV, 2006]. It requires the proof of an adequate performance of a detection system design for longitudinal airflow velocities up to $6\,\mathrm{m\,s^{-1}}$. This assumption is, however, supposed to represent the traffic-induced airflows. Furthermore, the guideline series VDI 6019 covers the smoke ventilation of buildings [VDI, 2006a], [VDI, 2006b]. In principle, Part 1 distinguishes the consideration of low-energetic and a high-energetic design fires. The purpose of a fire scenario with a comparatively low heat release is to assess "the influence of particular room-climatic conditions in the room on fire" and to prove the "effectiveness of the planned smoke removal system including the automatic fire detection and alarm systems" [VDI, 2006a]. In Part 2, the derivation of initial and boundary conditions based on the particular climatic situations of a building is postulated. Though focussed on inlet airflows, the annex is supplementarily concerned with processes related to both the washout of the plume and the disruption of the hot gas layer.

3.1.1 Climate Modelling

Airflows in underground stations – if considered at all – have usually been modelled with explicit initial and boundary conditions either for pressure or velocity [Carvel and Beard, 2005], [Flassak and Bächlin, 2012]. In this section, a data-driven approach is proposed, which incorporates temperature as the key determinant. The subsequent configuration based on field data is presented in the following section.

The first consideration to model different climatic conditions in the frame of an *FSE*-related analysis has been presented in [Schröder et al., 2014]. The climate model was conjunct with a representative station, which had been derived from field studies conducted in Germany [Borchert, 2014]. Based on field data collected by the Ruhr-University Bochum in the underground system of Dortmund, the principal correlation of temperature conditions and airflow velocities in the station determined by [Brüne, 2007] could be reproduced with *FDS*.

The introduced modelling approach exclusively utilises the definition of initial and boundary conditions for temperatures throughout the station. Firstly, the ambient temperature of the computational domain is assumed as the surface temperature. Moreover, all final staircases leading to the surface are fitted with boundary conditions representing the ambient temperature as well. Additional temperature boundary conditions are defined at the tunnel portals of U8 and U9. However, horizontal temperature gradients are not considered within one level. In order to accelerate the climate's transient phase, initial zones have been set up in all three levels of the station. In case of the platform levels, the initial temperatures are set equally to the boundary temperatures of the latter. The initial temperature of the concourse is assumed as the mean of the temperatures of surface and U9. A graphical summary is provided in Figure 3.1

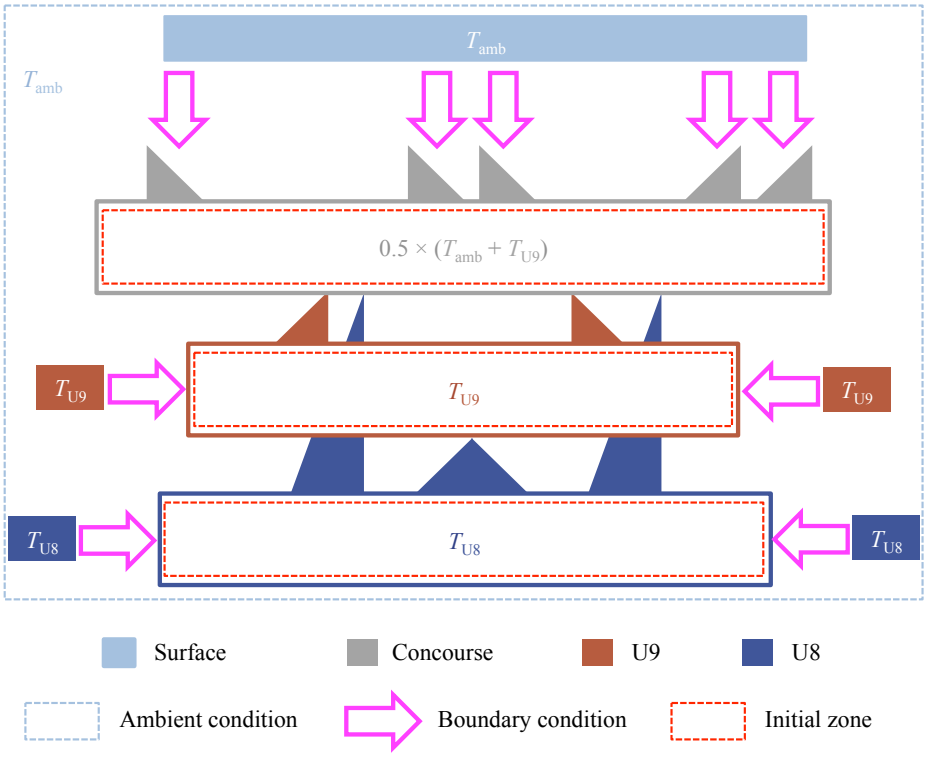

Figure 3.1: Overview of the climate model utilising ambient, initial, and boundary temperature conditions throughout the station. The triangles illustrate the staircases.

Moreover, the initial approach has been extended by the consideration of the built environment. On the basis of inside-wall measurements carried out by the Ruhr-University Bochum, the correlation between outside-wall and inside-wall-temperature has been determined. Given that, the initial temperature of all concrete building components has been adjusted according to Equation 3.1.

$$T_{\text{Wall}} = \frac{T_{\text{U8}} + T_{\text{U9}} + T_{\text{CL}}}{3} \cdot 0.75 + 4.124\,^{\circ}\text{C} \tag{3.1}$$

where:

T_{U8} is temperature at U8 in °C,

T_{U9} is temperature at U9 in °C,

T_{CL} is temperature at concourse in °C.

Finally, a period of 600 s of additional simulation time has been introduced prior to the consideration of any fire in order to engage the climatic conditions properly.

3.1.2 Data Basis

In the frame of the projects OrGaMIR and OrGaMIR Plus (see Section 1.3.3), a comprehensive dataset about climatic conditions in *Osloer Straße* has been collected by the Ruhr-University Bochum [Pflitsch and Brüne, 2016]. The time series are resolved in 10-minute-intervals and comprise a multitude of climatic quantities, such as temperature, airflow velocity, pressure amongst others. The data was collected with the help of six multi-criterial ultra-sonic measurement devices, which were placed in proximity to the tunnel portals of U8 and U9. In addition to that, two stations were set up temporarily inside the two staircases connecting U8 and concourse. Moreover, the ambient conditions have been recorded with a weather station at the surface. Recordings of the concourse are not available. In order to supply the afore-mentioned climate modelling approach, a selected subset of three data records has been utilised (see Table 3.1).

Table 3.1: Overview of measurement locations, which have been analysed to configure the climatic conditions.

Name	Location	No. Records	Quantities
`01__U8_G2_fn_o`	U8 track 2 → Franz Neumann Platz	146,900	T, v
`01__U9_G6_na_o`	U9 track 6 → Nauener Platz	118,985	T, v
`01__OB_OB`	Surface	176,641	T

This reduced selection was based on a number of different findings and requirements. Firstly, no remarkable differences between the measurements within one level have been found. Secondly, the data is intended to be used for simultaneous initial and boundary conditions of the *CFD* simulations. Hence, a temporal coincidence of the particular time series for both underground and surface had to be ensured. Since not all measurements were ran continuously due to operational and technical reasons, some of the remaining locations had to be excluded from the final analysis.

Within the preliminary studies in [Schröder et al., 2014], the temperatures underground and at the surface were sampled continuously within their statistical distri-

butions over the course of one year. In other words, a multitude of different climatic conditions has been incorporated, while the sampling did not include any additional constraints regarding the temporal coincidence of the surface and underground temperatures. Now, the data analysis focusses on the temperature differences between underground and surface. Regarding the latter, the emphasis is set on the upper and lower extrema in order to find representative climatic conditions of one summer and one winter case. Given this objective, a filter was applied to the datasets. In this respect, the summer period was assumed from July to September and the winter period from December to February. In additions to that, only recordings between 5:00 a.m. and 12:00 p.m. are included in the upcoming analyses.

In the following steps, the analysis workflow will briefly be presented concerning the winter configuration for the U8 level. Figure 3.2 provides the time series of the temperatures measured underground and at the surface as well as the resulting temperature difference.

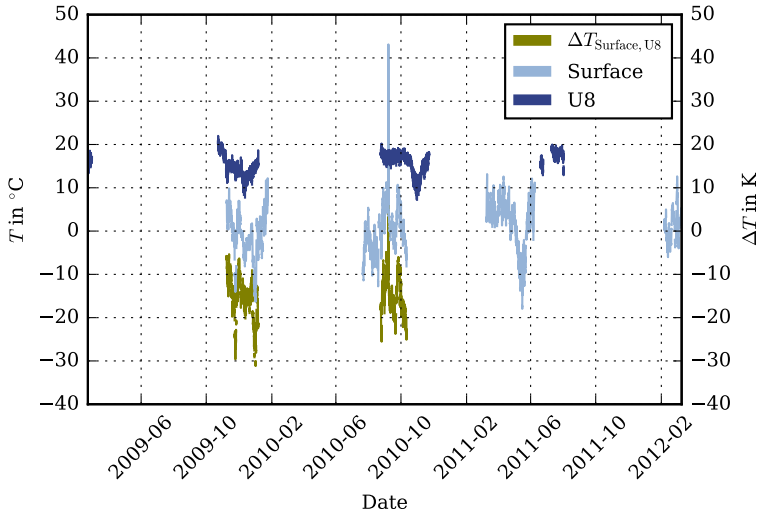

Figure 3.2: Winter conditions: time series of underground (U8) and surface temperatures and corresponding differences for coincident data.

It becomes evident that the dataset effectively allows for the evaluation of only two winter periods. Furthermore, the data proves the typical climate dynamics of underground stations: while the surface temperature provides a remarkable spread

between ± 15 °C (except outlier in 2010), the underground temperature varies in a much smaller range between 10 °C and 20 °C. Moreover, a more microscopic view to the data also revealed that there is a temporal delay between the individual courses of underground and surface temperature. The corresponding temperature differences consequently vary from −5 K to −30 K.

In the next step, the coincident data subset is analysed in more detail. For this purpose, the distributions of the particular temperatures are derived as shown in Figure 3.3.

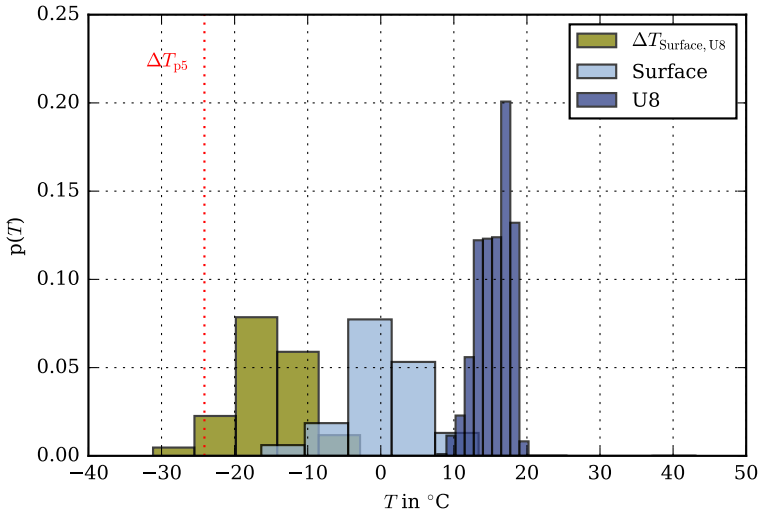

Figure 3.3: Winter conditions: distributions of underground (U8) and surface temperatures and corresponding difference when data series have been coincident. The dashed line illustrates the fifth percentile boundary, which has been applied to extract the most distinct temperature differences between surface and underground.

The distribution plot clearly illustrates the distinct fluctuations amongst the surface temperatures. In turn, the underground temperatures are distributed in more refined intervals. The vertical temperature difference between surface and underground is one of the key determinants of the underground climate. Hence, the ongoing analysis focusses on the distribution of the latter. In this respect, winter conditions are represented by the lower bound of this distribution or in other words: situations with maximal (negative) temperature differences between surface and underground.

In the sense of choosing a reasonable extent for the winter case, the temperature difference distribution is solely considered up to the fifth percentile from now on. For the summer case the distribution is considered beginning from the ninety-fifth percentile. Given these cut distributions, the underlying temperature components of surface and underground temperatures have been determined as shown in Figure 3.4.

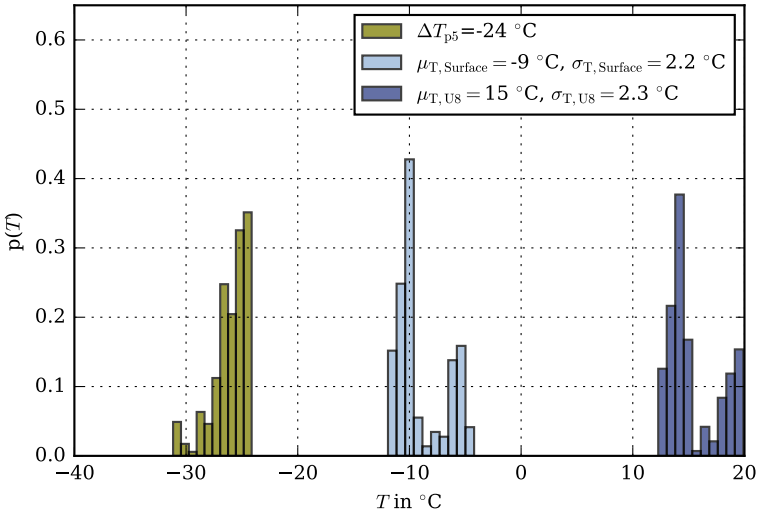

Figure 3.4: Winter conditions: illustration of temperature difference distribution bounded by the fifth percentile and the underlying components of underground (U8) and surface temperature.

The visualisation of the latter reveals a bipartite separation of the data, which looks like two separate distributions. This could be explained by two evaluated winter periods. Obviously, the distributions of both surface and underground are very similar and more or less shifted by the absolute value of the temperature difference. A higher number of observations could allow for a more robust parametrisation of these sub-distributions. With the given data however, the Gaussian mean and standard deviation have been derived in order to configure the climatic conditions. For the winter case, the temperatures of surface and U8 constitute $-9\,°C$ and $15\,°C$ respectively. The presented workflow was applied to summer conditions and and to the U9 level as well. The resulting configurations will be incorporated in the setup of the fire simulation ensemble in Section 4.3.3 and are provided in Table 4.6.

3.1.3 Results

The major objective of the presented modelling approach and data analysis was to obtain typical airflow conditions as they can be observed in underground stations. For both summer and winter case, Figure 3.5 visualises the velocity profiles that have established in the U8 after the transient phase of 600 s.

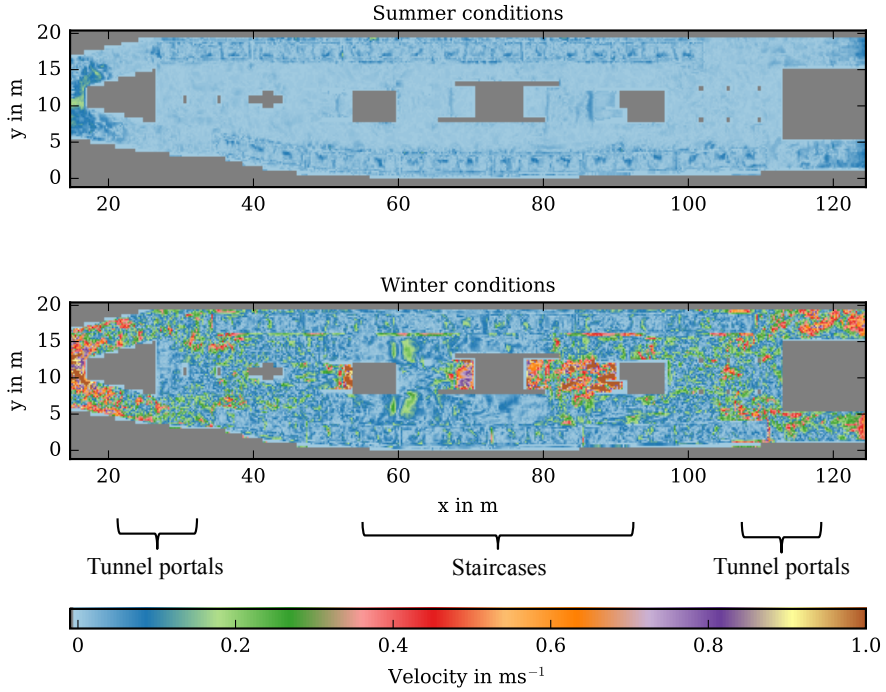

Figure 3.5: Horizontal slices of absolute velocities for summer and winter conditions. The slices refer to the U8 level at a height of 1.95 m after 600 s. For the winter case, velocities greater than 1 m s^{-1} have established in proximity to the tunnel portals and upward staircases.

Whereas almost no air movements can be observed within the summer configuration, distinct airflows establish for the winter case. Besides the tunnel portals, upward airflows especially form in proximity to the staircases. Moreover, almost the entire platform area is covered with slight velocity fluctuations.

3.2 Coupling of Fire and Evacuation Simulations

Prescriptive regulations do usually not consider the presence of any fire effects in escape routes. This is doubtlessly a reasonable requirement, which ensures a substantial degree of safety and it should, wherever possible, be straightforwardly fulfilled.

However, for specific building designs and uses, there may be scenarios that cannot exclude a spatiotemporal coincidence of building occupants and particular fire effects in general. In these cases, it is necessary to evaluate the extent and possible consequences of exposures and interactions. This task may include a multitude of different effects, e.g. "deciding to enter and continue through smoke or turn back and seek refuge, and on walking speed and wayfinding ability" [Purser and McAllister, 2016] or effects on an "evacuee's initial response" [Ronchi et al., 2013]. Henceforth, it requires a more conjunct analysis of the relevant subsystems.

The interactions between fire and evacuation dynamics are oftentimes reduced to the engineering timeline model presented in Chapter 2. But already the very beginning of the timeline requires a conjunction, e.g. when distinguishing between detection times of a detection system or individual occupants. In terms of route choice, fire modelling results and acceptance criteria are used to apply constraints to the temporal availability of the escape route system. With the aim of proofing tenability throughout an evacuation, this approach may be sufficient. But it assumes no interactions at all until a particular acceptance criterion is exceeded. However, there are interactions (e.g. re-routing due to smoke spread) that already may become relevant before a certain acceptance criterion is exceeded.

Beyond that, a deterministic life safety analysis of an existing design is not necessarily based on the principle that a coincidence of occupants and fire effects is impossible. This fact requires additional considerations about potential interactions, such as the reduction of walking speeds due to reduced visibility or impairment and incapacitation by toxic fire effluents.

The thoughts stated above were the cause for a number of submodels that have been added to the *JuPedSim* framework. In that regard, this section concerns *JPScore* – the simulation module of *JuPedSim*. Further information are provided in Section 5.1.1. As shown in Figure 3.6, a well-structured assignment of the particular submodels can be achieved in orientation to the hierarchy of motion.

Hierarchy of Motion Hoogendoorn [Hoogendoorn et al., 2002] proposed the hierarchy of motion in order to structure the diversity of aspects when modelling pedes-

trian dynamics as presented in Figure 3.6. It consists of the strategic, tactical, and operational level. The following information about the particular levels is extracted from the above-mentioned source.

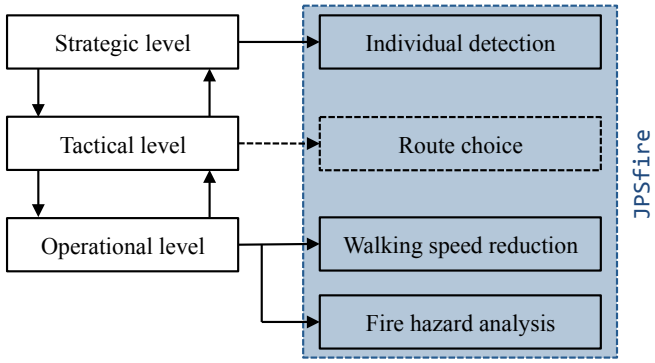

Figure 3.6: Hierarchy of motion [Hoogendoorn et al., 2002] and the assignment of relevant interactions between fire and pedestrian dynamics.

The strategic level concerns all aspects that are relevant prior to the movement of a pedestrian. From the perspective of a pedestrian, this stage is usually associated with no or incomplete information about conditions and alternatives. Beside the planning of a particular route, this also covers the fundamental decision to leave a building. This decision is the result of a complex process (see Section 1.3.2) and is depending on different cues. Doubtlessly, one of the latter is the sight of smoke, which is referred to as individual detection from now on. The latter represents the first interface between fire and evacuation simulations.

The tactical level consists of short-term decisions that become effective throughout the travel phase. These decisions are based on more detailed and localised information. In this respect, the potential effect of smoke spread on route choice is investigated as well.

Finally, the operational level includes all model characteristics that are related to the movement of pedestrians, e.g. the adoption of directions and walking speeds. The belonging interface to fire simulation data mainly consist of two aspects. The latter cover both reduced walking speeds in case of smoke obstruction as well as the impairment or prevention of the travel phase by fire hazards.

In the following sections, the extensions of the aforementioned levels are successively presented. The corresponding framework of these extensions is *JPSfire*, which involves the four major aspects illustrated in Figure 3.6.

JPSfire *JPSfire* is the interface between *JuPedSim* and *FDS* and is organised in two major levels: pre-processing of *FDS* data and incorporation by *JPScore*. The basic workflow and the quantities employed within this study and their relevance for the particular submodels are summarised in Figure 3.7.

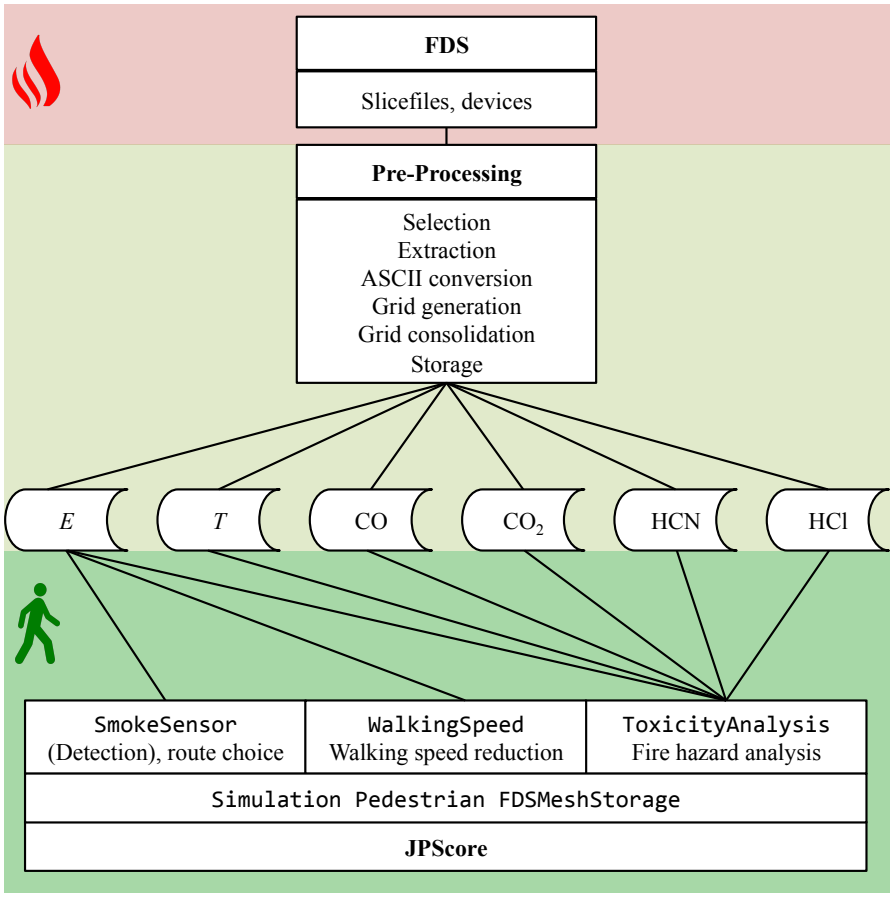

Figure 3.7: Overview of hierarchy and main functionalities of *JPSfire*, processed fire simulation data, and supplied classes of *JPScore*.

The first level represents the pre-processing interface, which conducts the selec-

tion, extraction, conversion, consolidation and storage of relevant fire simulation data. Besides extinction coefficient (E) and temperature (T), the gas concentrations of carbon monoxide (CO), carbon dioxide (CO_2), hydrogen cyanide (HCN), and hydrogen chloride (HCl) are evaluated. Once the relevant quantities and their evaluation locations are specified, information will either be gathered from *FDS* devices or slicefiles. Since the latter are stored in binary format, their incorporation initially requires a conversion to *ASCII* format. This is necessary in order to filter and consolidate the data in a flexible fashion. In the next step, the datasets are reshaped to their original spatial extends. In case of multi-mesh datasets, the latter are consolidated to single objects. Finally, the datasets of all specified quantities and evaluation locations are written out in order to make them accessible for *JPScore*, which sustains the second level of *JPSfire*. With regards to the simulation core, three classes are generically involved in the data incorporation. While the `Simulation` class controls the simulation of pedestrians based on a certain model in a specific scenario, the `Pedestrian` class hosts all relevant functions and parameters applicable to one particular pedestrian. Furthermore, the `FDSMeshStorage` class handles the inclusion and provision of the pre-processing data which is supplied by the first stage of *JPSfire*. The further implementations in *JPScore* depend on the particular submodels. Hence, these will be addressed separately in the following sections.

3.2.1 Individual Detection

The individual detection of fire cues has not inherently been implemented to *JPScore* yet. It will, however, be included within the design of experiment in Section 5.3.3. In concrete terms, the datasets prepared for the `SmokeSensor` class are utilised in order to determine the time, when smoke initially penetrates a particular subroom of the simulation geometry. Thus, the individual detection time is subroom-based and not agent-based currently.

3.2.2 Route Choice

Motivation Beside detecting a fire incident and engaging in a certain response, the sight of smoke may also influence the route choice of pedestrians and thus is relevant for the design of the tactical level. With regards to life safety analyses, these aspects can potentially affect the exposure to certain fire effects but also the load distribution in escape route systems and thus the location and extent of jam areas. If and why building occupants avoid or traverse smoke is a sophisticated question that has to

be assessed from a multi-disciplinary perspective. In principle, the initial question is wether multiple options are available at all. However, even in case of multiple options, occupants will move through smoke if there is a "good" reason for doing so [Künzer and Hofinger, 2016]. Similar thoughts are stated by engineers in [Gwynnee and Boyce, 2016, p. 2515]. According to Künzer and Hofinger, this decision however depends on multiple aspects, e.g. personal knowledge, experience, motivation, provided information, and social relations. The same is applicable if familiar exits are affected by smoke and alternatives are either unknown or subjectively less appealing. Moreover, any kind of stress may impair reasonable decisions.

Empiricism A few studies directly address the route choice of building occupants during fire incidents. In the year 1972, Wood conducted probably the most extensive work [Wood, 1972]. The interview study enquired about 1000 fire incidents in residential and public buildings and revealed that 60 % of the subjects traversed smoke. Further findings were that this number was in close relation to the familiarity with the building. Almost similarly, Bryan determined 63 % out of 584 interviewed subjects going through smoke during residential fires in the U.S. five years later [Bryan, 1977]. With an exclusive focus on a public occupancy, Fahy and Proulx provide numbers that have been collected upon the fire evacuation after the terrorist attacks at the World Trade Center in 1993 [Fahy and Proulx, 1997]. In this case, 94 % (Tower 1) and 70 % (Tower 2) of the evacuees encountered and traversed smoke while clearing the high-rises. Data related to underground systems can be derived from the incident study conducted in the course of the Daegu subway fire [Jeon and Hong, 2009]. Here, the authors found that more than 60 % of the subjects followed an evacuation route they had planned in advance. Only 25 % of this group were able to complete their planned passage, whereas the remaining 75 % deviated from their initial route. Another recent study was conducted by Çakici Alp, who interviewed 17 people present during a fire in a university building [Çakici Alp and Çağdaş, 2014]. In the knowledge that the number is small, the author found that approximately 30 % of the subjects deviated from their planned route due to smoke, while 46 % passed through smoke.

Implementation Inspired by these thoughts and numbers, a comprehensive proposal for a perception-based route choice algorithm has been presented in [Schröder et al., 2015]. The following information is a condensed excerpt of this source. Due to restrictions regarding the routing algorithms implemented in *JuPedSim*, the implementation is only functional for convex geometries currently. For that reason, it

will not be considered in the experimental design of the case study. Further work is necessary here.

The implementation has been carried out using an artificial test case as illustrated in Figures 3.8 and 3.9. It consists of a central assembly room, an adjacent room, and a corridor. The intention of the test case is that an assumed fire in the adjacent room yields increasing smoke spread into both the assembly room and the corridor. Initially, the smoke propagation will affect the corridor's upper exit due to the proximity to the fire. Later on, the lower exit of the assembly hall is affected as well since the smoke layer descends, when the ceiling jet reaches the lower wall.

In order to conjunct smoke dynamics and adaptive route choice, *JuPedSim*'s cognitive map routing framework has been extended. The latter has initially been introduced by [Haensel, 2014] and is continuously developed by Andresen [Andresen et al., 2016a], [Andresen et al., 2016b], [Andresen et al., 2017]. The basic idea of this routing framework is that the route choice depends on two major aspects: knowledge and perception. In terms of knowledge, every pedestrian has its individual, graph-based representation of the built environment, which is called metric map. Perception is represented by a set of so-called sensors which serve as individual input channels for each pedestrian. The purpose of these sensors is to provide the metric map with additional information, which is referred to as second order knowledge.

With regards to interdependences between fire and evacuation simulations, a `SmokeSensor` class has been implemented, which is supplied by *JPSfire*. The basic operation within the latter is to evaluate the line of sight from a pedestrian's current position towards a particular exit as it is demonstrated in Figure 3.8. With the help of spline interpolation of either optical density D or extinction coefficient E, the emerging line is used to extract the spatial course of the smoke conditions from the *FDS* field data. This process is conducted for all visible exits.

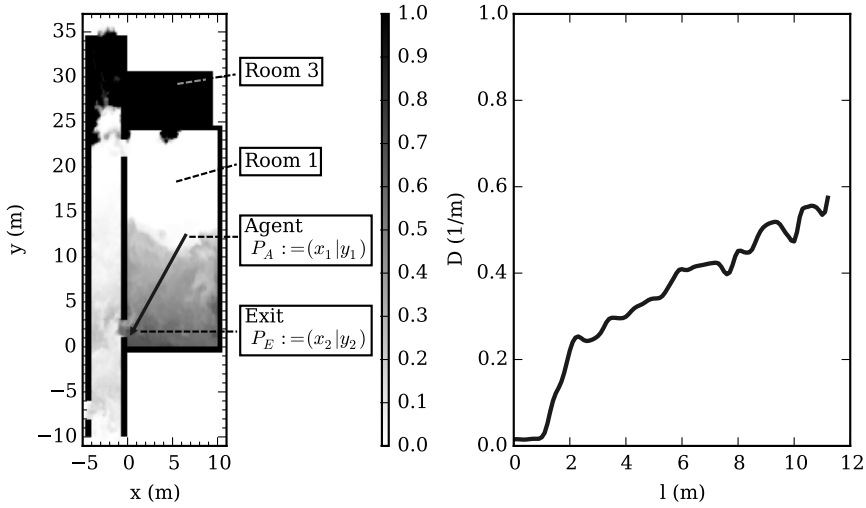

Figure 3.8: Extraction of optical density from fire simulation data with the help of spline interpolation.

In the subsequent step, the resulting data series are used to compute a weight factor for each visible exit. The factors then are used to modify the cost calculation, which is run on the metric map of each pedestrian. This process is conducted repetitively in order to account for the fire dynamics. For computational reasons, the weight factors are pre-computed and stored in a grid, which then is accessed by *JPScore*.

The functional verification of the introduced implementation reveals the route choice patterns illustrated in Figure 3.9.

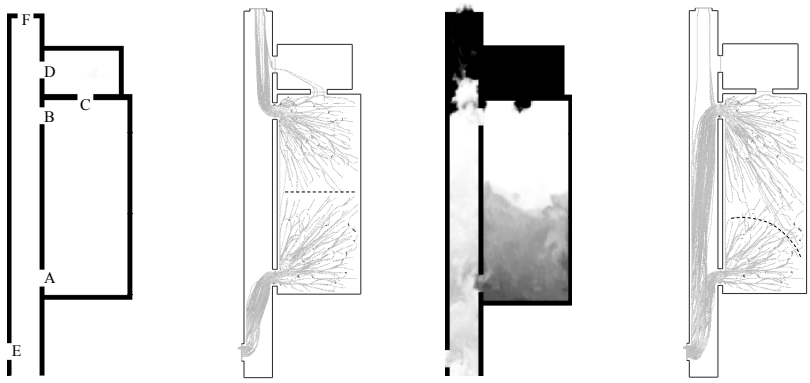

(a) Geometry (b) Shortest path (c) Smoke spread (d) Smoke sensor

Figure 3.9: Geometry and trajectory plots visualising the different route choice patterns. Under normal conditions, exits E and F are equally used (Subfigure 3.9b). In case of an assumed fire, exit F is increasingly avoided (Subfigure 3.9b).

It becomes apparent that the initial shortest path route choice (Subfigure 3.9b) changes in dependence to the current smoke spread conditions (Subfigure 3.9d). More precisely, the occupants increasingly use exit E, whereas exit F remains almost unused. With regards to the assembly room, the dashed line in Subfigure 3.9b represents the separation of the observed route choice due to the shortest path calculation under normal conditions. Subfigure 3.9c visualises the smoke spread in the geometry 165 seconds after ignition. Subfigure 3.9d shows the resulting route choice patterns with activated smoke sensor. With increasing smoke spread, the separation line relocates towards exit A, which is increasingly affected by smoke.

With regards to the vast uncertainties about the risk perception of individual pedestrians, the edge weighting routine has been added with certain randomness. The corresponding model parameter has been denoted as *risk tolerance*, which additionally modifies the cost calculation routine. A comprehensive sensitivity analysis about this artificial parameter as well proposals for its calibration with regards to the available empiricism have been conducted in [Hein, 2016].

3.2.3 Walking Speed Reduction

Motivation If there is a certain likelihood that smoke may spread into escape routes, the evacuation dynamics will be influenced by that. In general, the presence of smoke yields an increased extinction and, thus, obscures the sight of occupants.

The extent of these effects is heavily dependent on a multitude of factors. The most important aspects probably are the optical and chemical smoke characteristics, which in turn depend on the fuels and fire dynamics. But also the layout of a particular escape route system and lighting conditions will influence the visibility conditions. A number of incident and laboratory studies have identified the reduction of walking speeds as one of the major consequences of impaired visibility.

Empiricism In the past years, two major datasets have become available providing empirical relations between extinction coefficients and walking speeds. The very first was a Japanese study, which was conducted by Jin [Jin, 1978]. The second was conducted in Sweden by Frantzich & Nilsson [Frantzich and Nilsson, 2003]. Since the experimental conditions of both studies are slightly different from each other, the application of the data needs some further considerations. In general, both studies imply a reduction of walking speeds with increasing extinction coefficients. However, the extends of this effect are rather different. Firstly, the extinction coefficients in Jin's data are in the range of 0 to 1 m^{-1}, whereas the data collected by Frantzich & Nilsson covers 2 to 7 m^{-1}. Secondly, Jin predicts a more instant reduction than Frantzich & Nilsson. The reasons for these differences may be manifold. One of the most obvious factors, for instance, is the spatial configuration of the experiments. In Jin's experiment, the subjects were advised to traverse a corridor with a length of 20 m straight towards an emergency exit at its end. During the experiment conducted by Frantzich & Nilsson, the subjects were requested to pass through a 37 m long road tunnel including some obstacles. Furthermore, the obscuration of the sight was induced differently. In order to provoke irritant and non-irritant smoke characteristics, Jin used kerosene and wood grip fires. In contrast, Frantzich & Nilsson filled the experimental space with theatric fog. In a fraction of the experimental runs, the latter was additionally mixed with small amounts of acetic acid. Recently, additional data was generated by Fridolf when conducting evacuation experiments in a 200 m long rail tunnel [Fridolf et al., 2013b, 2015]. The objectives of the study were both the effectivity of way-finding systems and walking speeds in smoke-filled environments. Similarly to the study of Frantzich & Nilsson, smoke spread was simulated by theatric fog, which was mixed with acetic acid. The achieved extinction coefficients range from almost 0 to 2.2 m^{-1}. Thus, the optical conditions in the experimental space were less extensive but in turn represent a valuable addition to the dataset of Frantzich & Nilsson. A graphical overview of the introduced datasets can be found in Figure 3.10.

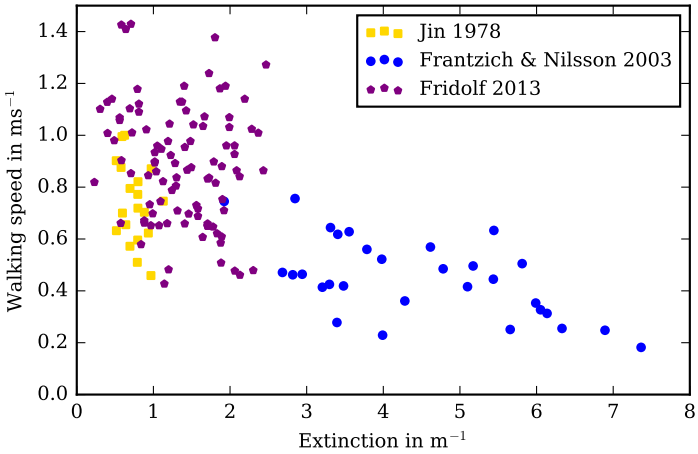

Figure 3.10: Experimental studies on the relation of extinction coefficient and walking speed applicable to non-irritant smoke.

Interpretations The data presented above clearly implies uncertainties about the physical performance of occupants forced to walk through smoke. In terms of fitting the data to a certain model, Frantzich & Nilsson propose an approximation by utilising a linear regression. Jin, on the other side, did not provide any recommendations for fitting the data. Recently, a logarithmic fit has been proposed by Purser in [Purser and McAllister, 2016]. In this work, he also discusses a consolidation and logarithmic approximation of both presented datasets. Further considerations of how to interpret the datasets have been made by Fridolf in [Fridolf et al., 2013a] by consolidating the dataset by Frantzich & Nilsson and his dataset. In order to account for the scatter of the data, he introduces a subdivision of the measurements into single classes that can be incorporated by means of descriptive statistics.

Besides the statistical analysis of the particular studies, additional questions arise when interpreting the data for the purpose of model implementation. One obvious question may be the influence of individual occupant characteristics on these data sets. Does reduced visibility uniformly decrease the current walking speed? Supposing that it does not, what is the contribution of the individual desired walking speed of a pedestrian? Another question is how to deal with the boundaries of the provided data domain. What assumptions should be made in ranges where no data is provided? Is there an absolute minimum speed? A well-structured and comprehensive study

concerning these and other related questions can be found in [Ronchi et al., 2013]. Based on an artificial case study, this contribution provides an interesting comparison of the mentioned datasets and interpretations. This work, in particular, addresses the implementation of (variable) functional relations sourced from the datasets and considers different interpretations of their corresponding boundaries.

Implementation For the analysis in this thesis, the dataset by Frantzich & Nilsson has been chosen. This decision has been made focussing on the fact that the study provides a wider coverage of extinction coefficients. In addition, it may be more appropriate for the application in complex built environments since the experimental setup was somewhat more demanding for the subjects in terms of avoiding obstacles and way-finding. Further on, its validity is to some extend supported by the dataset of Fridolf and both were conducted in the context of transportation infrastructure.

The implementation is carried out referring to interpretation number 2 in [Ronchi et al., 2013]. This means that not a single desired walking speed is globally determined by fitting the data but a normalised linear regression is utilised to recalculate the desired walking speed of an agent. The corresponding coefficients are provided in [Frantzich and Nilsson, 2003]. Since this regression could potentially yield in effective walking speeds very close to or even less than zero, a global minimum walking speed is set as shown in Equation 3.2.

$$v(E) = \max\left(v_{\min}, v_0 \cdot (1 + \frac{-0.057}{0.706} \cdot E)\right) \tag{3.2}$$

where:

E is extinction coefficient in m^{-1},

v_0 is desired walking speed in $\mathrm{m\,s}^{-1}$,

$v_{\min}$ is minimal walking speed. Here: $0.3\,\mathrm{m\,s}^{-1}$.

The walking speed reduction routine is triggered by the `Pedestrian` class whenever a desired walking speed is requested. The `WalkingSpeed` class itself accommodates Equation 3.2 and conducts the recalculation of the desired walking speeds. For this purpose, the `FDSMeshStorage` class is requested to deliver the optical conditions for time and space of a particular pedestrian. The necessary fire simulation data is prepared by *JPSfire* in advance.

3.2.4 Fire Hazard Analysis

Motivation Fundamentally, the determination of *ASET* is carried out by evaluating certain fire effects and their particular thresholds for tenability. This question opens up a highly complex interface between *FSE* and multiple disciplines of classical life sciences, e.g. physiology and toxicology.

Beginning with research on increasing fatalities in residential fires in the United Kingdom, major work and knowledge has been achieved by Purser since the 1980s. His most recent disquisitions on "Combustion Toxicity" and "Assessment of Hazards to Occupants from Smoke, Toxic Gases, and Heat" can be found in [Purser, 2016a] and [Purser and McAllister, 2016]. If not marked differently, the major contents of this section are derived from these sources.

In principle, these analyses come along with a large degree of underlying uncertainties. This covers both the *FSE* part in terms of determining the extent of fire effects as well as the life science part in terms of estimating the impact on a human being. Despite forensic studies that proved the proposed concept in general [Purser, 2016b], this drawback led to a very heterogenous acknowledgement and adoption of these insights into building codes and *FSE* practice.

However, this approach is particularly beneficial for analyses or scenarios that cannot solely be covered by prescriptive reasoning. In this respect, Purser rules out potential exposures caused by "sprinklered enclosures due to downdrag and loss of smoke buoyancy", or by the fact "that a system may be rendered inoperable". Finally, he also emphasises the appropriateness of "estimating the risk of injury and death throughout the life of the building [...] for a range of scenarios" [Purser, 2016a].

Relevant physiological processes for assessing life safety in the event of a fire are, e.g. incapacitation, irritation, visibility, and thermal stress. Thus, fire-related quantities of particular interest are gas concentrations, smoke densities, temperatures, and radiation. Depending on the chosen approaches in terms of fire modelling and data analysis, these quantities normally represent spatiotemporal data. They describe a certain condition at a certain location for a certain duration. The conjunction of these data with the occupants requires additional considerations. For this purpose, the concepts of fractional effective concentrations (*FEC*) and fractional effective doses (*FED*) have been implemented within this thesis.

Fractional Effective Concentrations The *FEC* concept is supposed to process information about a fire effect at a given time and space. This is especially appropriate when considering exposures that have an immediate effect on occupants. In principle,

an *FEC* term is simply composed by the fraction of a particular fire effect and the belonging tenability criterion as shown in Equation 3.3.

$$FEC = \frac{e}{e_\mathrm{t}} \tag{3.3}$$

where:

FEC is fractional effective concentration,

e is effect of fire,

e_t is tenability criterion of fire effect.

This fraction allows for the evaluation of a particular system performance, while unity represents the transition to untenability.

Fractional Effective Doses The *FED* concept extends the idea of *FEC* to the time dimension. In particular, this is beneficial for the assessment of accumulating exposures to fire effects. Its very basis is a general formulation of time-dose-relationships for particular fire effects according to Equation 3.4.

$$D = e \cdot t_\mathrm{e} \tag{3.4}$$

where:

D is dose,

e is effect of fire,

t_e is exposure time.

When considering the dynamics of fire-driven flows and crowd movements in built environments, it, however, is very unlikely that the quantities of fire effects are time-independent. In order to ensure an adequate representation of these spatiotemporal dynamics, the dose can be represented by the integral term presented in Equation 3.5.

$$D(t_\mathrm{e}) = \int_0^{t_\mathrm{e}} e(t)\ \mathrm{d}t \tag{3.5}$$

Except for comparative analyses, this expression does not allow for any evaluation up to now. Hence, the product of exposure and time has to be related to certain doses that are known to represent the thresholds of tenability. This relation yields the fractional effective dose as shown in Equation 3.6.

$$FED = \frac{D(t_e)}{D_t} \tag{3.6}$$

where:

FED is fractional effective dose,

D_t is dose representing the tenability threshold.

Again, unity represents the transition to untenability. In turn, the underlying exposure time component then represents $ASET$ – at least for the particular fire effect.

With regards to an occupant's evacuation, Purser distinguishes three different modes of consequences to which the *FEC* respectively *FED* concepts may be applied: impairment, prevention, and lethality. However, lethal time-dose-relationships only play a minor role since lethality has to be considered as a consequence of impairing and preventing exposures in advance. Hence, they will be excluded in the scope of this thesis.

So far, the presented *FED* concept is applicable to multiple fire effects and different consequence modes. The following paragraphs will now provide the derivation of concrete performance measures. Purser used the knowledge about relevant physical fire effects and gas components as well as their physiological effects in order to set up predictive models for the above-mentioned modes of consequences. The data mostly are derived from animal experiments and has been back-calculated to human beings. Further reading about underlying methods, validation, interactions between particular gas species, and limitations can be found in the literature referenced in [Purser, 2016a].

Impairment by Irritation Besides asphyxiant gas components, smoke may contain irritant components as well. This mostly is the case, when the present fuel consists of halogen compounds, e.g. chlorine. In order to derive information about irritation, the *FEC* concept can be applied to the expected irritant gas components as shown in Equation 3.7 and 3.8. In the scope of this thesis, only HCl has been implemented. Note: In accordance with the literature, the *FEC* is referred to as FIC (fractional irritant concentration) for this application. As discussed in section 2.4.2, the criteria for impairment and incapacitation are assumed to be 200 and 900 ppm respectively. The escape of an occupant is considered as impaired or prevented if the fraction exceeds unity.

$$FIC_{\mathrm{Im}} = \frac{\sigma_{\mathrm{HCl}}}{200\,\mathrm{ppm}} \tag{3.7}$$

$$FIC_{\mathrm{In}} = \frac{\sigma_{\mathrm{HCl}}}{900\,\mathrm{ppm}} \tag{3.8}$$

where:

FIC_{Im} is fractional irritant concentration for impairment by irritation,

FIC_{In} is fractional irritant concentration for incapacitation by irritation,

σ_{HCl} is volume concentration of HCl in ppm.

Impairment by Visibility In terms of occupants' potential exposure to smoke, Purser states that "their exit choice and movement speed (and hence their travel time) can be affected" [Purser, 2016a, p. 2316]. The empirical bases and the implementation of these points have already been addressed comprehensively within this chapter. However, there is still need for a particular measure that reports the spatiotemporal coincidence of occupants and smoke. Again, this is achieved by employing the *FEC* concept to the extinction coefficient. As presented in Section 2.4.2, the threshold extinction coefficient is supposed to roughly represent visibility conditions below 20 metres. Hence, the escape of an occupant is considered to be (at least temporarily) impaired while the fraction provided in Equation 3.9 exceeds unity.

$$FEC_{\mathrm{Smoke}} = \frac{E}{0.23\,\mathrm{m}^{-1}} \tag{3.9}$$

where:

FEC_{Smoke} is fractional effective concentration for impairment by visibility,

E is extinction coefficient in m^{-1}.

Impairment by Heat The assessment of exposures to heat needs to account for both the radiative as well as the convective impact from smoke present in an occupant's environment. For the derivation of tenability times representing tolerable conditions, Purser proposes an empirical relation that utilises the smoke temperature. If the smoke temperature is derived from a time series, the thermal impact can be expressed as a function of time. The integrated reciprocal of this empirical relation yields the fractional effective dose for heat as shown in Equation 3.10.

$$FED_{\mathrm{Heat}}(t_{\mathrm{e}}) = \int_0^{t_{\mathrm{e}}} \frac{1}{2 \cdot 10^{31} \cdot T(t)^{-16.963} + 4 \cdot 10^{8} \cdot T(t)^{-3.7561}} \mathrm{d}t \tag{3.10}$$

where:

FED_{Heat} is fractional effective dose for tolerable heat conditions,

T is smoke temperature in °C.

Prevention by Incapacitation On the basis of an extensive literature review, Purser identified incapacitation as the "key determinant" for fatalities during fires. In principle, the incapacitation of humans is mainly driven by asphyxiation. In general, smoke is a complex mixture of numerous chemical compounds. Its composition strongly depends on the present fuels, fire dynamics, ventilation conditions and many other factors. In this respect, the fire effects mentioned above represent gas concentrations. In order to account for varying toxicological potentials of particular smoke components, Equations 3.5 and 3.6 can be expressed as summation of gas concentration time series and corresponding tenability doses. This conjunction yields Equation 3.11.

$$FED_{\mathrm{In}}(t_{\mathrm{e}}) = \int_0^{t_{\mathrm{e}}} \sum_{\mathrm{i}=1}^{n} \frac{\sigma_i(t)}{D_{\mathrm{t,i}}} \mathrm{d}t \tag{3.11}$$

where:

FED_{In} is fractional effective dose for incapacitation,

σ_i is volume concentration of gas component i,

$D_{\mathrm{t},i}$ is dose representing tenability applicable to gas component i.

So far, this expression is conceptual and its application requires the introduction of concrete gas components and the corresponding threshold doses. In terms of asphyxiation, Purser identified carbon monoxide (CO) and hydrogen cyanide (HCN) as the two major gas components. While CO will occur in almost all combustion processes, the presence of HCN is dependent on the nitrogen content of the fuels. Since the physiological effects of both gases are very different, a separated consideration of both is inevitable. For instance, incapacitation by CO can be accurately predicted by a simple dose relationship as shown in Equation 3.4, while the Carboxyhemoglobin (COHb) concentration causing incapacitation is applied. COHb is the complex, which is formed by haemoglobin and CO in the blood of an exposed person. On the contrary, the incapacitation process by HCN is extremely non-linear. Here, concentrations smaller than 80 ppm result in a tenability of about one hour. In contrast, an increase of up to 180 ppm will decrease the tenability times to approximately two minutes [Purser, 2016a, p. 2359]. Furthermore, the concentrations of both oxygen (O_2) and carbon dioxide (CO_2) are relevant for the respiration of a human being. In principle, decreased O_2 concentrations induce hypoxia. The impact of CO_2 is more ambivalent: on the one hand, moderately increased concentrations result in higher respiration rates, which in turn cause an overall increased inhalation. On the other hand, very high concentrations inherently decrease the O_2 concentrations and result in hypoxia as well. The incapacitation of an occupant can be predicted according to Equation 3.12.

$$FED_{\mathrm{In}}(t_{\mathrm{e}}) = \int_0^{t_{\mathrm{e}}} \left(\left(\frac{3.317 \cdot \sigma_{\mathrm{CO}}(t)^{1.036}}{D \cdot 10^{-5}} + \frac{\sigma_{\mathrm{HCN}}(t)^{2.36}}{2.43 \cdot 10^{7}} \right) \cdot \dot{V}_R \cdot \exp\left(\frac{\sigma_{\mathrm{CO_2}}(t)}{5} \right) + \frac{1}{\exp\left(8.13 - 0.54 \cdot (20.9 - \sigma_{\mathrm{O_2}}(t))\right)} \right) \mathrm{d}t \tag{3.12}$$

where:

$\sigma_{\mathrm{CO_2}}$ is volume concentration of carbon dioxide in Vol%,

σ_{CO} is volume concentration of carbon monoxide in ppm,

σ_{HCN} is volume concentration of hydrogen cyanide in ppm,

$\sigma_{\mathrm{O_2}}$ is volume concentration of oxygen in Vol%,

D is % COHb causing incapacitation. Here: 20 %,

FED_{In} is fractional effective dose for incapacitation,

$\dot{V}_{\mathrm{R}}$ is respiration rate. Here: $50\,\mathrm{l\,min^{-1}}$.

It should be noted that additional terms, e.g. for nitrogen oxides (NO_x) may be incorporated into this concept. However, according to the recommendations by Purser, these can be omitted "without significant error" when assessing asphyxia [Purser, 2016a, p. 2372]. Furthermore, additional terms for lethal doses are excluded as argued above.

The specification of the respiration rate $\dot{V}_R$ and the COHb concentrations yielding incapacitation D deviate from the "default" parameter recommendations. In the scope of this thesis, the parametrisation shown in Equation 3.12 is supposed to account for the higher physical efforts during the evacuation of the underground station, i.e. when moving up stairs.

Implementation Based on the recommendations by Purser, the hazard analysis is triggered in "successive short periods ($<$ 1 min) at the breathing zone" of building occupants [Purser, 2016a, p. 2318]. Hence, the data extraction is conducted at 1.95 m above the ground. Assuming an average breathing rate of $20\,\mathrm{min^{-1}}$, the `ToxcityAnalysis` class is called by the `Simulation` class every three seconds of simulation time for each pedestrian object. The conduction of the hazard analysis routine is thus timed in an appropriate order of magnitude. Within the `ToxcityAnalysis` class, all relevant variables for the calculation of the afore-mentioned *FED* and *FEC* values are initialised. For a pedestrian's global time and position in the domain, the relevant fire simulation data are requested from the `FDSMeshStorage` class. Having a pedestrian's data available for a given time and space, the *FED* and *FEC* values are then computed and – where applicable – transferred to the pedestrian class. Finally, the results of the hazard analysis are consecutively written out in *XML* format. Compared to pure text-based formats, the tree structure of *XML* will allow for a more efficient exploration of the extensive data amounts during the subsequent post-processing.

Chapter 4

Fire Simulation

In this chapter, the subsystem *Fire* is addressed. Firstly, a brief documentation of numerical and computational aspects for the application of the Fire Dynamics Simulator is given. In the next step, relevant auxiliary specifications regarding the built environment, combustibles, and fire sources are discussed. An important part of this chapter is the setup of the simulation ensemble, which constitutes comprehensive considerations of fire locations, design fires, and climatic conditions. Followed by that, the simulation ensemble is examined in a first stand-alone analysis, which focusses on *ASET*. For this purpose, an advanced methodology for the assessment of multiple performance criteria in spacious domains is introduced.

4.1 Fire Model and Computation

Fire Model One of this study's components is the computation of a simulation ensemble of selected fire scenarios inside the station. For this purpose, the *CFD* model Fire Dynamics Simulator (*FDS*), Version 6.3.2 has been utilised. The Fortran-code has been developed at *NIST* since the late 1990s and is predominantly designated for the simulation of fire-driven flows in built environments. Several submodels allow for assessing a variety of relevant questions in fire safety engineering. The Navier-Stokes equations are solved via the finite difference method, while the applicability of the solution is limited to flow regimes with low Mach numbers. The spatial discretisation is based on a structured, uniform grid. With regards to *FSE* analyses, turbulences are usually resolved with the *LES* model. However, a *DNS* implementation is available as well. The distinctive feature in comparison to conventional *CFD* codes is the incorporation of "source terms and boundary conditions that describe the turbulent combustion of gaseous fuel and oxygen, [and] the transport of thermal radiation

through hot, soot-laden gases" [McGrattan et al., 2015a]. In the course of the development, the code has been parallelised for both *OpenMP* and *MPI*. The aforementioned features as well as the open-source distribution increased the popularity of *FDS* in both research and application during the past years.

Computation After a grid sensitivity study had been performed, a grid resolution of $\mathrm{d}x = 15\,\mathrm{cm}$ was chosen throughout the entire geometry. This is in accordance with the expected magnitudes of heat release and the characteristic fire diameter discussed in [McGrattan et al., 2015c] and [McGrattan et al., 2015b]. Furthermore, it allows for an adequate representation of filigree geometry components, which may be relevant in terms of the occurring fluid dynamics, e.g. stairs, lintels, or beams.

As illustrated in Figure 4.1, the domain has been decomposed into twelve meshes with a total number of approximately 26 million grid points. On the basis of the general principles postulated in [McGrattan et al., 2015c] and preliminary studies, the arrangement of the meshes has been optimised in terms of three additional criteria. Firstly, staircases are not intersected by any mesh transitions. The second principle is that the spatial extends of the mesh transitions were attempted to be minimised. In order to avoid slicing of the plume areas, the fire locations have been incorporated for the placement of the mesh transitions as well.

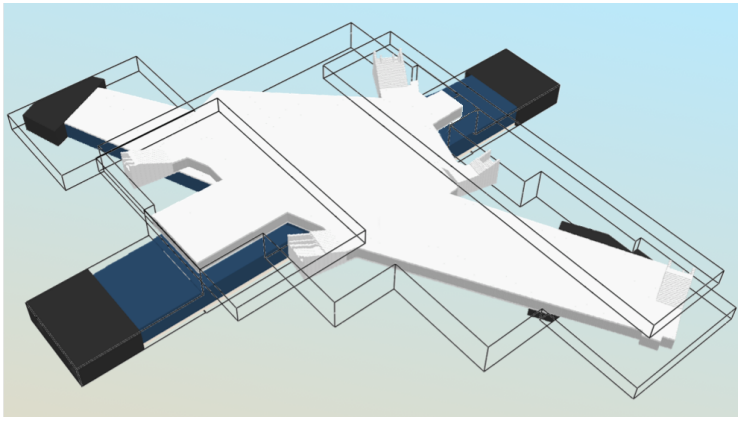

Figure 4.1: Decomposition of the computational domain into 12 meshes.

The high computational effort is distributed with the aid of a hybrid parallelisation strategy using both *MPI* and *OpenMP*. In concrete terms, each of the 12 meshes is assigned to one particular *MPI* task, which itself is divided into four *OpenMP* threads.

Hence, a total number of 48 cores per simulation is utilised. These resources can be provided by two compute nodes on the JURECA system at the Jülich Supercomputing Centre [Krause, 2015].

4.2 Auxiliary Specifications

4.2.1 Built Environment

Geometry The station layout and its representation as a generic geometry format has already been presented in Section 1.2.3. Here, the focus is set on the preparation of the geometry in order to conduct *CFD* simulations. For *FSE* tasks, especially, one of the most basic requirements is a "waterproof" representation of the model without unintended leakages. For this purpose, a mass balance analysis across all openings has been carried out in advance.

Additional considerations were necessary regarding the spatial discretisation's impact on the representation of the geometry. Since *FDS* solves the conservation equations on a structured grid, the representation of filigree building elements may imply weaknesses. This applies to all structural components that are slanted in the domain, e.g. staircases or non-orthogonal walls. In orientation to the V+V framework proposed by [Münch, 2013], simplified test cases were set up to cover these concerns. In terms of mass and heat transport, the results of these studies did not remarkably yield deviating results.

Thermal Properties In FDS, the conjunction of geometry elements and thermal properties is realised by defining materials, which are assigned to surfaces. In order to represent the structure and relevant interiors of the station, five major materials have been specified and assigned to four surfaces. In this respect, surfaces are specified by their thickness d and – if applicable – by their composition of multiple materials. Relevant material parameters are specific heat c_p, thermal conductivity λ, and density ρ. An overview of the configuration is given in Table 4.1. The applied values have been gathered from [Schneider, 2012].

Table 4.1: Overview of defined surfaces, materials including their particular properties, and major examples of their application.

Surfaces	**Materials**	**Application**
`SURF_CONCRETE`	`CONCRETE`	structural components
$d = 0.3\,\mathrm{m}$	$\lambda = 2.5\,\mathrm{W\,m^{-1}\,K^{-1}}$	
	$\rho = 2400\,\mathrm{kg\,m^{-3}}$	
	$c_p = 1.0\,\mathrm{kJ\,kg^{-1}\,K^{-1}}$	
`SURF_STEEL`	`STEEL`	railcar undercarriage
$d = 0.003\,\mathrm{m}$	$\lambda = 50\,\mathrm{W\,m^{-1}\,K^{-1}}$	
	$\rho = 7800\,\mathrm{kg\,m^{-3}}$	
	$c_p = 0.45\,\mathrm{kJ\,kg^{-1}\,K^{-1}}$	
`SURF_ALU_SANDWICH`	`ALU`	sandwich compound
compound:	$\lambda = 160\,\mathrm{W\,m^{-1}\,K^{-1}}$	railcar body
`ALU+INSU+ALU`	$\rho = 2800\,\mathrm{kg\,m^{-3}}$	
$d = 0.003$+0.1+0.003 m	$c_p = 0.88\,\mathrm{kJ\,kg^{-1}\,K^{-1}}$	
	`INSU`	
	$\lambda = 0.4\,\mathrm{W\,m^{-1}\,K^{-1}}$	
	$\rho = 100\,\mathrm{kg\,m^{-3}}$	
	$c_p = 1.03\,\mathrm{kJ\,kg^{-1}\,K^{-1}}$	
`SURF_GLAS`	`GLAS`	railcar glazing
$d = 0.01\,\mathrm{m}$	$\lambda = 1\,\mathrm{W\,m^{-1}\,K^{-1}}$	glass segments shopping area
	$\rho = 2500\,\mathrm{kg\,m^{-3}}$	
	$c_p = 0.75\,\mathrm{kJ\,kg^{-1}\,K^{-1}}$	

Openings A number of studies has shown that both fire and combustion dynamics strongly depend on the ventilation conditions that are provided by a built environment [Carvel and Beard, 2005], [Ingason, 2005], [Purser and Purser, 2008].

Across its three levels, the station model comprises 13 openings. Eight of them represent the tunnel portals of U8 and U9, which serve as interfaces to the adjacent tunnel system. The remaining five openings are the staircases connecting the concourse level with the surface. Throughout the entire station, a total cross-sectional area of about $180\,\mathrm{m^2}$ is available for inlet and outlet airflows. Moreover, two trains are considered on both U8 tracks and another one on the incoming U9 track. Additional considerations on smaller scales are necessary in order to specify the ventilation conditions inside the rail cars and shopping units.

Regarding the trains, the following assumptions were made. Firstly, all of the 18 carriage doors towards the platform are considered to be open. The different train models, which are operated by *BVG* on U8 and U9 and their expected effect

on ventilation conditions, are incorporated as well. Hence, both a trainset with six separate cars and a trainset with six continuously accessible cars will be examined. In this respect, the six car trainset yields a remarkable, but rather punctual release of heat and smoke with good thermal buoyancy. In case of the continuously accessible trainset, the smoke and heat release is expected to be less localised and, thus, less buoyant.

Finally, the performance of the carriage glassing needs to be addressed. In this respect, the integrity does not only depend on the glass type but also on its mounting [Bulk, 2015] – and of course on the fire scenario. In orientation to [Wilk, 2012], the windows of the affected carriage are assumed to collapse consecutively within a period of 720 to 1020 seconds after ignition. The structure of the car body is assumed to remain intact.

With regards to fire scenarios in the shopping units, some basic considerations about the ventilation conditions during compartment fires are necessary. The shopping units and concourse area are separated from each other by glass segments and glass doors without a qualified fire resistance. It is assumed that the doors are opened and that the glass segments remain intact. Depending on the fire scenario and the number and width of doors, the expected fire dynamics may thus be limited by the resulting cross-sections of the openings.

Smoke and Heat Extraction System The retail units inside the concourse level are equipped with a smoke and heat extraction system (*SHE*), whose ventilation ducts are wall-mounted. The control logic is triggered by the fire detection system and closes all vents except the ones in the compartment where a fire is detected. The system is assumed to operate fully one minute after detection. Depending on the floor space of the shopping units, the number of vents differs from one to five. Their effective area accounts to $0.076\,\mathrm{m}^2$. The volume flow of each retail unit has been excerpted from measurements, which were recorded after the installation [Eichelberger, 1998]. The technical specifications for the considered compartments are summarised in Table 4.2. The three locations associated to the particular retail units are taken up in Section 4.3.1.

Table 4.2: Technical specifications of the *SHE* system.

Retail Unit	**Openings** / A_{eff} **in** m^2	$\dot{V}_{\text{SHE}}$ **in** $\text{m}^3\,\text{h}^{-1}$
5 (location 1)	2 / 0.152	2539
17 (location 2)	5 / 0.380	4712
9 (location 3)	4 / 0.304	8313

4.2.2 Combustibles

In this section, the design fires, which are going to be introduced in Section 4.3.2, are assigned with combustibles. This specification is an influential part for the outcome of any *FSE* analysis. Initially, a representative fuel for a particular building use and a corresponding fire scenario has to be identified. In the next step, the production rates (yields) for the particular components to which the fuel is decomposed during the combustion process have to be specified.

In order to reduce the complexity of the entire simulation setup, two major fuels will be considered within this study. These are polyurethane (PUR) for the fire scenarios related to rolling stock and polyvinyl chloride (PVC) for the luggage and retail fire scenarios. Table 4.3 provides a brief overview of the conjunction of the design fires and the appurtenant fuels.

Table 4.3: Overview of design fires and assigned combustibles.

Design Fire	**PUR**	**PVC**
BR F	x	
BR H	x	
TR16	x	
Retail		x
Luggage		x
TRIn	x	

Polyurethane In orientation to *TRStrab BS* [TRStrab BS, 2014], polyurethane is assumed to be the major representative fuel whenever a fire scenario is related to rolling stock. Further on, the technical rule states CO, CO_2, and soot as relevant combustion products and provides the corresponding yields as shown in Table 4.4. It is notable that the extent of soot release is subdivided into two different stages. This is supposed to consider the worsening ventilation, respectively the incomplete

combustion conditions while *HRR* increases. Another major combustion product of PUR is HCN, which is, however, not considered. Henceforth, the fuel definition has been extended by HCN as fourth product species. Usually, a rough 1:13 relation based on the CO-yield is proposed for this purpose, e.g. in [vfdb, 2013]. However, this approach is only valid for very small nitrogen contents, which in turn may not be appropriate for PUR. Hence, the appurtenant production rate has been chosen in orientation to [Purser and Purser, 2008] and [Purser, 2016a] for well-ventilated conditions. Nevertheless, one of Purser's major findings is that the HCN-yield may significantly depend on the ventilation conditions. However, since the yields of CO and CO_2 are assumed to be constant, the same is assumed to be the case for HCN. Please note that these assumptions may involve significant uncertainties. In reality, each vehicle generation is likely to provide different fuel characteristics. In the frame of this work, however, the presented fuel configuration will be assigned to all rail car design fires without further differentiation.

Table 4.4: Overview of polyurethane fuel characteristics based on [TRStrab BS, 2014] and [Purser and Purser, 2008; Purser, 2016a].

Reaction Product	**Yield**	**Time**
Carbon monoxide	$\gamma_{CO} = 0.122\,\mathrm{g\,g^{-1}}$	constant
Carbon dioxide	$\gamma_{CO_2} = 1.274\,\mathrm{g\,g^{-1}}$	constant
Hydrogen cyanide	$\gamma_{HCN} = 0.070\,\mathrm{g\,g^{-1}}$	constant
Soot	$\gamma_{Soot} = 0.056\,\mathrm{g\,g^{-1}}$	$t \leq 600\,\mathrm{s}$
Soot	$\gamma_{Soot} = 0.129\,\mathrm{g\,g^{-1}}$	$t > 600\,\mathrm{s}$

The temporal subdivision of the soot release has been achieved by defining a dual reaction scheme. This means that one particular reaction is assigned to two differentiated combustion phases that incorporate the above-mentioned configurations. The transition between the two phases is controlled by ramping the fuel mass fluxes of the particular reaction. For this purpose and in accordance to *TRStrab BS*, the mean heat of combustion has been chosen as ΔH_c =18 770 kJ kg^{-1}.

Polyvinyl Chloride The design fires covering the luggage and the retail unit fires are assigned with polyvinyl chloride as major representative fuel. With regards to the variety of different materials which can be expected for both luggage or retail units, this assumption is doubtlessly a notable simplification. The configuration of the fuel characteristics has been extracted from an example presented in the *FDS* User's

Guide [McGrattan et al., 2015c] and is summarised in Table 4.5. In contrast to PUR, the combustion characteristics of PVC are assumed to remain constant throughout the entire observation time, which of course is an additional simplification.

Table 4.5: Overview of polyvinyl chloride fuel characteristics based on [McGrattan et al., 2015c].

Reaction Product	**Yield**	**Time**
Carbon monoxide	$\gamma_{CO} = 0.063\,\mathrm{g\,g^{-1}}$	constant
Carbon dioxide	$\gamma_{CO_2} = 0.676\,\mathrm{g\,g^{-1}}$	constant
Hydrogen chloride	$\gamma_{HCl} = 0.583\,\mathrm{g\,g^{-1}}$	constant
Soot	$\gamma_{Soot} = 0.172\,\mathrm{g\,g^{-1}}$	constant

4.2.3 Fire Sources

The derivation of design fires in Section 4.3.2 is not going to account for pyrolysis and flame spread modelling. However, by means of an adequate plume formation during the early stages of a fire, it is necessary to conjunct the explicitly defined heat release rates with a certain fire spread. For this purpose, the fire sources have been modelled with the help of the *FDSgeogen* framework, which is described in Section 4.4 in more detail. One of its convenient functionalities is the representation of fire spread across a rectangular surface. In concrete terms, the surface is discretised in finite elements, which are successively ignited. This process can be triggered by both common parameterised models, e.g. αt^2, but also by arbitrary *HRR* time series. The latter feature, especially, goes beyond the functionalities currently implemented in FDS. The outlined approach has been applied to the design fires presented above. An exemplary time series of the fire spread and the corresponding heat release rates applicable to the *BR F* design fire is illustrated in Figure 4.2.

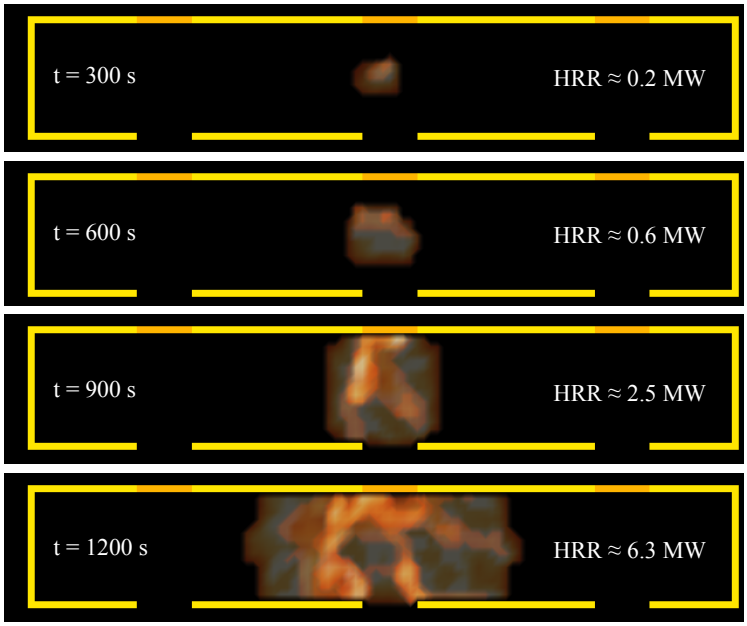

Figure 4.2: Top view of time, flame spread, and corresponding heat release rate in a carriage applicable to the design fire *BR F*.

In case of high-energetic rail car fires, the fire surfaces have been placed inside the car bodies with a total size of 14.4 m × 2.4 m. The surfaces have been subdivided into 384 subelements, whereas each subelement has an edge length of 0.3 m. In order to account for a proper plume formation, this edge length has been reduced to 0.15 m for the medium- and low-energetic fires. For the retail units, surfaces with a size of 2.1 m × 2.1 m have been implemented. For the sprinklered design fire, this complies quite well with the *HRRPUA* of 250 kW m^{-2} given by [DIN EN 1991-1-2/NA, 2015]. The luggage fire surface is represented by a simple rectangular box, whose top surface has an extent of 0.45 m × 0.60 m. The sideward surfaces of this idealised luggage item are not considered as fire surfaces. Finally, the self-extinguishing rail car fire is assumed to spread over a maximum area of 0.60 m × 0.60 m.

4.3 Fire Scenarios

In this study, the term "fire scenario" is supposed to unify the initial and boundary conditions applicable to fire locations, design fires, and climatic conditions. In the first

instance, the relevance of potential fire events are considered in general. With regards to the station and its use(s), three different fire events have been identified. These are a carriage fire, a retail unit fire, and a luggage fire. In the following paragraphs, these events are supplemented with additional, qualitative considerations and the expected potentials for challenging the achievement of the protection goals.

Carriage Fire With regards to underground stations, the fire of a carriage is supposed to be a severe fire scenario in manifold ways. Inevitably, a carriage consists of numerous combustibles that may contribute to a fire. In the past years, the fire performance of rolling stock vehicles has remarkably been improved, e.g. by advancing and harmonising standards such as EN 45545. However, recent incidents have proven that even state of the art vehicles still may burst into a fully developed fire [dpa, 2016], [EUB, 2016]. Within the METRO full-scale tests (see Section 1.3.3), ignition sources and interior material performance have been identified as the key answers to the question if a fire will spread or not [Ingason et al., 2012]. Unfortunately, these two factors are slightly diffuse. Firstly, many transportation companies obtain new vehicles more or less continuously. This results in diverse fleets with varying ages and product performances. Secondly, the standardised ignition models applicable to many interior components are intended to cover minor arson. More intense events, e.g. severe arson, luggage fires, or high-voltage failures, may exceed the performance level assured by the standards.

On the basis of the arguments stated above, four major fire scenarios have been identified as subsets of carriage fires. First of all, the two major generations of *BVG* vehicles serving on U8 and U9 will be incorporated. Hence, the models *BR F* and *BR H*, which represent varying operation times between approximately 10 and 30 years, are considered. Further on, a generalised fire scenario is utilised. The latter is supposed to represent a multitude of different train models, e.g. if no insights into the fire performance of a particular vehicle are available. Finally, a self-extinguishing fire scenario will be examined in order to account for either low ignition initials, advantageous material performance, and/or staff intervention.

With regards to the protection goal life safety, the occurrence of a fully developed fire would yield extensive heat release rates and fuel mass fluxes accordingly. The latter may result in a remarkable release of soot and toxic effluents, which are likely to affect the entire station. However, also a self-extinguishing fire may be challenging for the design. Since the lower heat release will result in a less buoyant hot gas layer, it may impede the formation of smoke-free layers.

Moreover, a fully developed car fire also challenges the structural integrity of the built environment. This problem will, however, not be addressed in this study.

Luggage Fire In the field of rail transport, luggage fires are associated with a considerable risk. For instance, they are considered as one of five designated ignition models during the design phase of rail vehicles [DIN EN 45545-1, 2013]. Consequently, luggage fires ought to be considered for the assessment of infrastructures as well. Studies on amounts of luggage in underground stations have been conducted in the frame of the METRO project (see Section 1.3.3). It has been found that 82 % of all passengers carried some sort of luggage. Depending on the weekday, the luggage weight per passenger varied between 3.5 and 4.5 kg. The most frequent contents were textiles, paper, and electronic devices [Ingason et al., 2012, pp. 28-30], while latter may represent a potential ignition source. The moderate heat and smoke release is supposed to represent the lower boundary of the overall scenario set. However, the work of Bulk showed that luggage fires may emit remarkable amounts of toxic and/or irritant effluents [Bulk, 2015]. Finally, another particularity is the fact that a luggage fire may effectively occur throughout the entire station.

With the goal of assessing life safety, the challenging characteristics of this scenario subset are mainly the limited stratification of a stable hot gas layer as well as the emission of irritant fire effluents. The impact on the structure is, however, expected to be negligible.

Retail Unit Fire Since the concourse level hosts multiple retail units, a corresponding fire has been considered as an additional fire scenario. Retail spaces, in particular, are characterised by high fuel loads and comparatively high fire growth rates. In order to cope with these characteristics, a number of safety measures has been implemented over the station's service time. The latter are considered for the configuration of this scenario subset as well. Firstly, an automatic fire suppression system is installed throughout all retail spaces. Secondly, the conventional ventilation system serves as smoke and heat extraction system once triggered by the fire detection system. The relevant technical specifications of both systems have been presented in this section as well as in Section 1.2.3. For the upcoming analyses, a proper operation of the sprinkler system is assumed. Moreover, the upcoming quantitative risk analysis as well as investigations concerning structural integrity will utilise an additional scenario subset without sprinkler intervention. This scenario will, however, be excluded within this study.

The intended challenges induced by the sprinklered scenario are manifold. For sure, the impact on the lower levels will be marginal. However, in spatial terms, the concourse level has a very strategic meaning since it unifies all means of escape. In this respect, a sprinklered scenario will yield moderate but remarkable heat and smoke spread into the concourse area. The latter provides a rather non-convex geometry, which is frequently obscured by massive pillars. With regards to the Daegu incident study (see Section 1.2.2), these circumstances may impact occupant-related processes, e.g. way-finding, or recognition of evacuation cues.

4.3.1 Fire Locations

Because of the spacious built environment and the non-trivial escape route system, an important role has been assigned to the locations that correspond to the aforementioned fire scenarios. A couple of studies support this focus. For instance, Chen et al. conducted numerical studies on the formation of stack effects during fire events in subway stations [Chen et al., 2003]. Their results imply that the propagation of smoke may distinctively depend on the question which opening is reached first. In other words, once a certain flow regime has established, the system may remain in equilibrium as long as further conditions only change marginally. Hence, labile systems may be prone to minor changes. In temporal terms, these kind of changes may be induced, e.g. by time-dependent heat release rates or background airflows. However, with respect to the spatial conditions, asymmetries may influence the smoke dynamics. The results of numerical studies on mechanical smoke extraction systems in [Schmidt, 2015] and [Schröder et al., 2016] back these thoughts. Similar findings of the importance of fire locations in connection to expected occupant scenarios are discussed in [Nilsson and Fahy, 2016].

Given the insights stated above, nine fire locations throughout the entire station have been defined. In this respect, each level is subdivided into three single locations. In case of the platform levels, they are – as far as possible – evenly distributed along one particular track. Hence, no further variations among the tracks of one platform level are made. To varying degrees, the final positions along the tracks were indicated by operational aspects (e.g. stopping points), the carriage dimensions, and mesh alignment limitations. Finally, three different locations have been distributed across the concourse level as well. Aiming at a reasonable placement of the luggage fire, the positions were slightly adjusted towards the platforms and concourse areas. A graphical overview of the nine fire locations is given in Figure 4.3.

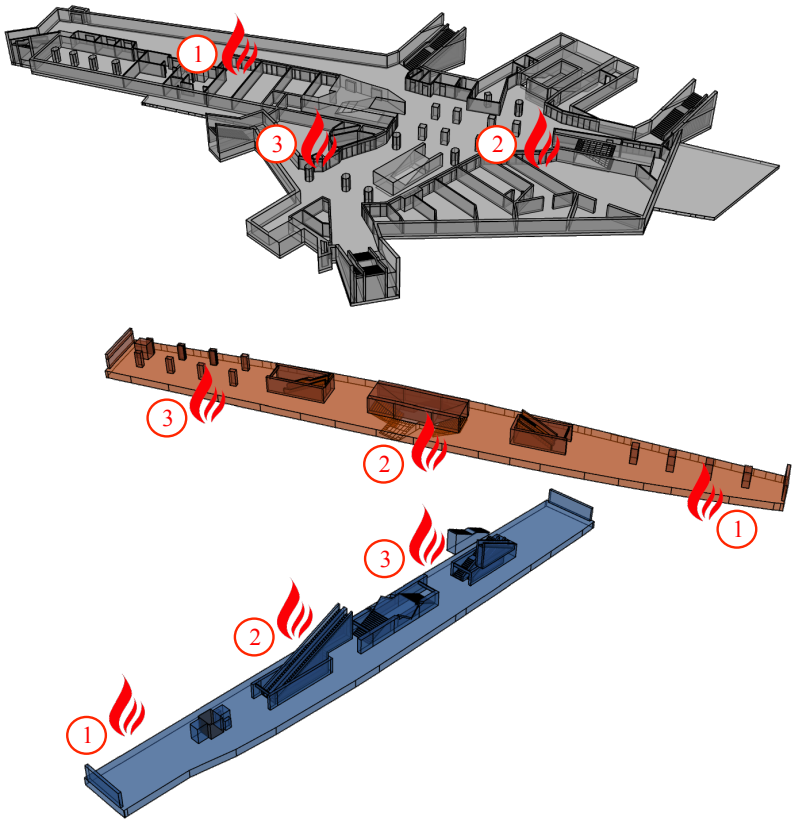

Figure 4.3: Distribution of nine fire locations across the station.

4.3.2 Design Fires

In order to quantify the fire scenarios verbally defined above, six different design fires have been selected. In principle, they can be grouped into fires with high, medium, and low heat releases. Obviously, the high-energetic fires comprise the fully developed rail car fires, whereas a medium heat release is represented by the sprinklered retail unit fire. Finally, low-energetic fires incorporate both a luggage fire and a self-extinguishing fire inside a rail car.

High-energetic Fires In general, a fully developed rail car fire yields multiple magnitudes of MW heat release. However, the development of heat release and/or other related quantities over time significantly depends on multiple factors, such as

ignition initials, material performance, or ventilation amongst many others. In order to cover a maximum variety concerning these questions, a set of three design fires has been agreed upon. Contrary to preliminary works, e.g. [Schröder et al., 2014] or [Schmidt, 2015], this study refrains from a t-squared approach for the formulation of a time-dependent heat release. Instead, existing studies of the fire performance of *BVG* rolling stock as well as a regulatory design fires are utilised.

Firstly, the operating rolling stock of *BVG* is considered. Both lines U8 and U9 are served by the vehicle generations *BR F* and *BR H*. A comprehensive study of the fire performance of the latter has been conducted in [Wilk, 2010]. The presented data for these two vehicles is extracted from this report.

BR F especially has successively been delivered and redesigned over a period of 21 years from 1973 to 1994 [BVG, 2007]. Since the retirement of the very first *BR F* vehicles is already ongoing, the F 84 generation has been chosen as a representative with intermediate age. Depending on the daytime, *BR F* can be operated in two-car, four-car and six-car configurations. Each single carriage is a separate unit with a length of approximately 16 m and has three doors per side. The design fire curve of *BR F* starts with an almost linear increase of *HRR* to roughly 500 kW within the first 10 minutes. In the period between the tenth and twentieth minute, *HRR* increases exponentially to 6.5 MW. The maximum *HRR* of approximately 16.5 MW is reached after about 25 minutes and lasts until the end of the observation time.

BR H has been delivered since 1995 and represents the most recent generation of *BVG* rolling stock. In contrast to *BR F*, it is exclusively operated as an inseparable six-car trainset with a total length of 98 m. The trainset is entirely accessible and provides a total number of 18 doors per side. Identical to *BR F*, *HRR* is initially predicted to increase to 500 kW within the first 10 minutes. Contrary to *BR F*, the *HRR* remains on this level for another five minutes but then also increases to 6.5 MW after 20 minutes. Beginning at that time, *HRR* advances exponentially up to 45 MW until 30 minutes after ignition.

In the sense of comparable and transferable results, the regulatory design fire agreed in *TRStrab BS* is considered as well [TRStrab BS, 2014]. The technical rule postulates the application of a generalised design fire if no other knowledge about the fire performance of a particular vehicle is available. Hence, the design fire is supposed to envelope the variety of different tram and underground vehicles operated in Germany. In general, it is determined by the length of a constructionally separated unit, which means that the plateau and decay phase are dependent on the length of one unit. Based on a single 16 m long *BR F* carriage, the corresponding curve has

been derived as follows. In comparison to the *BVG* curves, the *TRStrab BS* design fire initially yields a lower heat release rate. However, beginning at the second minute after ignition, a remarkably higher heat release is assumed, which results in an *HRR* of about 5.5 MW after 10 minutes. Finally, *HRR* reaches its maximum of 22 MW 19 minutes after ignition and starts decaying after 23 minutes.

Figure 4.4 provides an overview of the introduced design fires. Please note that both the time and the *HRR* axes have been subdivided in order to assure a better differentiation between the development and fully-developed fire phases.

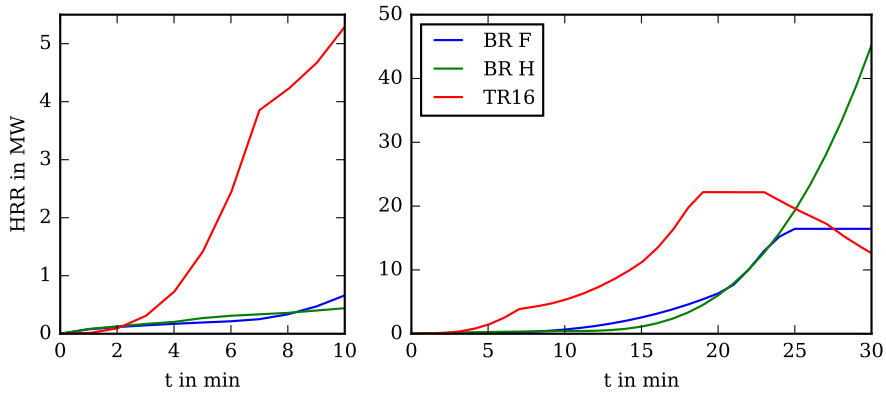

Figure 4.4: High-energetic design fires including *BVG* vehicle generations *BR F*, *BR H*, and the generalised *TR16* envelope curve.

Medium-energetic Fires The transition to medium heat release rates is represented by a design fire that serves for the fire scenarios in the retail units located in the concourse level, where an operating sprinkler system has been assumed. For this purpose, a quadratic formulation is applied in order to describe the dynamic development of heat release. For the parametrisation of the latter, the recommendations applicable to retail spaces given in [DIN EN 1991-1-2/NA, 2015] and [vfdb, 2013] are used. The expected fast fire growth is specified by $\alpha = 0.047\,\mathrm{kW\,s^{-2}}$. Accordingly, the heat release rate per unit area is assumed to be $250\,\mathrm{kW\,m^{-2}}$. In order to represent the intended intervention by the sprinkler system, it is important to consider the technical specifications of both the sprinkler system and the *SHE* system, which have been presented in Section 1.2.3. For the given geometries of all three retail unit locations (see Figure 4.3), preliminary studies revealed a maximum sprinkler activation time of

about 150 seconds. Referring to the squared fire growth, this yields an *HRR* of about 1 MW after activation. Regarding the sprinkler system, this result is based on the following specifications: $T_{\text{Activation}} = 68\,^{\circ}\text{C}$ and $RTI = 200\,\text{m}^{1/2}\text{s}^{1/2}$. Normal response sprinklers generally cover *RTI*s ranging from 80 to $200\,\text{m}^{1/2}\text{s}^{1/2}$ and assuming lower *RTI*s would yield lower activation times. Unfortunately, the manufacturer could not provide more detailed information. Thus, in the sense of conservatism, the upper bound has been applied in this situation. In addition to that, varied activation times of the *SHE* system have been found to be negligible for the determination of the sprinkler activation time. This insight can obviously be attributed to the comparatively low volume flows of the *SHE* system.

Once the sprinkler system has been activated, the fire is suppressed or extinguished. Representing a proper sprinkler intervention is an advanced topic that can be assessed in different ways. For instance, *FDS* includes a sprinkler model that directly interacts with the conservation equations and the combustion model. Another alternative is to describe the sprinkler intervention by empirical relations. For this purpose, a variety of different recommendations is available [VDI, 2006a; vfdb, 2013]. The ORPHEUS project agreed on the following approach. After activation, *HRR* remains constant for 300 seconds and than decays linearly down to zero for another 300 seconds. The constant phase especially may be considered as very conservative since some studies show a rather more effective suppression. However, in order to account for other uncertainties, e.g. shadowing effects, the constant phase appears to be appropriate. Nevertheless, the empirical approach implies some limitations. For instance, the disruption of a stratified hot gas layer will not be considered. This effect will surely be significant inside the considered compartment, but the ceiling jet entering the concourse area should already be less affected by that. In addition, vaporisation effects are neglected, which could have an influence on visibility or irritancy conditions inside the concourse area. The derived design fire for the sprinklered retail unit fire is visualised in Figure 4.5.

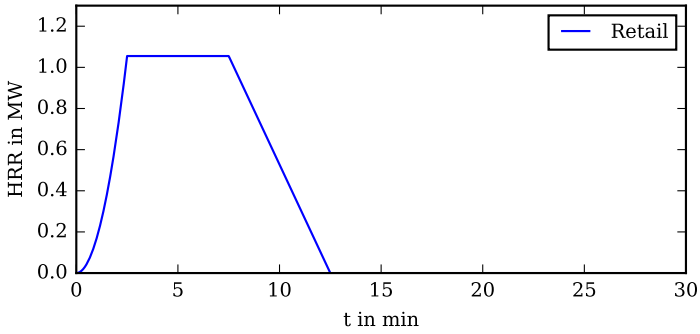

Figure 4.5: Medium-energetic design fire represented by a sprinklered retail unit fire (*Retail*).

Low-energetic Fires Finally, the low orders of heat release are represented by the design fires belonging to scenarios for a luggage fire on the platform and a self-extinguishing fire inside a rail car. Both are presented in Figure 4.6.

A number of studies on the fire behaviour of luggage items has been conducted throughout the past years [Ingason et al., 2012; Bulk, 2015]. In addition to that, standards such as [DIN EN 45545-1, 2013] provide ignition models that are supposed to cover these orders of magnitudes as well. The studies of Bulk probably provide the most reliable statistics in terms of experimentation. He tested a total number of eight different luggage types, which have been packed in order to represent a variety of different passenger types and travel purposes. According to the experimental results, the development phase has been approximated with an αt^2 approach, whereas the fire growth has been determined as $\alpha = 0.002\,931\,\mathrm{kW\,s^{-2}}$. The maximum *HRR* adds up to 120 kW and is reached after 200 seconds. This *HRR* is maintained for a duration of 18 minutes after ignition. Between the 20th and 60th minute, *HRR* linearly decreases to zero.

A rail car fire that does not advance to the full developed phase appears to be reasonable to cover variable outcomes once an ignition has taken place. However, the quantification of this scenario is a demanding task. Once again, the fire dynamics may be drastically influenced by ignition initial, vehicle performance, or extend and time of intervention. In order to ensure comparability and transferability of the results, the initial design fire postulated in *TRStrab BS* has been chosen [TRStrab BS, 2014]. Given this design fire, the development phase is represented by a linear increase

of *HRR* up to 120 kW within the first five minutes. The short-term peak *HRR* of 150 kW is reached after eight minutes. Beginning from that time *HRR* linearly decays to zero within the next 22 minutes. This design fire is intended to be the initial for the assessment of the ignition behaviour of a rail car's interior materials. In other words, its straight-forward application is based on the assumption that the interior materials will not contribute to the combustion process. In practice, however, this will be the case to some extend but the proper quantification of the underlying pyrolysis processes is a very sophisticated task, which has been excluded here. Further reading on underlying difficulties can be found in [Meunders et al., 2014]. The application in rail vehicles has been investigated in further works, e.g. [Camillo, 2013], [Bansemer, 2015], and [Bulk, 2015].

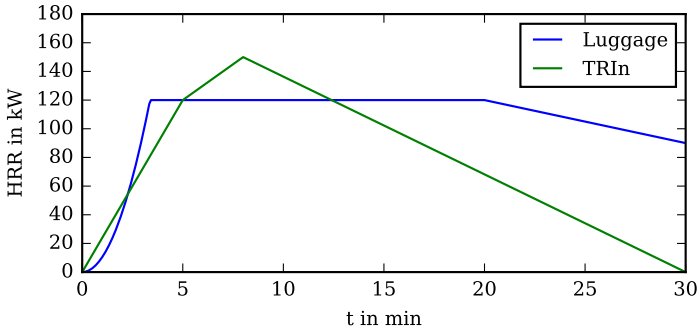

Figure 4.6: Low-energetic design fires representing a burning luggage item (*Luggage*) and a self-extinguishing fire inside a rail car (*TRIn*).

4.3.3 Climatic Conditions

One of the major objectives of this study is a more specific consideration of climatic conditions in the frame of *FSE* analyses. Hence, the definition of initial and boundary conditions plays an important role. A comprehensive summary of the data basis and the developed approach to implement climatic conditions has been presented in Chapter 3.1. Based on the assumption that the climate is predominantly temperature-driven, both summer and winter conditions shall be incorporated. In order to investigate possible differences to normal conditions, a default simulation configuration is included as well. Beside the definitions of global ambient conditions, the climate model consists of two additional components. Firstly, all openings are

endued with vents that are set on a specific gas temperature. Secondly, initial zones with the mean temperatures of the adjacent vents are placed on all three major levels. Moreover, the inner temperature of all concrete building elements is considered as well. For this purpose, a functional relation between the mean temperatures of all three initial zones and the inside wall temperatures has been derived from field measurements. The introduced configurations are summarised in Table 4.6. All remaining parameter specifications are kept unchanged.

Table 4.6: Overview of considered climatic conditions and subsequent definition of initial and boundary conditions.

Configuration	**Summer**	**Winter**	**Default**
Ambient conditions			
T_{amb} in °C	25	-9	20
Initial and boundary conditions			
T_{U8} in °C	24	15	20
T_{U9} in °C	29	15	20
T_{CL} in °C	27	3	20
T_{wall} in °C	24	12	20

4.4 Sampling

All relevant elements for the generation of multiple fire scenarios are now prepared. As discussed in Chapter 2, a bottom-up approach for life safety analysis in case of fire shall be conducted. Henceforth, no initial (risk-based) selection process is applied to the set of fire scenarios in advance. In other words, a full-factorial sampling approach that incorporates all discrete combinations of climatic conditions, fire locations, and design fires has been performed. In total, this approach yields 108 fire scenarios. In order to structure the experimental design, the fire simulation ensemble has been spilt up into three sub-ensembles each of them representing one of the three levels, U8, U9, and concourse. The corresponding matrices are provided in Appendix A.1.

The entire simulation setup was conducted with the help of *FDSgeogen*, which is a Python framework for the automated setup and processing of *FDS* simulations. The necessary inputs are provided in hierarchical *XML* format. This combination allows for a very convenient and powerful utilisation of conditional statements and constraints that shall be incorporated into the design of experiment. It has already been successfully applied during the preliminary studies in [Schröder et al., 2014] and

[Schmidt, 2015]. Additional reading – with a focus on optimisation problems – can be found in [Meunders et al., 2014].

The parametrisation conducted by *FDSgeogen* covers the implementation of the described design fires, fire locations, and all relevant initial and boundary conditions in order to represent climatic aspects. In addition to that, an extensive write-out of data needs to be set up for the upcoming post-processing. The built environment itself has been incorporated into the workflow as plain *FDS* input, utilising the third party software PyroSim. Once all relevant parametrisation tasks have been completed, *FDSgeogen* runs over all scenario specifications and builds the *FDS* input file for each scenario.

4.5 Preliminary Analysis

As soon as all simulations have been set up and computed, the focus can be set on the data analysis, which is probably the most challenging task. However, first of all, the basic requirements and needs for this task shall be reconsidered. With regards to the spatial extend of the built environment and the complexity of the introduced parameter space, the data analysis has to be advanced accordingly. Firstly, the analysis has to account for the spatial distribution of the fire simulation output data as discussed in Section 2.4.3. Secondly, an appropriate method is necessary to explore the responses of the simulation ensemble finally and derive generalisable information from the data.

Data Basis *FDS* provides spatiotemporal data of multiple physical quantities, which can be written out in a number of different ways. An overview of quantities that will be included in the upcoming analysis has been provided in Table 2.1. In this study, time series of planar slices throughout the computational domain are mainly utilised. This choice provides a two-dimensional coverage of all domain areas, which are aligned to the floor. Since the spatial discretisation of *FDS* does not allow for slanted slices, additional sensors (referred to as devices in *FDS*) provide time series of a certain quantity at a given place. This is particularly necessary for monitoring the staircase areas.

In *FSE* practice, data analysis is usually driven by the question if and when a certain threshold of an arbitrary quantity is exceeded. Hence, the analysis depends on certain numbers, which are referred to as tenability or acceptance criteria. The

ORPHEUS project has agreed upon a set of these criteria, which have been discussed in Section 2.4.2.

Challenges As introduced in Section 2.4, *ASET* is determined by evaluating the time series of a particular performance criterion at a given space. The violation of a corresponding threshold then represents *ASET*. This straightforward analysis was conducted in the frame of preliminary studies, e.g. [Schröder et al., 2014; Schmidt, 2015; Schröder et al., 2016].

However, the data exploration becomes more elaborate with increasing numbers of quantities that shall be included into the analysis, e.g. for the simultaneous assessment of optical conditions, temperatures, gas concentrations and so on. Consequently, the analysis then yields a set of different times, whose minimum is supposed to represent *ASET*. A generalised example of this understanding with two imaginary quantities a and b is illustrated in Figure 4.7.

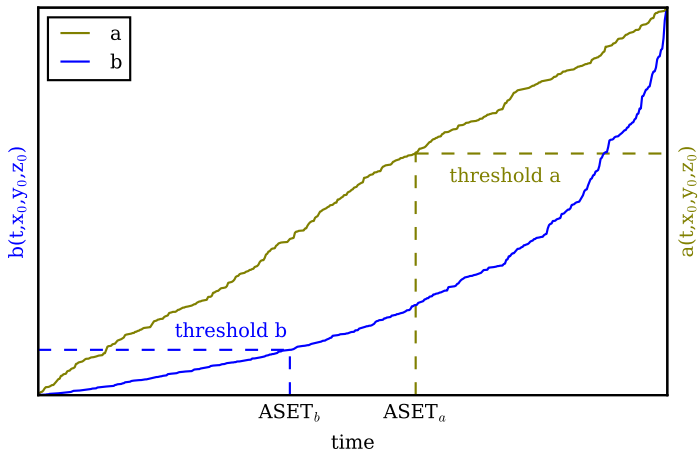

Figure 4.7: Schematic times series of two arbitrary quantities exceeding their corresponding thresholds.

Another challenge is the fact that the information retrieval is solely valid for one given location (x_0, y_0, z_0). In compartmentalised environments, this approach may provide a sufficient coverage of the spatiotemporal fire dynamics. However, in spacious environments, it may potentially result in both underestimations or overestimations. In particular, the case study of this work provides open-plan compartment areas of

multiple thousands square metres. Henceforth, the data analysis shall be conducted in a way that accounts for the spacious domain.

4.5.1 ASET Maps

In order to cope with the above-mentioned challenges, a map representation of *ASET* is introduced in order to get a better understanding of the spatiotemporal dynamics and the multi-criterial characteristics of this number. For demonstration purposes, the fire scenario `f001` is utilised, which represents a carriage fire in the U8 level as shown in Figure 4.8.

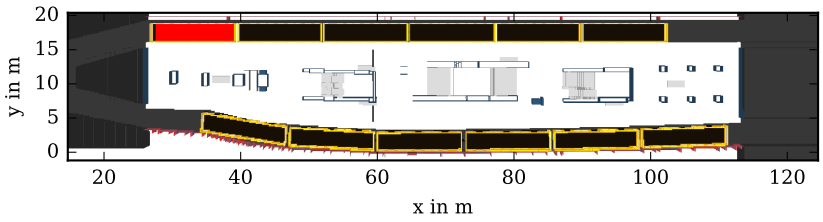

Figure 4.8: Top view on the U8 level. Four staircases connect the platform with the U9 level. Both tracks are occupied by a six-car trainset. The seat of fire is assumed in the carriage marked red.

The proposed method utilises the *FDS* slice files of the quantities introduced in Section 2.4.2. These two-dimensional time series provide a higher information content throughout the domain. An exemplary sequence of slices is provided in Figure 4.9 visualising the extinction coefficient inside the U8 level throughout the analysis time. The slices are aligned with the floor at a height of 1.95 m. Here, the intention of the proposed approach becomes apparent. The asymmetric configuration of this particular scenario yields a spatial distribution of the optical conditions along the platform.

With the help of a corresponding tenability criterion serving as threshold, it is possible to distinguish between areas with acceptable and unacceptable conditions. This insight, however, still relies on the actual time point which is evaluated. In other words: the introduced data format has to be extended by the time dimension. Prior to that, some discretisation aspects regarding time and space have to be considered.

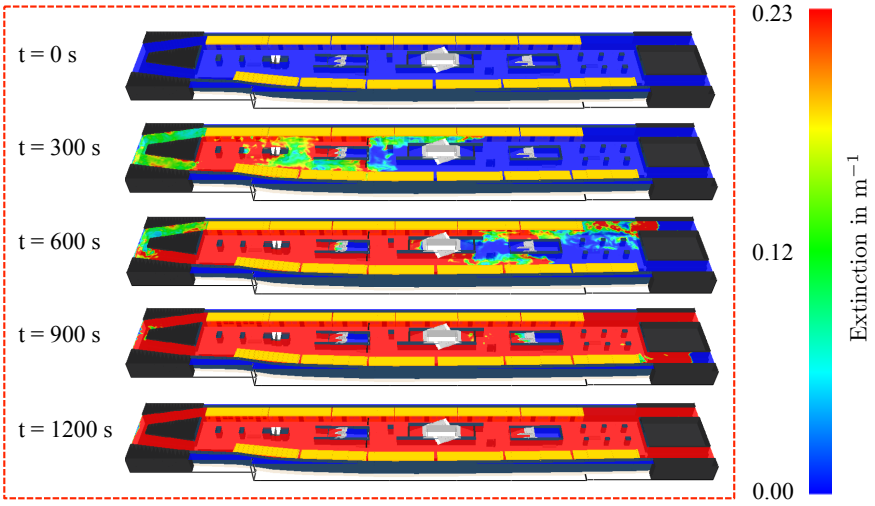

Figure 4.9: Two-dimensional slices through the U8 level aligned with the floor and visualising the state of extinction over a period of 20 minutes. Red areas indicate extinction coefficients greater than $0.23\,\mathrm{m}^{-1}$.

What time interval appears to be appropriate for determining *ASET*? For numerical reasons and depending on the specified dump times, *FDS* can provide enormous amounts of data resolved on a scale of split seconds. However, for the most engineering questions, coarser resolutions are sufficient, but what time scales are appropriate for assessing life safety in case of fire? seconds? minutes? The same applies to extents of safety and/or error margins. In terms of these questions, talking about minutes appears to be reasonable. Moreover, the spatial resolution of the analysis needs to be addressed. Since it is obviously not reasonable to decide about tenability within discretisation scales required by means of numerical accuracy, the latter is chosen as $\mathrm{d}x = 60$ cm. Larger scales may be prone to disregarding filigree building components.

With these conventions being established, a three-dimensional stack consisting of the two-dimensional slices can now be set up. The necessary data preparation is conducted by the *JPSfire* framework. In this respect, the stack's third dimension represents time. As discussed above, a time step of one minute results in a stack length of 21 slices in order to cover the overall analysis time of 20 minutes. Hence, the entire spatiotemporal dynamics of one particular quantity have been aggregated into one object. In the next step, the analysis routine iterates over every single control element and time step within this object. Based on the tenability criteria introduced

in Table 2.1, it can be decided for each iteration step if the evaluated value represents tenable or untenable conditions. In the latter case, the current iteration time step then represents *ASET* for a given location. If no tenability criterion is exceeded, *ASET* is assigned to a time of 21 minutes. The output of this process step is a time map representing the spatial distribution of *ASET* related to one particular quantity. In the next instance, this algorithm is applied to the entire set of quantities relevant for the upcoming life safety analysis. Three of the resulting *ASET* maps applicable to extinction coefficient, temperature, and carbon monoxide are exemplarily illustrated in Figure 4.10.

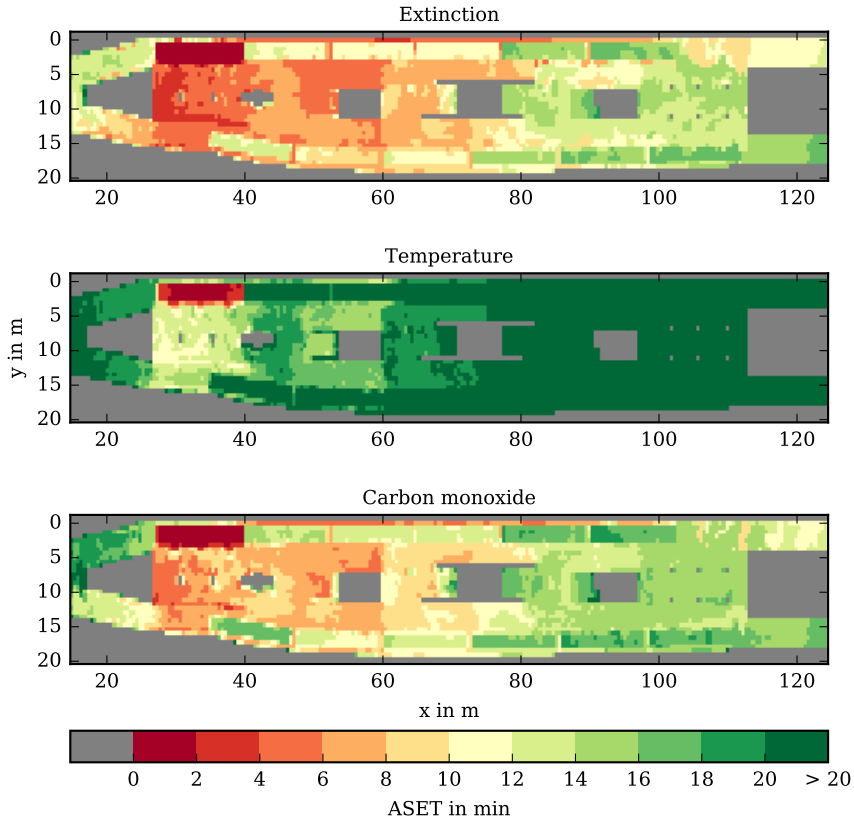

Figure 4.10: Single *ASET* maps exemplarily generated for extinction coefficient, temperature, and carbon monoxide. The colour map has been discretised into intervals of three minutes. Grey fields represent areas obstructed by the built environment.

Once all relevant single maps have been computed, the global minima out of all control elements and quantities are determined and stored in a consolidated *ASET* map. This final step yields a two-dimensional object describing the overall *ASET* for a set of locations in the domain. An exemplary map of the U8 level is illustrated in Figure 4.11. The basic logic of this routine is presented in Appendix B.1.

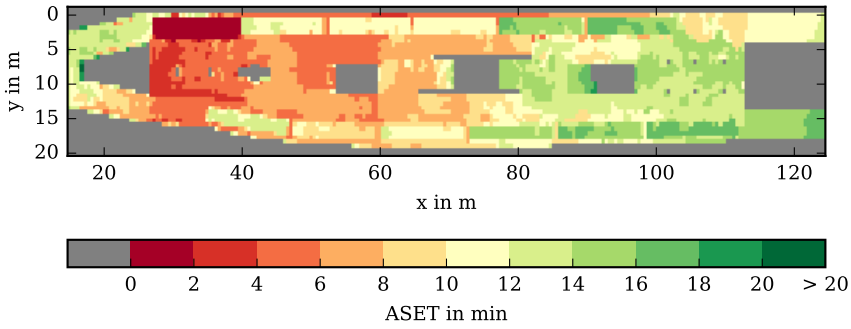

Figure 4.11: Consolidated *ASET* map derived from the entire set of incorporated quantities. Applicable for the U8 level and the fire scenario `f001`.

In comparison to the single *ASET* maps (see Figure 4.10), it can be concluded that *ASET* is predominantly determined by the extinction. For this particular fire scenario, it becomes evident that there is a spatial distribution of *ASET* throughout the platform level. In close proximity to the seat of fire (top left), untenable conditions establish within less than two minutes. More distant areas remain available for durations of up to 18 minutes.

Once a map representing *ASET* has been set up, it is possible to determine the distribution of *ASET* as shown in Figure 4.12. Technically, this conversion reduces the two-dimensional maps to a one-dimensional data series. However, the absolute number of control elements provides information on the spatial frequency of a particular *ASET*. In order to maintain this information, the distributions are intentionally visualised and handled non-normalised.

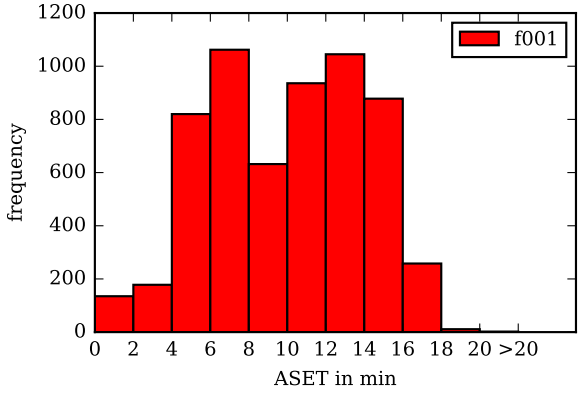

Figure 4.12: Histogram showing the frequencies of *ASET* in the U8 level applicable for the fire scenario `f001`.

The distribution clearly illustrates the wide range of *ASET*s that may occur for this particular scenario. The left bars of the distribution are control elements, where tenability thresholds have been exceeded rather immediately. The bars on the right side represent control elements, where tenability is maintained for up to 20 minutes.

In contrast to other works, e.g. [Schröder et al., 2014], [Albrecht, 2012] or [Kong et al., 2016], this distribution does not yet account for the variability induced by a set of fire scenarios but for the spatiotemporal dynamics of one fire scenario. In the next instance, the *ASET* distribution itself has to be understood as a function of every single sample within the design space. This data representation then truly accounts for the challenges discussed in Chapter 2.4.3. In order to obtain a better understanding of the distributions of *ASET* and the underlying impact of the design of experiment, a correlation analysis will be conducted.

4.5.2 Correlation Analysis

A correlation analysis requires a certain measure that allows for the comparison of the particular samples within the fire simulation ensemble. This measure will be derived from the comparison of distributions. For this purpose, a huge variety of distance metrics is available [Myatt, 2007]. However, not solely the similarity of distributions but also their proximity to the initial state shall be addressed. This state is represented by the histogram of an *ASET* map, whose control elements are entirely greater than 20 minutes (here: 21 minutes). The counterpart is the histogram of an *ASET*

map representing a particular fire scenario. Given these two distributions, a distance metric inspired by the earth mover's distance (*EMD*) has been applied [Pele and Werman, 2008, 2009]. It represents the effort which is necessary to transform the *ASET* map of the fire scenario to the *ASET* map representing the initial state. In contrast to conventional *FSE* analyses, this measure does not have a direct physical meaning. It basically represents the cumulative product of a particular time difference between *ASET* and the initial state and its number of occurrences. Since each observation corresponds to an area (0.36 m^2 per control element of the map in this case), it may also be understood as time × area, which is necessary to recover the initial state of a particular control element. Based on the *ASET* map of the U8 level, the basic idea is illustrated in Figure 4.13.

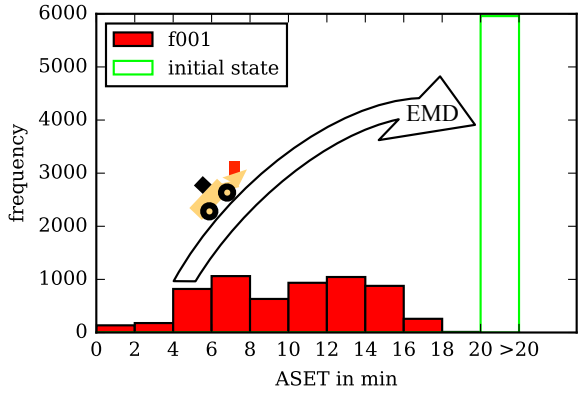

Figure 4.13: ASET map histograms of fire scenario `f001` (red) and initial state (green) in the U8 level. The frequency of control elements with an *ASET* less than and equal 21 minutes is illustrated. The *EMD*-inspired metric represents the necessary effort to transform `f001` to the initial state.

In order to facilitate the multivariate analysis of a multitude of scenarios, a scalar score is necessary to capture the development of *ASET* within the entire station. For this purpose, the *EMD*s of all three levels are summed up to a global score $EMD_{\text{ASET=21 min}}$. In this respect, a high score corresponds to a high effort in order to recover the initial state (*ASET* is 21 minutes). Figure 4.14 provides a first overview of the impact of the particular fire scenario parameters. For this purpose, all three locations, six design fires, and three climate conditions are plotted against the intro-

duced distance metric. The sequence of the design fires corresponds to the total heat release and the colouring visualises at which level a fire was assumed.

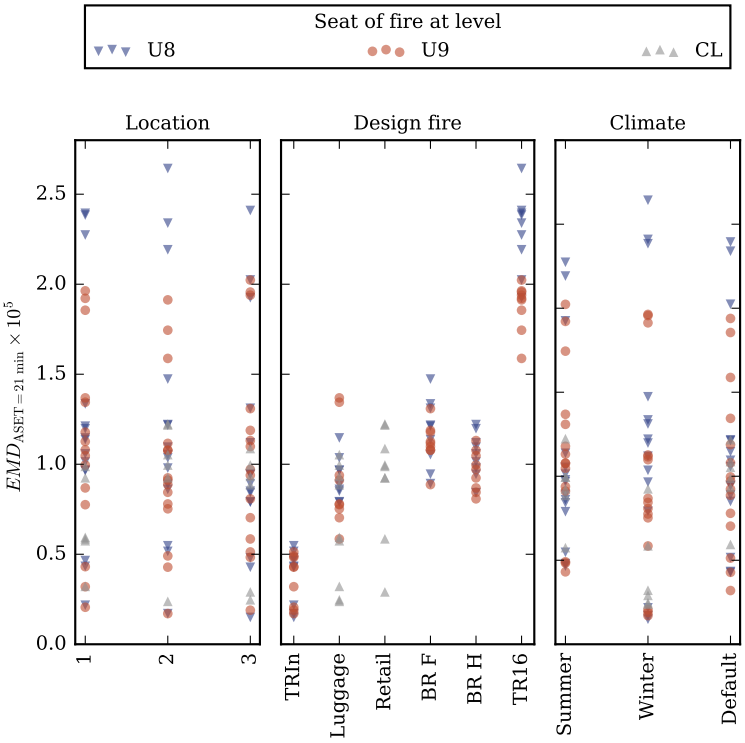

Figure 4.14: Scatter matrix illustrating the impact of the fire scenario parameters location, design fire, and climate on the *EMD*. Design fires are ordered by total heat release.

In principle, it becomes evident that the *EMD*s remarkably scatter in a range from almost zero up to $2.5{\times}10^5$. In other words, there are severe fire scenarios but also ones with minor consequences. In contrast to the outer scatter plots, the emerging structure illustrated in the central scatter plot demonstrates that the development of *ASET* is predominantly driven by the design fires. This fact is not surprising and generally acknowledged in the field of *FSE*. However, there are distinct fluctuations within the single design fires, which imply that both location and climate appear to be influential inside these scenario subsets. Another observation is that the most

severe *TR16* fire occurs in the lowest level (U8). Interestingly, this effect seems to vanish for the *BR F* and *BR H* fires. The same applies to the low-energetic fires, i.e. *TRIn* and *Luggage*. In this respect, the luggage fire yields remarkably variable impacts on *ASET* throughout the station. In comparison to the latter, the *Retail* fire yields comparable consequences.

In order to gather more insights into the impact of the fire location and climatic conditions, the correlation analysis has been separated based on the insight that the system is predominantly driven by the design fire. For this purpose, the classification into high-, medium-, and low-energetic fires, which has been introduced in Section 4.3.2, is applied. Figure 4.15 provides the associated results applicable to the high-energetic design fires, which exclusively occur in the platform levels.

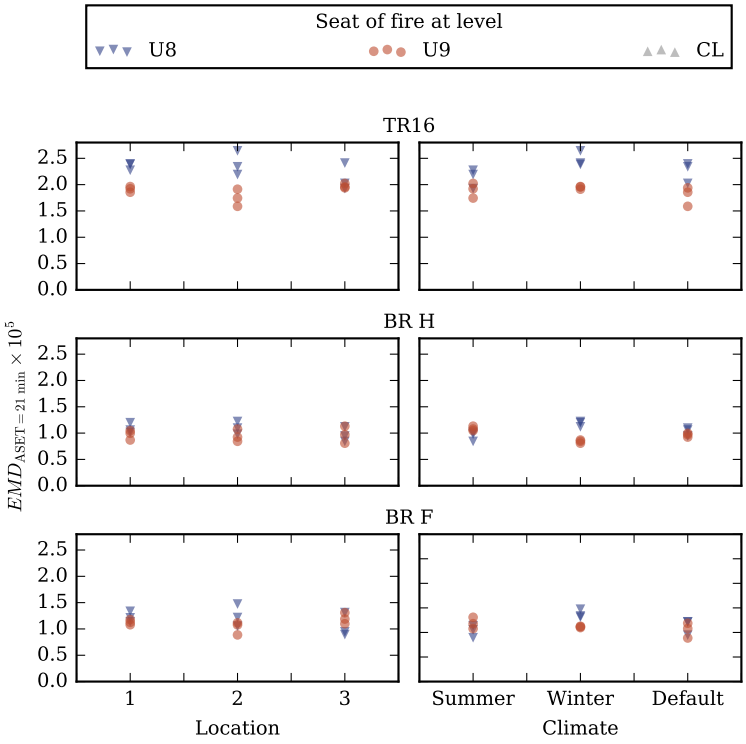

Figure 4.15: Separated analysis of high-energetic design fires regarding the impact of fire locations and climatic conditions on the *EMD*.

The differentiated analysis reveals additional insights into the impact of both fire locations and climatic conditions. For all three design fires, it becomes apparent that a fire in the centre of the U8 level (location 2) yields the most adverse impact on *ASET*. Contrary to that, the centred fire in the U9 level results in a more advantageous development of *ASET*. This finding only weakly applies to *BR H* fire since the inter-accessible trainset yields a less punctual emission of smoke and fire effluents. Moreover, a fire at location 3 on the U8 level appears to swap the observed hierarchy between the levels. This observation may be explained by the winding staircase towards the surface and the comparatively high hot gas layer temperatures in front of the latter. Finally, distinct climatic influences are observable for scenarios, where winter conditions have been set.

Figure 4.16 provides the correlation plots corresponding to the medium-energetic fire scenarios. Note that the latter only occur in the concourse level.

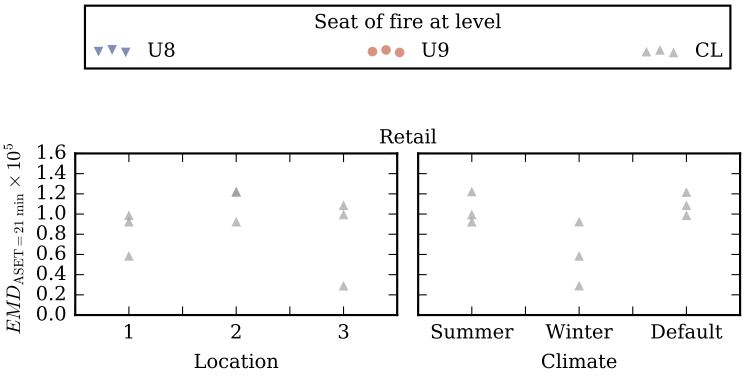

Figure 4.16: Separated analysis of medium-energetic design fires regarding the impact of fire locations and climatic conditions on the *EMD*.

Once again, the variations of fire location and climate lead to remarkably different results. With regards to the placement of the fire, location 2 yields the lowest *ASET*s throughout the concourse. In addition to that, a significant impact of the climatic conditions has been revealed. Winter conditions consequently result in less adverse developments of *ASET* than summer and default conditions. In conjunction with a fire located in close proximity to a staircase towards the surface, the majority of fire effluents is literally flushed out of the concourse.

Figure 4.17 comprises the correlation plots corresponding to the low-energetic fire scenarios. Here, the *Luggage* fires may occur throughout the entire station. The *TRIn* scenario is solely assumed in the platform levels.

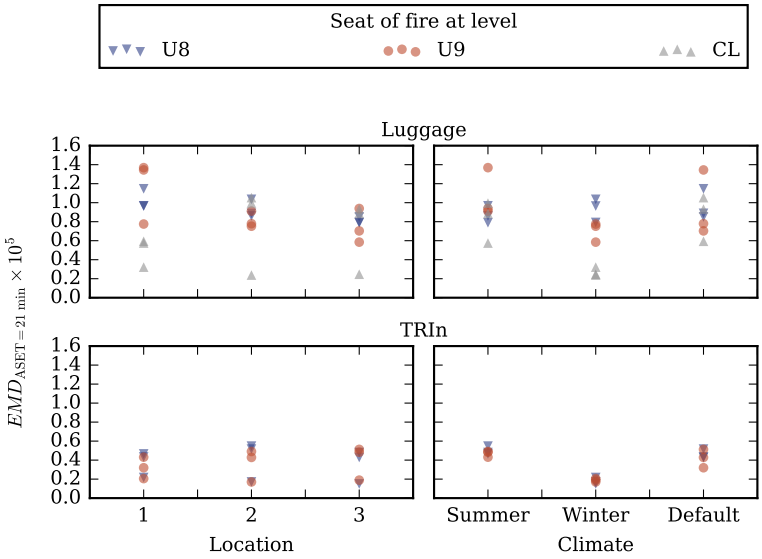

Figure 4.17: Separated analysis of low-energetic design fires regarding the impact of fire locations and climatic conditions on the *EMD*.

The low-energetic fire scenarios provide extremely fluctuating results regarding the development of *ASET*. With regards to the *TRIn* scenarios, the fire location yields rather similar findings as for to the high-energetic fires. A centred placement in the platform levels results in the most adverse effects. However, the most distinct influence is again caused by the climate since all scenarios configured with winter conditions are limited to very localised decreases of *ASET*. This observation can be explained by dilution, which is caused by the established air movements inside the station. Moreover, in case of summer and default climate conditions, the fires in the lowest level (U8) are slightly more severe. Regarding the *Luggage* scenarios, the development of *ASET* becomes more complex. For instance, the fires placed on the platform levels correspond to remarkable influences caused by the particular locations. Location 1 on both U8 and U9 especially yields comparatively severe consequences. In addition, no systematic differences between the fires either on U8 or U9 are observable.

Moreover, the fires occurring on the concourse yield slightly less severe consequences. Nevertheless, these findings again depend on the climatic conditions. The winter case, for instance, reveals the expected hierarchy between the levels. Obviously, this effect does, however, not apply to summer and default conditions. There may be multiple explanations for the observations stated above. On the one hand, the *Luggage* scenarios are assigned with different combustible characteristics. On the other hand, the source term may potentially be too extensive for dilution but still too marginal to affect three levels simultaneously. This probably is the reason for the higher consequences of the fires placed on U9 since they definitively affect the spacious concourse as well, which does not necessarily apply to fires in the U8 level. In addition to these thoughts, the low heat release implies a labile hot gas layer stratification and, thus, causes faster smoke spread into the staircases. In case of the platform levels, this mechanism may be an explanation for the increased importance of the fire locations.

4.6 Summary

The fire scenario ensemble has been set up with the aim to introduce certain variabilities to the subsystem. For this purpose, three main parameters have been varied: design fire, fire location and climatic conditions. The latter have been incorporated by a full-factorial sampling, which yielded 108 fire scenarios. For quantifying the consequences of all samples, multiple quantities have been utilised to compute *ASET* maps for each level of the station. Inspired by a commonly used distance metric (*EMD*), the effort to transform the *ASET* maps of a particular scenario to an initial state has been computed. This scalar score describes the development of *ASET* throughout the entire station and represents the consequences corresponding to a particular fire scenario.

The subsequent correlation analysis revealed distinct margins of consequences within the fire scenario ensemble. As expected, the design fires have been identified as the key determinant for that. In concrete terms, the consequences of the design fires can be ranked as follows: *TR16*, *BR F*, *Luggage*, *BR H*, *Retail*, and finally *TRIn*. It is notable here that both *Luggage* and *Retail* fires may yield upper margins of consequences, which are comparable to the *BVG* carriage fires. Additionally, these design fires correspond to highly variable consequences. In order to gain a better understanding of these variabilities, the correlation analysis has been separated based upon the particular design fires.

This analysis step revealed interesting insights concerning the impact of the fire locations. For instance, the impact of the level at which a fire is occurring is more complex than initially assumed. Only in case of the *TR16* scenarios, a fire on the lowest level (U8) yields the most adverse consequences with regards to the entire station. In case of the remaining two carriage fires as well as the low-energetic fires, this effect, however, seems to be superposed by additional influences. The latter are, for instance, the varied locations within one level. Here, it has been found that a centred location in U8 and the outer ones in U9 yield the most severe consequences. For the *Retail* fire, the opposite observations were made. In this case, the fire location most remote from any staircase causes the most adverse conditions. In other words, the proximity to upward staircases obtains an important role.

Besides these spatial aspects, also the climatic conditions have been found to affect the development of *ASET*. With regards to high-energetic fires on the U8 level, winter conditions yield more severe developments of *ASET*. In these cases, the established airflows obviously abet the smoke spread into more remote areas. However, this does not equally apply to similar fires on the U9 level. In case of both medium- and low-energetic fires, opposite observations were made. In concrete terms, winter conditions induce higher *ASET*s throughout the station. These findings can mainly be explained by two observed effects. On the one hand, the airflows within the station dilute the smoke effluents and on the other hand, the established air movements additionally support the natural ventilation towards the surface.

Up to now, the analysis has been based on the spatial and temporal extent of *ASET* throughout the station. However, this summarised view does not yet account for the relations to the subsystem *Evacuation*. In other words, the globally most adverse development of *ASET* may not necessarily provide the most challenging conditions for a certain set of evacuation scenarios. The development of the latter will therefor be addressed in the following chapter.

Chapter 5

Evacuation Simulation

This chapter covers the subsystem *Evacuation*. Firstly, a brief summary of the applied software framework and computational aspects is given. In the following section, the geometrical representation of *Osloer Straße* is discussed. One of the chapter's centrepieces is the configuration of the occupant scenario ensemble. The basic components of the latter are subdivided into built environment, safety measures, occupancy & occupants as well as hazard. The consolidation of these components as occupant scenarios is discussed within the design of experiment section. Finally, a preliminary analysis of the reference evacuation ensemble is presented. The latter is based on an extended approach utilising maps for the representation of *RSET*.

5.1 Evacuation Model and Computation

5.1.1 Evacuation Model

Besides ensemble simulations for multiple fire scenarios, another ensemble is set up for the subsystem *Evacuation*. For the computation of the latter, the Jülich Pedestrian Simulator (*JuPedSim*) version 0.8 has been utilised [Kemloh et al., 2016]. The software framework covers the simulation, analysis, and visualisation of pedestrian dynamics and is developed at Forschungszentrum Jülich. It arose from the *OpenPedSim* framework [Kemloh Wagoum et al., 2014] in 2013 and has been developed continuously in the frame of multiple research projects. The framework consists of four major components: *JPScore*, *JPSvis*, *JPSreport*, and *JPSeditor*. The *JPScore* module performs the microscopic computation of the pedestrian's trajectories. *JPSvis* can be used for the visualisation of the geometry and the trajectories. *JPSreport* provides multiple methods for analysing pedestrians' trajectories and *JPSeditor*, finally, allows

for the setup of geometries. Further reading can be found in [Kemloh Wagoum et al., 2015].

The primary purpose of *JuPedSim* is academic use. It is supposed to equip researchers with a convenient software framework which provides major features for investigating pedestrian dynamics. In turn, the focus is exclusively set on particular research interests. As a consequence of this philosophy, *JuPedSim* or especially *JPScore* involves a variety of implementations throughout all model levels. In this respect, model levels refer to the hierarchy of motion as introduced in Section 1.3.1. The submodels, which have been applied within this thesis are summarised in the following paragraphs.

Operational Level This level covers the modelling of the pedestrian's movement within the computational domain, which is represented in continuous space. Amongst others, a velocity-based model introduced by Tordeux [Tordeux et al., 2016] is available and applied in this thesis. It represents a collision-free, first-order model, which consists of two submodels. The first submodel computes an optimal velocity depending on the minimum spacing in front of a given pedestrian. The computation of the movement direction is covered by the second submodel. Moreover, the model assumes a pedestrian as a symmetrical circle, whose diameter represents the shoulder width.

Tactical Level *JPScore* provides a multitude of different route choice models. In principle, every route choice algorithm is based on a navigation graph, which is generated out of the specified geometry. Moreover, variable algorithms can be applied to the navigation graph resulting in varying route choice patterns such as local shortest, global shortest, or quickest path. A comprehensive summary of the different implementations can be found in [Kemloh Wagoum, 2013]. In the frame of this thesis, the global shortest path router is applied.

5.1.2 Computation

Since the computational effort of evacuation simulations is moderate in comparison to the *CFD*-based fire simulations, a serial computation strategy has been chosen for each simulation run. Pedestrian simulation models usually utilise a randomised initialisation, which is controlled by a so-called seed value. The purpose of this approach is to introduce a certain variability of selected criteria such as initial agent positions, distributions for walking speeds, or pre-movement times amongst others. Having said

that, a particular simulation setup requires multiple computational realisations in order to achieve converging results.

Convergence of Results General or minimum recommendations for a sufficient number of realisations are rarely provided, e.g. in the German RiMEA guideline, which states a minimum of ten realisations [RiMEA, 2016]. A more specific estimate can be made with the help of a convergence analysis. However, determining the convergence of evacuation simulations is a rather sophisticated task which heavily depends on the utilised model, the scenario specifications, and finally the evaluated convergence criteria. A potential approach utilising the differences between the evacuation curves (time t vs. number of occupants N) has been proposed by Lovreglio [Lovreglio et al., 2014]. One limitation of this approach is that these curves can solely be derived for one particular exit.

In order to capture the spatiotemporal dynamics of the evacuation process, the utilisation of the raw simulation output may be valuable, namely the pedestrians' trajectories. However, determining the difference of trajectories is computationally demanding and may probably yield no convergence at all. In this study, a new method is introduced, which is based on a map representation of the pedestrian dynamics. In concrete terms, the pedestrians' trajectories are used to map the maximum clearing time corresponding to each discrete map element. These so-called *RSET* maps are further described in Section 5.5.1.

The basic idea of the convergence analysis is the following: given the *RSET* maps for two realisations of a scenario, another map representing the ninety-fifth percentile of the two latter is calculated. After that, the number of realisations is increased and the ninety-fifth percentile maps are continuously determined. At a certain point the ninety-fifth percentile maps will not change anymore if additional realisations are incorporated to the analysis. Having said that, an appropriate metric for quantifying the difference of two maps or distributions is necessary. For this purpose, the Kullback–Leibler divergence has been utilised [Kullback and Leibler, 1951]. For a variety of different scenario characteristics, it has been found that a total number of 15 realisations yields converging results throughout all three building levels. This separated analysis on the basis of all three building levels is a convenient benefit of the above-mentioned *RSET* map generation. Figure 5.1 exemplarily demonstrates the decreasing divergence and a simultaneously increasing number of realisations.

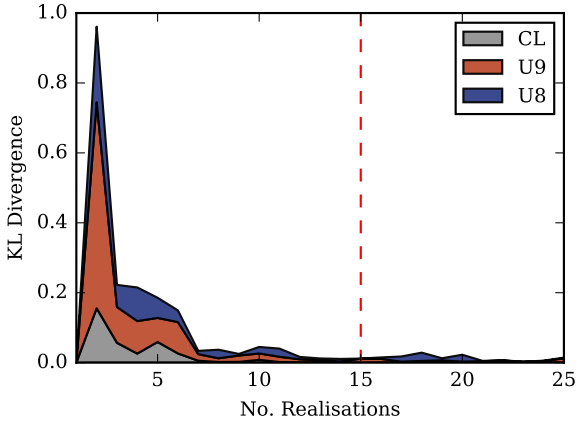

Figure 5.1: Development of Kullback-Leibler Divergence for *RSET* probability density functions with increasing numbers of realisations.

Given the above-mentioned number of 15 realisations per scenario, the computation of the evacuation ensemble basically represents a high throughput computing problem. In order to cope with these circumstances, a general purpose cluster operated at the Jülich Supercomputing Centre (JSC) has been used. The cluster was set up during the HERMES project especially for the purpose of large scale pedestrian simulations [Kemloh Wagoum, 2013, p. 30].

5.2 Geometry

In *JuPedSim*, a building is represented by an agglomeration of rooms and subrooms, with each of them being defined by an arbitrary set of vertices. Since the computational domain is represented by continuous space, the vertices can be set with arbitrary accuracy. The necessary data has been aggregated from floor plans and supplementary field measurements conducted in [Osterkamp, 2015]. The representation of the built environment is based on the convention that a room either represents an entire level or a staircase. Given that, a (set of) subroom(s) is supposed to refine a particular room. The connection between rooms is realised by transitions, while subrooms are linked by crossings. Subrooms may also be specified as inclined stairs in order to connect different levels. Additional building elements, such as pillars, benches, or vending machines are included as obstacles. A top view on the geometry representation of *Osloer Straße* is provided in Figure 5.2.

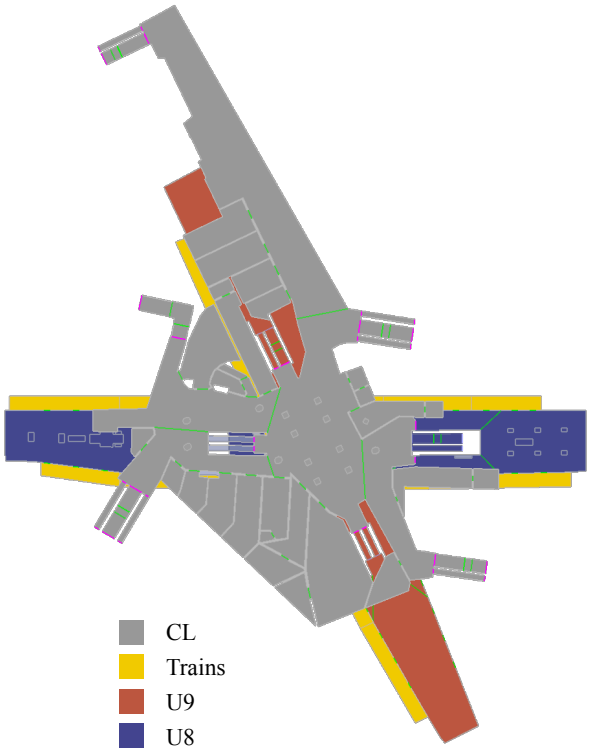

Figure 5.2: Vertex-based geometry of *Osloer Straße* including the levels U8, U9, CL, and three trains. Magenta lines illustrate transitions between rooms and green lines represent crossings between subrooms.

5.3 Occupant Scenarios

Beside the static geometry, the subsystem *Evacuation* is essentially composed by occupant scenarios. In common literature and guidelines, a multitude of different classifications for all relevant degrees of freedom are available [Nilsson and Fahy, 2016], [ISO/TS 29761, 2015], [RiMEA, 2016]. A comprehensive summary of available documents has been given by [Konrad, 2014]. In this respect, it appears to be a tremendous task to account for all requirements, theories, and scientific insights when defining occupant scenarios.

However, according to the current work on DIN 18009–2 [Jäger and Schröder,

2016] the occupant scenarios within this study will be specified based on the four major components shown in Figure 5.3. The entire process has to understood as an iterative process, whose steps are not necessarily sequential since many specifications are interdependent. Firstly, potential influences by the built environment will be discussed. In the next step, relevant considerations about safety measures and organisational aspects are included. Subsequently, the broad topic area related to occupancy and occupants is presented. Finally, the incorporation of potential (fire) hazards over the course of the evacuation is addressed. The above-mentioned components are extended in the following sections in order to vitalise the engineering timeline that has been introduced in Section 2.4. Having said that, the main objective is to account for the multitude of scenarios that may be associated with the subsystem *Evacuation* in real life.

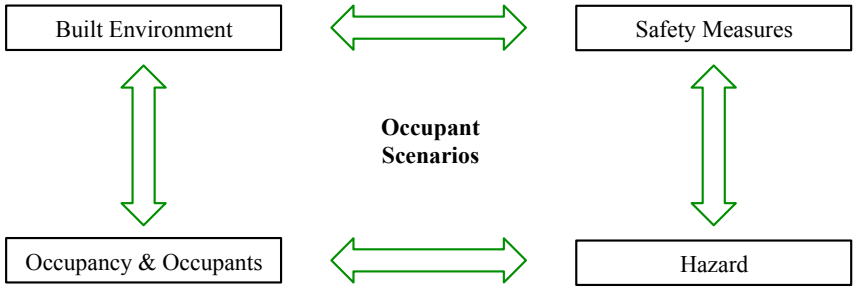

Figure 5.3: Major components for the specification of occupant scenarios.

In the frame of preliminary works, a comprehensive study on multivariate occupant scenarios applied to *Osloer Straße* has been conducted in [Axnich, 2016]. Beside the technical proof-of-concept, the major purpose of this work was to establish a well-informed understanding of the occurring pedestrian dynamics such as total evacuation times or jam formation amongst others.

5.3.1 Built Environment

In contrast to other sources, such as [Nilsson and Fahy, 2016] or [ISO/TS 29761, 2015], the following considerations of the built environment will have a less distinct reference to the subsystem *Fire* since those aspects have been addressed in Section 2.5.1 and are included in Section 5.3.4. Therefore, the focus is set on additional characteristics that may be relevant for the simulated pedestrian dynamics.

Technical Building Equipment The retail units in the concourse and all duty rooms are monitored by a fire detection system, which automatically triggers an evacuation siren in this area. Moreover, *Osloer Straße* is equipped with a personal announcement (*PA*) system, which is assumed to be functional throughout the entire station.

Egress Paths Regarding the egress paths of the station, a number of assumptions are made. Besides all stairs, escalators leading to the surface are assumed to be used by the occupants as well. Despite the emergency task to stop escalators towards lower levels in order to provide additional capacity, the latter are not considered as egress path. The same applies to the two elevators of the station. The width of all conventional staircases is shortened by the dimensions of handrails. Moreover all emergency exits which require traversing the tunnel system are excluded from the analysis. Finally, the trains that are assumed in the station are represented by subrooms as part of the built environment. In this respect, two six-car trainsets are placed on the U8 level and one on the U9 level. For every individual trainset, all 18 doors towards the platform are assumed open.

5.3.2 Safety Measures

Procedural Detection Before the *BVG* control centre is able to raise an evacuation alarm, a fire needs to be detected, confirmed, and reported. This process may involve multiple bodies and conditions inducing different outcomes. Besides installed technical systems, a fire can be detected either by *BVG* staff or by customers. In case of a detection by staff – most probably a driver – the detection procedure will be rather short. Once a potential risk is identified, she or he will immediately inform the control centre. If a fire is detected by a customer, she or he will most probably inform the public fire service, which in turn will report the fire to the *BVG* control centre.

In orientation to [TRStrab BS, 2014], an assumed train fire requires the consideration of an additional component: the maximum travel time into the station. For *Osloer Straße*, this number ranges between one and two minutes. The guideline also assumes an additional time period of one minute for exploring and reporting fire incident since the driver has to carry out a variety of different tasks in a very short period of time. With these numbers in mind, the procedural detection time is expected to range between 120 seconds and and 180 seconds.

Evacuation Alarm Once the *BVG* control centre is informed about a fire incident, the emergency routine is initiated. This is assumed to happen instantaneously if the confirmed fire is reported by a driver. In case of an incident reported by a third party, the situation is likely to be confirmed before any further action is undertaken. The same may apply to an emergency call forwarded by the fire service. Thus, the alarm times are assumed ranging between 0 and 120 seconds.

If the fire is confirmed, the evacuation alarm via the *PA* system is triggered by the control centre. For the further analysis the detection and alarm times yield the pre-alarm time. It is assumed to end when the evacuation alarm is activated by the control centre via the *PA* system. Given that, potential preceding instructions via the train-mounted *PA* systems are only considered to have a local effect.

Regarding the presented thoughts and numbers about potential detection and alarm sequences, the pre-alarm time is expected to range between 120 and 300 seconds and will become a variable in the design of experiment.

Staff Intervention During normal operations, no permanent *BVG* staff is present at *Osloer Straße*. In the event of a fire, mobile security services can be dispatched to the station. Moreover, a maximum number of three trains can be present at the station for operational reasons. Except the corresponding number of train drivers, no further staff intervention is assumed. The only exception are the retail areas, where the presence of salespersons is incorporated into the analysis by means of adapted pre-movement times.

5.3.3 Occupancy and Occupants

An essential part of the setup of occupant scenarios is the specification of occupancies and corresponding occupant characteristics. While occupancy is understood as one or multiple building use(s), occupant characteristics are seen as a set of versatile attributes that may be relevant for the purpose of an evacuation analysis. Both components are oftentimes conjunct by defining "standard populations" as proposed in [RiMEA, 2016]. A step forward is proposed in [ISO/TS 29761, 2015], where a so-called "occupant characteristics matrix" is requested. Moreover, [ISO/TR 13387, 1999] accounts for "seasonal variations" when estimating population numbers. However, no further advice is provided on generating a population out of particular occupant groups. With regards to the eleventh behavioural fact (see Section 1.3.1), heterogenous populations are thus insufficiently covered. In order to account for multiple building uses, temporal dynamics, heterogeneity and uncertainty when composing

a particular simulation population, this study utilises an alternate approach, which is inspired by the so-called *persona* method. Its conception has been proposed by [Schäfer et al., 2014] for the purpose of an evacuation analysis. A first practical implementation using *JuPedSim* has been conducted in [Zinke et al., 2017]. Originally, the *persona* method has been introduced by [Cooper et al., 2007] and represents a product design tool for describing the needs and habits of costumers. Using the example *Osloer Straße*, the basic idea of the method is as follows. The focus is set on fictional characters (*personas*) with varying premises and demands by means of a safe evacuation out of the station. In the end, a *persona* represents a "close narrative description of [a] real-world user or a cluster of users based on valid observations" [Schäfer et al., 2014]. Given these thoughts, the setup of an appropriate methodological framework as well as the relevant *persona* attributes are addressed in the following paragraphs.

Setting up Personas In order to cover the expected variety of building occupants, a set of seven *personas* has been created. In principle, they are distinguished by their current goals of activity and their ages. The different activities consist of travelling, shopping, or working in the station. The expected margins of different ages have been aggregated to youth, adult, and elderly. Of course, there are a multitude of additional characteristics that my be influential, e.g. group affiliation, gender, and so forth. However, the above-mentioned *personas* shall serve as a starting point and are finally listed in Table 5.1.

Table 5.1: overview of specified *personas*.

	Passenger	**Shopper**	**Salesperson**
Youth	x	x	-
Adult	x	x	x
Elderly	x	x	-

In the next instance, the *personas* have to be specified in detail. Initially, the qualitative (narrative) description of selected *persona* features has to be conducted. Once a *persona* is set up qualitatively, the specifications have to be prepared for the upcoming population generation. In this study, an *XML*-based container is used as interface. Using the example of adult passengers, this process is illustrated in Figure 5.4.

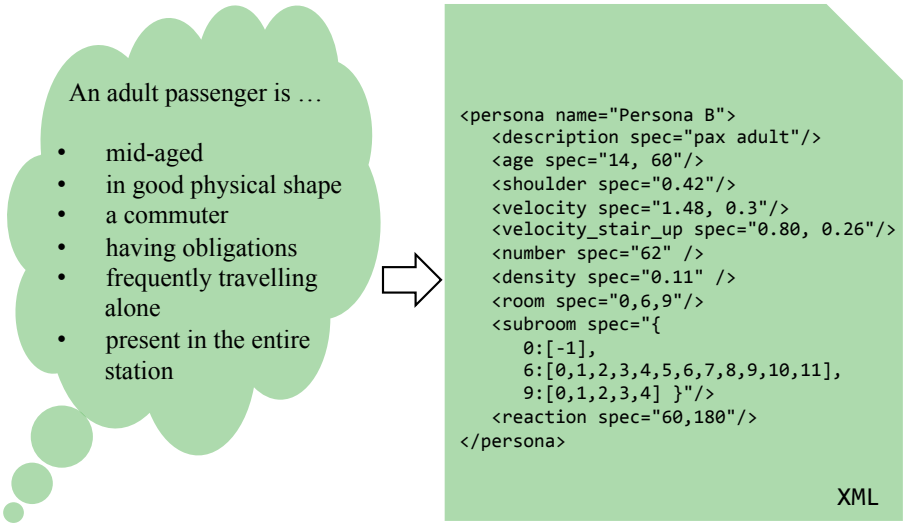

Figure 5.4: Exemplary translation of narrative *persona* characteristics into numeric values.

The quantitative characteristics of each *persona* are stored in the *XML* container and can be interpreted with *Python*. This allows for utilising a number of different data types for the *persona* specification. In this respect, single values are directly adopted, while a pair of values is used to describe a certain attribute by means of a distribution. Moreover, key-value pairs (dictionaries) are used in order to distribute a *persona* over particular `rooms` or `subrooms`. The parametrisation of common physiological parameters such as `shoulder` width, `velocity` and `velocity_stair_up` aims at the realistic representation of the movement characteristics. The attributes `number` and `density` can be tuned in order to establish the occupant load of the entire station and the attribute `reaction` specifies the pre-movement time (distribution) of a given persona. The parametrisation of the above-mentioned attributes and the corresponding empiricism is discussed in the following paragraphs.

Physiological Characteristics The physiological occupant characteristics cover movement speed when walking on the plain and up stairs as well as the pedestrians' shoulder width. Regarding the desired movement speeds, the data has been chosen in orientation to the Weidmann data as it is provided in [RiMEA, 2016]. The shoulder widths have been set using the literature reviewed in [Weidmann, 1994]. For the three different age classes, Table 5.2 provides an overview of the specified parameters.

Table 5.2: overview of physiological occupant characteristics. The distribution parameters μ and σ are incorporated refer to a Gaussian distribution.

	Youth	**Adult**	**Elderly**
$v_{0,\text{ plain}}$ in $\text{m}\,\text{s}^{-1}$	$\mu = 1.60$ $\sigma = 0.3$	$\mu = 1.48$ $\sigma = 0.3$	$\mu = 1.07$ $\sigma = 0.2$
$v_{0,\text{ stair up}}$ in $\text{m}\,\text{s}^{-1}$	$\mu = 0.86$ $\sigma = 0.26$	$\mu = 0.80$ $\sigma = 0.26$	$\mu = 0.58$ $\sigma = 0.25$
l_{shoulder} in m	0.30	0.42	0.38

In orientation to [Holl and Seyfried, 2010], the above-mentioned parameter sets have been investigated using simplified test cases. The plausibility of the obtained results was checked on the basis of experimental data [Seyfried et al., 2009] as well as hand calculation methods provided in the NFPA 130 guideline [NFPA, 2014].

Individual Detection Apart from one global detection time, the process of detecting a fire may not necessarily have the procedural character as discussed in Section 5.3.2. In anticipation of Figure 5.5, the sight of smoke may for instance serve as initial cue for an occupant prior to any official report to the control centre. In order to account for this mechanism – which is also discussed in [ISO/TR 16738, 2009] – the fire simulation data is processed regarding the question if and when an occupied room or subroom is affected by smoke. The associated time represents the individual detection time for a given position of an occupant.

Pre-movement Time Besides the pedestrians' physiological characteristics, numerous works identified the pre-movement time as one of the key determinants of evacuation processes [Zhang et al., 2008], [Albrecht et al., 2010], [Rogsch et al., 2015]. The pre-movement phase itself consists of recognition and response. Unfortunately, the quantification of these processes is a tremendous task with enormous underlying uncertainties. The pre-movement time is also referred to as reaction time in [RiMEA, 2016] and is occasionally mixed up with preceding time fractions such as detection or alarm times. Recapitulating the engineering time line introduced in Section 2.4, this paragraph will exclusively account for the pre-movement time.

In order to obtain a more informed understanding of the occupant recognition and response, it is inevitable to understand the latter as the result of an entire decision making process. Comprehensive knowledge on that insight is provided by Kuligowski

in terms of the protective active decision model (*PADM*) in Section 1.3.2. According to *PADM*, the bases of the decision making process are manifold. Besides current activities and goals, it essentially depends on the cues and information, which are provided to an individual or group. Moreover, "social context, personal characteristics, past experience and hazard knowledge" are further key aspects of the outcome of the decision making process. In terms of response behaviour, it is important to note that insufficient or lacking information necessarily results in further "information-seeking" instead of responding. In this respect, a so-called decomposition diagram is a useful tool in order to point out the numerous ambiguities when modelling the pre-movement phase. In orientation to [Kuligowski, 2016, p. 2094] and employing the incident studies presented in Section 1.2.2, such a partial diagram has been set up applicable to a passenger in Figure 5.5.

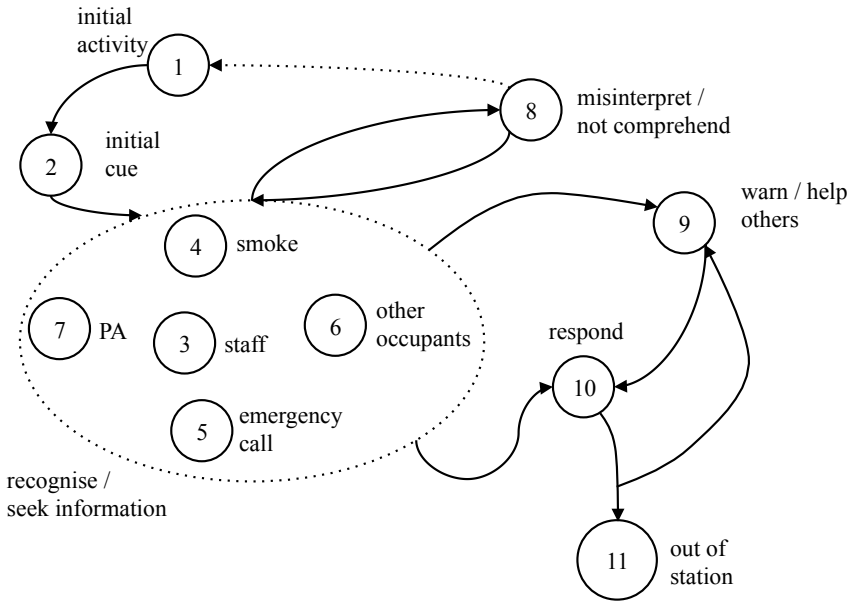

Figure 5.5: Partial decomposition diagram applicable to a passenger.

From this perspective, it becomes apparent that modelling a population's response behaviour requires reasonable fluctuations. In order to explore the lower and upper bounds of the latter, a brief review on available data is given in the following paragraph. Moreover, this study investigates a facility that hosts multiple building uses

simultaneously: transportation and retail. Hence, the data review has to be conducted for both building uses.

On a generic basis, the selection of response times is addressed in multiple guidelines and standards. An application-oriented example is the German RiMEA guideline [RiMEA, 2016], which in general distinguishes between three different cases. Initially, a "rapid" response is represented by a detection time of zero. Although being useful for the assessment of congestions, this specification is not further considered in this study. In the next instance, a "speedy" response is assumed whereat the individual response times are uniformly distributed between zero and one minute(s). Finally, the response time is specified with respect to the infrastructural and organisational circumstances in case of a "slow" response. For this purpose, the application of Purser's empirical data collection [Purser, 2003] is proposed. The latter also provides data for transportation structures ranging from one minute and a half to greater than 15 minutes. This data is excluded from the guideline due to a limited empirical basis. With a subsequent restriction, the data is, however, provided for orientation purposes in the standards [ISO/TR 16738, 2009] and [BSI 7974-6, 2004]. Moreover, the German technical guideline for light rails [TRStrab BS, 2014] assumes a response time of one minute without any additional specifications.

Notable research on the response behaviour in transportation facilities has been conducted by Sime and Proulx in the 1990s. In [Proulx and Sime, 1991], a field study on five different evacuation procedures was conducted at an underground station in Newcastle. The different trials revealed remarkably different response times depending on the provided information. The incorporation of these insights into engineering applications has been addressed in [Sime, 1995] later-on. Finally, further data on response times in mercantile facilities is collected in [Gwynnee and Boyce, 2016]. For this particular building use, the response times range from zero to approximately two minutes.

The summary of the above-mentioned data about response behaviour is provided for both building uses in Table 5.3

Table 5.3: overview of relevant and applicable data concerning occupant's pre-movement times t_{pre}. All values are in seconds.

Source	$t_{\textbf{pre, min}}$	$t_{\textbf{pre, max}}$	**Notes**
General			
[RiMEA, 2016]	0	60	"fast"
Retail			
[RiMEA, 2016]	120	300	"slow"
			category B M2 B3 A2
[Gwynnee and Boyce, 2016]	0	100	Siren used
Transport			
[ISO/TR 16738, 2009]	90	240	category E M2 B3 A3
	120	300	category E M3 B3 A3
[TRStrab BS, 2014]	60	-	Fixed value
[Proulx and Sime, 1991]	495	540	Bell
	135	180	2 staff
	75	460	Non-directive *PA*
	75	90	*PA* and staff
	60	90	*PA*

Based on the data listed above, it becomes evident that the field studies to some extend revealed lower response times than the enveloping numbers of the guidelines and standards. Hence, the emphasis is slightly moved to the field data.

In the next step, ranges of pre-movement times have to be assigned to the introduced *personas*. Without doubt, this is an arbitrary task, which depends on various additional parameters and relations such as group behaviour or gender. However, in the sense of composing variable populations, this challenge has been solved rather straightforwardly. The basic assumptions of this conceptual demonstration are as follows: Young occupants are likely to be more adventurous than adults and elderly people. In turn, the latter may be impaired by sensory limitations. In the platform areas an operated directive *PA* system but a temporarily delayed staff intervention is assumed. The automatic fire detection system mounted in the retail areas triggers an immediate but non-directive evacuation alarm in this part of the station. Finally, it is assumed that salespersons will take care for clearing and securing their stores before

they respond to the evacuation cue(s). Because of that, a positive staff intervention can be expected in the retail areas. The resulting configurations are presented in Table 5.4. It is to be noted that these ranges represent the bounds of the pre-movement times and are not directly implemented into the upcoming simulations. Further details are provided within the design of experiment in Section 5.4.

Table 5.4: overview of the *personas* and the assigned pre-movement time ranges. All values are in seconds.

Persona	$t_{\mathbf{pre,\ min}}$	$t_{\mathbf{pre,\ max}}$	**Notes**
Passenger Youth	90	240	adventurous
Passenger Adult	60	210	
Passenger Elderly	90	180	sensory impairments
Shopper Youth	30	100	adventurous
Shopper Adult	0	100	
Shopper Elderly	30	100	sensory impairments
Salesperson	100	180	clear and secure the store

In reference to the *PADM*, the assumptions presented above are intended for the perception of aural evacuation cues given by the alarm and/or *PA* system. However, another evacuation cue may be the perception of smoke, whose impact on the response behaviour has not been sufficiently investigated yet. A literature review given by Kuligowski revealed that a perceived cue "smoke" not necessarily yields immediate responses by test subjects [Kuligowski, 2016, p. 2098]. However, with regards to the high variability, which will be incorporated by the fire scenario ensemble (see Chapter 4), a certain relation between smoke spread and response appears to be necessary. In this respect, the following – rather simplistic – assumption has been made: the perceived risk of an aural alarm is less than the one induced by the sight of smoke. Hence, the assigned response time boundaries of an occupant are reduced by 50 % if smoke is perceived.

Setting up the RSET Timeline In the preceding paragraphs, all relevant time components for detection, alarm and occupant response have been discussed and quantified. In order to set up the *RSET* part of the engineering timeline, the different courses of events and the introduced time ranges are summarised in Figure 5.6. The time ranges will be incorporated into the design of experiment in Section 5.4

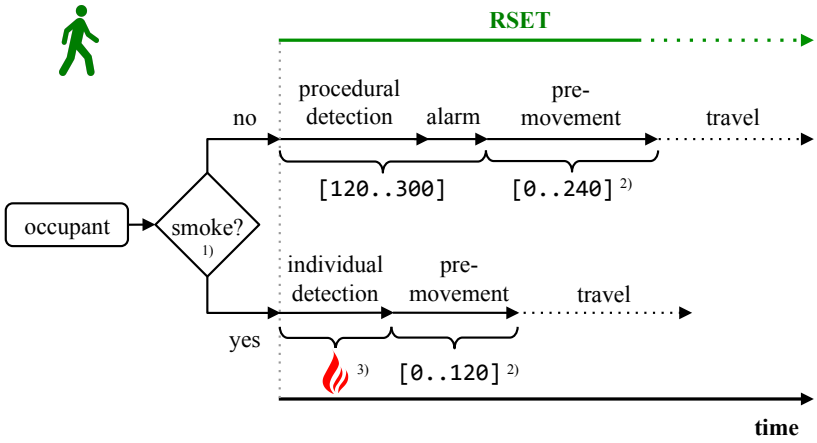

1) is smoke visible before procedural detection and alarm time?
2) depending on applicable persona
3) depending on the fire scenario

Figure 5.6: Engineering timeline setup for *RSET*.

Route Choice In spacious structures, especially route choice can remarkably impact the pedestrian dynamics. In turn, typical evacuation characteristics like travel times or jam areas can then be closely correlated to an occupant's spatiotemporal exposure to fire effects. Route choice itself is again driven by a multitude of factors, such as available alternatives, behaviour of others, group affiliation, or received instructions. Another question is an occupant's knowledge of a certain built environment. In this respect, the recent works of Andresen [Andresen et al., 2016a,b] provide a promising framework in order to model differing degrees of knowledge as well as a perception-based wayfinding. Moreover, incident studies such as [Jeon and Hong, 2009] revealed that the built environment may drastically impair the wayfinding abilities, e.g. because of massive pillars as they can also be found in the concourse level.

In order to investigate these potential dynamics, the route choice of the population has been varied in terms of three different strategies. For this purpose, the five final exits connecting concourse and surface have been equipped with goals. The first routing strategy assumes the entire population to use the local shortest path towards the closest goal. In regard to the shape of the escape route system, this results in movement patterns where exits F and J are almost solely used (see Figure 5.7).

The second routing strategy explicitly assigns goals to particular occupants and induces a uniform usage across all five exits. Moreover, a field study on exit choice in *Osloer Straße* has been conducted in [Hofinger et al., 2016] and revealed interesting imbalances regarding the particular exit usages. In concrete terms, exits leading to connection services such as bus or tramway were used more frequently. In reference to familiarity (see Section 1.3.1), occupants tend to use commonly used exits during an evacuation. Given these insights, the third route choice strategy randomly assigns goals to occupants according to the distributions gathered from field data. Figure 5.7 provides a qualitative illustration of the movement patterns that are induced by the three route choice strategies inside the concourse.

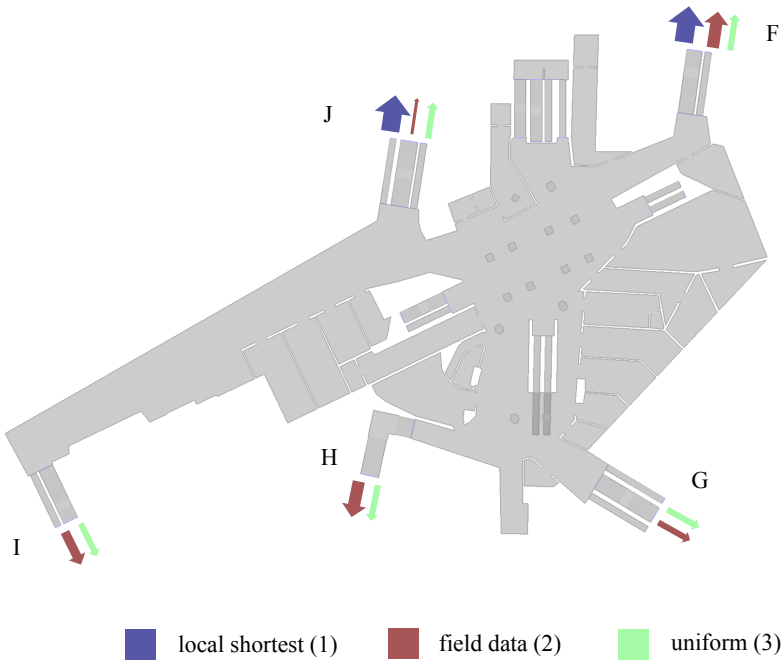

Figure 5.7: Major movement patterns of different route choice strategies. The width of the arrows indicates how frequently a particular exit is chosen.

Population Generation At the beginning of this section, the *persona* method has been introduced in order to capture the heterogeneity amongst occupants. Upon the definition of seven representative *personas*, the considered degrees of freedom such as physiological characteristics, individual detection, response, and route choice have

been discussed. The subsequent step is to merge *personas* in order to obtain varying populations regarding both composition and size. In the first instance, the population generation will be addressed.

The population generation is supposed to address two different purposes. Firstly the temporal fluctuations of the overall occupant load shall be covered. Secondly, the variability in terms of different population compositions is incorporated. These variations are of particular interest, e.g. in oder to facilitate subsequent probabilistic analyses, where the occurrence of particular population characteristics have to be conjunct with probabilities. In this respect, comprehensive data of the principal characteristics of public transportation has been gathered by Weidmann [Weidmann, 1994]. In terms of quantifying the temporal fluctuations, he determined the relative distribution of the traffic load in three German cities [Weidmann, 1994, p. 138]. Besides Hagen and Hannover, Hamburg is assumed to be the city, which is most comparable to Berlin. The Hamburg data henceforth is used as representative for the transport use. Similar statistical data is available for the course of shopping activities during weekdays in Germany [GfK, 2013]. Please note that the original data is resolved in two-hour bins and has been refined to one-hour intervals. Figure 5.8 provides a graphical overview of the afore-mentioned time series.

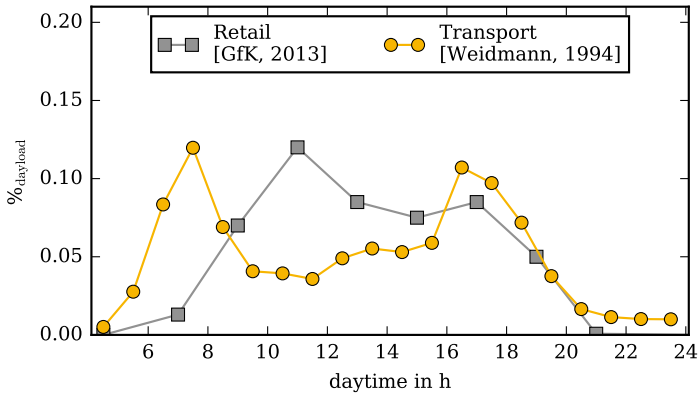

Figure 5.8: Relative occupant loads for retail and transport use throughout a weekday. The integrals of the curves equal 100 %.

Despite two double-peak structures, there are differences between the two utilised datasets. While the transportation load reaches its maximum during the morning from 5 to 7:30 am, the retail occupant load grows slowly and reaches its maximum in

the late forenoon. In turn, the noon time represents the least frequented daytime for the transport use. Furthermore, both peaks during the afternoon are rather similar. Finally, retail use ceases in the late evening, whereas transportation maintains a lower but constant level. Given these insights and numbers, it is possible to model coinciding building uses with respect to a workday. Of course, additional variations may emerge during other times, e.g. weekends or major events. These aspects are not further considered in this study.

Moreover, the variability in terms of different population compositions consisting of multiple *personas* is not incorporated yet. It is generally acknowledged that, e.g. age or travel purpose vary remarkably throughout the day. For instance, Weidmann qualitatively concluded that commuters dominate the scene during the morning hours, whereas elderly people are increasingly present in the forenoon and pupils prevail at noon. The afternoon hours again are characterised by elderly people and families. Finally, the evening peak is dominated by commuters [Weidmann, 1994, p. 245]. Precise quantitative fractions could not be found in literature. However, these fractions would heavily depend on many local factors such as demographics or the surrounding infrastructure (education, commerce, business, transport, sights). In order to capture this variability, a data-driven approach for generating representative populations has been developed. The subsequent workflow is only demonstrated here for the passenger subpopulation.

Initially, the given qualitative observations of Weidmann were used for defining upper and lower percentage constraints for the fractions of a particular *persona*. Table 5.5 provides an overview of the derived upper and lower constraints.

Table 5.5: Fractions of *personas* for population composition.

Daytime	**Youth**		**Adult**		**Elderly**	
	min	max	min	max	min	max
4:30 p.m.	0	10	90	100	0	0
8:00 a.m.	10	30	60	80	1	10
10:00 a.m.	1	10	1	20	60	90
12:00 a.m.	20	30	20	30	50	60
2:00 p.m.	20	30	20	30	60	70
5:00 p.m.	20	30	60	80	1	10
11:30 p.m.	0	10	80	100	0	10

In the next step, $5,000$ so-called candidate populations are generated using a randomised Dirichlet distributor [MacKay, 2003]. In principle, this method yields three

random numbers whose sum equals one and each of them describes the percentage of one persona. Subsequently, all generated triples are checked for compliance with the specified constraints of each persona. Once a total number of 50 compliant populations is found, the generation routine is completed. Figure 5.9 illustrates the 50 randomly composed populations which in turn constitute the overall occupant load introduced in Figure 5.8.

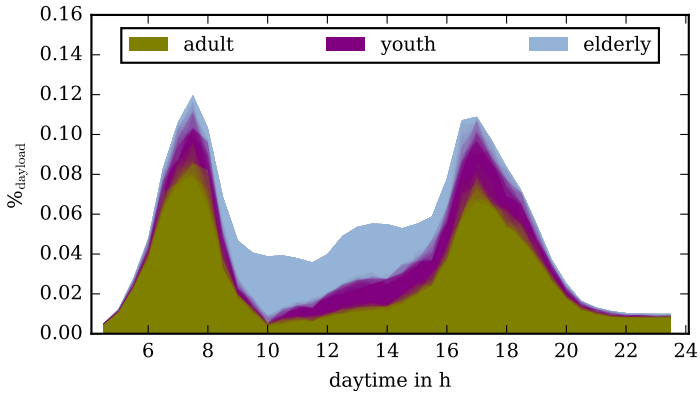

Figure 5.9: Stack plot of 50 variable populations consisting of adult, youth, and elderly people. The varying population compositions are illustrated by the blurred overlaps of the curves.

It becomes apparent that the desired variability could successfully be introduced to the populations. However, for conducting simulations, it is necessary to chose a set of samples out of this agglomeration. One potential approach is a continuous sampling along the time axis, whereat daytime would become the parameter determining the population characteristics. However, a closer look at these time series reveals daytimes with similar characteristics, e.g. during the early morning, forenoon, or late evening. In contrast, high variabilities are expected during the peak times. Hence, the computational effort shall be focussed on the most variable and busiest daytimes.

In order to achieve that, the parameter space containing the 50 populations is explored using k-means clustering. The latter is a data analysis approach, which iteratively forms optimised clusters based on the Euclidian distances between a set of observations. It is a so-called supervised method since the desired number of clusters is explicitly specified in advance. Further reading can be found in [Myatt, 2007]. In this case, an observation is understood as a three-dimensional point comprising the

following information: fraction of adults, fraction of youth, and fraction of elderly. In the period from 4:30 a.m. to 11:30 p.m., the relative occupant loads are interpolated by half-hour intervals which yields 38 observations. In conjunction with the 50 generated populations, a parameter space with $38 \times 50 = 1900$ observations is set up. The latter can now be clustered by means of very similar and very unique observations. In order to emphasise the peak times, the weighting of the observations has been modified. Therefore, a higher score has been applied to the relative occupant load of the entire population which equals the sum of all three *persona* fractions. The output of this analysis is a set of 15 clusters representing the 50 populations based on optimised Euclidian distances between the *persona* fractions. These clusters are summarised in Table 5.6 and referred to as population clusters.

Table 5.6: Population clusters with corresponding relative occupant loads $\%_{\text{dayload}}$, occupant numbers N, and represented daytimes. The derivation of the concrete occupant numbers is taken up in the following paragraph.

Cluster	$\%_{\text{dayload}}$ (transport/retail)	N	**Daytimes**
0	0.05 / 0.10	814	8:30, 19:00
1	0.04 / 0.24	707	10:30, 11:00, 11:30
2	0.01 / 0.00	99	4:30, 5:00, 20:30, 21:00, 21:30, 22:00, 22:30, 23:00, 23:30
3	0.11 / 0.03	1567	6:30, 7:00
4	0.11 / 0.17	1672	16:30, 17:00, 17:30
5	0.06 / 0.17	916	9:30, 12:30, 13:00, 13:30, 14:00, 14:30, 15:00
6	0.03 / 0.05	450	19:30, 20:00, 20:30
7	0.10 / 0.08	1532	8:00
8	0.04 / 0.19	697	10:00
9	0.08 / 0.14	1284	17:30, 18:00, 18:30
10	0.05 / 0.02	762	5:30, 6:00
11	0.04 / 0.21	700	11:30, 12:00, 12:30
12	0.05 / 0.14	773	9:00, 15:00
13	0.08 / 0.16	1237	15:30, 16:00
14	0.12 / 0.05	1785	7:30

It becomes evident that the k-means algorithm aggregated daytimes with fewer variability and overall load to single clusters, e.g. cluster 2. This means that many daytimes with similar characteristics in terms of occupant load and population composition are unified to one cluster. In turn, daytimes with high occupant loads and/or

expected variabilities in terms of population characteristics are represented more exclusively, e.g. clusters 7 and 14. Finally, the population cluster ID is going to become the single design parameter determining both the relative occupant load and the population composition.

Population Size In the preceding paragraph, the data-driven generation of populations has been introduced. So far, only the relative occupant loads have been utilised for that. In order to quantify the population size(s), these percentages are transformed to absolute numbers or densities respectively. The population size represents a crucial factor for evacuation analyses. Aiming at severe but reasonable boundaries for that, several recommendations and data have been utilised. Moreover, the multipurpose use of the station requires the assessment of both retail and transport use. In this respect, [ISO/TR 16738, 2009] qualitatively specifies both uses to have "high" occupant densities without giving further advice.

The retail use in the concourse has been quantified based on a variety of common standards and guidelines. In this respect, it is important to consider the particular retail units as well as the floor plan of the concourse in more detail. The concourse provides a total area of approximately $3000\,\mathrm{m}^2$ whereof two-thirds serve as traffic area, which will additionally be occupied by passengers. The retail units offer different goods and services and their areas range from 10 to $120\,\mathrm{m}^2$. In common guidelines, the proposed occupant densities for different store types are in range from 0.1 to 0.36 persons per m^2 [RiMEA, 2016], [vfdb, 2013].

In terms of transportation, initially, the passenger capacities of the six-car-trainsets are addressed. Both *BR F* and *BR H* can carry approximately 750 passengers, while the fraction of standing passengers is higher in case of *BR H*. Having this number, the applicable German technical guideline for light rail [TRStrab BS, 2014] allows for two principal approaches. Firstly, the maximum occupancies inside the trains plus thirty additional percent on the platforms is assumed throughout the entire station. This requirement applies to new stations. If available and applicable to stations in service, the occupancy can be estimated based upon counting data. In this case the average across the peak hour is supposed to cover the expected traffic load. In this study, the second approach has been chosen based on Berlin's recent transportation report [Stadt Berlin, 2014] as well as own field studies conducted in *Osloer Straße* [Hofinger et al., 2016]. Over the course of an average weekday, the transportation report states a total number of approximately $90,000$ passengers using the U8 and U9 services [Stadt Berlin, 2014, p. 54]. According to this source, this number is divided up into

roughly 55,000 passengers in U8 and 35,000 in U9. In this respect, it is important to recapitulate that the U9 platform serves as final stop. Moreover, field studies were conducted during rush hour on a Monday evening in January 2016 [Hofinger et al., 2016]. In this study, the occupant loads on all three departure platforms have been recorded shortly before the arrival of a train. The collected occupant numbers range from 30 to 230 per single track.

The data discussed above shall serve as basis for a reasonable estimate of the population sizes. All information and recommendations are briefly summarised in Table 5.7.

Table 5.7: Information for estimation of population size.

Source	N	D **in** m^{-2}	**Notes**
Retail			
[RiMEA, 2016]	-	0.18 – 0.36	Stores
[vfdb, 2013]	-	0.3	General stores
	-	0.1	Convenient stores
[ISO/TR 16738, 2009]	-	High	Category B1
[Hofinger et al., 2016]	35 – 65	-	Field data (1 h, weekday)
Transport			
[TRStrab BS, 2014]	750	-	maximum train capacity per track
	225		30 % train capacity on platform per track
[Stadt Berlin, 2014]	$\approx 90,000$	-	Through traffic on U8 and U9 (entire weekday)
[ISO/TR 16738, 2009]	-	High	Category E
[Hofinger et al., 2016]	30 – 230	-	Single Platform Field data (1 h, weekday)
[BVG, 2007]	216 / 534	- / 4.0	*BR F* (seats / stances)
	168 / 580	- / 4.0	*BR H* (seats / stances)

Regarding the retail use, a maximum occupant density of $0.1\,\mathrm{m}^{-2}$ has been chosen as design value. This rather low value corresponds to the gross areas of the retail units, which does not account for installed obstructions, e.g. furniture. Moreover, the resulting numbers of approximately 100 shoppers would be in good but conservative

agreement with the data collected in the field studies. Finally, salespersons are distributed with a very low occupant density of $0.02\,\mathrm{m}^{-2}$ in order to account for smaller and larger retail units. However, the distribution routine will at least allocate one single agent.

Aiming at a simplified incorporation of the counting data provided in [Stadt Berlin, 2014], a total load of $30,000$ passengers is assumed per track, while U9 is only occupied by one train. It is important to reconsider that these numbers cover the passengers occupying the trains. Moreover, this number has been increased by 20 % for several reasons. Firstly, the data basis of the transportation report was gathered back in 2007, while the overall transportation performance by *BVG* increases constantly [Stadt Berlin, 2014, p. 53]. Finally, the numbers represent averaged values for weekdays which may underestimate temporal peaks, e.g. during non-vacation periods. These thoughts yield a total number of $36,000$ passengers per track throughout one day. The breakup of this number for the specification of short-termed occupant scenarios can be achieved by combining the temporal course of the occupant load presented in Figure 5.8 and operational aspects. The assumption that approximately 12.5 % of the daily load emerges in the peak hour during the morning yields $4,500$ passengers per track. Given the applicable operation interval of 12 rotations per hour, a maximum number of about 375 passengers is assumed per train. Moreover, the occupant load on the platforms is estimated to be 30 % of the persons inside the trains. For this purpose, the maximum occupant density for the transport use has been tuned to $0.11\,\mathrm{m}^{-2}$.

Finally, the question may arise if it is reasonable to quantify the population size by only half of the maximum train capacity. However, this approach utilises all available data and appears to represent the station's regular operation based on own observations. In addition to that, *Osloer Straße* is a rather remote station in Berlin's underground network. This results in commuter traffic either inbound from or outbound to the city centre, which has been proved by the field studies presented in [Hofinger et al., 2016]. Moreover, the platform countings of this study correspond well with the 30 % assumption applied to the specified occupant load of 375 passengers per train. The final configuration of the population sizes as well as the distribution across the geometry are summarised in Table 5.8.

Table 5.8: Population size and distribution.

Persona	N	D **in** m^{-2}	**U8**	**U9**	**CL**	**Notes**
Retail						
Shopper	-	0.10	-	-	x	retail units, concourse
Salesperson	(1)	0.02	-	-	x	retail units
Transport						
Passenger	-	0.11	x	x	x	platforms, concourse
Passenger	6×63	-	x	x	-	per six-car trainset

The design values provided above correspond with the maximum total occupant load during the morning peak as introduced in Figure 5.8. In case of less frequented daytimes, the design values are reduced accordingly. This mechanism is triggered by the population clusters.

5.3.4 Hazard

According to [Jäger and Schröder, 2016], the consideration of hazards over the course of an occupant's evacuation is supposed to have multiple aspects. This study only accounts for fire hazards and their subsequent impact on the evacuation dynamics. Initially, traces of fire may serve as evacuation cue, which has already been addressed in terms of individual detection times in Section 5.3.3. For multiple reasons, the spatiotemporal data induced by a particular fire scenario is an essential input variable for each occupant scenario. The presence of smoke, for instance, yields a reduction of walking speeds as discussed in Section 3.2.3. On the other hand, physiological effects of potential coincidences between occupants and fire effluents are monitored according to the model implementations presented in Section 3.2.4. Consequently, each occupant scenario requires a conjunction with all specified fire scenarios. These aspects are revisited within the consolidated ensemble introduced in Chapter 6. However, the further procedure within this chapter corresponds to a so-called reference evacuation ensemble which is initially set up without considering a fire scenario.

5.4 Sampling

In this section all specifications discussed earlier are unified in order to generate an ensemble of occupant scenarios. The relevant design parameters are the following: pre-alarm time, pre-movement time, route choice, and population cluster. Hence, a four-dimensional parameter space has to be set up. As introduced in Section 2.6.1, a Latin Hypercube Sampling (*LHS*) has been applied. Based on a downsampling study, the occupant scenario ensemble here is specified by 80 samples. Technically, an *LHS* design yields a matrix with n rows and k columns, whereat n represents the number of samples and k the dimensionality. Hence, the *LHS* matrix of the occupant scenario ensemble has a shape of 80×4. Within the design space, each sample point consists of its four coordinates, which range from zero to one. In this respect, it is important to note that the design includes both continuous and discrete parameters. While the continuous parameters (pre-alarm time, pre-movement time) are directly incorporated into the design, the discrete parameters (route choice, population cluster) are assigned based on rounding operations. Moreover, the pre-movement time distributions require additional explanation. The latter are unique for each *persona* (see Table 5.4). In this respect, only the upper bound of an assumed uniform distribution is affected by the sampling. In concrete terms, a sample close to zero percent yields a narrow pre-movement time distribution around $t_{\text{pre, min}}$. In turn, a sample in proximity to one hundred percent results in a wide distribution between $t_{\text{pre, min}}$ and $t_{\text{pre, max}}$. The stated parameters as well as their corresponding ranges are summarised in Figure 5.10.

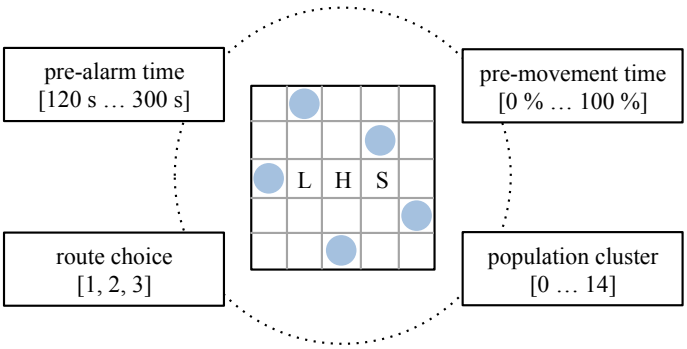

Figure 5.10: Design of experiment occupant scenario ensemble.

5.5 Preliminary Analysis

In order to obtain a principal understanding of the subsystem *Evacuation*, a reference ensemble is specified based on the method presented in Section 5.4. As stated above, the reference ensemble does not yet incorporate any fire hazards throughout the evacuation process. In preparation of this, the basic data analysis workflow is briefly discussed.

Data Basis The application of microscopic pedestrian models is based on the movement of individuals (agents) constituting the overall evacuation process. The movement of an agent can be described by a trajectory – the agent's path through space and time. *JPScore* computes a set of three-dimensional trajectories, which can be enriched by any additional data. In contrast to solely time-based analyses, this format can yield large amounts of data. The data extent especially depends on the population size, the temporal resolution, and the extent of further information,

Challenges The interpretation of computer-simulated evacuation processes is commonly reduced to local information, such as the clearing time of a particular space. As long as these analyses are sufficiently refined, the evacuation dynamics may be covered appropriately. However, information remains rather discrete and the analyses may have limitations with increasing numbers of evaluation points. Likewise, the subsequent conjunction with other spatiotemporal information like fire simulation data evolves to a more and more complex task.

Inspired by the *ASET* maps introduced in Section 4.5.1, a unified data format with an improved spatiotemporal resolution of the evacuation dynamics is utilised for the ongoing analyses.

5.5.1 RSET Maps

Once again, this data format is a map representing the spatial distribution of the required safe egress time (*RSET*) in this case. The generation of these maps is conducted as follows. Firstly, the three-dimensional trajectories are filtered by the z-elevation, i.e. a particular building level. This is achieved by a grid, which slices the trajectories. It has a grid resolution of $\mathrm{d}x = 0.6\,\mathrm{m}$ and is initialised with NaN (not a number) values. In the next instance, the routine determines the time, when a cell has been traversed by an agent for the last time. The corresponding grid element then is set to this time. If a grid elements has not been traversed at all, its value

will remain NaN. This approach is illustrated in Figure 5.11 using a simple corridor which is traversed by one single pedestrian over a period of 60 seconds.

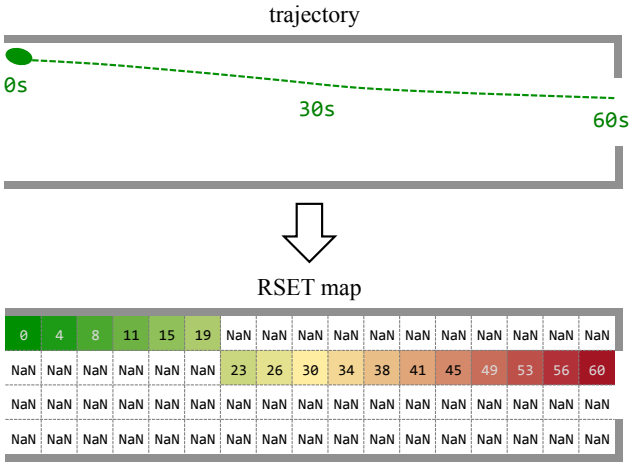

Figure 5.11: RSET map generation on the basis of a pedestrian's trajectory.

As stated above, the necessary information is provided by the trajectories of every realisation computed for one occupant scenario. In order to account for the randomness of the latter, all maps are stacked and the *RSET* map representing the ninety-fifth percentile is determined. Since non-occupied areas within the map remain NaN, they are excluded from the percentile calculation. Finally, this process is repeated for every level of the station. The corresponding analysis routine is provided in Appendix B.2. An exemplary *RSET* map derived for the occupant scenario `e013` in the U8 level is provided in Figure 5.12.

The *RSET* map provides comprehensive information about the evacuation dynamics of the exemplary occupant scenario. In principle, the U8 level is cleared in less than 11 minutes and it becomes apparent that two major jam areas are forming in front of the staircases towards the concourse level.

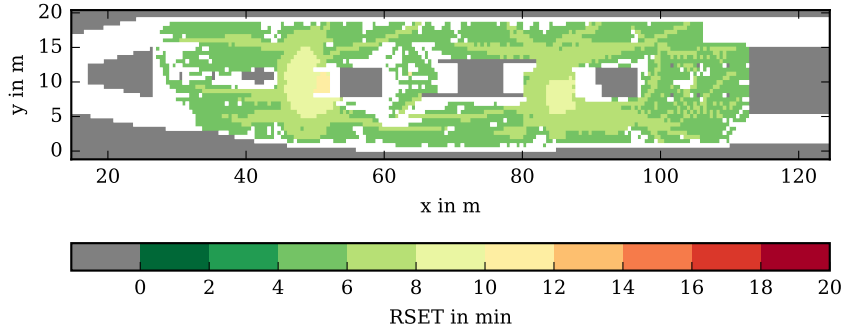

Figure 5.12: Exemplary map illustrating the ninety-fifth percentile of *RSET* in the U8 level. The colour map has been discretised into intervals of two minutes. Grey fields represent areas that are obstructed by the built environment. White areas have not been traversed at all.

Recapitulating the discussions conducted in Section 2.4, it again is possible to transform the *RSET* map to a distribution applicable to the relevant occupant scenario. The derivation of these distributions only accounts for areas within the domain which have been occupied by agents. Moreover, obstructed areas are excluded as well. The corresponding *RSET* distribution is provided in Figure 5.13.

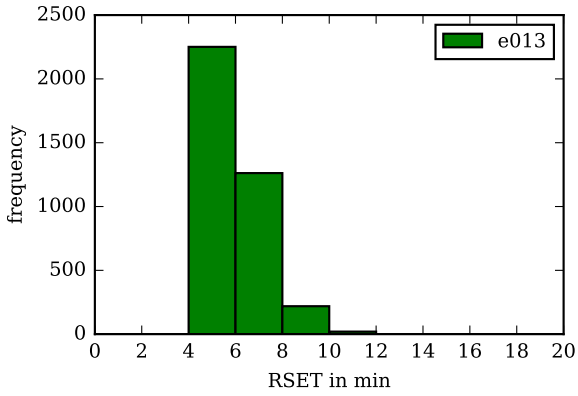

Figure 5.13: Distribution of the ninety-fifth percentile of *RSET* in the U8 level.

This exemplary case reveals a remarkable offset along the time axis which is in-

duced by the specified pre-alarm and pre-movement times. Moreover, the shape of these distributions will heavily depend on the interaction amongst fire and occupant scenarios. Similar to the distributions derived for *ASET* (see Section 4.5.1), it is again possible to source additional information from this data format. For instance, the frequencies of the higher *RSET*s within the map allow for deductions of the spatial extend of jam areas.

5.5.2 Correlation Analysis

Given the data analysis introduced above, it is possible to apply a correlation analysis to the reference occupant scenario ensemble. As discussed in Section 5.4, the latter consists of 80 scenarios, whereat four parameters are varied. These were pre-alarm time, pre-movement-time, route choice, and population cluster. The major purpose of this preliminary analysis is to establish a general understanding of the occurring evacuation dynamics. This covers the orders of magnitudes in terms of total evacuation times and it also aims at investigating the impact of the particular design parameters.

The ultimate quantity for the description of evacuation processes is time, e.g. evacuation times. In this respect, it is usually impossible to refer to exact numbers since these processes have underlying uncertainties. The design of experiment as well as the data preparation presented above are supposed to account for these aspects. Hence, the evacuation times have to be represented as margins. In this respect, the station's total evacuation time can be determined as the maximum value stored in the *RSET* map of the concourse level. The conjunction of this value with the occupant numbers corresponding to the population clusters yields the correlation plot shown in Figure 5.14.

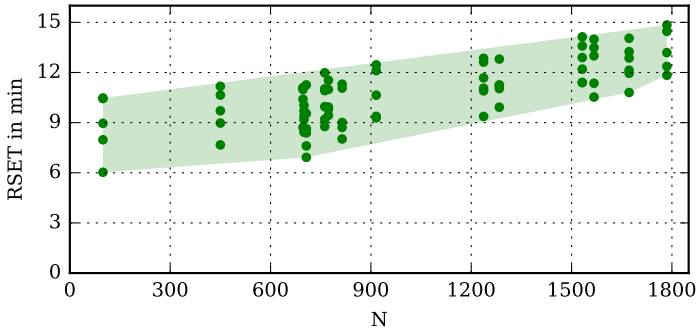

Figure 5.14: Reference occupant scenario ensemble: correlation of occupant number and *RSET*. The light green polygon illustrates the margin in which *RSET* is expected to range.

As expected, an increasing relationship between occupant numbers and total evacuation time has been determined. In concrete terms, the station's total *RSET* ranges from six up to 15 minutes. However, apart from the occupant numbers, the design of experiment obviously induces further fluctuations in the subsystem *Evacuation*. It becomes apparent that the *RSET* margins of the single design populations spread between three and five minutes. These margins are obviously affected by the remaining parameters. As shown in Figure 5.15, the pre-alarm time has been found to have remarkable influence, too.

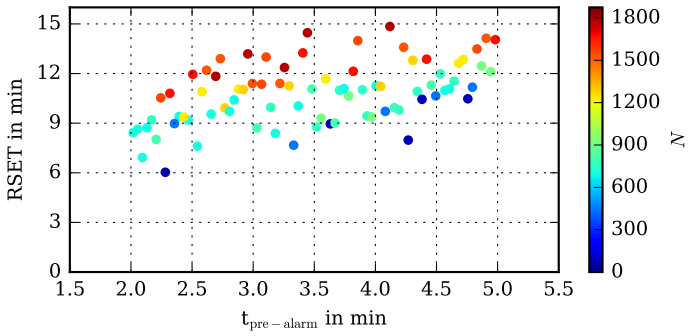

Figure 5.15: Reference occupant scenario ensemble: impact of pre-alarm time on *RSET*.

The pre-alarm corresponds to an increasing relation with *RSET*. Moreover, this relation is additionally shifted depending on the population size. These insights may be redundant when solely considering the pedestrian dynamics. However, for the upcoming consolidation of fire and occupant scenarios this mechanism will potentially influence the coincidence of occupants and fire effluents and the associated interactions.

Similar observations have been made regarding the population's route choice strategy. Figure 5.16 provides the corresponding correlation plot.

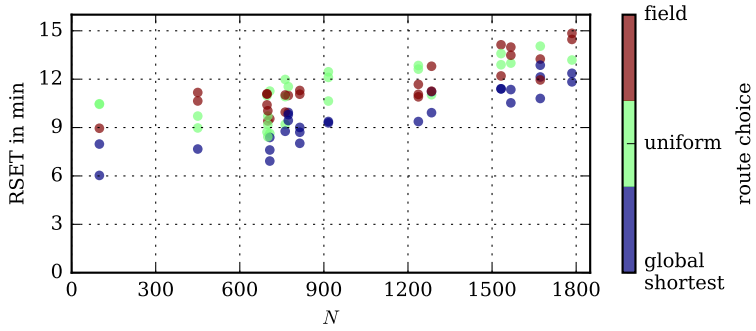

Figure 5.16: Reference occupant scenario ensemble: impact of route choice on *RSET*.

It becomes evident that route choice mode 1 (global shortest) consequently yields the lowest evacuation times. In turn, the route choice modes 2 and 3 (uniform and field data) cause higher evacuation times. This observation can be explained by the longer passages inside the concourse associated with these modes. However, no distinct separation between the latter is observable. So far, the specified pre-movement times have only minor influences on the overall evacuation time of the reference ensemble.

5.6 Summary

The occupant scenario ensemble has been set up with the aim to add certain variabilities to the subsystem. For this purpose, the following four parameters have been varied: pre-alarm time, pre-movement time, route choice, and population composition. The latter have been varied inspired by the *persona* method in conjunction with an automated agent distribution routine. The subsequent design of experiment consists of 80 occupant scenarios which have been generated with an *LHS* sampling.

Inspired by the map-based analysis of the fire scenarios within Chapter 4, the observed pedestrian dynamics are assessed with a similar approach: *RSET* maps. For every grid cell of the latter, the computed three-dimensional pedestrian trajectories are used to determine the time, when a cell has been traversed for the last time. Once repeated for every level of the station, the resulting two-dimensional maps provide comprehensive information about the evacuation process.

The preliminary analysis is based on a reference occupant scenario ensemble which does not consider any interdependences to a fire scenario. The outcome of the particular occupant scenarios has been assessed with a correlation analysis which is based on the above-mentioned *RSET* maps. The focus of the preliminary analysis was exclusively set on the station's total evacuation time. The analysis revealed *RSET*s expected in a margin from six to 15 minutes. As expected, the occupant number significantly correlates with *RSET* as it is demonstrated by the linear increasing relation of these numbers. Nevertheless, also pre-alarm time, route choice, and the varied population compositions incorporate remarkable variabilities resulting in a wide margin of *RSET*s.

These preliminary findings are intended to provide a principal overview of the simulation of the subsystem *Evacuation*. In other words, fire scenario-related interdependences, such as accelerated detection times or reduced walking speeds are not considered. The latter steps as well as the conjunction of both *ASET* and *RSET* maps will subsequently be conducted in the following chapter.

Chapter 6

Life Safety Analysis

In this chapter, the subsystems *Fire* and *Evacuation* are combined to one ensemble. After the demonstration of the corresponding workflow, the ensemble is initially assessed with a semi-macroscopic analysis which is based on difference maps derived from the introduced *ASET* and *RSET* maps. The negative fractions of the difference map distributions are used to compute the consequences of a particular combination of a fire scenario and an occupant scenario. In the next step, the Euclidean distances between the consequences of all scenario combinations are computed and stored in a distance matrix. The latter then is reassembled by an agglomerative clustering routine which allows for grouping similar observations to scenario clusters. Afterwards, these clusters are assessed in the frame of an enrichment analysis which is supposed to determine the main contributing design parameters. Furthermore, the combinatoric relations within the clusters are investigated. In the subsequent step, the scenario clusters are analysed based on the microscopic scale. The purpose of this analysis is to supplement the scenario clusters with an alternative measure of consequences, which is the concept of fractional effective doses (*FED*). In this case, the consequences are derived from the individual exposure of occupants to toxic smoke effluents. Finally, the correspondence of the two utilised consequence measures is investigated.

6.1 Ensemble Combination

According to Nilsson and Fahy's findings, a deterministic life safety analysis has to be understood as a "process of finding combined scenarios, i.e. combined fire and occupant scenarios, which challenge the [...] fire safety design" [Nilsson and Fahy, 2016, p. 2048]. The authors, moreover, state that the proper selection of combined design scenarios is "not necessarily intuitive" since the complexity of the overall system increases with a growing number of degrees of freedom.

Based on the formation of subsystems, the preceding two chapters addressed the design of experiment of the fire and occupant scenario ensembles. Now both subsystems are combined in order to conduct the overall life safety analysis. For the combination of fire and occupant scenarios, potential interactions between the latter (e.g. building use-related fire scenarios or occupant intervention) may play a certain role. In the frame of this study, however, none of these dependencies are considered.

Henceforth, a full-factorial combination of the introduced fire and occupant scenarios has been conducted as illustrated in Figure 6.1. Given that the fire ensemble consists of 108 fire scenarios and each of the underlying occupant ensemble includes 80 scenarios, a total ensemble size of $8,640$ combinations is analysed.

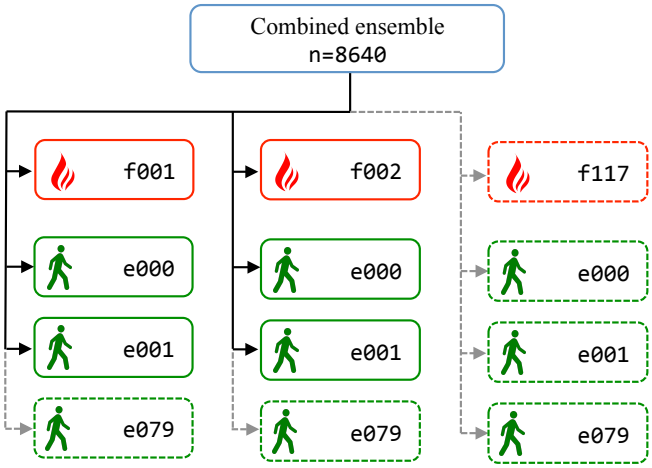

Figure 6.1: Principal structure of the combined ensemble for the life safety analysis.

As illustrated in Figure 6.1, fire scenarios are denoted by a preceding `f` and occupant scenarios by a preceding `e`. Both denotations refer to the naming of the two subsystems *Fire* and *Evacuation* and are followed by the particular scenario ID. It is to be noted that the maximum fire scenario ID `f117` is higher than the considered ensemble size for the following reason. For the further work within the ORPHEUS project, the ensemble comprises nine additional fire scenarios for questions regarding structural fire safety. The latter are not included in the life safety analysis.

6.2 Workflow

Assuming a completed fire scenario ensemble, the first stage of the overall workflow is the processing of the fire simulation data. As presented in Chapter 3, the *JPSfire* framework conducts a multitude of different operations. Firstly, *FDS* field data representing the extinction coefficient is processed in order to supply the routines determining individual detection times and reduced walking speeds in smoke. In addition to that, further life-safety relevant quantities such as temperatures and gas concentrations are prepared for the import by *JPScore*. Moreover, the above-mentioned data is utilised for the computation of the *ASET* maps introduced in Chapter 4. Once these steps are completed for a particular fire scenario, the underlying occupant ensemble is generated according to Chapter 5. In the following stage, the occupant scenarios are computed. After all trajectories have been computed, an intermediate post-processing routine calculates the *RSET* maps of each occupant scenario as presented in Chapter 5. Upon completion of one computational realisation ($8,640 \times 15$ in total), the generated output data is successively compressed and transferred to a designated file storage system. The described workflow is illustrated in Figure 6.2.

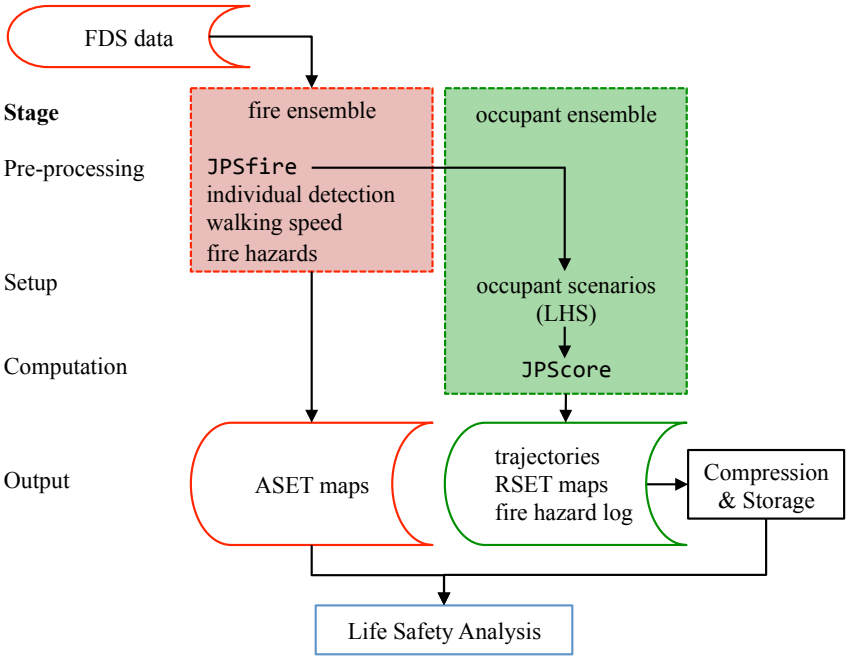

Figure 6.2: Pre-processing, setup, and computation of combined ensemble.

The workflow yields the following outputs: semi-macroscopic maps resolving *ASET* and *RSET* spatially as well as agent-based (microscopic) data, such as trajectories and fire hazard logs. In principle, the life safety analysis is conducted on the semi-macroscopic level and on the microscopic level.

6.3 Semi-macroscopic Analysis

The semi-macroscopic analysis aims at resolving the *ASET-RSET* concept in space based on the entire evacuation process. For this purpose, the previously introduced *ASET* and *RSET* maps are subtracted from each other. This operation yields a difference map which is supposed to quantify the comparison of *ASET* and *RSET* in space. With regard to [Purser, 2016a], this kind of analysis allows for the conclusion, if and to which extent the dynamics of an occupant scenario may be *impaired* by a certain fire scenario. Moreover, this approach is extended by a cluster analysis in order to group similar observations throughout the extensive ensemble. The parametric origins and relations found in the identified clusters then are investigated in the frame of an enrichment analysis.

6.3.1 Difference Maps

Assuming both maps of *ASET* and *RSET* as three-dimensional surfaces with the dimensions x, y, and time, the basic idea of the upcoming analysis is the following. A scenario combination complies with the *ASET-RSET* concept, if the *ASET* surface is above the *RSET* surface (in terms of time) and if the two do not intersect each other. The distances between these surfaces are a measure for quantifying the safety margin. If both surfaces intersect each other, the area, where the difference of *ASET-RSET* is less than zero, allows for localising and quantifying the failure. This comprehension is captured by a map representing the subtraction of *ASET* and *RSET*, which is computed for each level of the station. This process step facilitates the spatial resolution of the central question if *ASET* is greater than *RSET*. The corresponding analysis routine is provided in Appendix B.3. An exemplary difference map applicable to the U8 level is illustrated in Figure 6.3. It refers to the combination of fire scenario `f001` and occupant scenario `e013`. Both were presented in the two preceding chapters.

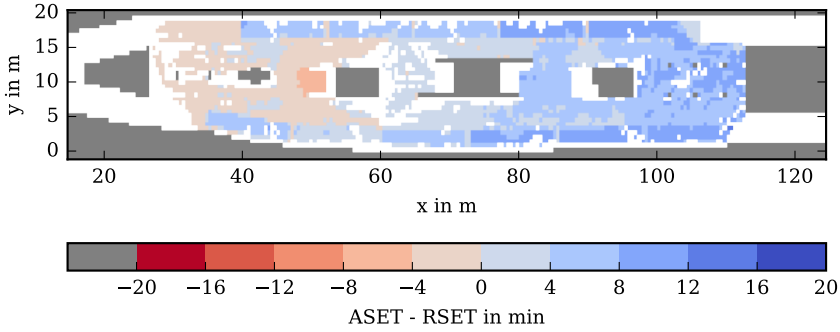

Figure 6.3: Exemplary difference map unifying *ASET* and *RSET*. The colour map has been discretised into intervals of four minutes. Grey fields represent areas that are obstructed by the built environment. White areas have not been traversed at all.

The difference map introduced above clearly indicates that the *ASET-RSET* requirement is not entirely fulfilled for this scenario combination. In particular, this applies to regions in close proximity to the seat of fire and jam areas in front of the staircases. Here, the acceptance criteria have been exceeded for up to eight minutes. In turn, the more distant areas provide a sufficient time difference of more than eight minutes. These conclusions illustrate that this analysis is able to capture the spatial distribution of the safety margin. For this purpose, the map representation can again be transformed to a distribution as illustrated in Figure 6.4.

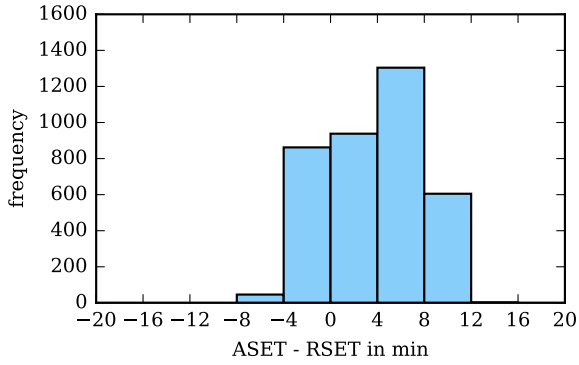

Figure 6.4: *ASET-RSET* difference map distribution.

In principle, the distribution allows for distinguishing between failure and fulfilment of the *ASET-RSET* concept. If the distribution of a subtraction map is entirely located on a range greater than zero, a particular scenario combination fulfils the *ASET-RSET* requirement. In engineering practice, this state should, of course, rely on a sufficient safety margin. However, for the ongoing analysis, $ASET - RSET = 0$ will serve as limiting state.

Quantification of Consequences The next step is to derive a measure from these maps in order to quantify the consequences of a particular scenario combination and to facilitate the comparison between the latter. Also in this case, it is possible to determine the effort which is necessary to recover a certain state of the system. The corresponding measure can be computed similarly to the *EMD*-inspired metric, which has been applied to the *ASET* distributions analysed in Chapter 4. With regard to the difference map distribution, the limiting state $ASET - RSET = 0$ is used. With this in mind, the measure is determined by consecutively summarising the bin-wise products of frequency and time difference throughout the histogram fraction less than zero as illustrated in Figure 6.5.

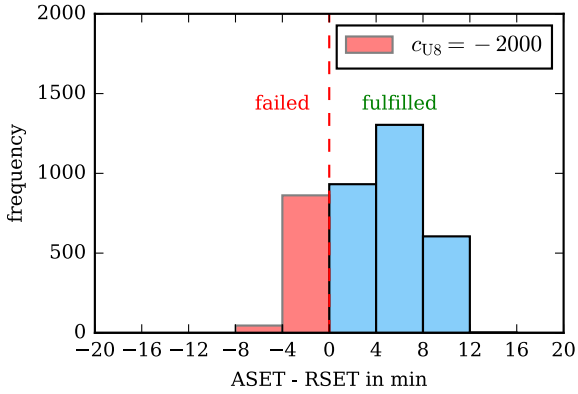

Figure 6.5: Quantification of consequences based on *ASET-RSET* difference map distribution applicable to the U8 level.

The introduced consequence measure is denoted as c and is either zero or increases negatively the more $ASET - RSET$ exceeds the limiting state. In order to capture the entire station, the consequences of all three station levels are summed up to the total consequences c_{total}. This measure is supposed to represent the consequence

corresponding to a particular combination of a fire and an occupant scenario. Since this approach incorporates spatiotemporal distributions, it is important to note that both c and c_{total} are artificial scores but they do not represent intuitive quantities, such as a time or an area. It is the product of time differences derived from *ASET-RSET* and the underlying frequencies instead. A meaning which probably is more comprehensible can be obtained as follows. With regards to the frequency, each single observation corresponds to one control element of the difference map. While every control element has an area of $0.36\,\text{m}^2$, the introduced consequence measure can also be understood as exceeding time per area. However, for the ongoing analyses, c and c_{total} are exclusively treated as a dimensionless scores.

Frequency of Consequences With regards to the entire simulation ensemble, it is valuable to investigate the frequency of the total consequences. For this purpose, the consequences of all $8,640$ scenario combinations are initially represented by a histogram as demonstrated in Figure 6.6.

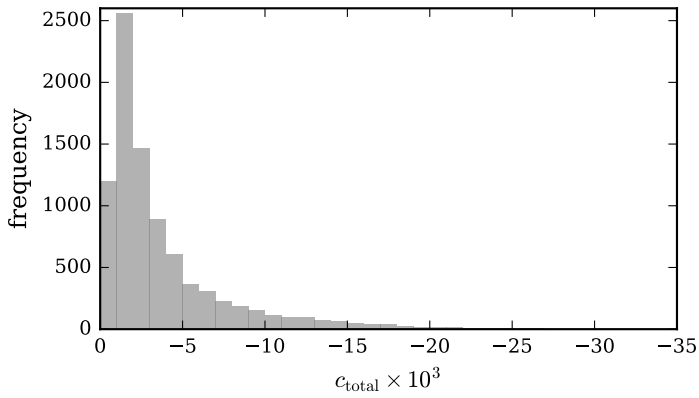

Figure 6.6: Histogram illustrating the frequency of consequences.

The total consequences range from -72 to $-32,540$. However, it turns out that more than 95 % of all scenario combinations yield consequences less severe than 50 % of the maximal observed consequences. Of course, this insight may depend on the experimental design and it may not be misinterpreted in terms of probabilities.

In addition to this summarised view, it is also possible to evaluate the consequences of each level separately. In order to gain a more refined understanding of the system's

response, Figure 6.7 opposes the total consequences and the particular consequences per level.

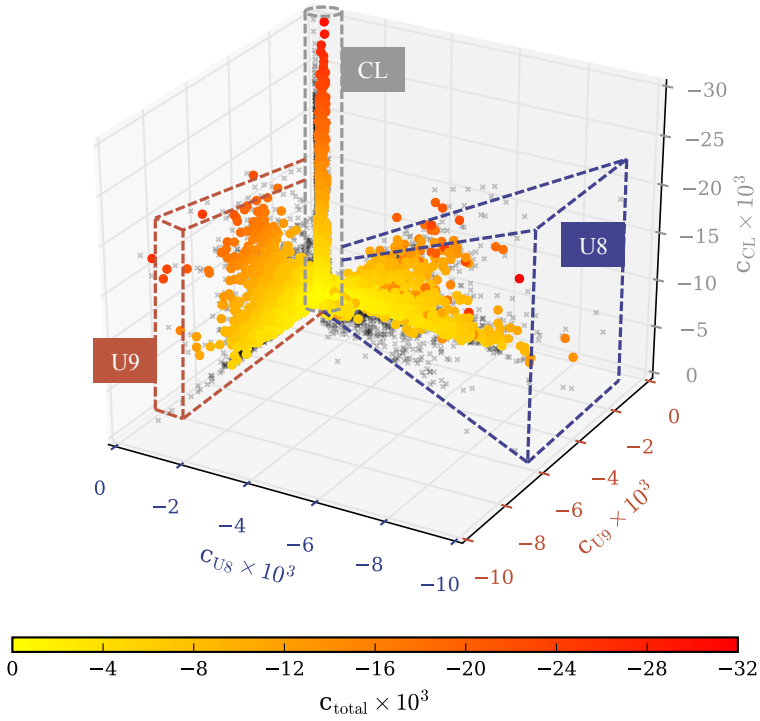

Figure 6.7: Single consequences observed on the levels U8, U9, CL, and the resulting total consequences. Scatter points represent scenario combinations and grey crosses illustrate their projection to the plains for better spatial comprehension. The dashed enclosures demonstrate the influence of the level where a fire is assumed. Note: z-axis is not to scale.

The scatter plot consists of three axes which represent the calculated consequences for all three levels of the station. Since every data point represents one combination of a fire scenario and an occupant scenario, a total number of $8,640$ points is illustrated. The fourth dimension is covered by the colouring of the data points and represents the summarised total consequences. In terms of a better spatial comprehension, the grey crosses illustrate the design points' projection to the particular plains of the plot. The illustration reveals first qualitative insights into the system behaviour. In principle, a

comparatively large agglomeration of data points represent only minor consequences, while higher consequences can be observed less frequently but on all three levels. In principle, the formation of three subdomains comes into view. These subdomains are illustrated by the dashed enclosures in Figure 6.7 and correspond to the level, where a fire was assumed. With this in mind, it becomes apparent that the consequences in the platform levels provide remarkable fluctuations. This especially applies to the observed consequences on U9, which are increasingly influenced by severe fires on U8. Consequently, the enclosure involving fires on the U8 level spans a wide space. Furthermore, fires on the U9 level induce a less extensive plain in the domain since these scenarios predominantly affect two levels. The concourse level obviously obtains a superordinate role. This is also applicable by means of quantitative comparison. It may be affected by up to $c = -30,000$, whereas the maximum consequences observed on the platform levels only range up to $c = -10,000$. This observation can be explained by two different perspectives. On the one hand, the concourse is more spacious than the platform levels. On the other hand, it is the final component of the escape route system, which inherently yields the highest *RSET*s throughout the station.

This (visual) data exploration reveals first patterns within the output of the simulation ensemble. For a more detailed analysis, the generated scenario combinations are grouped into scenario clusters based on their similarity.

6.3.2 Cluster Identification

Distance Metric The formation of scenario clusters requires a certain distance metric which is applied to all scenario combinations. In order to account for the *ASET*-*RSET* relation throughout all three levels of the station, the corresponding consequence measures are summarised to one scalar value, i.e. c_{total}. For a set of two scenario combinations i and j, the pairwise Euclidean distance between these two scalars is computed according to Equation 6.1. The distance then is stored in a distance matrix.

$$d(i,j) = \sqrt{((c_{\text{U8},i} + c_{\text{U9},i} + c_{\text{CL},i}) - (c_{\text{U8},j} + c_{\text{U9},j} + c_{\text{CL},j}))^2} \tag{6.1}$$

where:

d is Euclidean distance,

c is consequences.

Distance Matrix The distance matrix has a shape of $8,640 \times 8,640 = 72,649,600$ elements and is symmetrical. Hence, only one diagonal set of combinations needs to be processed. The resulting diagonal matrix is illustrated in Figure 6.8.

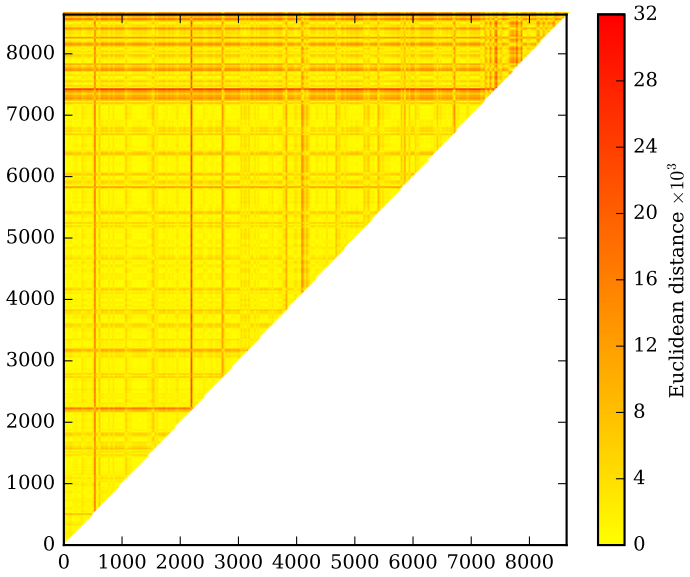

Figure 6.8: Distance matrix of all 8,640 scenario combinations.

So far, the matrix is ordered by the sequence of the labels corresponding to the fire and occupant scenarios, i.e. `f001/e001`, `f001/e002`, and so forth. However, the contrastive lines in Figure 6.8 indicate considerably different consequences of the particular scenario combinations, which are investigated in more detail.

Agglomerative Clustering In the next instance, the distance matrix is processed with an agglomerative clustering analysis, which represents a "hierarchical method for grouping observations" [Myatt, 2007, p. 111]. With regards to the scenario selection process, the method represents a bottom-up approach based on comparable consequences of a particular scenario combination. This means that all observations are initially considered as separate clusters. In the subsequent steps, these initial clusters are consecutively merged to condensed clusters based on their distances. The distances between a single observation and a cluster are determined with the help of linkage rules, e.g. *average*, *single*, or *complete*. Further reading about these rules

can be found in [Myatt, 2007, pp. 113]. The final result of the entire process is one single cluster which then consists of all processed observations. The visualisation of the cluster formation can be achieved by a dendrogram as presented in Figure 6.9.

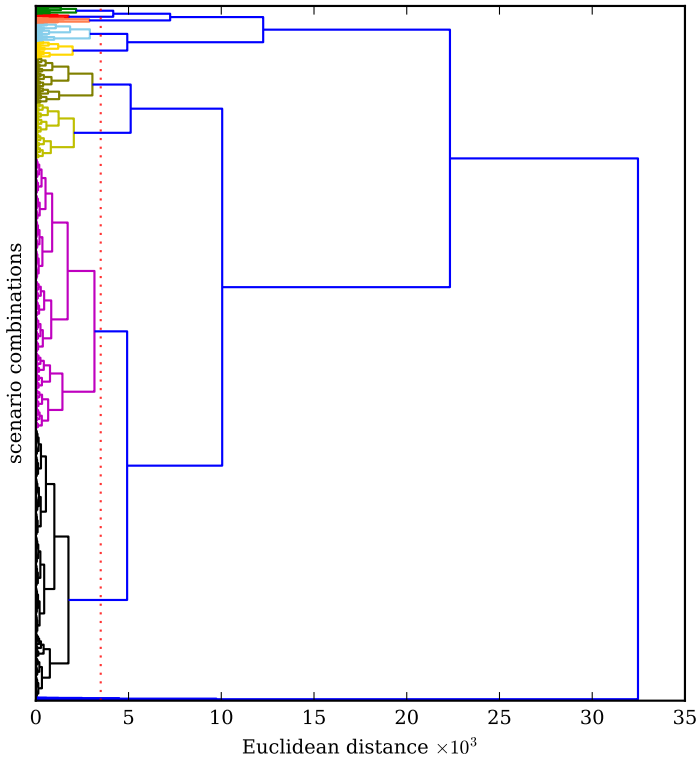

Figure 6.9: Dendrogram illustrating agglomerative clustering applied to the entire simulation ensemble. Note: one of the small clusters is in close proximity to the x-axis.

This illustration of the cluster tree can be understood as follows. The x-axis represents the distance between single observations and/or clusters. Normally, the observation labels of the particular scenario combinations are located on the y-axis. For reasons of clearness, the latter are removed in this case. Therefore, it is important to note that the sequence of these labels would now be adjusted according to the affiliation to a cluster. In general, the transition from all single observations towards one final cluster is illustrated by traversing the tree from left to right. The vertical links

mark the points where a cluster has been formed and the horizontal links represent the distances which have to be bridged for that. These aspects are important for determining a precise number of clusters, which is supposed to represent the variability within the data. This is either achieved by setting a certain cut-off distance or by defining an explicit number of clusters. In that regard, there is no golden rule for determining an appropriate number of clusters since there are distinct interdependences between the data, the applied distance metric, the linkage rules and so forth.

The formation of clusters is a trade-off between reducing the extent and conserving the information of a particular problem. Thus, multiple configurations were investigated over the course of this study. Finally, the cluster tree has been generated with the *complete* linkage rule and a predefined number of ten clusters. The corresponding threshold distance is approximately $3,500$ and is illustrated by the dotted line in Figure 6.9. Table 6.1 provides an overview of the identified clusters, their total sizes, the numbers of unique fire and occupant scenarios, and the observed consequences inside the clusters. It is to be noted that the sequence of the cluster IDs does not correspond to the rank of consequences. For this reason, additional cluster names ranging from A to J are introduced which are consecutively assigned according to the increase of consequences.

Table 6.1: Overview of identified scenario clusters.

Name	**ID**	**Size**	**Fire**	**Occupant**	$\mathbf{c}_{\min}$	$\mathbf{c}_{\max}$
Cluster A	2	3354	108	80	-72	-1832
Cluster B	1	3367	106	79	-1834	-4996
Cluster C	3	688	69	73	-5006	-7056
Cluster D	5	562	47	64	-7070	-10122
Cluster E	4	208	39	45	-10142	-12130
Cluster F	6	227	31	39	-12160	-15074
Cluster G	7	152	27	28	-15158	-19334
Cluster H	9	55	18	14	-19524	-22402
Cluster I	8	24	12	6	-22804	-27298
Cluster J	10	3	3	1	-28846	-32540

The cluster formation reveals rather heterogenous characteristics. The first two clusters, namely A and B, involve over three quarters of all observations, while almost all single fire and occupant scenarios occur at least once. In turn, with increasing consequences, the cluster sizes decrease, while their characteristics become more and

more unique. In this respect, unique means that the variability of the contributing fire and occupant scenarios becomes less.

In addition to this summarised view, the characteristics of the individual clusters are analysed in more detail in the next section.

6.3.3 Enrichment Analysis

The purpose of the enrichment analysis is to explore patterns in the parametrisation of the identified clusters. In this respect, an essential question is if the consequences are either driven by the fire scenarios or by the occupant scenarios.

For this purpose, radar plots are applied (e.g. Figure 6.10). Within a particular cluster, these diagrams oppose the design of experiment of the two subsystems *Fire* and *Evacuation* with the frequency of observations. In terms of a more meaningful visualisation of the design fires and population clusters, the sequence of the frequency bars has been sorted by the overall heat release and by the corresponding occupant numbers. Moreover, the labels of the population cluster IDs are supplemented by the occupant numbers.

In addition to the frequency of single observations, the parametric relations of the particular scenarios may reveal further insights into the system's behaviour. Therefore, parallel coordinate plots are utilised in order to illustrate the combinatorics inside one cluster (e.g. Figure 6.11). These plots are set up as follows: the upper subplot represents the fire scenarios and the lower subplot describes the occupant scenarios. Moreover, the upper subplot includes the linkage between a fire and an occupant scenario, which is illustrated by a grey line. While the x-axes involve the particular parameters of the two mentioned subsystems, the y-axes consist of the levels of each parameter. For a particular combination of a fire and an occupant scenario, a polyline consisting of eight vertices can be populated across the two subplots. In order to visualise the formation of patterns, more frequent polylines are emphasised by increased line widths and more intense colouring.

In the following paragraphs, an exemplary excerpt of four clusters is analysed in more detail. These are the scenario clusters A, B, F, and J (see Table 6.1). The sequence of the clusters represents the severity of the incorporated consequences. The examination of the remaining clusters can be found in Appendix C. For a better comprehension of the less intuitive parameter levels, especially fire locations and design fires, it may be valuable to recapitulate Section 4.3.1 and Section 4.3.2 in advance. Please note that some interpretations are not exclusively derived on the basis of one cluster but also in reference to adjacent clusters.

Scenario Cluster A Scenario cluster A represents the lowest margin of consequences observed in the entire ensemble. The cluster has a total size of 3354 scenario combinations, while every fire scenario and every occupant scenario occurs at least once. The underlying design parameters are illustrated in Figure 6.10.

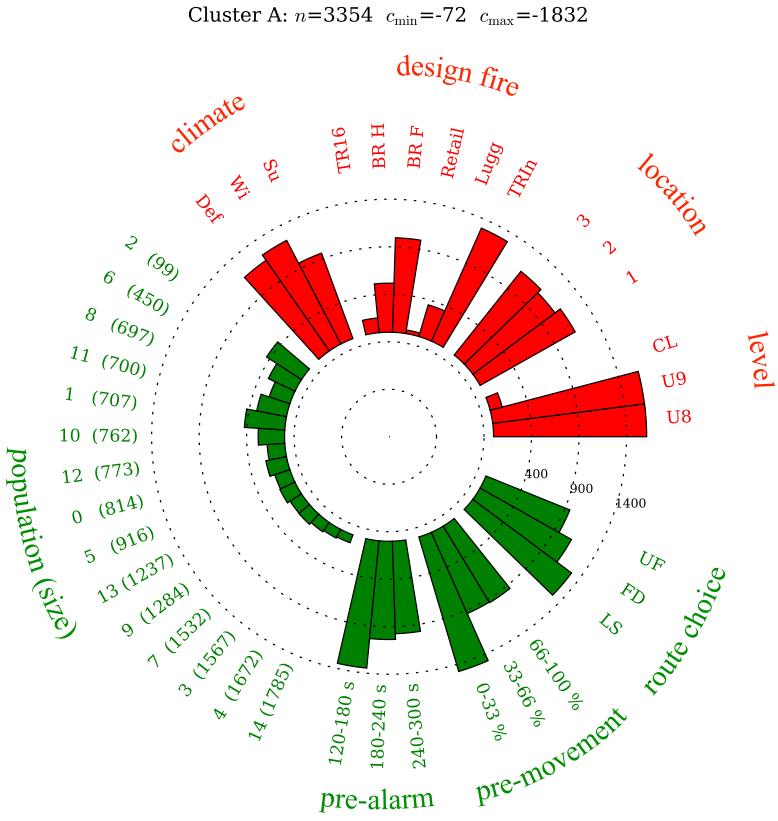

Figure 6.10: Radar plot illustrating the parametric origin of cluster A.

With regards to the fire scenarios, the cluster is predominantly driven by the design fires *TRIn*, *BR F*, and *BR H*, i.e. low-energetic and moderately increasing high-energetic fires. Consequently, the fires placed in the platform levels clearly represent the largest portion in the cluster. In terms of the occupant scenarios, the cluster mainly accumulates populations with less or equal than one thousand occupants. Moreover, it becomes evident that the lowest modes of both pre-alarm times and pre-movement times obtain a superordinate role. The same applies to the route choice

where shortest path configuration can be observed most frequently. A more specific view on the relations between the subsystem's parameters is provided in Figure 6.11.

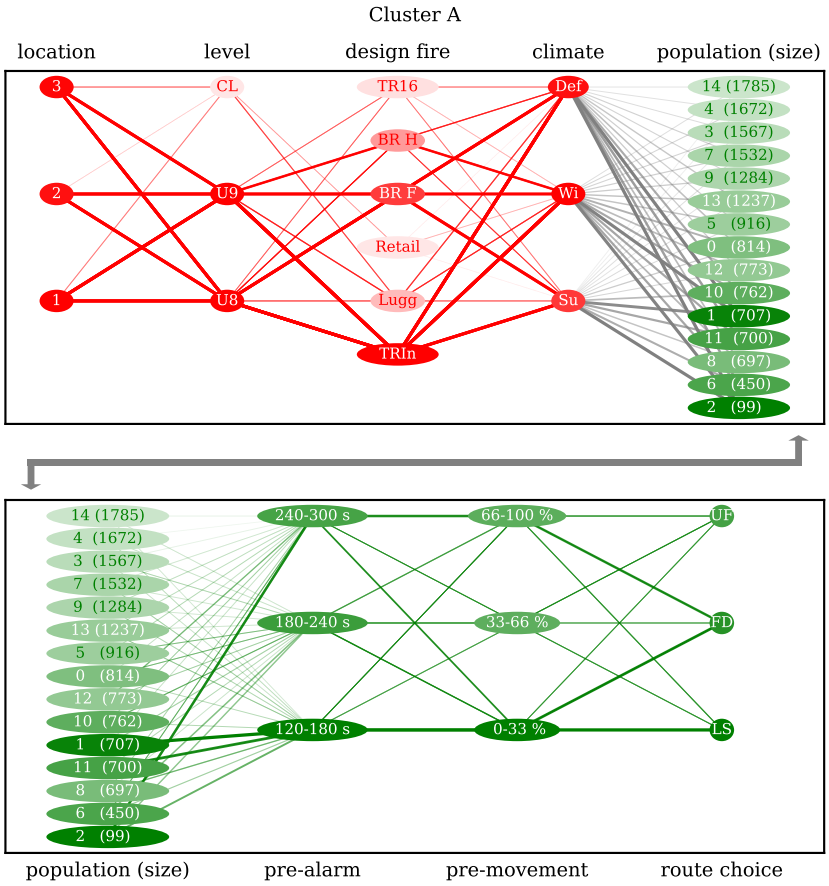

Figure 6.11: Parallel coordinate plot illustrating the parametric relations of cluster A.

It turns out that the few fires assumed in the concourse are predominantly located at the more remote locations 1 and 3 (see Section 4.3.1). These cases are oftentimes associated with *Luggage* fires, while the *Retail* fires play a subordinate role – if at all in conjunction with winter conditions. With regards to the fires in the platform levels, it becomes evident that the moderate consequences of the *TRIn* fire are almost independent from the remaining parameters. Similar observations can be made for the *BR F* fire. However, despite comparable initial heat releases, the *BR H* fire is

found to be less adverse on the U9 level and in connection with winter conditions. In terms of the climatic influences, contrary observations can be made for the *TR16* fire which is more frequently associated with summer and default conditions in this cluster.

With regards to the occupant scenarios, the accumulation of smaller populations is emphasised by the grey linkage lines. The populations can be conjunct with the specified pre-alarm times. Here, it is shown that this cluster involves a certain balance between the population sizes and pre-alarm times in order to cope with worsening conditions and to maintain the lowest margin of consequences simultaneously.

Scenario Cluster B The subsequent margin of consequences is represented by cluster B, whose size is almost similar in comparison to cluster A. Again, the radar plot shown in Figure 6.12 provides the corresponding design parameters.

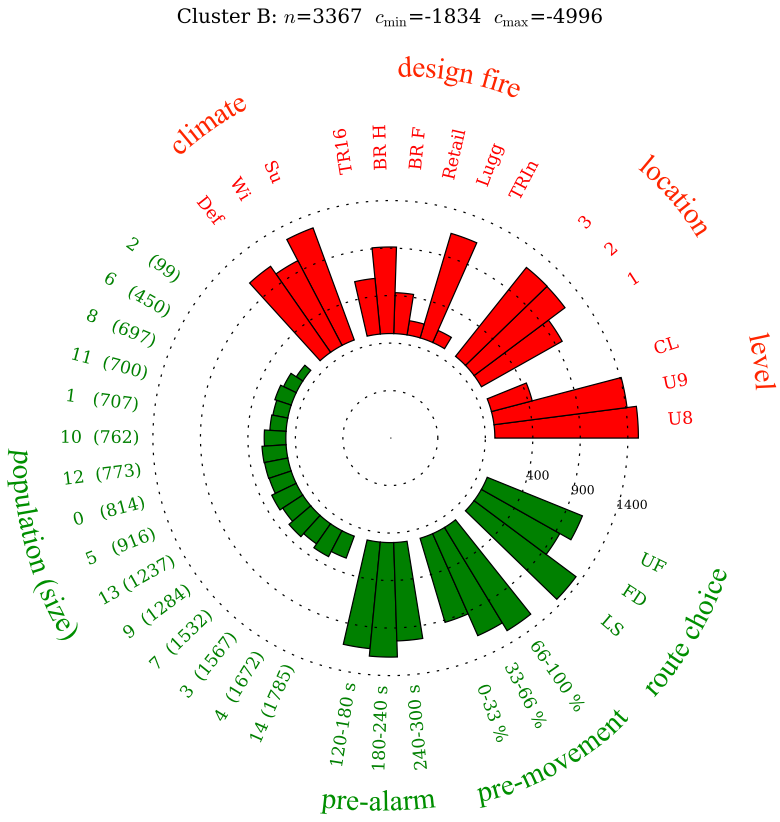

Figure 6.12: Radar plot illustrating the parametric origin of cluster B.

At a glance, the parametrisation of the fire scenarios reveals patterns similar to cluster A. However, the impact of the design fires is different since the relevance of the *Luggage* fire increases. Moreover, the influence of the design fires *BR H* and *TR16* becomes more distinct, while the importance of *BR F* decreases. The transition from *BR F* to *BR H* is an unexpected response since the stand-alone analysis of the fire simulation ensemble revealed that the development of *ASET* corresponding to *BR H* is less adverse than in case of *BR F*. This can be explained by the inter-accessibility of the *BR H* carriage which results in widespread smoke emission.

Simultaneously, the contributing occupant scenarios provide interesting trends. For instance, population clusters with occupant numbers greater than one thousand gain importance. Moreover, the time components set for the pre-alarm and pre-movement phases start shaping up to their upper boundaries. In addition to the frequency of observations, the connection between the particular parameter levels is illustrated in Figure 6.13.

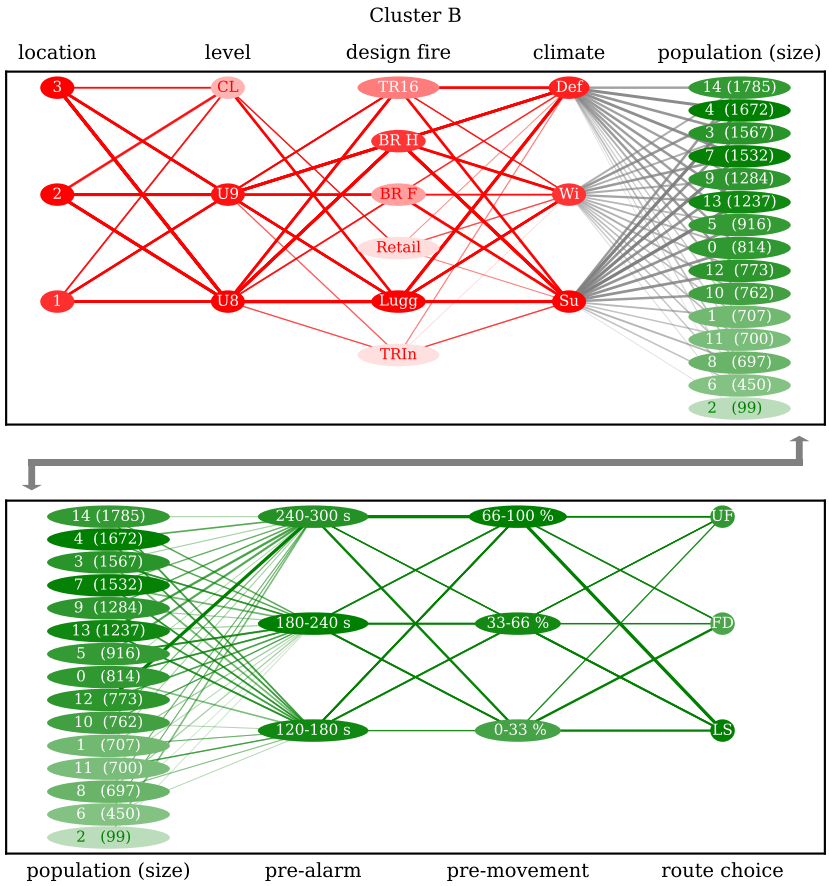

Figure 6.13: Parallel coordinate plot illustrating the parametric relations of cluster B.

In this range of consequences, the visualisation emphasises the superordinate roles of the *Luggage* and the *BR H* fires. For both of them, no distinct influence of the remaining fire scenario parameters can be derived. In turn, the scenarios associated

with the *TR16* fire are composed differently. For instance, it turns out that the U8 level is observed more frequently than the U9 level. Moreover, the climate parameters indicate that summer and default conditions correspond to minor consequences in this case. With regards to cluster A, the predicted consequences of a *BR F* fire are contrarily more severe on the U9 level compared to the U8 level. The few cases when the *TRIn* fire yields higher consequences, correspond to default and summer conditions, while the level is not influential. In reference to cluster A, the implication that the consequences of the *Retail* fires are smaller during winter conditions persist in cluster B as well.

The occupant scenarios reveal a rather uniform distribution of the particular populations. Again, a balance between population sizes and pre-alarm times can be observed. However, the spread of the linkages is wider compared to cluster A, which can be explained by the distinct variability regarding the pre-movement times and route choice. Between the latter two, only one pattern has formed: high pre-movement times frequently correspond to local shortest path route choice.

Scenario Cluster F An intermediate margin of consequences is covered by scenario cluster F, which has a size of 227 observations. This comparatively small subset of the design space consists of 31 different fire scenarios and 39 occupant scenarios. The contributing design parameters are presented in Figure 6.14.

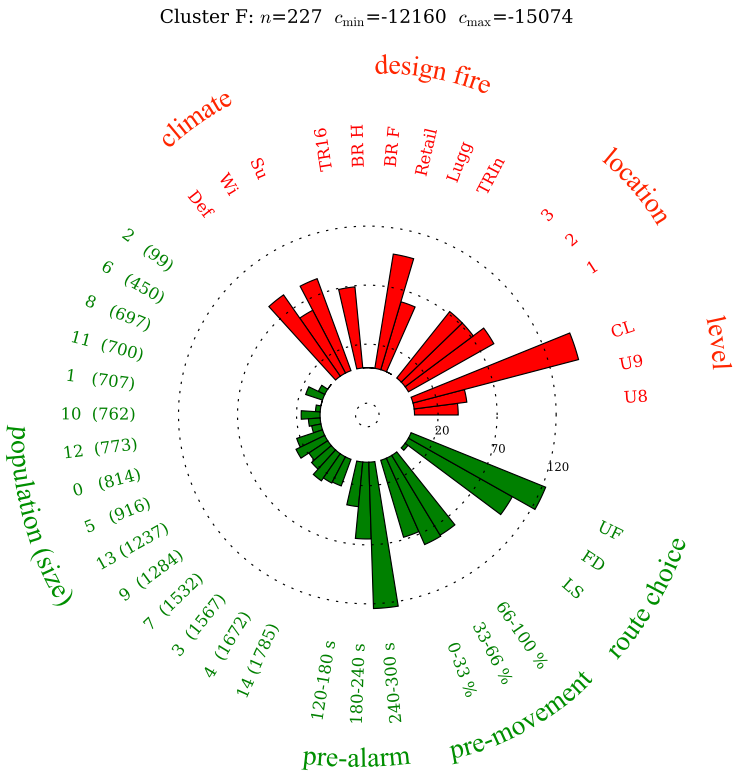

Figure 6.14: Radar plot illustrating the parametric origin of cluster F.

Meanwhile, the relations between the parameters have changed and start pointing the direction towards the scenario combinations with the most adverse consequences. In terms of the fire scenarios, fire locations inside the concourse level have become the superordinate design parameter within this cluster. Consequently, the *Retail* and *Luggage* design fires are the most frequent observations. However, also the *TR16* fire persists in this cluster, which mainly represents the remaining fires placed in both U8 and U9. Moreover, it could be observed that the contribution of winter conditions decreases, which may be explained by their advantageous effect on the ventilation of

the concourse level. With regards to the occupant scenarios, the frequency of the population clusters increasingly shifts towards higher occupant loads. However, some fluctuations within the range of 450 to 800 occupants, i.e. daytimes with smaller but more diverse populations, are observable. The parametrisation of the pre-alarm time is now predominantly driven by the highest mode, i.e. 240 to 300 seconds. Contrary to that, the pre-movement times are almost uniformly distributed. Finally, the underlying route choice configurations are almost equally associated with uniform exit usage and route choice derived from collected field data. In the next instance, the relations between the parameter levels of cluster F are investigated using Figure 6.15.

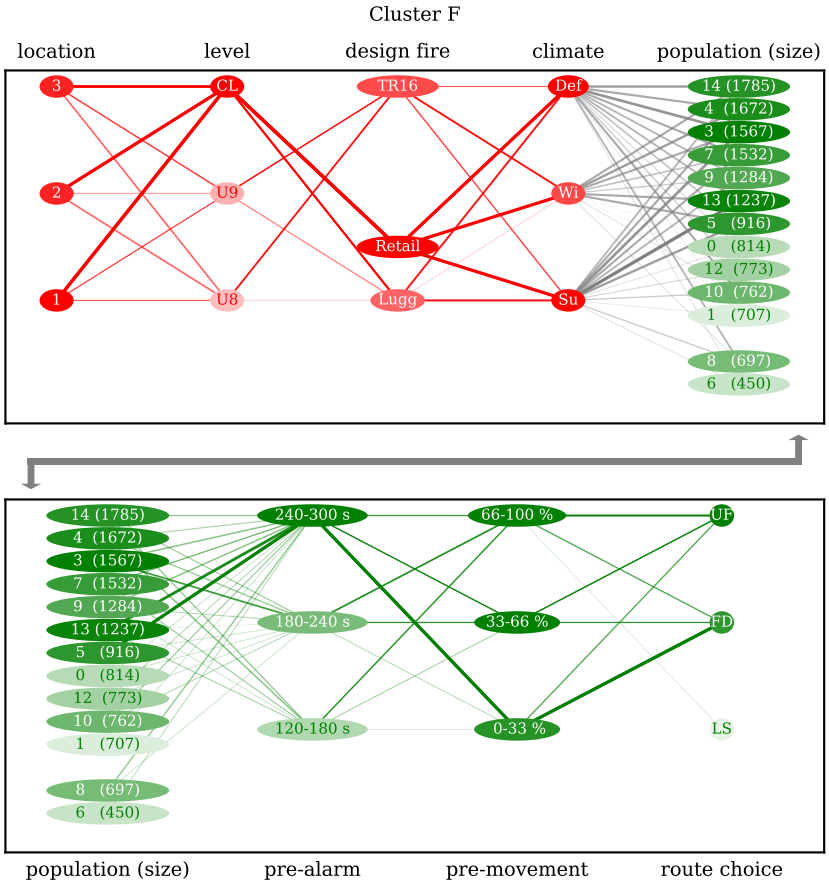

Figure 6.15: Parallel coordinate plot illustrating the parametric relations of cluster F.

Within the intermediate margin of consequences, the Parallel coordinate plot of cluster F starts diminishing. In concrete terms, only the design fires *Luggage*, *Retail*, and *TR16* remain in this cluster and two of the smaller populations are not represented anymore. The superordinate design fire is the *Retail* fire. Here, the impact of the climatic conditions inverts since cluster F represents the transition, when the more favourable winter conditions start being superposed by the more adverse default or summer conditions. Similar findings apply to the *Luggage* fire. In this case, it turns out that the majority of the corresponding fire scenarios are located in the concourse, while they are also most frequently conjunct either with default or summer conditions. Contrary to these findings and in contrast to cluster B, the (intermediate) consequences induced by the *TR16* fire are increasingly related to winter conditions.

The linked occupant scenarios are dominated by larger populations. A notable insight is that mid-sized populations frequently correspond to high pre-alarm times paired with low pre-movement times. Finally, this constellation is oftentimes related to route choice according to field data.

Scenario Cluster J The tenth and final scenario cluster represents the most adverse margin of consequences that has been observed throughout the entire design space. In comparison to the aforementioned clusters, it is extremely small since it only consists of three single observations. These observations are composed by three unique fire scenarios and one single occupant scenario. A more detailed view of the design parameters is provided in Figure 6.16.

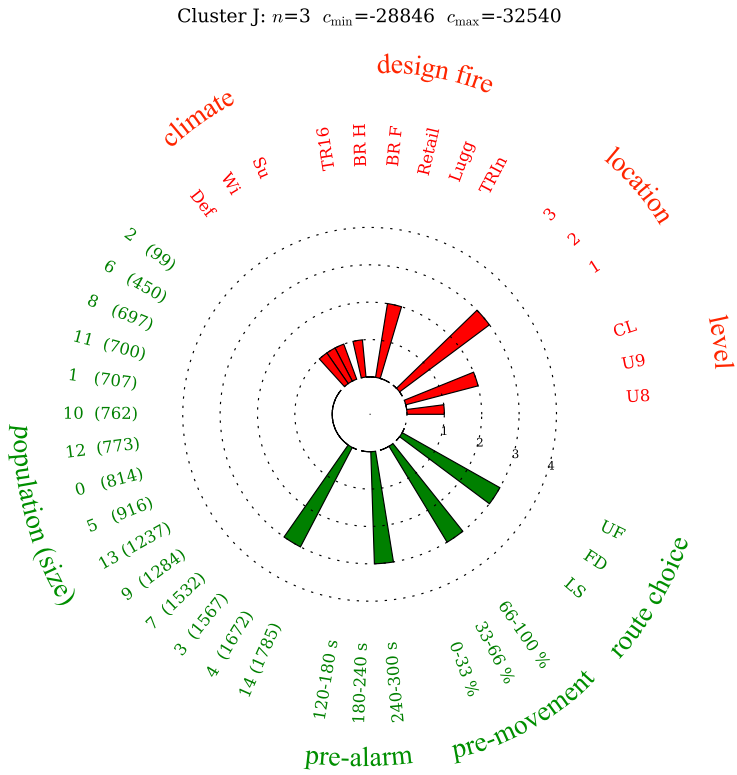

Figure 6.16: Radar plot illustrating the parametric origin of cluster J.

The three fire scenarios of this cluster cover two *Retail* fires placed in the concourse level and one *TR16* fire located in the U8 level. Moreover, it becomes apparent that the cluster reveals the most critical placement in the two particular levels. This is location 2 in both cases, which is either the centre of the U8 level or the large retail unit on the concourse level closest to the staircases towards the underground. It is notable that this scenario cluster involves all three climatic conditions, which is

a vivid demonstration of the complex interdependences between the fire dynamics, ambient temperatures, and background airflows.

At a glance, the single occupant scenario yields expected results, e.g. the maximum assigned times for both pre-alarm and pre-movement phase and an exit choice that is based on field data. However, a noteworthy finding is that the cluster including the most severe consequences does not include the globally largest population (population cluster 14) but the second largest population (population cluster 4). A more detailed view on the relations between the parameters of the three fire scenarios is provided in Figure 6.17.

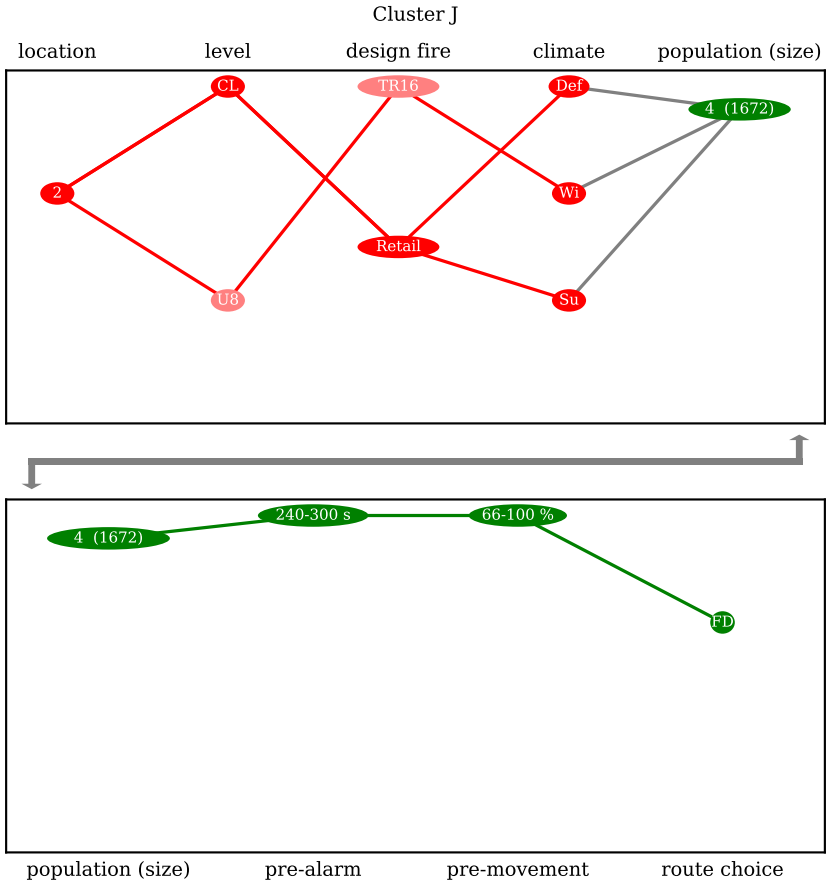

Figure 6.17: Parallel coordinate plot illustrating the parametric relations of cluster J.

In accordance with the conclusions drawn from the preceding clusters, the Parallel coordinate plot reveals that the two *Retail* fires can be traced back to default and summer conditions. These induce only limited capabilities of natural ventilation of the concourse level. The opposite effect can be observed for the single *TR16* fire in the underground paired with winter conditions. Here, the propagation of heat and smoke is adversely supported by the establishing temperature zones and airflows.

Moreover, the fact that only the second largest population corresponds with the most severe consequences can be explained as follows. Population cluster 14 represents the morning peak which is the busiest daytime at all. However, during this time, the population mainly consists of adults and young people and the building use is predominantly transportation. Contrary to that, population cluster 4 is supposed to cover the afternoon peak. In this case, the population is slightly smaller but its composition is rather diverse, e.g. with a higher number of elderly people. Moreover, this time of the day comes along with two overlapping building uses, i.e. transportation and shopping, which additionally affects the occupant distribution throughout the station.

6.4 Microscopic Analysis

The semi-macroscopic analysis has aimed at structuring the big data problem based on the similarity of the *ASET-RSET* relation involving all scenario combinations. The main deliverable of an *ASET-RSET* analysis is whether and to which spatiotemporal extent the dynamics of an occupant scenario may be *impaired* by a certain fire scenario, but it does not readily provide an answer to the question if the evacuation process may be *prevented* at all [Purser, 2016a]. For this purpose, a microscopic analysis using fractional effective doses (*FED*), as introduced in Chapter 3, is utilised. More precisely, this analysis is supposed to supplement the identified scenario clusters with the *FED* applicable to incapacitation (FED_{In}). Firstly, this step aims at providing the scenario clusters with more meaningful figures which are common in the field of *FSE*. In addition to that, an essential question is if there is a correspondence between the proposed *ASET-RSET* consequence measure and the *FED* analysis.

The FED_{In} measure has been logged agent-wise throughout all scenario combinations and computational realisations, which yields 129,600 fire hazard logs. For a particular scenario cluster, the aforementioned fire hazard logs are transferred to *FED* histograms as presented in the following paragraphs. This data transformation covers the combination of all fire scenarios and occupant scenarios belonging to one

cluster. The histograms allow for conclusions about the expected consequences corresponding to a scenario cluster. For this purpose, the FED_{In} axis has been divided into three different ranges which represent different extends of consequences. In this regard, Purser and McAllister proposed design thresholds of $FED_{\mathrm{In}} = 0.3$ appropriate for "the general population" and $FED_{\mathrm{In}} = 0.1$ applicable to "particularly sensitive groups" [Purser and McAllister, 2016, p. 2343]. In the final instance, $FED_{\mathrm{In}} = 1.0$ implies loss of consciousness. Across all scenarios combinations within a specific cluster, the y-axis represents the mean number of occupants who are affected by a particular range of consequences. The mean values have been chosen, in order to characterise the consequences in a more global fashion rather than overestimating the impact of single observations. Moreover, in contrast to a normed illustration of the histograms, a concrete number is assumed to be more intuitive. In order to keep track of lower occupant numbers, a logarithmic scale has been chosen.

Again, the four clusters discussed in Section 6.3 are examined in more detail, while their sequence corresponds to the consequences determined within the semi-macroscopic analysis. The investigation of the remaining clusters can be found in Appendix C. In order to distinguish between the levels, where a fire was assumed, the histograms are subdivided accordingly.

Scenario Cluster A In terms of *ASET-RSET*, scenario cluster A includes 3354 scenario combinations and involves the most moderate consequences. The corresponding *FED* histogram is provided in Figure 6.18.

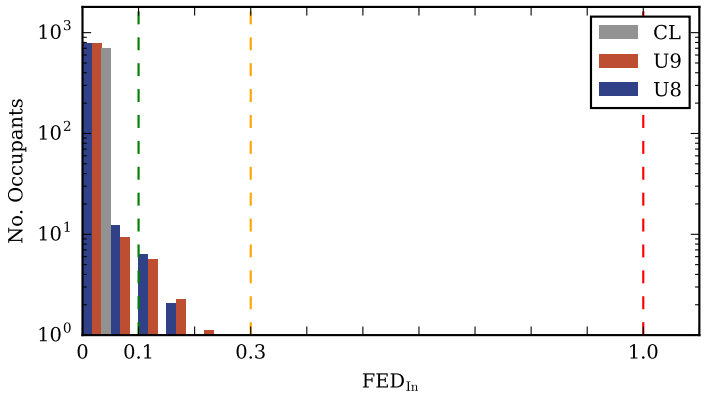

Figure 6.18: *FED* histogram of scenario cluster A.

As discussed in Section 6.3.3, cluster A accumulates occupant scenarios with small occupant numbers, which can be recognised by the limited extend of the histogram's bars. Further on, it becomes apparent that none of the scenarios in cluster A includes occupants being observed with an $FED_{\mathrm{In}} > 0.3$. On average, only a small fraction of less than 20 occupants exceeds the $FED_{\mathrm{In}} = 0.1$ threshold. In addition to these findings, the system behaviour is rather similar to fires originating in both U8 and U9. Contrary to that, scenario combinations associated with fires in the concourse level, show different outcomes. Here, none of the corresponding scenarios even reached the $FED_{\mathrm{In}} = 0.1$ threshold. This insight can be explained in terms of different aspects. Firstly, the concourse level is the final means of escape, which results in small exposure times in comparison to fires in the subjacent levels. Secondly, the underlying occupant scenarios within cluster A predominantly imply a shortest path route choice strategy. Moreover, the sprinkler-affected fires start decaying during the evacuation process. On the one hand, this may yield small *ASETs*. On the other hand, the conditions may improve in the later stages of the evacuation process which yields lower exposures to fire effects. Finally, the fire scenarios in the concourse are exclusively assigned with a PVC combustion reaction so that FED_{In} is not additionally influenced by HCN in these cases.

Scenario Cluster B The second scenario cluster involves 3367 scenario combinations and represents the second margin of consequences. The associated *FED* histogram is illustrated in Figure 6.19.

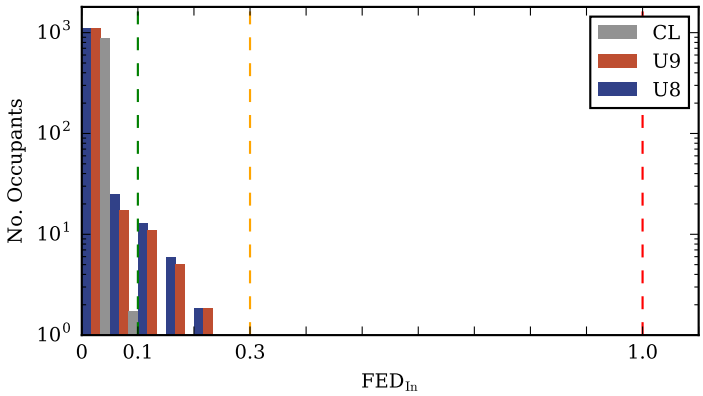

Figure 6.19: *FED* histogram of scenario cluster B.

Except for higher overall occupant numbers, the observed response is rather similar to scenario cluster A. Again, none of the scenario combinations exceeds the $FED_{\mathrm{In}} > 0.3$ threshold. However, the subset of observations in the range from $FED_{\mathrm{In}} = 0.1$ to $FED_{\mathrm{In}} = 0.3$ has increased and starts shifting towards the upper boundary. To a smaller extent, similar observations can be made for the scenario combinations representing fires in the concourse, which increasingly result in doses close to the $FED_{\mathrm{In}} = 0.1$ threshold. All in all, the latter cases remain less adverse than the ones in the subjacent levels.

Scenario Cluster F An intermediate range of consequences is represented by scenario cluster F, which consists of 227 scenario combinations. Figure 6.20 provides the corresponding *FED* histogram.

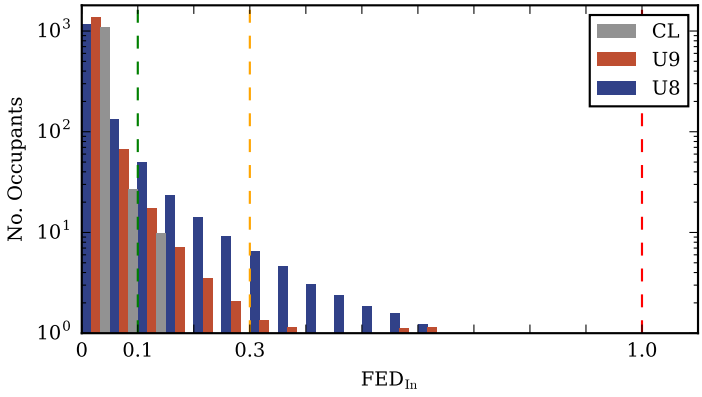

Figure 6.20: *FED* histogram of scenario cluster F.

Scenario cluster F reveals notable changes regarding the system's response. At first view, it becomes evident that the $FED_{\mathrm{In}} = 0.3$ threshold is now exceeded in a number of observations, while the majority is represented by scenarios with a fire assumed in the U8 level. Having said that, the aforementioned similarity of the consequences of fires placed in the platform levels starts fading. With regards to fires located in the concourse area, the analysis now also yields single occupants who have exceeded the $FED_{\mathrm{In}} = 0.1$ threshold. In summary, a rather systematic stacking of the single histograms (per level) has formed.

Scenario Cluster J Finally, scenario cluster J involves the maximum consequences determined with *ASET-RSET*. It is noteworthy that the uniqueness of the agglomerated observations yields a very small cluster which only consists of three different fire scenarios paired with one single occupant scenario. The appurtenant *FED* histogram can be found in Figure 6.21.

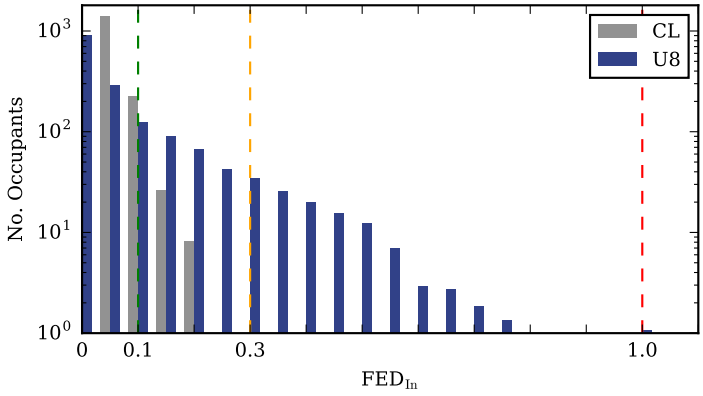

Figure 6.21: *FED* histogram of scenario cluster J.

At first sight, it becomes obvious that cluster J does not contain a fire scenario associated with the U9 level. A clear separation between the histograms of the U8 level and the concourse can be observed, too. With regards to the U8 level, on average, a number of 300 occupants is expected to exceed the $FED_{\mathrm{In}} = 0.3$ threshold. The two fire scenarios located in the concourse also reveal increasing numbers of occupants above the $FED_{\mathrm{In}} = 0.1$ threshold, while $FED_{\mathrm{In}} = 0.3$ remains unaffected in all cases.

An understanding which probably is more comprehensive in terms of higher margins of consequences, including U9 scenarios, can be achieved by considering scenario cluster I as well (see Appendix C). The analysis of the latter reveals that there may also be scenario combinations where a few occupants were observed in close proximity to the $FED_{\mathrm{In}} = 1.0$ threshold. This finding and the stacking patterns in the *FED* histograms indicate that the most adverse consequences of *ASET-RSET* may not necessarily imply corresponding responses in terms of an *FED* analysis. Having said that, the relation between these two approaches finally is investigated in more detail.

6.5 Comparison of Semi-macroscopic and Microscopic Analysis

In order to compare the outcomes of *ASET-RSET* and *FED*, a correlation analysis opposing these two approaches is conducted. For this purpose, the outputs of both analyses have to be incorporated as scalars. Regarding the *ASET-RSET* approach, the consequence measure introduced in this chapter is applied. Moreover, the *FED* analysis is expressed by the average number of occupants which have been observed exceeding the FED_{In} thresholds introduced in the previous section. In the following scatter plots, every data point represents one scenario combination. Once again, the data points are separated based on the level, where a fire was assumed. In this respect, Figure 6.22 provides the scatter plot corresponding to the range $0.1 < FED_{\mathrm{In}} < 0.3$.

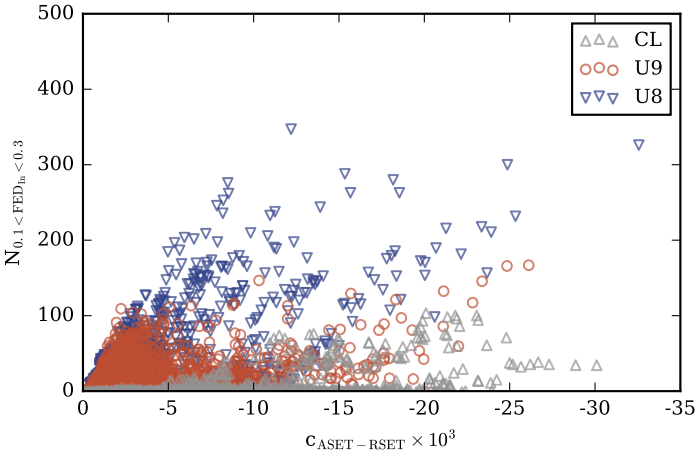

Figure 6.22: Correspondence of *ASET-RSET* analysis and *FED* analysis applicable to $0.1 < FED_{\mathrm{In}} < 0.3$.

The plot presented above fulfils one of the initial expectations. To a small extent, there is an increasing relation between the consequences determined with *ASET-RSET* and *FED*. However, there are distinct fluctuations within the data, which apparently have different origins. Also here, a clear separation between the different levels comes into view since the consequences of the U8 scenario combinations are above the U9 and CL cases. The maximum average number of occupants whose doses are in the range of $0.1 < FED_{\mathrm{In}} < 0.3$ is less than 400. With regards to the concourse

fires, it becomes evident that there is a delay ($c \approx -5,000$) before doses exceeding the $FED_{\mathrm{In}} = 0.1$ threshold respond to the violation of *ASET-RSET*. In contrast to that, fires originating in U8 or U9 instantaneously yield a relation between violating *ASET-RSET* and increasing effective doses. Another notable observation is that, in case of U8 and CL fires, the maximum doses do not straightforwardly correspond to the maximum consequences in terms of *ASET-RSET*. In case of the U8 level, this is a singular observation (at $c \approx 11,000$, $N \approx 350$), but a rather systematic one for the concourse level (beginning from $c \approx 24,000$, $N \approx 100$). In summary, it turns out that even scenario clusters representing the lower third of consequences in terms of *ASET-RSET* may approach the upper consequence boundaries in terms of fractional effective doses.

In the next instance, a similar analysis is conducted using the number of occupants whose doses correspond to $FED_{\mathrm{In}} > 0.3$ as shown in Figure 6.23.

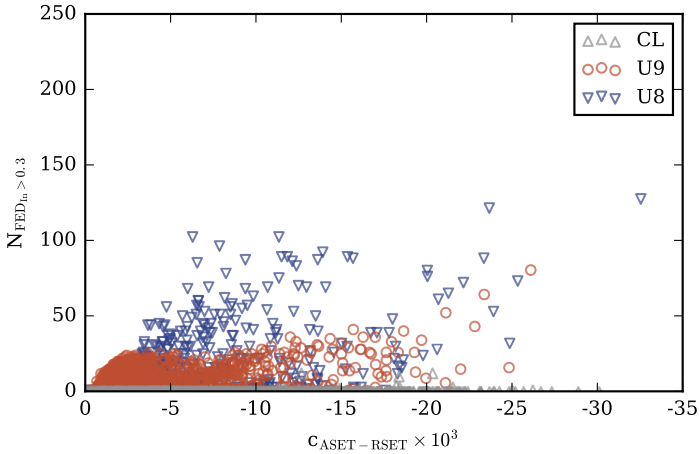

Figure 6.23: Correspondence of *ASET-RSET* analysis and *FED* analysis applicable to $FED_{\mathrm{In}} > 0.3$.

The scatter plot applicable to $FED_{\mathrm{In}} > 0.3$ reveals similar patterns compared to the preceding threshold. Once again, the FED_{In} consequences determined for the U8 scenario combinations are above the U9 cases. However, for this particular threshold, the concourse scenarios equals zero almost entirely. Moreover, the average number of affected occupants is far less than 150. Increasing relation between *ASET-RSET* and *FED* can only be observed in isolated subdomains. For instance, fires

in the U8 level instantaneously imply a correspondence between both consequence measures. However, there are also delayed responses of *FED* in the range of higher consequences ($c > 10,000$) regarding *ASET-RSET*. Different observations can be made for fires located at the U9 level. Here, the *FED* response forms a plateau up to $c = 10,000$ before a slightly increasing relation between the two consequences measures becomes apparent.

6.6 Summary

The life safety analysis unified the two subsystems *Fire* and *Evacuation*. For this purpose, a semi-macroscopic and a microscopic analysis were conducted, while these two approaches were finally related to each other.

The semi-macroscopic analysis utilised the map representations of both *ASET* und *RSET* as they were introduced in the preceding chapters. These maps were used in order to compute a difference map which represents the spatial relation of *ASET* and *RSET* for a combination of a fire and an occupant scenario. Having done that, the fraction of the negative times in the difference map distribution can be used to quantify the consequences inspired by the earth mover's distance (*EMD*). This measure has been used to calculate the Euclidean distance between all $8,640$ scenario combinations. The resulting distance matrix serves as input for an agglomerative clustering which revealed ten scenario clusters unifying similar observations. These clusters then were assessed with the help of an enrichment analysis. The latter allows for identifying patterns in the underlying parametrisation of the two subsystems *Fire* and *Evacuation*.

Subsequently, the microscopic analysis has aimed at providing the identified clusters with supplementary numbers which are more figurative and common in the field of *FSE*. In concrete terms, the concept of fractional effective doses (*FED*) was applied for this purpose. To some extent, a relationship between these two analyses has been found. However, the conjunction of both outputs raised questions concerning particular fluctuations which have finally been discussed in a correlation analysis opposing the results of both approaches. One of the main findings is that there is a non-trivial dependency between both location and spatial extend of violating *ASET* and *RSET* and the corresponding doses that are accumulated by the occupants.

Chapter 7

Closing Remarks

7.1 Conclusions

The main contribution of this study is the methodological extension of the life safety assessment in case of fire. For this purpose, the underground station *Osloer Straße* served as case study in the frame of the ORPHEUS project. In order to cope with uncertainties, the analysis has been conducted in orientation to the principles of multivariate analysis. In this regard, uncertainties may emerge from different levels, e.g. input specification, model configuration but also from the analysis itself. Having said that, the focus of this study was especially set on the specification of model inputs, i.e. the definition of scenarios, and on the spatiotemporal resolution of a well-established concept of analysing life safety in case of fire – the comparison of available safe egress time ($ASET$) and required safe egress time ($RSET$).

The system formation, the definition of its subsystems, underlying elements, and boundaries have been conducted inspired by the principles of *Systems Engineering*. In this regard, the superordinate system *Fire Incident during Operation* is decomposed to the subsystems *Fire* and *Evacuation*. In the first instance, the subsystems have been concerned separately and were consolidated later on.

The methodological frame was set up in orientation to the performance-based design process, while the specification and evaluation of any protective measures have been excluded from the scope of the study. The emphasis was set on the assessment of the infinite scenario space associated with the two defined subsystems instead. In practice, it is necessary to reduce this space to a few relevant scenarios, e.g. due to limited resources in terms of computation but also by means of a feasible analysis and visualisation of the generated output. This reduction usually is a trade-off consideration of consequences and probabilities of a particular combination of fire and occupant scenarios. In order to provide this process with an informed data basis, this

study intentionally used a more refined view. In concrete terms, the scenario space has been explored with a simulation ensemble consisting of 8,640 design points. The latter has been composed of 108 fire scenarios × 80 occupant scenarios, which were sampled with the help of systematic design of experiment (*DoE*) strategies.

In the frame of preparative works, a data-driven approach for representing varying climatic conditions in *FDS* simulations has been introduced. Moreover, the *JuPedSim* framework has been extended in order to incorporate fire simulation data.

For the preliminary analysis of the fire simulation ensemble, a multi-criterial and spatially resolved method for determining *ASET* has been introduced. The proposed method computes *ASET* on a map and allows for the determination of a scalar score which describes the consequences of a particular fire scenario. The subsequent analysis identified the design fires as the system's key determinants. However, the remaining parameters such as level and location of an assumed fire induce remarkable fluctuations within the particular design fire subsets. In this regard, the key factors are the spatial extent of the affected areas as well as the temporal extent of *ASET* itself. Moreover, it was found that varying climatic conditions may significantly influence the development of the evaluated performance criteria throughout the station.

For each of the 108 fire scenarios, an underlying ensemble containing 80 occupant scenarios has been computed. This full-factorial combination was necessary in order to account for the dependencies between the fire scenarios and pedestrian dynamics, e.g. individual detection, or decreased movement speeds in areas affected by smoke. The stand-alone analysis of a reference scenario revealed that the most influential parameters of these sub-ensembles were the population characteristics, the pre-alarm time, and the route choice. With regard to the specification of occupant scenarios, an alternative approach has been introduced that accounts for dynamic occupant loads and varying population compositions. The application of the latter showed that a particular *RSET* may correspond to multiple populations with diverse sizes and characteristics.

The life safety analysis conjuncted all fire scenarios and occupant scenarios. Having this conjunction, the aspired bottom-up approach has been conducted in order to group the consequences of all scenario combinations, i.e. finding scenario clusters with comparable consequences. It is noteworthy that this process has been conducted deterministically, i.e. the probabilities of a particular outcome had not been considered so far. The consequences have been computed with the help of difference maps derived from the subtraction of the introduced *ASET* and *RSET* maps. The cluster formation was conducted for ten clusters whose parametric origins revealed that

the relation between *ASET* and *RSET* has a certain trade-off character between the severity of fire scenarios and the capability of occupant scenarios to cope with these fire scenarios. The most severe consequences correspond to a small subset of scenario combinations, which includes one single occupant scenario and three different fire scenarios. Interestingly, the assigned simulation population accounts for 93 % of the maximal assumed population size. This population is only the second largest but a more heterogenous one. The fire scenarios include a single high-energetic carriage fire at the centre of the station's lowest level paired with winter climate conditions. Moreover, the remaining two fire scenarios are sprinklered fires in different retail units inside the concourse paired with summer and default climate conditions. Finally, the consequences derived from the *ASET-RSET* subtraction were supplemented and compared with an analysis using the concept of fractional effective doses (*FED*). This analysis revealed interesting differences between the spatiotemporal development of *ASET-RSET* and the microscopically tracked doses which inherently correlate with the exposure times induced by the levels and locations, where a fire is assumed. In other words: *ASET-RSET* is an appropriate concept to answer the question if and to which extent an occupant scenario may be impaired by a fire scenario. However, in case of a violation of *ASET-RSET*, the relation between the extent of the violation an the corresponding exposures to fire effects, i.e. dose-time-relationships, is not trivial. In these cases, the distinct dynamics of coincident fire and evacuation processes may not be sufficiently represented by *ASET-RSET*.

7.2 Outlook

This study raised a number of tasks and questions which are worth investigating in more detail. In terms of application, the introduced analysis steps need to be supplemented with a more convenient data processing and have to be provided to the community. This especially applies to the utilised maps representing *ASET*, *RSET*, and the difference between these two measures.

With regards to the field of fire simulation, the modelling of fuel characteristics may significantly impact the outcome of the analyses. The same applies to the design fires, in the course of which the modelling of the sprinkler intervention may be a crucial aspect. In this respect, the robustness of the analysis could be checked under consideration of alternative approaches. Moreover, it may be valuable to conduct the determination of *ASET* with alternative performance criteria thresholds and to reassess the system's response. In this study, commonly applied values for exposure

times of up to 30 minutes have been applied. However, the estimations of *RSET* may also allow for lower exposure times.

In terms of evacuation simulation, the response and route choice of occupants require further research and model development. In this study, the detection time has been distinguished into procedural and individual detection. In the same fashion, pre-movement times were explicitly controlled by the experimental design. However, a more inherent consideration of perceiving and agglomerating evacuation cues may be a potential research topic. The same applies to the route choice of occupants, which has been found to be very influential in built environments with large spatial extents and complex escape route systems. This insight is a clear motivation for further work on route choice modelling, e.g. considering individual knowledge or perception (of smoke). Moreover, the generation of occupant scenarios utilised the *persona* method which introduced simulation populations with variable sizes and compositions. This approach may be extended by additional *persona* characteristics, e.g. group affiliation, herding, or varying spatial knowledge. This also applies to the definition of initial conditions which represent different activity stages inside a building, e.g. ingress, circulation, or egress.

In regard to the life safety analysis, the map representation of *ASET*, *RSET*, and their difference is an appropriate approach to capture the spatial distribution of these measures. In order to facilitate the incorporation into probabilistic analyses, it is necessary to discuss the quantification and interpretation of the introduced consequence measure, but also alternative approaches. Moreover, agglomerative clustering has been successfully applied to the field of fire safety engineering. It represents a powerful tool for explorative data analysis and it may be valuable to investigate the cluster formation with alternative approaches and/or configurations. With respect to practice, its application may also be valuable for smaller design spaces consisting of a full-factorial combination of a only a few fire and occupant scenarios. This is, in particular, appropriate when multiple, different criteria shall be evaluated per scenario combination. Beside *ASET*-*RSET*, the similarity calculation could then be expanded by performance criteria addressing jams or even by probabilities. Conceptually, the inclusion of probabilities corresponding to a scenario combination would then facilitate the agglomeration of scenarios which are similar in terms of both consequences and probabilities. Irrespective of the underlying uncertainties in general, the proposed analysis workflow would then be capable to deliver risk-based scenario clusters as they were introduced in Section 2.5.3. Having said that, the conduction of similar studies on other building types and corresponding building uses could provide

a valuable knowledge base to many of the stakeholders within the performance-based design process in *FSE* practice.

On the basis of *ASET-RSET*, a set of clusters has been formed successfully. Nevertheless, the conjunction with an analysis based on fractional effective doses (*FED*) revealed that there is only a limited correspondence between *ASET-RSET* and *FED*. With this in mind, *ASET-RSET* is an appropriate indicator for the compliance and violation of particular performance criteria. However, it has limitations in terms of predicting the exposures associated with a particular violation. Further investigations are necessary here, e.g. under consideration of other extensive escape route systems or design fires that start decaying in a comparatively early stage.

Appendix A

Design of Experiment

A.1 Fire Simulation

A.1.1 U8 Level

ID	Location	Design Fire	Climate
f001	1	*BR F*	Summer
f002	1	*TRIn*	Default
f003	3	*TR16*	Summer
f004	2	*BR H*	Default
f005	3	*Luggage*	Winter
f006	2	*BR H*	Summer
f007	3	*TR16*	Winter
f008	3	*TR16*	Default
f009	2	*TRIn*	Winter
f010	2	*Luggage*	Default
f011	1	*BR H*	Winter
f012	3	*BR F*	Winter
f013	2	*BR F*	Default
f014	1	*Luggage*	Default
f015	1	*BR H*	Summer
f016	3	*BR F*	Summer
f017	2	*BR F*	Winter
f018	1	*BR F*	Winter
f019	3	*Luggage*	Default
f020	1	*TR16*	Summer
f021	1	*Luggage*	Summer
f022	3	*BR F*	Default
f023	2	*TR16*	Summer
f024	3	*BR H*	Summer
f025	3	*BR H*	Default
f026	3	*TRIn*	Summer

ID	Location	Design Fire	Climate
f027	2	*TRIn*	Default
f028	1	*TR16*	Winter
f029	2	*Luggage*	Summer
f030	3	*TRIn*	Default
f031	3	*Luggage*	Summer
f032	1	*TRIn*	Summer
f033	3	*BR H*	Winter
f034	1	*TRIn*	Winter
f035	2	*TR16*	Winter
f036	2	*BR F*	Summer
f037	2	*BR H*	Winter
f038	2	*TRIn*	Summer
f039	1	*TR16*	Default
f040	1	*Luggage*	Winter
f041	1	*BR H*	Default
f042	2	*TR16*	Default
f043	1	*BR F*	Default
f044	3	*TRIn*	Winter
f045	2	*Luggage*	Winter

A.1.2 U9 Level

ID	Location	Design Fire	Climate
f046	1	*BR F*	Summer
f047	1	*TRIn*	Default
f048	3	*TR16*	Summer
f049	2	*BR H*	Default
f050	3	*Luggage*	Winter
f051	2	*BR H*	Summer
f052	3	*TR16*	Winter
f053	1	*TR16*	Default
f054	2	*TRIn*	Winter
f055	2	*Luggage*	Default
f056	1	*BR H*	Winter
f057	3	*BR F*	Winter
f058	2	*BR F*	Default
f059	1	*Luggage*	Default
f060	1	*BR H*	Summer
f061	3	*BR F*	Summer
f062	2	*BR F*	Winter
f063	1	*BR F*	Winter
f064	3	*Luggage*	Default
f065	1	*TR16*	Summer
f066	3	*Luggage*	Summer

ID	Location	Design Fire	Climate
f067	3	*BR F*	Default
f068	2	*TR16*	Summer
f069	3	*BR H*	Summer
f070	3	*BR H*	Default
f071	3	*TRIn*	Summer
f072	2	*TRIn*	Default
f073	1	*TR16*	Winter
f074	2	*Luggage*	Summer
f075	3	*TRIn*	Default
f076	1	*Luggage*	Summer
f077	1	*TRIn*	Summer
f078	3	*BR H*	Winter
f079	1	*TRIn*	Winter
f080	2	*TR16*	Winter
f081	2	*BR F*	Summer
f082	2	*BR H*	Winter
f083	2	*TRIn*	Summer
f084	3	*TR16*	Default
f085	1	*Luggage*	Winter
f086	1	*BR H*	Default
f087	2	*TR16*	Default
f088	1	*BR F*	Default
f089	3	*TRIn*	Winter
f090	2	*Luggage*	Winter

A.1.3 Concourse Level

ID	Location	Design Fire	Climate
f091	3	*Retail no Spr.*	Winter
f092	2	*Luggage*	Summer
f093	2	*Retail no Spr.*	Summer
f094	3	*Retail*	Default
f095	1	*Retail no Spr.*	Default
f096	2	*Retail no Spr.*	Default
f097	2	*Retail*	Default
f098	1	*Luggage*	Default
f099	3	*Luggage*	Winter
f100	3	*Retail no Spr.*	Default
f101	3	*Luggage*	Default
f102	2	*Retail*	Summer
f103	3	*Retail no Spr.*	Summer
f104	2	*Luggage*	Default
f105	1	*Retail no Spr.*	Summer
f106	2	*Luggage*	Winter

ID	Location	Design Fire	Climate
f107	1	*Luggage*	Summer
f108	2	*Retail no Spr.*	Winter
f109	1	*Luggage*	Winter
f110	2	*Retail*	Winter
f111	3	*Luggage*	Summer
f112	1	*Retail*	Winter
f113	1	*Retail*	Default
f114	1	*Retail no Spr.*	Winter
f115	3	*Retail*	Winter
f116	1	*Retail*	Summer
f117	3	*Retail*	Summer

A.2 Evacuation Simulation

ID	Pre-Alarm	Pre-Movement	Route Choice	Population Cluster
e000	204 s	81.9 %	Uniform	4
e001	213 s	45.6 %	Global Shortest	5
e002	240 s	50.6 %	Field Data	1
e003	222 s	60.6 %	Uniform	12
e004	297 s	14.4 %	Field Data	5
e005	249 s	84.4 %	Global Shortest	12
e006	123 s	11.9 %	Field Data	1
e007	173 s	53.1 %	Uniform	13
e008	175 s	65.6 %	Field Data	9
e009	135 s	64.4 %	Global Shortest	3
e010	144 s	44.4 %	Uniform	11
e011	128 s	15.6 %	Field Data	8
e012	227 s	1.9 %	Field Data	5
e013	180 s	76.9 %	Global Shortest	7
e014	229 s	48.1 %	Global Shortest	4
e015	267 s	8.1 %	Uniform	0
e016	274 s	39.4 %	Field Data	8
e017	186 s	51.9 %	Field Data	3
e018	261 s	38.1 %	Field Data	10
e019	195 s	86.9 %	Global Shortest	14
e020	139 s	69.4 %	Global Shortest	4
e021	245 s	54.4 %	Field Data	6
e022	276 s	49.4 %	Uniform	8
e023	290 s	16.9 %	Uniform	3
e024	164 s	31.9 %	Field Data	7
e025	283 s	18.1 %	Field Data	13
e026	294 s	40.6 %	Uniform	7
e027	216 s	0.6 %	Uniform	13

ID	Pre-Alarm	Pre-Movement	Route Choice	Population Cluster
e028	184 s	30.6 %	Global Shortest	3
e029	159 s	29.4 %	Uniform	1
e030	285 s	90.6 %	Field Data	2
e031	130 s	89.4 %	Field Data	10
e032	189 s	41.9 %	Uniform	10
e033	299 s	99.4 %	Field Data	4
e034	218 s	74.4 %	Uniform	2
e035	279 s	35.6 %	Field Data	12
e036	157 s	94.4 %	Uniform	7
e037	263 s	73.1 %	Field Data	2
e038	132 s	85.6 %	Global Shortest	0
e039	191 s	36.9 %	Global Shortest	1
e040	209 s	78.1 %	Uniform	0
e041	177 s	88.1 %	Field Data	14
e042	270 s	58.1 %	Uniform	6
e043	254 s	21.9 %	Field Data	7
e044	265 s	68.1 %	Global Shortest	4
e045	236 s	63.1 %	Global Shortest	12
e046	231 s	93.1 %	Uniform	3
e047	141 s	95.6 %	Field Data	6
e048	200 s	33.1 %	Global Shortest	6
e049	243 s	56.9 %	Global Shortest	9
e050	238 s	9.4 %	Global Shortest	5
e051	256 s	5.6 %	Global Shortest	2
e052	182 s	79.4 %	Global Shortest	0
e053	193 s	28.1 %	Global Shortest	7
e054	292 s	25.6 %	Field Data	5
e055	272 s	66.9 %	Field Data	10
e056	155 s	96.9 %	Uniform	13
e057	252 s	70.6 %	Global Shortest	12
e058	137 s	26.9 %	Global Shortest	2
e059	148 s	4.4 %	Field Data	11
e060	166 s	61.9 %	Global Shortest	9
e061	126 s	3.1 %	Global Shortest	1
e062	234 s	98.1 %	Uniform	10
e063	171 s	75.6 %	Uniform	8
e064	247 s	43.1 %	Uniform	14
e065	168 s	71.9 %	Field Data	11
e066	281 s	19.4 %	Field Data	13
e067	150 s	91.9 %	Uniform	4
e068	202 s	6.9 %	Uniform	11
e069	207 s	34.4 %	Uniform	14
e070	220 s	24.4 %	Global Shortest	0
e071	121 s	10.6 %	Field Data	11

ID	Pre-Alarm	Pre-Movement	Route Choice	Population Cluster
e072	153 s	20.6 %	Global Shortest	1
e073	225 s	59.4 %	Uniform	8
e074	211 s	13.1 %	Global Shortest	10
e075	258 s	80.6 %	Uniform	9
e076	146 s	83.1 %	Global Shortest	13
e077	288 s	23.1 %	Uniform	6
e078	162 s	55.6 %	Global Shortest	14
e079	198 s	46.9 %	Uniform	9

Appendix B

Data Analysis Routines

Note: The following Python code snippets are not readily working since they depend on pre-computed data and specific file paths. However, they are supposed to provide the basic logic for applying the *ASET-RSET* concept with the help of maps.

B.1 ASET Map Generation

Listing B.1: ASET map generation routine

```
'''This script computes the ASET maps based on the specified
   quantities incorporated from an FDS fire simulation.'''

import argparse
import os
import glob
import numpy as np

#-----------------------------------------------


#--------------- Functions --------------------
def pull_JPSfire_data(q, l):
    '''This function collects the spatiotemporal data provided
        by JPSfire for a given quantity and returns a single 3
       D-stacked array'''

    raws_path = 'C_toxicity_analysis/2_toxicity_grids/%s/%s/'
       %(q, l)
    raws = glob.glob(raws_path+'t_*.csv')
    raws = sorted(raws, key=lambda name: int(name[ name.rfind(
       '_')+1 : -11]))
```

```
    stack_tuple = ()
    for raw in raws:
        stack_tuple += (np.loadtxt(raw, skiprows=3, delimiter=
            ','),)

    quantity_stack = np.dstack(stack_tuple)

    r = open(raw)
    header = r.readlines()[2][:-1]
    r.close()

    return quantity_stack, header

def determine_exceedance_times(q, l, quantity_stack,
    all_aset_tuple):
    '''This function determines the particular exceedance
        times for all considered fire effects. For that purpose
        , it sets up an equally shaped array with exceedance
        times of 21 minutes. Then, it moves the time axis to
        axis 0 and iterates over the latter. For each time it
        is checked if the acceptance criteria are met. If yes,
        the belonging indices are used to set the exceedance
        time'''

    #array with temporary exceedance times
    temp = np.ones(np.shape(quantity_stack)[0:2])*21

    #bring time axis to pos 0
    quantity_stack = np.moveaxis(quantity_stack, -1, 0)

    #iterate over t and identify exceedance times
    for i, cond_at_time in enumerate(quantity_stack):

        exceed = np.where(cond_at_time>acceptance_criteria[q])
        temp[exceed] = i

        #determine minimum ASET at a given space
        exceedance_times = np.minimum(exceedance_times, temp)

    #fill tuple with exceedance_times arrays for all
        quantities
    all_aset_tuple += (exceedance_times, )

    return exceedance_times, all_aset_tuple

def determine_all_aset(all_aset_tuple, l):
```

```
    '''This function grabs all exceedance_times arrays for all
        quantities in one level and determines the particular
       minimum exceedance times. These than yield the overall
       ASET irrespective of the quantities. Finally, the ASET
       2D arrays are stacked level-wise and saved'''

    # load dummy aset map with obsts = -1 and open space = 22
    all_aset = np.loadtxt('%s/obsts/obst_%s.csv'%(script_path,
        l), delimiter=',')

    for q in all_aset_tuple:
        all_aset = np.minimum(all_aset, q)

    np.savetxt('0ASET/ASET_%s.txt'%(l), all_aset, header=
       header)

    return all_aset

#-------------------------------------------------


#-------------- Main Program -------------------

# z-levels to be analysed
levels = ['Z_28.950000', 'Z_33.750000', 'Z_37.050000']

# list of FSE relevant quantities
quantities = [
    'SOOT_EXTINCTION_COEFFICIENT',
    'CARBON_MONOXIDE_VOLUME_FRACTION',
    'HYDROGEN_CHLORIDE_VOLUME_FRACTION',
    'HYDROGEN_CYANIDE_VOLUME_FRACTION',
    'CARBON_DIOXIDE_VOLUME_FRACTION',
    'TEMPERATURE']

# dictionary containing the thresholds of FSE relevant
   quantities
acceptance_criteria = {
    'SOOT_EXTINCTION_COEFFICIENT':0.23,
    'TEMPERATURE':45,
    'CARBON_MONOXIDE_VOLUME_FRACTION':0.0001,
    'CARBON_DIOXIDE_VOLUME_FRACTION':0.01,
    'HYDROGEN_CYANIDE_VOLUME_FRACTION':0.000008,
    'HYDROGEN_CHLORIDE_VOLUME_FRACTION':0.00020}

try:
    print(firesim_id)
```

```
    os.chdir(firesim_id)

    if not os.path.exists('0ASET'):
        os.makedirs('0ASET')

    for l in levels:

        all_aset_tuple = ()
        for q in quantities:
            print(l, q)

            if q in os.listdir('C_toxicity_analysis/2
               _toxicity_grids/'):
                #-> FUNCTION CALL
                quantity_stack, header = pull_JPSfire_data(q,l
                   )
            else:
                # continue if a quantity has not been computed
                    (e.g. HCl)
                print(q, 'skipped')
                continue

            header_content = [float(i) for i in header.split('
               ,')]
            dim1 = np.arange(header_content[2], header_content
               [3], header_content[0])
            dim2 = np.arange(header_content[4], header_content
               [5], header_content[1])

            #-> FUNCTION CALL
            exceedance_times, all_aset_tuple =
               determine_exceedance_times(q, l, quantity_stack
               , all_aset_tuple)

        #-> FUNCTION CALL
        all_aset = determine_all_aset(all_aset_tuple, l)

except:
    print(' '-> contains no or corrupt JPSfire data -> skipped
       ')
    pass

#--------------- DONE ------------------
```

B.2 RSET Map Generation

Listing B.2: RSET map generation routine

```
'''This script computes the RSET maps based on the specified
   trajectory files incorporated from a JuPedSim pedestrian
   simulation.'''

import os
import glob
import argparse
import zipfile
import numpy as np
import xml.etree.ElementTree as ET

#--------------- FUNCTIONS --------------------

def determine_dimensions(traj_root, level):
    '''Determine the spatial minima and maxima of the
       trajectories.'''

    x_min = y_min = float("inf")
    x_max = y_max = -float("inf")

    for step in traj_root.findall('./frame/agent'):
        #print( float(step.attrib['x']) )
        if float(step.attrib['z']) == level:
            x_min = min(x_min, float(step.attrib['x']) )
            y_min = min(y_min, float(step.attrib['y']) )
            x_max = max(x_max, float(step.attrib['x']) )
            y_max = max(y_max, float(step.attrib['y']) )

    return round(x_min,0), round(x_max,0), round(y_min,0),
       round(y_max,0)

def setup_rset_map(x, y):
    '''Setup of a dummy RSET map filled with NaNs'''
    rset_map = np.zeros((len(y), len(x)))
    rset_map[:] = np.nan

    return x,y,rset_map

def determine_rsets(traj_root, level, x,y, rset_map):
    '''Iterate over all frames in the trajectory root. (Re-)
       write the traversal times for all x and y coordinates
       of an agent to the RSET map. '''
```

```
    for frame in traj_root.findall('./frame'):
        frame_id = int( frame.attrib['ID'] )

        for agent in frame.findall('agent'):
            if float(agent.attrib['z']) >= level-0.1 and float
               (agent.attrib['z']) <= level+0.1:
                agent_x, agent_y = float(agent.attrib['x']),
                   float(agent.attrib['y'])

                #determine the belonging indeces to access
                   rset_map
                ix = (np.abs(x-agent_x)).argmin()
                iy = (np.abs(y-agent_y)).argmin()

                rset_map[iy,ix] = frame_id*fps/60

    return rset_map


def process_rset_maps(level, percentile):
    '''Collect the rset_maps of all seeds in a tuple. The
       latter is converted to a 3D stack. Then, it calculates
       the nth percentile of RSET for each control element and
        sets them to a major map. The seed maps are than
       deleted'''

    raws = sorted(glob.glob('1RSET/RSET_*_%.2f.txt'%level))
    if len(raws)==0:
        print('No raw RSET maps found!')
    rset_maps = ()

    for raw in raws:
        print(raw)
        rset_maps +=  (np.loadtxt(raw, skiprows=1),)
        # delete raw data of single seeds (may be disc quota
           consuming otherwise)
        os.remove(raw)

    rset_stack = np.dstack(rset_maps)
    rset_percentiles = np.zeros((np.shape(rset_stack)[0], np.
       shape(rset_stack)[1]))

    for i, row in enumerate(rset_stack):
        for j, col in enumerate(row):
            rset_percentiles[i,j] = np.nanpercentile(
               rset_stack[i,j, :], percentile)
```

```
    return rset_percentiles
#-------------------------------------------


#---------------- MAIN PROG ------------------

# general variables
fps = 1

# shape parameters of upcoming RSET maps
delta=0.6
x = np.arange(-79.8, 79.8+0.01, delta)
y = np.arange(-24, 126+0.01, delta)

if not os.path.exists('1RSET'):
    os.makedirs('1RSET')

# the trajectories of every seed are assumed as zipped XML
   file in the current working directory
zips = sorted(glob.glob('*.zip'))

for zip in zips:
    try:
        with zipfile.ZipFile(zip) as myzip:
            traj = 'traj_%s.xml'%zip[:-4]
            traj_xml = ET.parse( myzip.open(traj) )
    except:
        print(traj, 'skipped')
        continue

    print(''->', traj)
    traj_root = traj_xml.getroot()

    for level in levels:

        #-> FUNCTION CALL
        x_min, x_max, y_min, y_max = determine_dimensions(
           traj_root, level)

        #-> FUNCTION CALL
        x,y,rset_map = setup_rset_map(x, y)

        #-> FUNCTION CALL
        rset_map = determine_rsets(traj_root, level, x,y,
           rset_map)

        header = 'x_min=%i, x_max=%i, y_min=%i, y_max=%i'%(\
```

```
        x_min, x_max, y_min, y_max)
        np.savetxt('1RSET/RSET_%s_%.2f.txt'%(traj[-8:-4],
           level), rset_map, header=header)

for level in levels:
    percentile=95
    #-> FUNCTION CALL
    rset_percentiles = process_rset_maps(level, percentile)
    header = 'x_min=%i, x_max=%i, y_min=%i, y_max=%i'%(\
    x_min, x_max, y_min, y_max)
    np.savetxt('1RSET/%iRSET_%.2f.txt'%(percentile, level),
       rset_percentiles, header=header)

#--------------- DONE ------------------
```

B.3 Difference Map Generation

Listing B.3: RSET map generation routine

```
'''This script conducts the ASET RSET comparison for a
   particular fire scenario and an evacuation scenario, i.e.
   the difference map is computed.'''

import os
import sys
import argparse
import numpy as np

#----------------- FUNCTIONS --------------------

def collect_ASET(cwd, level):
    '''Go to firesim dir and collect ASET maps. The raw ASET
       map is then  broadcasted to a bigger map in order to be
        aligned with the RSET map for the later analysis'''

    raw = 'ASET_%s.txt'%fire_levels[level]
    raw_map = np.loadtxt(cwd+'/0ASET/'+raw, skiprows=1)

    # prepare larger aset_map in order to ensure alignment
       with rset_map
    delta = 0.6
    x_map = np.arange(-79.8, 79.8+0.01, delta)
    y_map = np.arange(-24, 126+0.01, delta)
    aset_map = np.zeros((len(y_map), len(x_map)))

    aset_map[:]=np.nan

    r = open(cwd+'/0ASET/'+raw)
    header = r.readlines()[0][1:]
    r.close()
    header_content = [float(i) for i in header.split(',')]

    x_min = header_content[2]
    y_min = header_content[4]

    #determine the belonging indeces to broadcast raw_map into
        aset_map
    ix = (np.abs(x_map-x_min)).argmin()
    iy = (np.abs(y_map-y_min)).argmin()

    # broadcast raw_map into larger aset_map
    aset_map[ iy:iy+np.shape(raw_map)[0] , ix:ix+np.shape(
```

```
        raw_map)[1] ] = raw_map

    return aset_map, x_map, y_map

def collect_RSET(cwd, level):
    '''Go to pedsim dir and collect nth percentile ASET maps
       '''

    raw = '95RSET_%.2f.txt'%level
    print(raw)
    rset_map = np.loadtxt(cwd+'/1RSET/'+raw, skiprows=1)
    rset_map[rset_map==0] = np.nan
    return rset_map


def analyse_ASET_RSET(aset_map, x_map, y_map, rset_map):

    diff_map = aset_map - rset_map
    np.savetxt('2ASETvsRSET/2ASETvsRSET_%s.txt'%level,
       diff_map)

    return

#---------------- MAIN PROG --------------------

parser = argparse.ArgumentParser()
parser.add_argument("firesim_dir", type=str, help="firesim_dir
   ")
parser.add_argument("pedsim_dir", type=str, help="pedsim_dir")

try:
    cmdl_args = parser.parse_args()
    firesim_dir = cmdl_args.firesim_dir
    pedsim_dir = cmdl_args.pedsim_dir
except:
    sys.exit('No fire_id resp. ped_id specified!')

# this dict assigns the RSET (pedestrian) z_elevations to the
   belonging ASET (slice) elevations:
fire_levels = { 27.3:'Z_28.950000', 32.26:'Z_33.750000', 35.3:
   'Z_37.050000'}

levels = [27.3, 32.26, 35.3]   # z_elevations of rset maps


ped_id = int(pedsim_dir[1:])
```

```
print( firesim_dir, pedsim_dir )

log = []

for level in levels:

    #--> FUNCTION CALL
    aset_map, x_map, y_map = collect_ASET(firesim_path+
       firesim_dir, level)

    os.chdir(pedsim_path+firesim_dir+'/'+pedsim_dir)

    #--> FUNCTION CALL
    rset_map = collect_RSET(os.getcwd(), level)

    if not os.path.exists('2ASETvsRSET'):
        os.mkdir('2ASETvsRSET')

    #--> FUNCTION CALL
    analyse_ASET_RSET(aset_map, x_map, y_map, rset_map)

#----------------- DONE --------------------
```

Appendix C

Life Safety Analysis

C.1 Scenario Cluster C

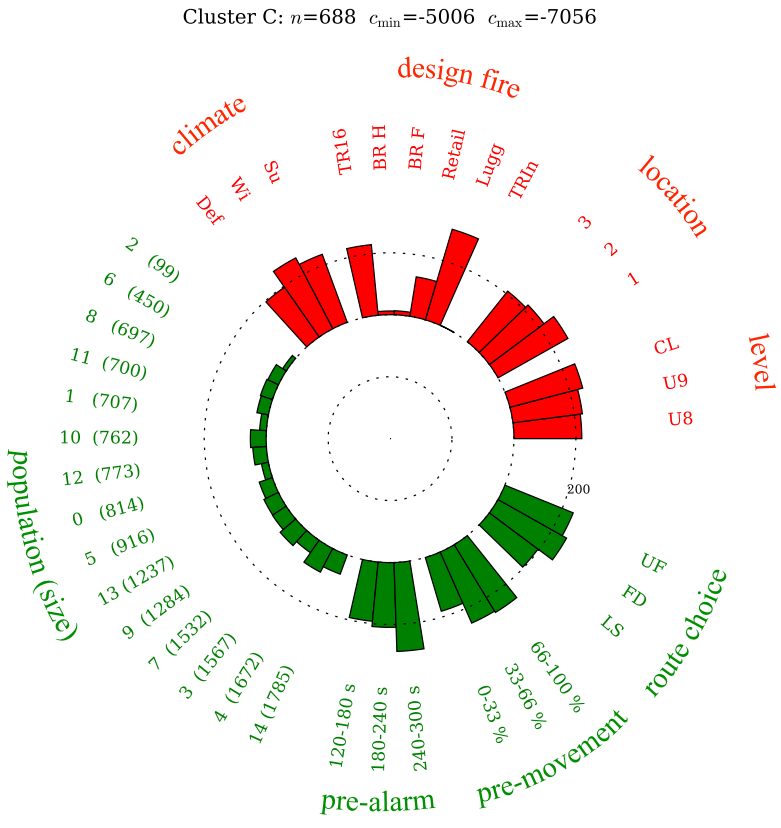

Figure C.1: Radar plot illustrating the parametric origin of cluster C.

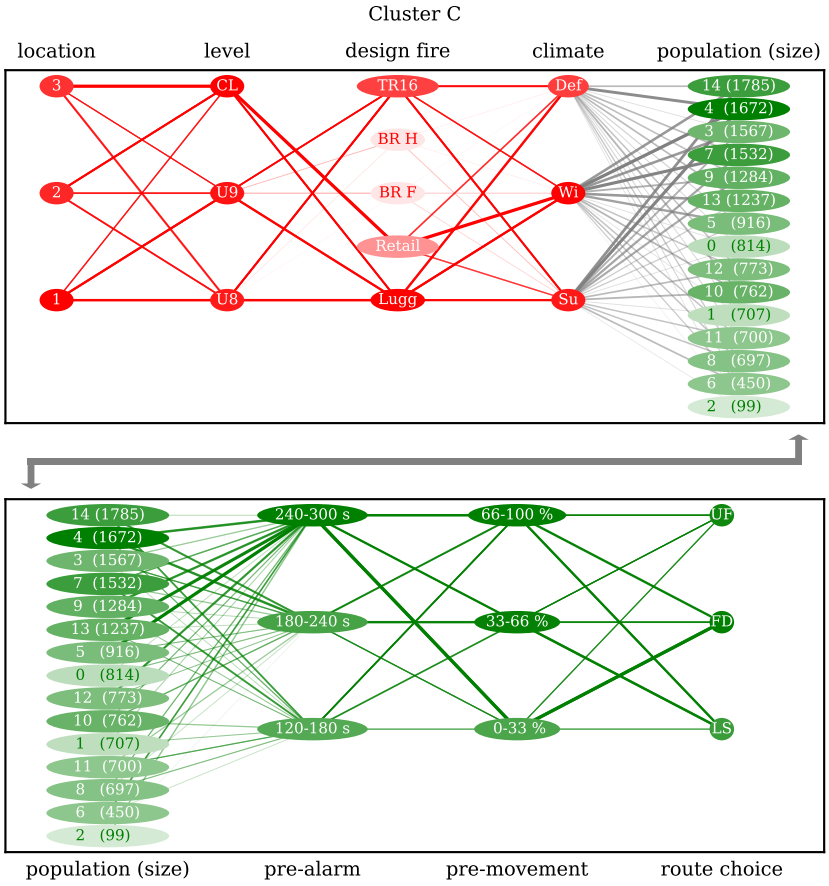

Figure C.2: Parallel coordinate plot illustrating the parametric relations of cluster C.

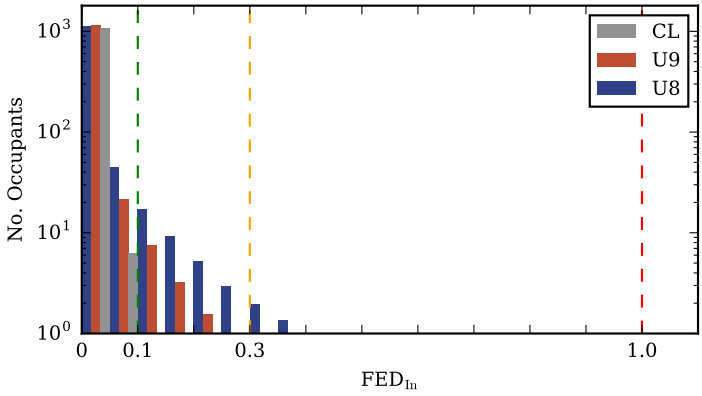

Figure C.3: *FED* histogram of scenario cluster C.

C.2 Scenario Cluster D

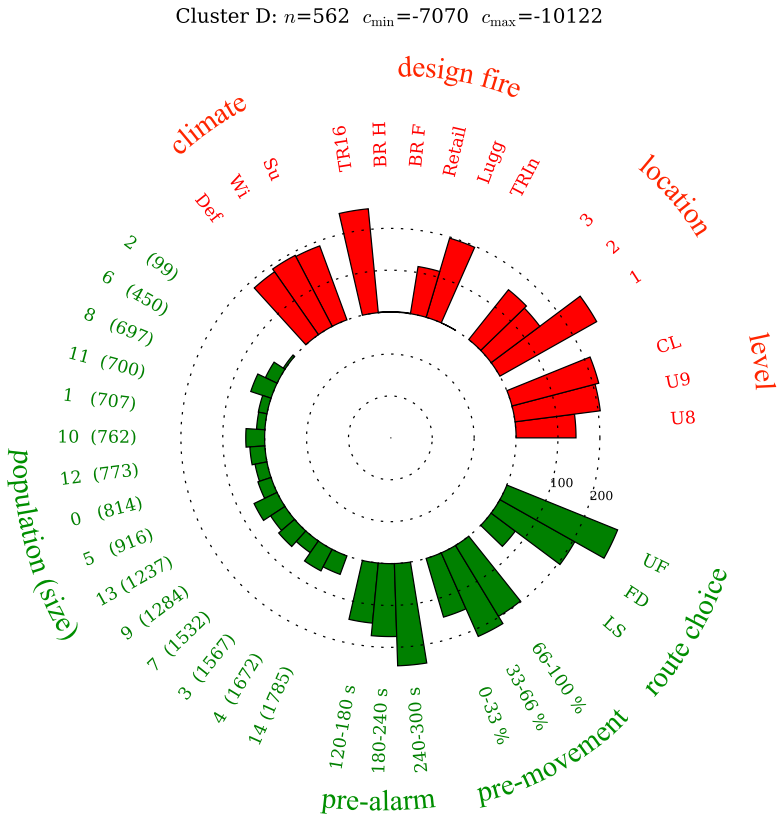

Figure C.4: Radar plot illustrating the parametric origin of cluster D.

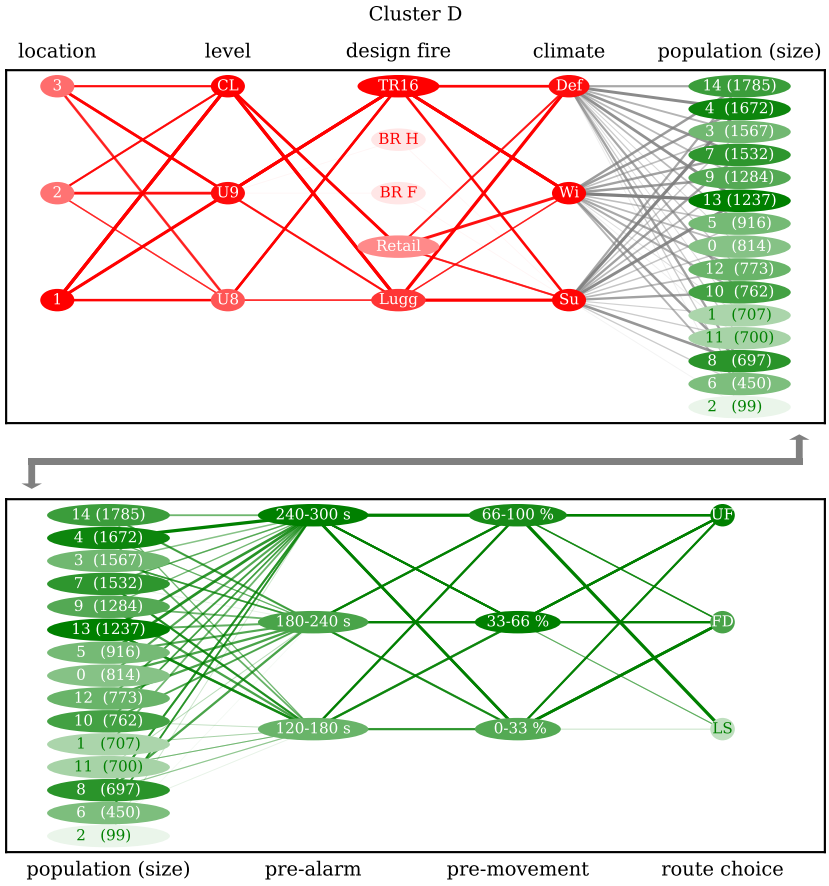

Figure C.5: Parallel coordinate plot illustrating the parametric relations of cluster D.

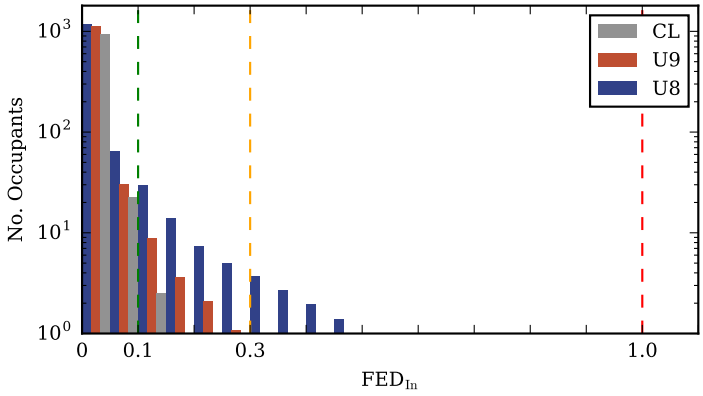

Figure C.6: *FED* histogram of scenario cluster D.

C.3 Scenario Cluster E

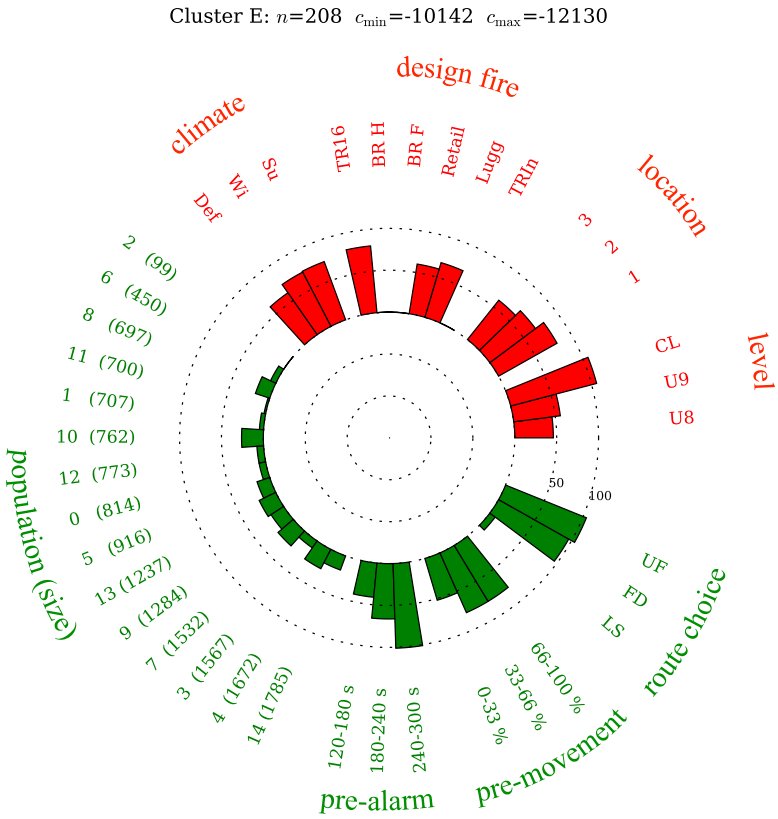

Figure C.7: Radar plot illustrating the parametric origin of cluster E.

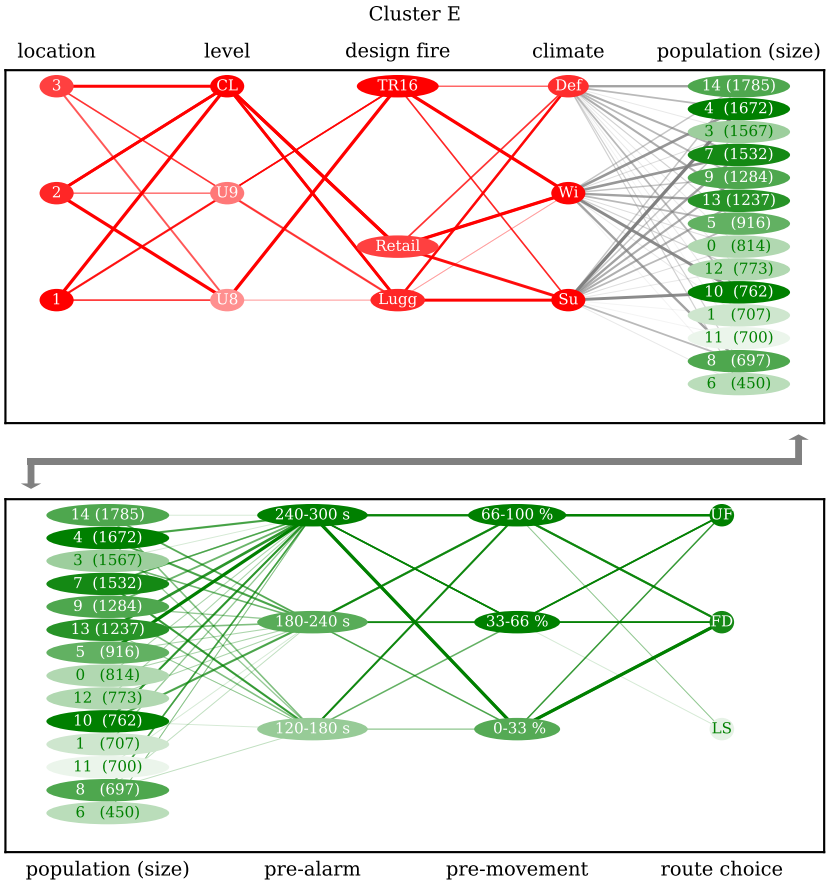

Figure C.8: Parallel coordinate plot illustrating the parametric relations of cluster E.

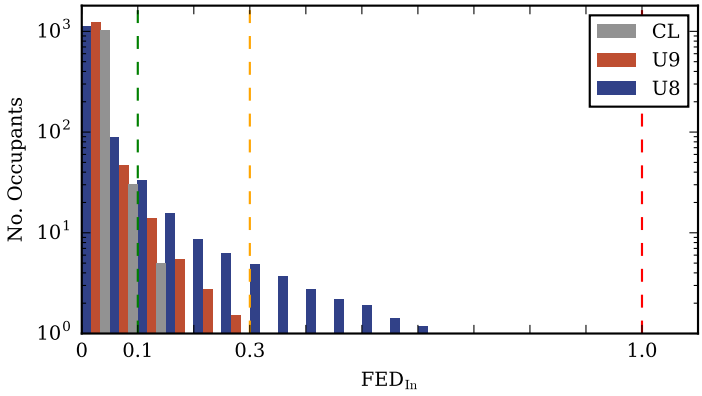

Figure C.9: *FED* histogram of scenario cluster E.

C.4 Scenario Cluster G

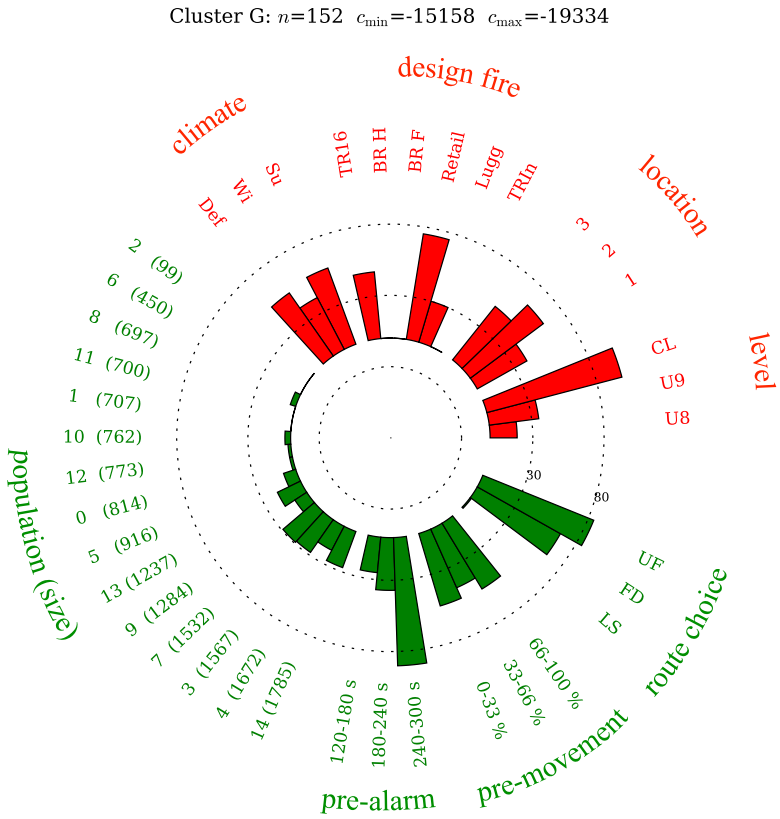

Figure C.10: Radar plot illustrating the parametric origin of cluster G.

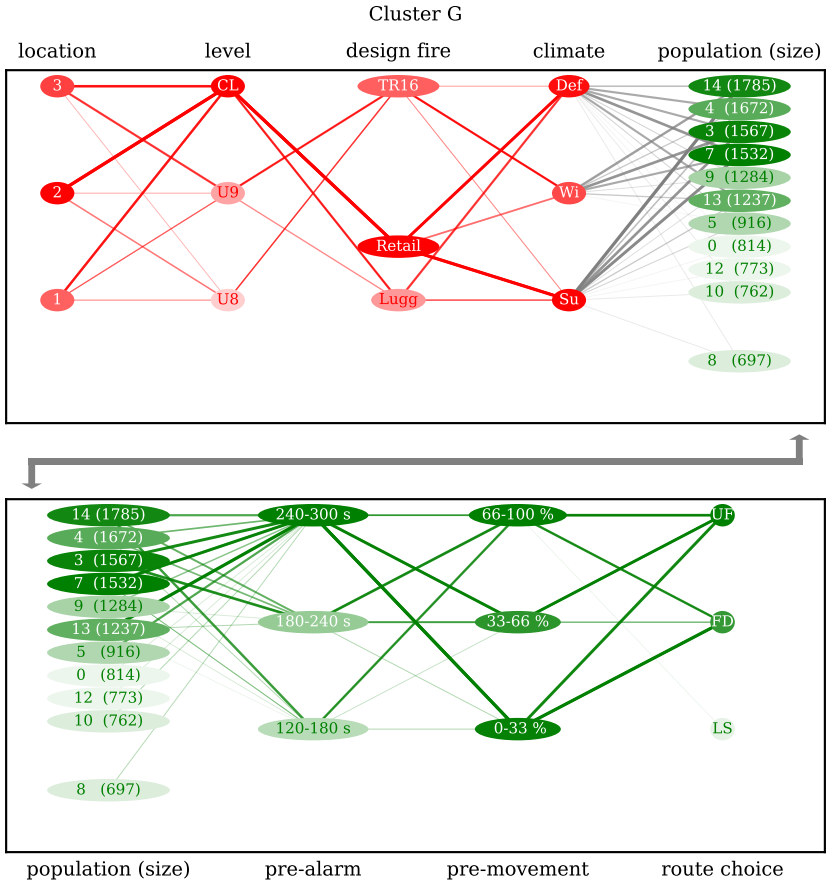

Figure C.11: Parallel coordinate plot illustrating the parametric relations of cluster G.

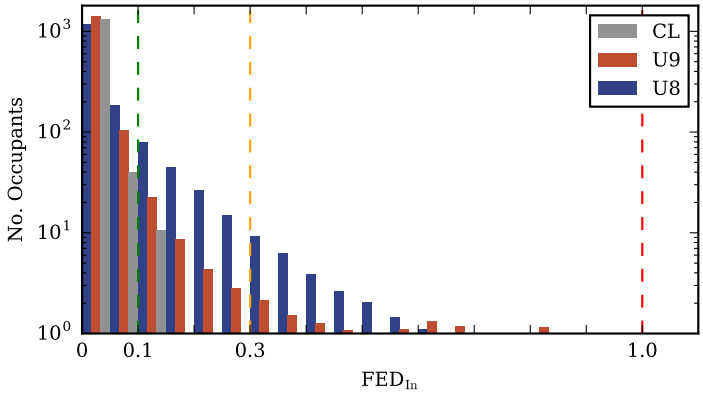

Figure C.12: *FED* histogram of scenario cluster G.

C.5 Scenario Cluster H

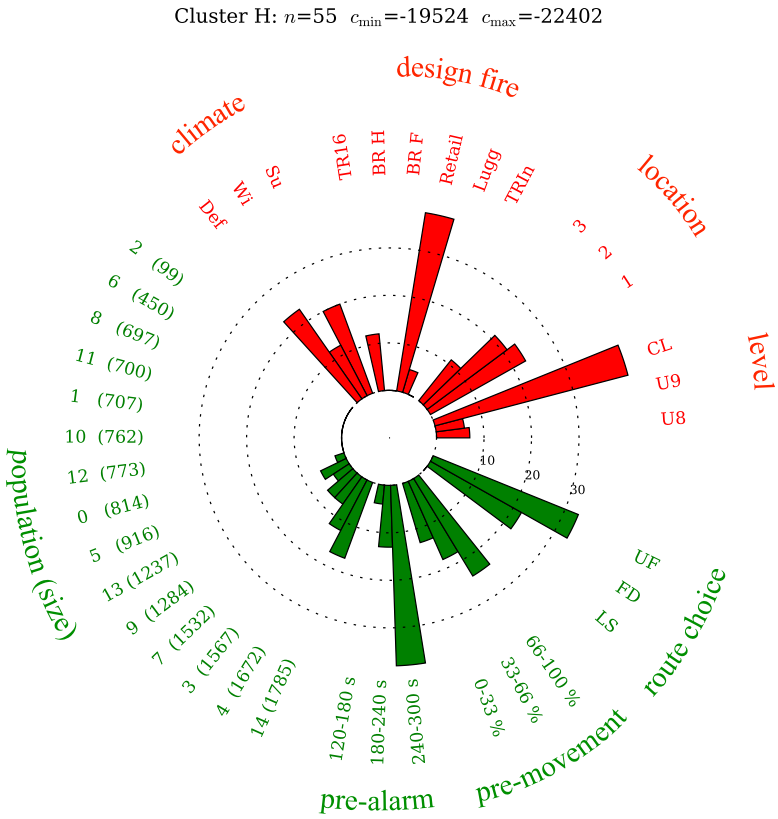

Figure C.13: Radar plot illustrating the parametric origin of cluster H.

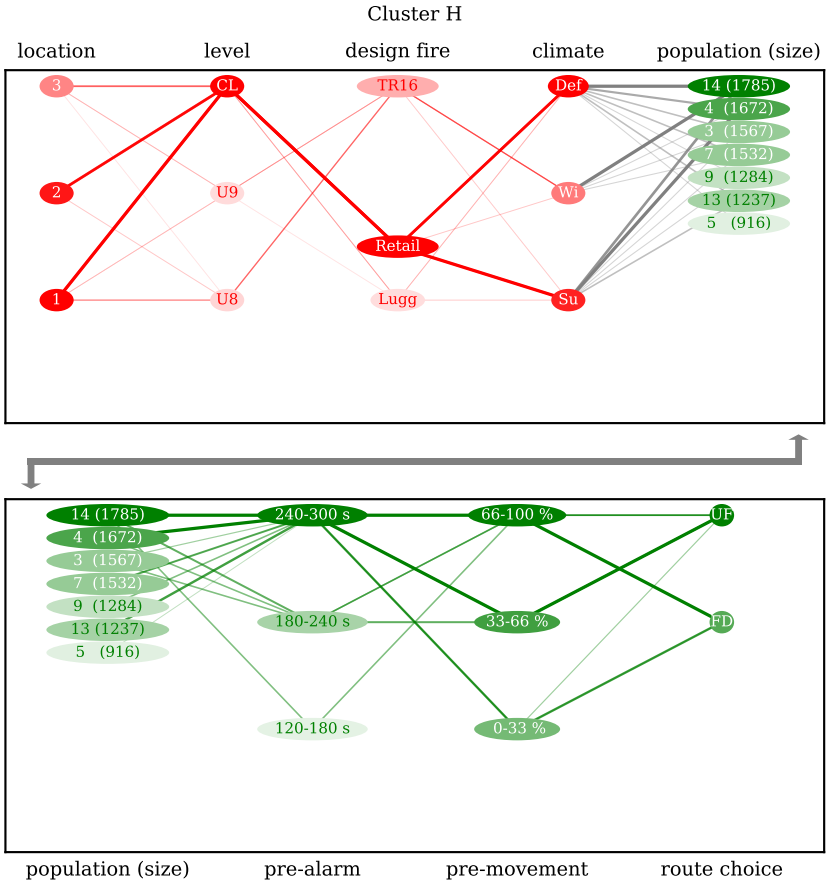

Figure C.14: Parallel coordinate plot illustrating the parametric relations of cluster H.

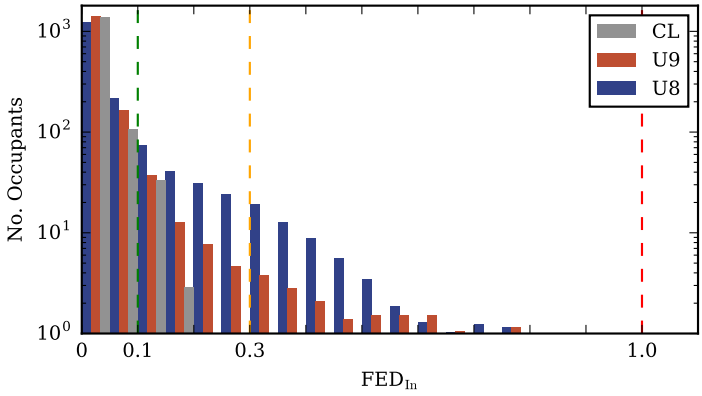

Figure C.15: *FED* histogram of scenario cluster H.

C.6 Scenario Cluster I

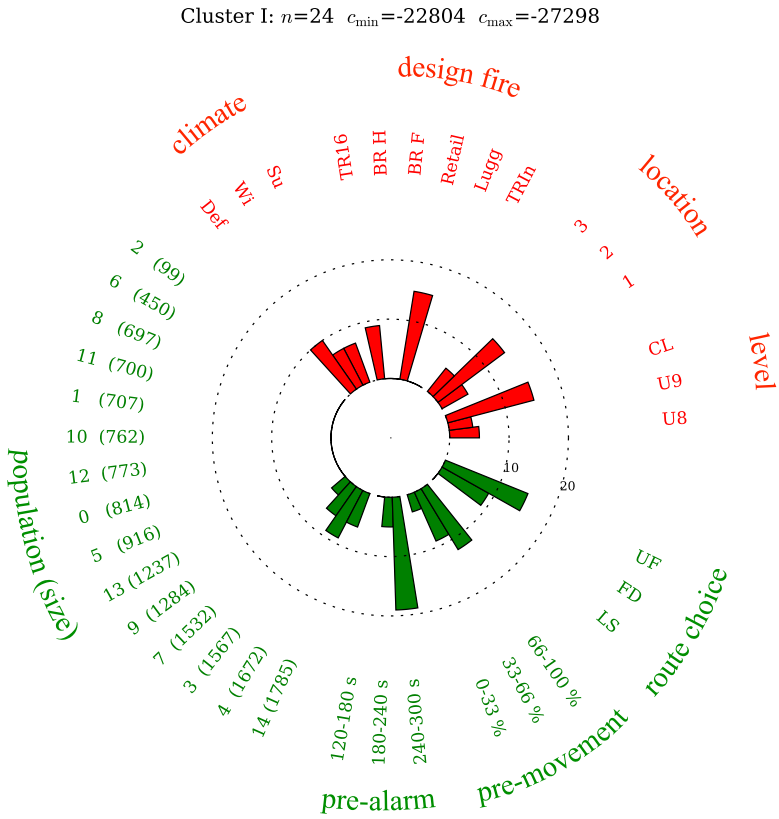

Figure C.16: Radar plot illustrating the parametric origin of cluster I.

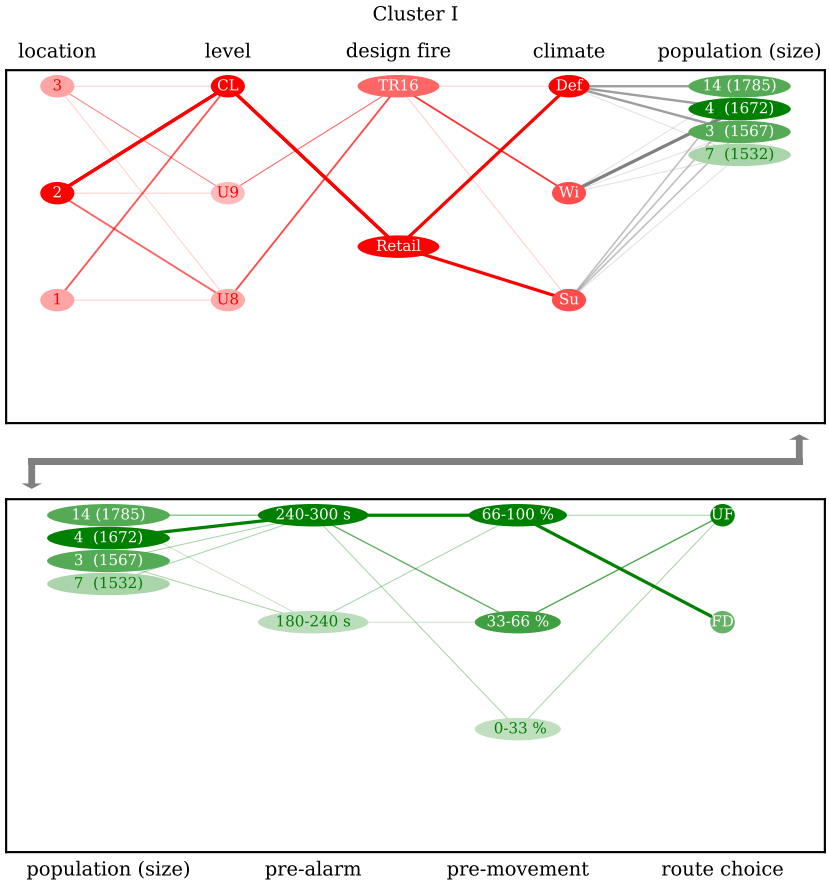

Figure C.17: Parallel coordinate plot illustrating the parametric relations of cluster I.

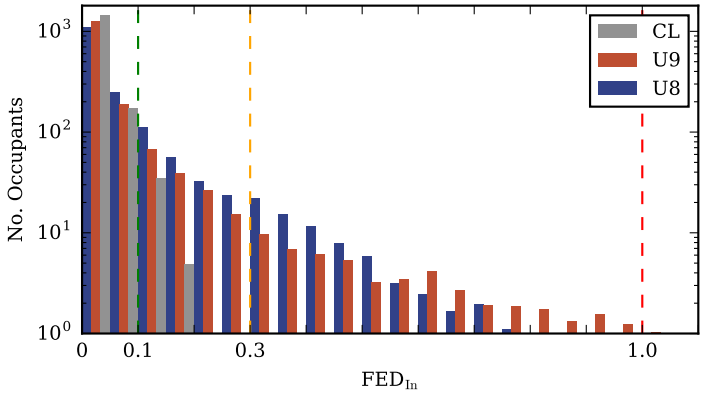

Figure C.18: *FED* histogram of scenario cluster I.

Appendix D

List of Publications

Written Contributions

Zinke, Robert; Künzer, Laura; Schröder, Benjamin; Schäfer, Christina. *Integrating Human Factor Aspects into Evacuation Simulation – Application of the Persona Method for Generating Populations.* In 14th International Conference on Information Systems for Crisis Response And Management; Albi; 2017.

Hofinger, Gesine; Zinke, Robert; Künzer, Laura; Schröder, Benjamin; Andresen, Erik; *Human Factors in Pedestrian Simulation: Field Studies in Underground Stations*; The 8th International Conference on Pedestrian and Evacuation Dynamics (PED 2016); Heifei; 2016.

Schröder, Benjamin; Arnold, Lukas; Meunders, Andreas; Schmidt, Sven; *Smoke and Heat Extraction in Underground Stations*; Interflam 2016; London; 2016.

Jäger, Gregor; Schröder, Benjamin; *Evacuation and Life Safety Assessment in Germany*; 11th Conference on Performance-Based Codes and Fire Safety Design; Warsaw; 2016.

Schröder, Benjamin; Andresen, Erik; Haensel, David; Chraibi, Mohcine; Arnold, Lukas; Seyfried, Armin; *Knowledge- and perception-based route choice modelling in case of fire*; 6th International Human Behaviour in Fire 2015 Symposium; Cambridge; 2015.

Jäger, Gregor; Kitzlinger, Manuel; Schröder, Benjamin; Seyfried, Armin; *Normierung von Personenstromsimulationen in DIN 18009-2*; Braunschweiger Brandschutztage; Braunschweig; 2015.

Schröder, Benjamin; Arnold, Lukas; Brüne, Markus; Meunders, Andreas; Schmidt, Sven; *High parametric CFD-analysis of fire scenarios in underground train stations using statistical methods and climate modelling*; 10th International Conference on Performance-Based Codes and Fire Safety Design Methods; Gold Coast; 2014.

Schröder, Benjamin; *Systematische Umsetzung der Lärm- und Vibrations-Arbeitsschutzverordnung am Beispiel der Energiewirtschaft*; sicher ist sicher; 6/2012; Erich Schmidt Verlag GmbH & Co. KG; 2012.

Talks

Schröder, Benjamin; *Multivariate Brandsimulation am Beispiel einer uPVA*; 10. Anwendertreffen der FDS Usergroup; Berlin; 2016.

Schröder, Benjamin; *Hello CS&E – My Home Institute and Research Topics*; Introductory Talk Univsersity of Minnesota; Minneapolis; 2016.

Schröder, Benjamin; *Numerische Brandsimulation – Möglichkeiten und Grenzen anhand einfacher und komplexer Beispiele*; Fortbildung Feuerwehr München; München; 2016.

Schröder, Benjamin; *Wissens- und wahrnehmungsbasierte Modellierung der Routenwahl im Brandfall*; Doktorandenseminar Brandsimulation; Wuppertal; 2015.

Schröder, Benjamin; *Das (un-) berechenbare Feuer*; Jahresabschlusskolloquium Jülich Supercomputing Centre; Jülich; 2014.

Schröder, Benjamin; *Coupling of fire and pedestrian simulations*; Workshop Neue Ideen in der Modellierung von Transportproblemen; München; 2014.

Schröder, Benjamin; *High parametric CFD-analysis of fire scenarios in underground train stations*; Doktorandenseminar Brandsimulation; Berlin; 2014.

Schröder, Benjamin; *Ansätze zur Kopplung von Brand- und Evakuierungssimulationen*; Doktorandenseminar Brandsimulation; Jülich; 2013.

Schröder, Benjamin; *Grunddaten der Personendynamik in Schienenfahrzeugen*; Workshop Rechnergestützte Modellierung in der Sicherheitsforschung; Koblenz; 2013.

Bibliography

Albrecht, C. (2012). *A risk-informed and performance-based life safety concept in case of fire*. PhD Thesis, Technische Universität Braunschweig.

Albrecht, C., Siemon, M., and Hosser, D. (2010). Application of sensitivity analysis to specific problems in Fire Protection Engineering to identify the most critical parameters and to reduce dimensionality. In *Proceedings of the 8th International Probabilistic Workshop in Szczecin*, pages 13–26, Szczecin.

Andresen, E., Chraibi, M., and Seyfried, A. (2016a). The impact of perception and wayfinding on pedestrian movements. In *Proceedings of the 8th International Conference on Pedestrian and Evacuation Dynamics (PED2016)*.

Andresen, E., Haensel, D., Chraibi, M., and Seyfried, A. (2016b). Wayfinding and cognitive maps for pedestrian models: In print! In *Proceedings of Traffic and Granular Flow 2015*.

Andresen, E., Haensel, D., Chraibi, M., and Seyfried, A. (2017). Wayfinding and cognitive maps for pedestrian models: Submitted (in review). *Transportmetrica A: Transport Science*.

Axnich, R. (2016). Parameterstudie zur Evakuierung einer unterirdischen Personenverkehrsanlage mit dem Jülich Pedestrian Simulator. Master's Thesis, Bergische Universität Wuppertal.

Bansemer, B. (2015). *Numerische Simulation von Schienenfahrzeugbränden auf der Basis experimentell ermittelter Materialkennwerte*. Pro Business. ISBN 978-3-86386-947-2.

Berchtold, F., Knaust, C., Thöns, S., and Rogge, A. (2016). Risk analysis in road tunnels – most important risk indicators. In *Seventh International Symposium on Tunnel Safety and Security*, Montreal.

BMBF (2015). Bundesministerium für Bildung und Forschung. http://www.sifo.de/. Bekanntmachung "Schutz von Verkehrsinfrastrukturen.

Borchert, G. (2014). Charakterisierung unterirdischer Bahnhöfe hinsichtlich des vorbeugenden und abwehrenden Brandschutzes. Bachelor's Thesis, Bergische Universität Wuppertal.

BOStrab (2007). Verordnung über den Bau und Betrieb der Straßenbahnen. Bundesministerium für Verkehr und digitale Infrastruktur.

Braha, D., Minai, A., and Bar-Yam, Y. (2006). *Complex Engineered Systems: Science Meets Technology*. New England Complex Systems Institute series on complexity. Springer.

Brüne, M. (2007). Ermittlung und Beschreibung der natürlichen Hintergrundströmung in U-Bahn-Systemen während der Betriebszeiten am Beispiel der Dortmunder U-Bahn unter besonderer Berücksichtigung der Außenwitterung. Diploma Thesis, Ruhr-Universität Bochum.

Bryan, J. (1977). Smoke as a Determinant of Human Behavior in Fire Situations (Project People). Technical Report NBS-GCR-77-94, University of Maryland. Grant No. 4-9027.

BSI 7974-6 (2004). PD 7974-6:2004 The application of fire safety engineering principles to fire safety design of buildings – Human factors: Life safety strategies – Occupant evacuation, behaviour and condition (Sub-system 6). BSI – British Standards.

Bulk, J. (2015). *Brandschutz in Schienenfahrzeugen - Experimentelle und numerische Untersuchungen zu Reisegepäck als sekundäres Zündinitial*. PhD Thesis, Bergische Universität Wuppertal.

BVG (2007). Typenbuch U-Bahn. Berliner Verkehrsbetriebe.

Camillo, A. (2013). *Multi-scale investigation of fire behaviour of a seat and a wall panel from European railway transport system*. PhD Thesis, l'Ecole Doctorale Sciences et Ingénierie en Matériaux, Mécanique, Enerǵtique et Aŕonautique (SIMMEA).

Carvel, R. and Beard, A. (2005). The influence of tunnel ventilation on fire behaviour. In Beard, A. and Carvel, R., editors, *The Handbook of Tunnel Fire Safety*, book section 9, pages 184–197. Thomas Telford, London.

Carvel, R. and Marlair, G. (2005). A history of fire incidents in tunnels. In Beard, A. and Carvel, R., editors, *The Handbook of Tunnel Fire Safety*, book section 1, pages 3–41. Thomas Telford, London.

Çakici Alp, N. and Çağdaş, G. (2014). Occupants Emergency Behaviour in Turkey. In Weidmann, U., Kirsch, U., and Schreckenberg, M., editors, *Pedestrian and Evacuation Dynamics 2012*, pages 1123–1133. Springer International Publishing.

Chen, F., Chien, S.-W., Jang, H.-M., and Chang, W.-J. (2003). Stack effects on smoke propagation in subway stations. *Continuum Mechanics and Thermodynamics*, 15(5):425–440, doi:10.1007/s00161-003-0117-5.

Cooper, A., Reimann, R., and Cronin, D. (2007). *About Face 3: The Essentials of Interaction Design*. Wiley.

DIN 18009-1 (2015). E DIN 18009-1:2015-04 Brandschutzingenieurwesen – Teil 1: Grundsätze und Regeln für die Anwendung. Deutsches Institut für Normung.

DIN EN 1991-1-2/NA (2015). DIN EN 1991-1-2/NA:2015-09 Nationaler Anhang – National festgelegte Parameter – Eurocode 1: Einwirkungen auf Tragwerke – Teil 1-2: Allgemeine Einwirkungen – Brandeinwirkungen auf Tragwerke. Deutsches Institut für Normung.

DIN EN 45545-1 (2013). DIN EN 45545-1:2013-08 Bahnanwendungen – Brandschutz in Schienenfahrzeugen – Teil 1: Allgemeine Regeln. Deutsches Institut für Normung.

Donald, I. and Canter, D. (1990). Behavioural aspects of the King's Cross Disaster. In Canter, D., editor, *Fires and human behaviour*, book section 2, pages 15–30. David Fulton Publishers, London.

dpa (2016). Regionalzug brennt aus – Rund 180 Fahrgäste in Sicherheit. *FAZ*. 06.01.2016.

Dudenredaktion (2006). *Duden – Deutsches Universalwörterbuch*. Bibliographisches Institut & FA Brockhaus AG , Mannheim, 6th edition.

Eichelberger (1998). Meßprotokoll Volumenstrommessung. Technical Report 976909, Eichelberger Ventilatorenfabrik GmbH & Co. U-Bahnhof Osloer Str.

EUB (2016). Untersuchungsbericht – Fahrzeugbrand, 25.06.2012, Eilendorf Hp – Aachen-Rothe Erde. Report 60uu2012-06/168-3323, Bundesministerium für Verkehr und digitale Infrastruktur. Eisenbahn-Unfalluntersuchungsstelle des Bundes.

Fahy, R. and Proulx, G. (1997). Human Behavior in the World Trade Center Evacuation. In *5th International Symposium on Fire Safety Science*, pages 713–724, Melbourne.

Fennell, D. (1988). Investigation into the King's Cross Underground Fire. Report, Department of Transport.

FGSV (2006). *Richtlinien für die Ausstattung und den Betrieb von Straßentunneln*. FGSV Verlag, Köln. Forschungsgesellschaft für Straßen- und Verkehrswesen e.V.

Fiedler, J. (2005). *Bahnwesen: Planung, Bau und Betrieb von Eisenbahnen, S-, U-, Stadt- und Straßenbahnen*. Werner Verlag.

Flassak, T. and Bächlin, W. (2012). Organisationsübergreifende Gefahrenabwehr zum Schutz von Menschen und kritischen Infrastrukturen durch optimierte Prävention und Reaktion (AZ 18VERKEHR07) : ORGAMIR; Teilvorhaben: Simulation (TP 3). Electronic resource.

Frantzich, H. and Nilsson, D. (2003). Utrymning genom tät rök: beteende och förflyttning. Technical Report 3126, Lund University.

Fridolf, K., Andre, K., Nilsson, D., and Frantzich, H. (2013a). The impact of smoke on walking speed. doi:10.1002/fam.2217 10.1002/fam.

Fridolf, K., Ronchi, E., Nilsson, D., and Frantzich, H. (2013b). Movement speed and exit choice in smoke-filled rail tunnels. *Fire Safety Journal*, 59(0):8–21, doi:http://dx.doi.org/10.1016/j.firesaf.2013.03.007.

Fridolf, K., Ronchi, E., Nilsson, D., and Frantzich, H. (2015). The relationship between obstructed and unobstructed walking speed: Results from an evacuation experiment in a smoke filled tunnel.

GfK (2013). Verteilung der Einkäufe unter der Woche in Deutschland nach Uhrzeit im Jahr 2013. Focus 41/2013, October 7th 2013, p. 82.

Gwynnee, S. and Boyce, K. (2016). Engineering Data. In Hurley, M., editor, *SFPE Handbook of Fire Protection Engineering*, book section 64. Society of Fire Protection Engineers, 5th edition.

Hadjisophocleous, G. V. and Mehaffey, J. R. (2016). Fire Scenarios. In Hurley, M., editor, *SFPE Handbook of Fire Protection Engineering*, book section 38. Society of Fire Protection Engineers, 5th edition.

Haensel, D. (2014). A knowledge-based routing framework for pedestrian dynamics simulation. Diploma Thesis, Technische Universität Dresden.

Hedefalk, J. and Wahlstrom, B. (1998). Lessons from the Baku underground railway/metro fire. In *3rd International Conference on Safety in Road and Rail Tunnels*, pages 15–28, Nice.

Hein, B. (2016). Sensitivity analysis of a perception-based route choice algorithm for a continuous evacuation model. Bachelor's Thesis, Technische Hochschule Köln.

Heuze, B. (2012). TRANSFEU – Transport Fire Safety Engineering in the European Union. Final report, Laboratoire national de métrologie et d'essais (LNE).

Hofinger, G., Zinke, R., Künzer, L., Schröder, B., and Andresen, E. (2016). Human Factors in Pedestrian Simulation: Field Studies in Underground Stations. In *The 8th International Conference on Pedestrian and Evacuation Dynamics (PED 2016)*, Hefei.

Holl, S. and Seyfried, A. (2010). Validität von Evakuierungssimulationen. *vfdb-Zeitschrift*, 1:35–41.

Hoogendoorn, S. P., Bovy, P., and Daamen, W. (2002). Microscopic pedestrian wayfinding and dynamics modelling. In Schreckenberg, M. and Sharma, S., editors, *Pedestrian and Evacuation Dynamics*, pages 123–155.

Hurley, M., Gottuk, D., Hall, J., Harada, K., Kuligowski, E., Puchovsky, M., Torero, J., Watts, J., and Wieczorek, C. (2016). *SFPE Handbook of Fire Protection Engineering*. Springer, New York, 5th edition.

Hurley, M. J. and Rosenbaum, E. R. (2016). Performance-Based Design. In Hurley, M., editor, *SFPE Handbook of Fire Protection Engineering*, book section 37. Society of Fire Protection Engineers, 5th edition.

iBMB (2015). *Braunschweiger Brandschutz-Tage 2015*. Institut für Baustoffe, Massivbau und Brandschutz (iBMB). Tagungsband Session 4 "Heißrauchversuche".

Ingason, H. (2005). Fire dynamics in tunnels. In Beard, A. and Carvel, R., editors, *The Handbook of Tunnel Fire Safety*, book section 10, pages 231–263. Thomas Telford, London.

Ingason, H., Kumm, M., Nilsson, D., Lönnermark, A., Claesson, A., Li, Y., Fridolf, K., Åkerstedt, R., Nyman, H., Dittmer, T., Forsén, R., Janzon, B., Meyer, G., Bryntse, A., Carlberg, T., Newlove-Eriksson, L., and Palm, A. (2012). The METRO Project. Final report, Mälardalen University.

ISO 9000 (2015). ISO 9000:2015 Quality management systems — Fundamentals and vocabulary. International Organization for Standardization.

ISO/TR 13387 (1999). ISO/TR 13387 Fire safety engineering Part 8: Life safety — Occupant behaviour, location and condition. ISO - International Organization for Standardization.

ISO/TR 16738 (2009). ISO/TR 16738 Fire-safety engineering – Technical information on methods for evaluating behaviour and movement of people. ISO – International Organization for Standardization.

ISO/TS 16733 (2006). ISO/TS 16733:2006 Fire safety engineering – Selection of design fire scenarios and design fires. International Organization for Standardization.

ISO/TS 29761 (2015). ISO/TS 29761:2015 Fire safety engineering – Selection of design occupant behavioural scenarios. International Organization for Standardization.

Jäger, G. and Schröder, B. (2016). Evacuation and Life Safety Assessment in Germany. In *11th Conference on Performance-Based Codes and Fire Safety Design*, Warsaw.

Jeon, G. and Hong, W. (2009). Characteristic Features of the Behavior and Perception of Evacuees from the Daegu Subway Fire and Safety Measures in an Underground Fire. *Journal of Asian Architecture and Building Engineering*, 8(2):415–422, doi:10.3130/jaabe.8.415.

Jin, T. (1978). Visibility through fire smoke. *Fire Flammability*, 9(2):135–155.

Kemloh, U., Chraibi, M., and Sesser, F. (2016). JuPedSim/JuPedSim: JuPedSim v0.8.1. doi:10.5281/zenodo.160168.

Kemloh Wagoum, A. U. (2013). *Route choice modelling and runtime optimisation for simulation of building evacuation*. PhD Thesis, Bergische Universität Wuppertal.

Kemloh Wagoum, A. U., Chraibi, M., Eilhardt, C., Nowak, S., Kulkov, I., Weber, D., Sauer, K., Klüpfel, H., and Schadschneider, A. (2014). OpenPedSim: A framework for pedestrian flow analysis. In Weidmann, U., Kirsch, U., and Schreckenberg, M., editors, *Pedestrian and Evacuation Dynamics 2012*, pages 1323–1330. Springer International Publishing.

Kemloh Wagoum, A. U., Chraibi, M., Zhang, J., and Lämmel, G. (2015). JuPedSim: An Open Framework for Simulating and Analyzing the Dynamics of Pedestrians. In *3rd Conference of Transportation Research Group of India*.

Kirchner, F. (2000). Feuer im U-Bahnhof Deutsche Oper. *Brandschutz*, 54(9):883–893. Berliner Feuerwehr.

Kleijnen, J. P. (2008). *Design and Analysis of Simulation Experiments*. International Series in Operations Research and Management Science. Springer, New York.

Kong, D., Lu, S., and Ping, P. (2016). A Risk-Based Method of Deriving Design Fires for Evacuation Safety in Buildings. *Fire Technology*, doi:DOI: 10.1007/s10694-016-0600-8.

Konrad, I. (2014). Normen und Leitfäden für Räumungssimulationen – Vorschläge zur Weiterentwicklung. Master's Thesis, Bergische Universität Wuppertal.

Kosow, H. and Gaßner, R. (2008). Methoden der Zukunfts- und Szenarioanalyse Überblick, Bewertung und Auswahlkriterien. WerkstattBericht Nr. 103.

Krause, D. (2015). JURECA: Jülich Research on Exascale Cluster Architectures. *Innovatives Supercomputing in Deutschland*, 13(1):92–95. FZJ-2015-04901.

Kuligowski, E. D. (2016). Human Behavior in Fire. In Hurley, M., editor, *SFPE Handbook of Fire Protection Engineering*, book section 58. Society of Fire Protection Engineers, 5th edition.

Kullback, S. and Leibler, R. A. (1951). On information and sufficiency. *Ann. Math. Statist.*, 22(1):79–86, doi:10.1214/aoms/1177729694.

Künzer, L. and Hofinger, G. (2016). Das Verhalten von Menschen in Rauch. *FeuerTRUTZ Magazin*, 2016(5):2–4.

Lindell, M. K. and Perry, R. W. (2012). The protective action decision model: theoretical modifications and additional evidence. *Risk Analysis*, 32(4):616–632.

Lovreglio, R., Ronchi, E., and Borri, D. (2014). The validation of evacuation simulation models through the analysis of behavioural uncertainty. *Reliability Engineering & System Safety*, 131:166–174, doi:http://dx.doi.org/10.1016/j.ress.2014.07.007.

MacKay, D. J. (2003). *Information Theory, Inference, and Learning Algorithms*. Cambridge University Press.

Mahajan, S. (2014). *The Art of Insight in Science and Engineering: Mastering Complexity*. MIT Press.

MBO (2012). Musterbauordnung (German Model Building Code) – MBO. ARGEBAU Fachkommission Bauaufsicht der Bauministerkonfererenz.

McGrattan, K., Hostikka, S., McDermott, R., Floyd, J., Weinschenk, C., and Overholt, K. (2015a). *Fire Dynamics Simulator Technical Reference Guide*, volume Volume 1: Mathematical Model. National Institute of Standards and Technology, Gaithersburg, Maryland, USA, 6.3.2 edition.

McGrattan, K., Hostikka, S., McDermott, R., Floyd, J., Weinschenk, C., and Overholt, K. (2015b). *Fire Dynamics Simulator Technical Reference Guide*, volume Volume 3: Validation. National Institute of Standards and Technology, 6.2 edition.

McGrattan, K., Hostikka, S., McDermott, R., Floyd, J., Weinschenk, C., and Overholt, K. (2015c). *Fire Dynamics Simulator User's Guide*. National Institute of Standards and Technology, 6.2.0 edition.

Meunders, A., Baker, G., Arnold, L., Schröder, B., Spearpoint, M., and Pau, D. (2014). Parameter Optimization and Sensitivity Analysis for Fire Spread Modelling with FDS. In *10th Conference on Performance-Based Codes and Fire Safety Design*, Gold Coast.

Michel, J.-B., Shen, Y. K., Aiden, A. P., Veres, A., Gray, M. K., Team, T. G. B., Pickett, J. P., Hoiberg, D., Clancy, D., Norvig, P., Orwant, J., Pinker, S., Nowak, M. A., and Aiden, E. L. (2011). Quantitative analysis of culture using millions of digitized books. *Science*, 331(6014):176–182, doi:10.1126/science.1199644.

Münch, M. (2013). *Konzept zur Absicherung von CFD-Simulationen im Brandschutz und in der Gefahrenabwehr*. PhD Thesis, FU Berlin.

Myatt, G. J. (2007). *Making Sense of Data – A Practical Guide to Exploratory Data Analysis and Data Mining*. Wiley, Hoboken, NJ.

NFPA (2014). *NFPA 130 Standard for Fixed Guideway Transit and Passenger Rail Systems, 2014 Edition*. National Fire Protection Association.

Nilsson, D. and Fahy, R. (2016). Selecting Scenarios for Deterministic Fire Safety Engineering Analysis: Life Safety for Occupants. In Hurley, M., editor, *SFPE Handbook of Fire Protection Engineering*, book section 57. Society of Fire Protection Engineers, 5th edition.

ORPHEUS (2015). Projekt ORPHEUS: Optimierung der Rauchableitung und Personenführung in U-Bahnhöfen: Experimente und Simulationen. http://www.orpheus-projekt.de/.

Osterkamp, M. (2015). Simulation der Räumung einer unterirdischen Personenverkehrsanlage mit dem Juelich Pedestrain Simulator. Bachelor's Thesis, Bergische Universität Wuppertal.

PBefG (2016). Personenbeförderungsgesetz. Bundesministerium für Verkehr und digitale Infrastruktur.

Pele, O. and Werman, M. (2008). A linear time histogram metric for improved sift matching. In *Computer Vision–ECCV 2008*, pages 495–508. Springer.

Pele, O. and Werman, M. (2009). Fast and robust earth mover's distances. In *2009 IEEE 12th International Conference on Computer Vision*, pages 460–467. IEEE.

Pflitsch, A. and Brüne, M. (2016). Dataset: Climate Osloer Straße (BER_Ol). Time series collected between 2009 and 2015.

Pflitsch, A., Brüne, M., Killing-Heinze, M., Ringeis, J., Agnew, B., and Steiling, B. (2013). Natural ventilation as a factor controlling the dispersal of airborne toxins in subway systems in a disaster situation. *Journal of Transportation Safety & Security*, 5(1):78–92, doi:10.1080/19439962.2012.721872.

Pflitsch, A., Brüne, M., Steiling, B., Killing-Heinze, M., Agnew, B., Irving, M., and Lockhart, J. (2012). Air flow measurements in the underground section of a uk light rail system. *Applied Thermal Engineering*, 32:22–30, doi:10.1016/j.applthermaleng.2011.07.030.

Proulx, G. (1995). Evacuation time and movement in apartment buildings. *Fire Safety Journal*, 24(3):229 – 246, doi:http://dx.doi.org/10.1016/0379-7112(95)00023-M.

Proulx, G. and Sime, J. (1991). To Prevent 'Panic' in an Underground Emergency: Why Not Tell People the Truth? In Cox, G. and Langford, B., editors, *Fire Safety Science Proceedings of the third International Symppsium*, Edinburgh. ELSEVIER APPLIED SCIENCE.

Purser, D. (2003). Behaviour and Travel Interactions in Emergency Situations and Data Needs for Engineering Design. In *Second International Conference in Pedestrian and Evacuation Dynamics (PED)*, pages 355–369, Greenwich.

Purser, D. A. (2016a). Combustion Toxicity. In Hurley, M., editor, *SFPE Handbook of Fire Protection Engineering*, book section 62. Society of Fire Protection Engineers, 5th edition.

Purser, D. A. (2016b). Developments in tenability and escape time assessment for evacuation modelling simulations. In Cuesta, A., Abreu, O., and Alvear, D., editors, *Evacuation Modeling Trends*, pages 25–53. Springer International Publishing, Cham.

Purser, D. A. and McAllister, J. (2016). Assessment of Hazards to Occupants from Smoke, Toxic Gases, and Heat. In Hurley, M., editor, *SFPE Handbook of Fire Protection Engineering*, book section 62. Society of Fire Protection Engineers, 5th edition.

Purser, D. A. and Purser, J. (2008). HCN Yields and Fate of Fuel Nitrogen for Materials under Different Combustion Conditions in the ISO 19700 Tube Furnace and Large-scale Fires. In Karlsson, B., editor, *Fire Safety Science – Ninth International Symposium*, pages 1117–1128. International Association of Fire Safety Science.

Quintiere, J. G. (2006). *Fundamentals of Fire Phenomena*. John Wiley & Sons.

Rennen, G., Husslage, B., Van Dam, E. R., and Den Hertog, D. (2010). Nested maximin Latin hypercube designs. *Structural and Multidisciplinary Optimization*, 41(3):371–395, doi:10.1007/s00158-009-0432-y.

RiMEA (2016). Richtlinie für Mikroskopische Entfluchtungsanalysen. Version 3.0.0, RiMEA e.V.

Rogsch, C., Galster, R., Luthardt, T., and Mohr, D. (2015). User Inputs and their Influence on the Dynamics of Pedestrian Movement in Evacuation Simulations. In *Human Behaviour In Fire Symposium*, Cambridge.

Ronchi, E., Gwynne, S. M. V., Purser, D. A., and Colonna, P. (2013). Representation of the impact of smoke on agent walking speeds in evacuation models. *Fire Technology*, 49(2):411–431, doi:10.1007/s10694-012-0280-y.

Schadschneider, A., Klingsch, W., Kluepfel, H., Kretz, T., Rogsch, C., and Seyfried, A. (2009). Evacuation dynamics: Empirical results, modeling and applications. In Meyers, R. A., editor, *Encyclopedia of complexity and system science*, volume 5, pages 3142–3176. Springer, Berlin, Heidelberg.

Schäfer, C., Zinke, R., Künzer, L., Hofinger, G., and Koch, R. (2014). Applying persona method for describing users of escape routes. In *The Conference on Pedestrian and Evacuation Dynamics 2014*, pages 636–641.

Schmidt, S. (2015). Entrauchung unterirdischer Personenverkehrsanlagen – Eine Untersuchung verschiedener Konzepte mittels hochparametrischer CFD-Simulationen. Master's thesis, Bergische Universität Wuppertal.

Schmundt, H. and Wassermann, A. (2014). Der vergessene Schornstein. *Spiegel*, 19:28–31.

Schneider, K.-J. (2012). *Bautabellen für Ingenieure*. Werner Verlag.

Schomacker, M. (2009). Berliner Untergrundbahn. http://www.berliner-untergrundbahn.de/. Accessed: 2016-01-10.

Schröder, B., Andresen, E., Haensel, D., Chraibi, M., Arnold, L., and Seyfried, A. (2015). Knowledge- and perception-based route choice modelling in case of fire. In *Human Behaviour In Fire Symposium*, Cambridge.

Schröder, B., Arnold, L., Brüne, M., Meunders, A., and Schmidt, S. (2014). High parametric CFD-analysis of fire scenarios in underground train stations using statistical methods and climate modelling. In *10th Conference on Performance-Based Codes and Fire Safety Design*, Gold Coast.

Schröder, B., Arnold, L., Meunders, A., and Schmidt, S. (2016). Smoke and Heat Extraction in Underground Stations. In *Interflam 2016*, London.

Seyfried, A., Jäger, G., Kitzlinger, M., and Schröder, B. (2015). Normierung von Personenstromsimulationen in DIN 18009-2. In *Braunschweiger Brandschutztage 2015*, Braunschweig.

Seyfried, A., Passon, O., Steffen, B., Boltes, M., Rupprecht, T., and Klingsch, W. (2009). New insights into pedestrian flow through bottlenecks. *Transportation Science*, 43(3):395–406, doi:10.1287/trsc.1090.0263.

SFPE (2014). Case Studies. In *10th Conference on Performance-Based Codes and Fire Safety Design*, Gold Coast.

Sime, J. (1995). Crowd psychology and engineering. *Safety Science*, 21(1):1–14.

Sime, J. D. (1983). Affiliative behaviour during escape to building exits. *Journal of Environmental Psychology*, 3(1):21 – 41, doi:http://dx.doi.org/10.1016/S0272-4944(83)80019-X.

Stadt Berlin (2014). Berliner Verkehr in Zahlen 2013. Report, Senatsverwaltung für Stadtentwicklung und Umwelt.

Tordeux, A., Chraibi, M., and Seyfried, A. (2016). Collision-Free Speed Model for Pedestrian Dynamics. In Daamen, W. and Knoops, V., editors, *Traffic and Granular Flow '15*. Springer (to be published).

TRStrab BS (2014). Technische Regeln für Straßenbahnen – Brandschutz in unterirdischen Betriebsanlagen. Bundesministerium für Verkehr und digitale Infrastruktur.

United Nations (2012). *The 2011 Revision: World Urbanization Prospects*. New York.

URP (2011). *Fundamental requirements for urban rail systems, design, construction, manufacture, operations & maintenace*. UITP Urban Rail Platform. Recommended basic reference for developing a minimum set of standards for voluntary use in the field of urban rail according to mandate M/486 EN.

VDI (2006a). VDI 6019 Part 1 Engineering methods for the dimensioning of systems for the removal of smoke from buildings. Fire curves, verification of effectiveness. Guideline ICS 13.220.99, VDI-Gesellschaft Technische Gebäudeausrüstung, Düsseldorf.

VDI (2006b). VDI 6019 Part 2 Engineering methods for the dimensioning of systems for the removal of smoke from buildings. Engineering methods. Guideline ICS 13.220.99, 91.140.30, VDI-Gesellschaft Technische Gebäudeausrüstung, Düsseldorf.

vfdb (2013). *Leitfaden Ingenieurmethoden des Brandschutzes*. Hosser, Dietmar, Altenberge. TB 04-01.

Viana, F. A. C. (2013). Things you wanted to know about the Latin hypercube design and were afraid to ask.

Weidmann, U. (1994). *Der Fahrgastwechsel im öffentlichen Personenverkehr*. PhD Thesis, ETH Zürich.

Wilk, E. (2010). Risikoanalyse zu brandtechnischen Eigenschaften der Schienenfahrzeuge der Berliner Verkehrsbetriebe. Technical Report G 077 / 09, Brandschutz Consult Ingenieurgesellschaft mbH Leipzig.

Wilk, E. (2012). Anwenderhinweise zur Berechnung der Bauteilbelastung der Bemessungsbrände der DB Station & Service AG. Technical Report G 137 / 11, Brandschutz Consult Ingenieurgesellschaft mbH Leipzig.

Winzer, P. (2013). *Generic Systems Engineering ein methodischer Ansatz zur Komplexitätsbewältigung*. Springer, Berlin u.a.

Wood, P. (1972). The Behaviour of People in Fires. Technical Report 953, Loughborough University of Technology. Fire Research Note.

World Bank (2015). Dataset: Urban population. Retrieved from: http://data.worldbank.org/indicator/SP.URB.TOTL.

Zhang, J., Song, W., and Xu, X. (2008). Experiment and multi-grid modeling of evacuation from a classroom. *Physica A: Statistical Mechanics and its Applications*, 387(23):5901 – 5909, doi:http://dx.doi.org/10.1016/j.physa.2008.06.030.

Zinke, R., Künzer, L., Schröder, B., and Schäfer, C. (2017). Integrating Human Factors into Evacuation Simulations – Application of the Persona Method for Generating Populations. In *14th International Conference on Information Systems for Crisis Response And Management*, pages 127–138, Albi.

Schriften des Forschungszentrums Jülich
IAS Series

Band / Volume 22
Three-dimensional Solute Transport Modeling in Coupled Soil and Plant Root Systems
by N. Schröder (2013), xii, 126 pages
ISBN: 978-3-89336-923-2
URN: urn:nbn:de:0001-2013112209

Band / Volume 23
Characterizing Load and Communication Imbalance in Parallel Applications
by D. Böhme (2014), xv, 111 pages
ISBN: 978-3-89336-940-9
URN: urn:nbn:de:0001-2014012708

Band / Volume 24
Automated Optimization Methods for Scientific Workflows in e-Science Infrastructures
by S. Holl (2014), xvi, 182 pages
ISBN: 978-3-89336-949-2
URN: urn:nbn:de:0001-2014022000

Band / Volume 25
Numerical simulation of gas-induced orbital decay of binary systems in young clusters
by A. C. Korntreff (2014), 98 pages
ISBN: 978-3-89336-979-9
URN: urn:nbn:de:0001-2014072202

Band / Volume 26
UNICORE Summit 2014
Proceedings, 24th June 2014 | Leipzig, Germany
edited by V. Huber, R. Müller-Pfefferkorn, M. Romberg (2014), iii, 60 pages
ISBN: 978-3-95806-004-3
URN: urn:nbn:de:0001-2014111408

Band / Volume 27
Automatische Erfassung präziser Trajektorien in Personenströmen hoher Dichte
by M. Boltes (2015), xii, 308 pages
ISBN: 978-3-95806-025-8
URN: urn:nbn:de:0001-2015011609

Band / Volume 28
Computational Trends in Solvation and Transport in Liquids
edited by G. Sutmann, J. Grotendorst, G. Gompper, D. Marx (2015)
ISBN: 978-3-95806-030-2
URN: urn:nbn:de:0001-2015020300

Schriften des Forschungszentrums Jülich
IAS Series

Band / Volume 29
Computer simulation of pedestrian dynamics at high densities
by C. Eilhardt (2015), viii, 142 pages
ISBN: 978-3-95806-032-6
URN: urn:nbn:de:0001-2015020502

Band / Volume 30
Efficient Task-Local I/O Operations of Massively Parallel Applications
by W. Frings (2016), xiv, 140 pages
ISBN: 978-3-95806-152-1
URN: urn:nbn:de:0001-2016062000

Band / Volume 31
A study on buoyancy-driven flows: Using particle image velocimetry for validating the Fire Dynamics Simulator
by A. Meunders (2016), xxi, 150 pages
ISBN: 978-3-95806-173-6
URN: urn:nbn:de:0001-2016091517

Band / Volume 32
Methoden für die Bemessung der Leistungsfähigkeit multidirektional genutzter Fußverkehrsanlagen
by S. Holl (2016), xii, 170 pages
ISBN: 978-3-95806-191-0
URN: urn:nbn:de:0001-2016120103

Band / Volume 33
JSC Guest Student Programme Proceedings 2016
edited by I. Kabadshow (2017), iii, 191 pages
ISBN: 978-3-95806-225-2
URN: urn:nbn:de:0001-2017032106

Band / Volume 34
Multivariate Methods for Life Safety Analysis in Case of Fire
by B. Schröder (2017), x, 222 pages
ISBN: 978-3-95806-254-2
URN: urn:nbn:de:0001-2017081810

IAS
Band / Volume 34
ISBN 978-3-95806-254-2